AN ABSTRACT OF THE DISSERTATION OF

Patrick I. Bennett for the degree of Doctor of Philosophy in Botany and Plant Pathology presented on May 10, 2018.

Title: Genetic Structure in Populations of the Douglas-fir Swiss Needle Cast Fungus *Nothophaeocryptopus gaeumannii*

Abstract approved: _____

Jeffrey K. Stone

The fungus *Nothophaeocryptopus gaeumannii* is the causative agent of Swiss needle cast (SNC), a foliar disease of Douglas-fir. Disease is characterized by premature loss of foliage and reduced growth resulting from the inhibition of photosynthesis due to the occlusion of stomata by the ascocarps of *N. gaeumannii.* Although the disease was first reported from Douglas-fir plantings in Europe, the fungus that causes the disease is endemic to the native range of Douglas-fir in western North America. The focus of this dissertation is to evaluate the factors that influence the genetic structure of native and introduced populations of *N. gaeumannii* and determine whether population structure is related to SNC severity.

Native populations of this fungus in western North America are subdivided into two lineages that may constitute cryptic species. Evidence suggests that one of these lineages (Lineage 2) may be more aggressive, as it appears to be more abundant relative to Lineage 1 where SNC is most severe. We determined that the two lineages are highly

differentiated and do not appear to interbreed but are sympatric at very fine spatial scales. In addition to this population subdivision, homothallic reproduction, inferred based on the presence of repeated multilocus genotypes (MLGs), was found to be a major factor influencing the genetic structure of *N. gaeumannii* in native and introduced populations worldwide. Spatial genetic variation in these populations allowed us to infer gene flow and migration at various hierarchical scales. For instance, in New Zealand, human-mediated migration of infected trees between sites seemed to be the most parsimonious explanation for the observed spatial distributions of repeated MLGs, as some MLGs were shared at sites over 1,000 km apart. This suggests that the movement of infected Douglas-fir seedlings by the timber or ornamental nursery trades may be a significant factor influencing the contemporary structure of this introduced population.

In Chapter four a dataset consisting of MLGs from 3,829 *N. gaeumannii* isolates from North America, South America, Europe, New Zealand, and Australia was analyzed to assess diversity and genetic structure in the global *N. gaeumannii* population. Approximate Bayesian computation (ABC) allowed for the identification of the most probable introduction pathways. This computational tool was used to test various demographic scenarios, each of which represented hypotheses about the origins of the introduced populations. This analytical framework also allowed for an assessment of the influences of founding events and population bottlenecks on the genetic structures of introduced populations. The demographic scenarios with the highest statistical support suggested that *N. gaeumannii* was first introduced from North America to Europe, and more recently from North America to New Zealand and South America. The *N.*

gaeumannii population in Australia was likely introduced from Europe, and thus the populations in Australia and New Zealand were introduced from different sources despite the relative proximity of the two countries.

The results presented in Chapter five suggested that environment is also an important factor shaping the genetic structure of native *N. gaeumannii* populations. The same environmental variables that were associated with SNC severity were also correlated with genetic variation in the pathogen population. For instance, the geographic distribution of Lineage 2 had a strong positive correlation with mean winter temperature. At both the landscape level and the stand level, it appeared that the spatial distribution of Lineage 2 was correlated with SNC severity. However, after accounting for the environmental differences between each of the sites associated with their relative coastal proximity, there was no evidence to suggest a relationship between the relative proportion of Lineage 2 and SNC severity. This suggests that the superficial association between *N. gaeumannii* Lineage 2 and disease severity is likely a reflection of the environmental influences on the disease and the differential environmental preferences of the two pathogen lineages. There was also strong genetic differentiation between the *N. gaeumannii* isolates collected from sites with the highest SNC severity and those collected from the sites with the lowest SNC severity, suggesting that there may have been genetic variation associated with disease or environment independent of the relative abundances of the two lineages. The evidence presented here suggested that climate is an important determinant of SNC severity, but also that climate has influenced the structure of *N. gaeumannii* populations.

©Copyright by Patrick I. Bennett
May 10, 2018
All Rights Reserved

Genetic Structure in Populations of the Douglas-fir Swiss Needle Cast Fungus *Nothophaeocryptopus gaeumannii*

by
Patrick I. Bennett

A DISSERTATION

submitted to

Oregon State University

in partial fulfillment of
the requirements for the
degree of

Doctor of Philosophy

Presented May 10, 2018
Commencement June 2018

Doctor of Philosophy dissertation of Patrick I. Bennett presented on May 10, 2018

APPROVED:

Major Professor, representing Botany and Plant Pathology

Head of the Department of Botany and Plant Pathology

Dean of the Graduate School

I understand that my dissertation will become part of the permanent collection of Oregon State University libraries. My signature below authorizes release of my dissertation to any reader upon request.

Patrick I. Bennett, Author

ACKNOWLEDGEMENTS

I must first express my sincerest gratitude and appreciation to all who have contributed to my academic and professional success during my time as a graduate student. To my mentor, my advisor, and my greatest advocate, Dr. Jeff Stone, for his kind patience and great wisdom to which I owe a great deal of my success. His confidence in my abilities allowed me to have confidence in myself. Thank you to Dave Shaw, Gabi Ritóková, and all of the members of the OSU Swiss Needle Cast Cooperative (SNCC) who provided the knowledge and resources that made all of this research possible. Thank you to Dan Omdal and Amy Ramsey for providing assistance with the sampling in Washington, and for helping to secure the funds that allowed us to process those samples. Special thanks to the members of the Grünwald lab including Nik, who challenged me to think more deeply about evolutionary biology and population genetics, and provided guidance and support at key stages throughout my academic career. To Javier Tabima and Zhian Kamvar, two inspirational scientists who not only opened my mind and my heart to population genetics, and were also great friends and role models. To Dr. Jeff Chang who, as both an instructor and a committee member, had a strong influence on my development as a scientist. Thank you for your willingness to share your wisdom about work, life, and the biological sciences. To my graduate committee representative, Barb Lachenbruch, who always had my best interest at heart. Special thanks to Lynda Ciuffetti who did everything in her power to make sure that each and every graduate in her department had access to the resources necessary to be successful, and who was always willing to listen and respond to the concerns of the graduate students in BPP. Thank you

to Melodie Putnam, who not only provided me with a research assistantship that allowed me to gain valuable experience working with the plant clinic, but gave me significant opportunities for advancement in many other ways. A very special thanks to the invaluable assistance provided by Wendy Sutton, who allowed me to advance my knowledge of molecular biology techniques and was always willing to help around the lab in any way that she could. Thanks to Paul Reeser, whose knowledge of media preparation, microscopy, culture maintenance, and many other laboratory techniques helped me to advance my skills in those areas. Many thanks to the members of the Western International Forest Disease Work Conference (WIFDWC) who have always offered a welcoming atmosphere, an outlet for my research findings, and good times around the campfire. Thank you to Richard Sniezko and the kind folks at the U.S.D.A. Forest Service Dorena Genetic Resource Center for providing many opportunities for advancement and valuable educational experiences in forest pathology. Thank you to Joey Spatafora, who served as a mentor and teacher that greatly advanced my knowledge in the fields of evolutionary biology and mycology. I am confident that his patience and kindness will make him a great leader for BPP.

Funding for this research was provided by The Swiss Needle Cast Cooperative, the Portland Garden Club Katherine R. Pamplin Scholarship, the Puget Sound Mycological Society Ben Woo Scholarship, the Cascade Mycological Society Freeman Rowe Scholarship, the Oregon Mycological Society, Washington Department of Natural Resources (WA DNR), U.S.D.A. Forest Service, the Oregon State University Graduate School, and the Oregon Lottery. A very special thank you is also owed to Ian Hood and

Scion, without whom the analyses of population structure of *N. gaeumannii* in New Zealand could not have been completed.

To all of my fellow BPP graduate students, past and present, thank you for being good friends. I appreciate all that were there to celebrate, to commiserate, and to share their knowledge and experiences. And a very special thank you to my fellow graduate students who have become some of my best friends, and who have helped me to grow and to become the person that I am today- Zolton Bair, Dabao Lu, Duncan Kroese, Hannah Rivedal, Brent Warneke, Kristen Finch, and Ryan Lenz.

I am eternally grateful to have the loving companionship of my wife Michelle Bennett, whose unwavering support and kindness has been truly uplifting. I am also very grateful to my family, especially my mother Suzanne, my sister Kristyn, and my grandmother Ellyn Johnson who all had a hand in raising me and guiding me toward the path to success.

CONTRIBUTION OF AUTHORS

Chapter 2: J. K. Stone assisted in designing the study, interpreting the results, and editing the manuscript.

Chapter 3: J. K. Stone sampled Douglas-fir foliage from New Zealand, isolated *N. gaeumannii* in culture, coordinated the molecular data acquisition, and assisted in designing the study, interpreting the results, and editing the manuscript. Ian Hood coordinated funding, assisted in sampling Douglas-fir foliage in New Zealand, and assisted in editing the manuscript.

Chapter 4: J. K. Stone sampled foliage from New Zealand, isolated the *N. gaeumannii* cultures from those sites, coordinated the molecular data acquisition, and assisted in designing the study, interpreting the results, and editing the manuscript.

Chapter 5: J. K. Stone assisted in designing the study, interpreting the results, and editing the manuscript.

TABLE OF CONTENTS

Page

Chapter 1. Introduction 1
1.1 Swiss Needle Cast (SNC) 2
1.1.1 Global distribution 2
1.1.2 Emergence in western Oregon and Washington 6
1.1.3 Measurement of SNC severity 8
1.1.4 Climate and SNC 11
1.1.5 Ecological Interactions 14
1.1.6 SNC Management 16
1.2 The Douglas-fir Swiss Needle Cast Fungus *Nothophaeocryptopus gaeumannii* (T. Rohde) Videira, C. Nakash., U. Braun & Crous 18
1.2.1 Infection biology 19
1.2.2 Mechanisms of pathogenicity 20
1.2.4 Taxonomy 22
1.3 Douglas-fir (*Pseudotsuga menziesii* (Mirb.) Franco) 23
1.4 Population Genetics of Fungal Plant Pathogens 27
1.4.1 Factors Influencing the Genetic Structure of Pathogen Populations 27
1.4.2 Fungal Speciation 29
1.4.3 Population structure of *N. gaeumannii* 32
1.5 Dissertation Outline 33
1.6 Literature Cited 35
1.7 Figures and Tables 42

Chapter 2. Hierarchical Genetic Structure in Populations of the Douglas-fir Swiss Needle Cast Fungus *Nothophaeocryptopus gaeumannii* in Coastal Oregon and Washington Forests 51
2.1 Abstract 52
2.2 Introduction 53
2.3 Materials and Methods 57

TABLE OF CONTENTS (Continued)

Page

2.3.1 Foliage Sampling 57
2.3.2 Isolation of *N. gaeumannii* from Infected Foliage 58
2.3.3 DNA Extraction, Multiplex PCR, and SSR Genotyping 58
2.3.4 Data Analysis 60
2.4 Results 64
2.4.1 Genetic diversity 64
2.4.2 Spatial distributions of multilocus genotypes 65
2.4.3 Population structure and differentiation 66
2.5 Discussion 69
2.6 Acknowledgements 77
2.7 Literature Cited 78
2.8 Figures and Tables 82
2.9 Supplementary Figures 100

Chapter 3. The Genetic Structure of Populations of the Douglas-fir Swiss Needle Cast Fungus *Nothophaeocryptopus gaeumannii* in New Zealand 102
3.1 Abstract 103
3.2 Introduction 104
3.3 Materials and Methods 107
3.3.1 Field Sampling, Isolations, and Culturing 107
3.3.2 Molecular techniques 108
3.3.3 Data analysis 108
3.4 Results 112
3.4.1 Genetic diversity 112
3.4.2 Population structure and differentiation 113
3.4.3 Spatial distributions of multilocus genotypes 114
3.5 Discussion 115

TABLE OF CONTENTS (Continued)

Page

3.6 Acknowledgements 125
3.7 Literature Cited 126
3.8 Figures and Tables 130
3.9 Supplementary Figures 138

Chapter 4. Global Population Structure, Diversity and Introduction Pathways of the Douglas-fir Swiss Needle Cast Fungus *Nothophaeocryptopus gaeumannii* 141
4.1 Abstract 142
4.2 Introduction 143
4.3 Materials and Methods 146
4.3.1 Field Sampling, Isolations, and Culturing 146
4.3.2 Molecular techniques 147
4.3.3 Data Analysis 148
4.4 Results 153
4.4.1 Diversity and Richness 153
4.4.2 Population Structure and Differentiation 154
4.4.3 Demographic History and Routes of Introduction 156
4.5 Discussion 157
4.6 Acknowledgements 171
4.7 Literature Cited 172
4.8 Figures and Tables 175
4.9 Supplementary Figures and Tables 187

Chapter 5. Environmental Variables Associated with Swiss Needle Cast Severity and *Nothophaeocryptopus gaeumannii* Population Structure in Western Oregon and Washington 201
5.1 Abstract 202
5.2 Introduction 203

TABLE OF CONTENTS (Continued)

Page

5.3 Materials and Methods 206
5.3.1 Foliage Sampling 206
5.3.2 Isolation of *N. gaeumannii* from Infected Foliage 207
5.3.3 DNA Extraction, PCR, and SSR Genotyping 207
5.3.4 Data Analysis 209
5.4 Results 212
5.4.1 The Spatial Distributions of *N. gaeumannii* Lineages in Relation to SNC Severity 212
5.4.2 Variations in Disease Severity, Geography, and Environment Across Sites 213
5.4.3 Correlations Between Environment, Disease, and the Genetic Structure of *N. gaeumannii* Populations 214
5.5 Discussion 216
5.6 Acknowledgements 225
5.7 Literature Cited 226
5.8 Figures and Tables 230
5.9 Supplementary Figures 242

Chapter 6: Conclusions 244
6.1 Literature Cited 254

LIST OF FIGURES

Figure Page

Figure 1.1: Douglas-fir trees exhibiting symptoms of Swiss needle cast including chlorosis (yellow-brown foliage), and thin crowns resulting from premature foliage loss 42

Figure 1.2: Maps showing correspondence between the *Picea sitchensis* vegetation zone in Oregon and Washington and the spatial distribution of Swiss needle cast (SNC) severity 43

Figure 1.3: Ascocarps (pseudothecia) of *Nothophaeocryptopus gaeumannii* cause Swiss Needle Cast (SNC) by blocking the stomata in Douglas-fir needles 44

Figure 1.4: Phylogenetic tree from Winton et al. (2007b) based on combined SSU and LSU sequences placing *Phaeocryptopus gaeumannii* (marked with a star) in the Mycosphaerellaceae and *P. nudus* in Dothideales. 45

Figure 1.5: A portion of the phylogenetic tree from Schoch et al. (2009) based on a combined LSU, SSU, TEF1, RPB1 and RPB2 sequence dataset showing placement of *P. gaeumannii* (marked with a star) in the Mycosphaerellaceae, supporting the findings of Winton et al. (2007b). 46

Figure 1.6: A portion of the phylogenetic tree presented in Videira et al. (2017) based on an alignment of LSU, RPB2, and ITS, which placed the former *P. gaeumannii* in the new genus *Nothophaeocryptopus* (marked with a star). 47

Figure 2.1: Maps showing the geographic locations of each site from which Douglas-fir foliage was sampled for isolation of *Nothophaeocryptopus gaeumannii* 85

Figure 2.2: Distributions of two *Nothophaeocryptopus gaeumannii* lineages in A) 24 sites in western Oregon (overlapping pie charts were pooled for two sites), B) 11 sites in western Washington 87

Figure 2.3: Bar plots showing the abundances of *Nothophaeocryptopus gaeumannii* SSR genotypes (MLGs) that were shared between A) Oregon and Washington, B) sites within Oregon, C) sites in Washington 89

Figure 2.4: Estimates of the standardized multilocus index of association (r_d) (Agapow and Burt, 2001) based on SSR genotypes from *Nothophaeocryptopus gaeumannii* isolates collected in Oregon and Washington 93

LIST OF FIGURES (Continued)

Figure Page

Figure 2.5: A) Bar plot from discriminant analysis of principal components (DAPC) showing posterior membership probabilities of 663 *Nothophaeocryptopus gaeumannii* genotypes (MLGs) in clusters representing Oregon (OR) and Washington (WA), from a clone-censored dataset including MLGs from 35 sites. B-G) DAPC scatterplots showing differentiation among the coastal and inland sites within each sampling block 96

Figure 2.6: UPGMA dendrogram from bootstrap analysis of Nei's genetic distance showing divergence between genotypes corresponding to two *Nothophaeocryptopus gaeumannii* lineages from Oregon and Washington (clone-censored, N = 663). Node labels represent bootstrap statistics (≥ 70%) from 10,000 replicate trees. 97

Figure 2.7: Bar plot showing the numbers of SSR multilocus genotypes of *Nothophaeocryptopus gaeumannii* recovered from 150 Douglas-fir trees in Oregon and Washington 98

Figure 2.8: UPGMA dendrograms from bootstrap analyses of Nei's genetic distance for *Nothophaeocryptopus gaeumannii* genotypes isolated from individual Douglas-fir needles from western Washington sites 99

Figure S2.1: Genotype accumulation curve showing the number of *Nothophaeocryptopus gaeumannii* multilocus SSR genotypes (MLGs) from the Oregon and Washington dataset observed in 1,000 random samples with numbers of loci ranging from 1 to *n*-1. 100

Figure S2.2: Rarefaction curve showing the observed genotypic richness in *Nothophaeocryptopus gaeumannii* Lineages 1 and 2 from Oregon and Washington samples 101

Figure 3.1: Locations of 32 sampling sites from which foliage was collected for isolation of *Nothophaeocryptopus gaeumannii* in New Zealand 130

Figure 3.2: Estimates of the unbiased index of association (r_d) (Agapow and Burt, 2001) based on SSR genotypes from *Nothophaeocryptopus gaeumannii* isolates collected in New Zealand 134

LIST OF FIGURES (Continued)

Figure Page

Figure 3.3: A) Bar plot from discriminant analysis of principal components (DAPC) showing posterior membership probabilities of 468 *Nothophaeocryptopus gaeumannii* genotypes (MLGs) in clusters representing the North (N) and South (S) Islands of New Zealand. B) DAPC scatterplot showing clustering among multilocus genotypes (MLGs) from 32 sites 135

Figure 3.4: UPGMA dendrogram from a bootstrap analysis of Nei's genetic distance showing divergence among *Nothophaeocryptopus gaeumannii* multilocus genotypes (MLGs) corresponding to two lineages from New Zealand (clone-censored, $N = 468$). Node labels represent bootstrap statistics (≥ 70%) from 10,000 replicate trees. 136

Figure 3.5: Bar plot showing the abundances of four *Nothophaeocryptopus gaeumannii* Lineage 2 SSR genotypes (MLGs) at six sites in the North and South Islands of New Zealand 137

Figure S3.1: Genotype accumulation curve for *Nothophaeocryptopus gaeumannii* in New Zealand, with the vertical axis showing the observed number of multilocus genotypes (MLGs), and the horizontal axis showing the numbers of SSR loci for which 1,000 random samples were selected without replacement 138

Figure S3.2: Genotypic richness curves with horizontal axes showing the numbers of *N. gaeumannii* isolates, and vertical axes showing the numbers of expected MLGs from A) Lineage 1, and B) Lineage 2. 139

Figure S3.3: Abundances of the 60 *Nothophaeocryptopus gaeumannii* SSR genotypes (MLGs) shared between the North (N) and South (S) Islands of New Zealand 140

Figure 4.1: Locations from which Douglas–fir foliage was sampled for the isolation of *Nothophaeocryptopus gaeumannii*. 175

Figure 4.2: UPGMA dendrogram from a bootstrap analysis of Nei's genetic distance among multilocus SSR genotypes from 1,260 *Nothophaeocryptopus gaeumannii* isolates collected from five regions that included nine countries 179

Figure 4.3. Scatterplot from discriminant analysis of principal components (DAPC) showing clustering among *Nothophaeocryptopus gaeumannii* Lineage 1 genotypes from a clone–censored dataset, with clusters representing the five regions from which samples were collected. 182

LIST OF FIGURES (Continued)

Figure Page

Figure 4.4: A) Scatterplot from discriminant analysis of principal components (DAPC) with clusters representing the five countries in Europe from which *Nothophaeocryptopus gaeumannii* was sampled. B) Bar plot from DAPC showing the probability of membership for each isolate in each of five clusters representing the countries from which *N. gaeumannii* was sampled in Europe 183

Figure 4.5: Scatterplot from DAPC with clusters representing the six states in the U.S. from which *Nothophaeocryptopus gaeumannii* was sampled 184

Figure 4.6: Graphical representation of the demographic scenario with the highest posterior probability from the preliminary *DIYABC* analysis. 185

Figure 4.7: Graphical representation of the demographic scenario with the highest posterior probability from the final *DIYABC* analysis 186

Figure S4.1: Genotype accumulation curve showing the number of *Nothophaeocryptopus gaeumannii* multilocus SSR genotypes (MLGs) from the global dataset observed in 1,000 random samples of *n*-1 loci sampled without replacement. 188

Figure S4.2: Fifteen *DIYABC* scenarios designed to test hypotheses about the evolutionary and geographic origin(s) of the *Nothophaeocryptopus gaeumannii* populations in Europe (EU), North America (NA), Australia (AUS), and New Zealand (NZ) 191

Figure S4.3: Principal components analysis (PCA) from the preliminary *DIYABC* analysis (Figures 4.6, S4.2) showing how well the summary statistics calculated from the observed dataset (yellow point) fit with the summary statistics calculated from simulated datasets 194

Figure S4.4: Sixteen *DIYABC* scenarios designed to test hypotheses about the evolutionary and geographic origin(s) of the invasive *Nothophaeocryptopus gaeumannii* population in Chile 197

Figure S4.5: Principal components analysis (PCA) from the final *DIYABC* analysis (Figures 4.7, S4.4) showing how well the summary statistics calculated from the observed dataset (yellow point) fit with the summary statistics calculated from simulated datasets 200

LIST OF FIGURES (Continued)

Figure Page

Figure 5.1: Swiss needle cast aerial survey maps (Ramsey et al., 2015; Ritóková et al., 2016) with pie charts showing the geographic distributions of *Nothophaeocryptopus gaeumannii* Lineage 1 (white) and Lineage 2 (black) in A) 24 sites in western Oregon (for two of the pie charts, data from adjacent sites were pooled to avoid overlap), and B) 11 sites in western Washington. 235

Figure 5.2: The relationships between distance from the coast (km) and A) the relative proportion of isolates corresponding to *Nothophaeocryptopus gaeumannii* Lineage 2, B) average foliage retention (AFR) (%), and C) the colonization index (i.e. the average proportion of stomata occluded by *N. gaeumannii* pseudothecia). D) The relationship between the relative proportion of Lineage 2 and average foliage retention when the distance from the coast (a major confounding variable) is not taken into account.... 237

Figure 5.3: The relationship between average foliage retention (AFR) (%) and the relative proportion of *Nothophaeocryptopus gaeumannii* Lineage 2, after accounting for distance from the coast. 238

Figure 5.4: The relationship between average foliage retention (AFR) (%), estimated for ten Douglas-fir trees from each of the 34 sites, and the colonization index (CI), an estimate of the average percentage of stomata occluded by pseudothecia of *Nothophaeocryptopus gaeumannii*. 239

Figure 5.5: Non-metric multidimensional scaling (NMDS) ordination based on the genetic distances between 33 sample sites calculated from multilocus SSR genotypes of *Nothophaeocryptopus gaeumannii* isolates 240

Figure S5.1: Diagnostic plots for the linear model of average foliage retention as a function of the relative proportion of *Nothophaeocryptopus gaeumannii* Lineage 2 and distance from the coast (km) 242

Figure S5.2: Stress plot from the non-metric multidimensional scaling ordination (NMDS) based on the genetic distances between sites from which *Nothophaeocryptopus gaeumannii* isolates were collected 243

LIST OF TABLES

Table Page

Table 1.1: Summary of studies that have investigated the relationships between Swiss needle cast (SNC) and climate. 48

Table 2.1: Sample sizes and diversity estimates for the two *Nothophaeocryptopus gaeumannii* lineages. 82

Table 2.2: Sample sizes and diversity estimates for the 35 sites in Oregon and Washington from which *Nothophaeocryptopus gaeumannii* isolates were collected for this study. 83

Table 2.3: Pairwise geodesic distances between sites in Oregon and Washington with shared *Nothophaeocryptopus gaeumannii* multilocus genotypes (MLGs). 90

Table 2.4: Analysis of molecular variance (AMOVA) showing the partitioning of genetic variance and estimates of differentiation among *Nothophaeocryptopus gaeumannii* subpopulations. Isolates clone-censored, $N_{isolates}$ = 663. 92

Table 3.1: Sample sizes and diversity estimates for the *Nothophaeocryptopus gaeumannii* isolates collected from 32 sites in the North and South Islands of New Zealand. 131

Table 3.2: Hierarchical analysis of molecular variance (AMOVA) performed with clone-corrected dataset including unique SSR multilocus genotypes from 468 *Nothophaeocryptopus gaeumannii* isolates collected from 32 sites in the North and South Islands of New Zealand. 133

Table 4.1: Estimates of genetic diversity for native and introduced *Nothophaeocryptopus gaeumannnii* populations worldwide. 176

Table 4.2: Allelic richness for nine microsatellite loci (Winton et al., 2007) across nine countries from which *Nothophaeocryptopus gaeumannii* was sampled for this study. All calculations were performed with rarefaction sample sizes of 10 isolates. 177

Table 4.3: Analysis of molecular variance (AMOVA) table showing genetic variation and estimates of differentiation among *Nothophaeocryptopus gaeumannii* populations from a hierarchical sampling of 14 subpopulations covering nine countries and five regions. Samples are from a clone-censored dataset. 178

Table 4.4: Estimates of population differentiation (G'_{ST}) (Hedrick, 2005) for the five regions from which Douglas–fir foliage was sampled for isolation of *Nothophaeocryptopus gaeumannii* 180

LIST OF TABLES (Continued)

Table Page

Table 4.5: Estimates of population differentiation (G'_{ST}) (Hedrick, 2005) between each of the fourteen regional *Nothophaeocryptopus gaeumannii* subpopulations. 181

Table S4.1: Summary of locus characteristics for the SSR markers used to genotype *Nothophaeocryptopus gaeumannii* isolates for this study. 187

Table S4.2: Prior distributions and analysis parameters for the preliminary *DIYABC* analysis of *Nothophaeocryptopus gaeumannii* populations in North America, New Zealand, Europe, and Australia (Figures 4.6, S4.2). 192

Table S4.3: Posterior prob. and 95% confidence intervals for the 15 scenarios from the preliminary *DIYABC* analysis of *Nothopaeocryptopus gaeumannii* populations in North America, New Zealand, Europe, and Australia (Figures 4.6, S4.2). 193

Table S4.4: Prior distributions and analysis parameters for the final *DIYABC* analysis (Figures 4.7, S4.4). 198

Table S4.5: Posterior probabilities and 95% confidence intervals for the 16 scenarios from the final *DIYABC* analysis that included the South American *Nothophaeocryptopus gaeumannii* population (Figures 4.7, S4.4). 199

Table 5.1: Site variables, sample sizes, and disease severity estimates for the 35 sites from which Douglas-fir foliage was collected for isolation of *Nothophaeocryptopus gaeumannii*. 230

Table 5.2: Summary of variations in geographic, disease, and environmental variables across the 35 sites in Oregon and Washington from which Douglas-fir foliage was sampled for isolation of *Nothophaeocryptopus gaeumannii*. 233

Table 5.3: Pearson's correlation coefficients (*r*) for the relationships between each of the environmental and geographic variables used for this study. Numbers in parentheses represent computed P-values for the correlation coefficient..... 236

Table 5.4: Environmental, geographic, and disease variables used in the joint-plot for the NMDS analysis based on the genetic distance *Nothophaeocryptopus gaeumannii*. . 241

Chapter 1. Introduction

1.1 Swiss Needle Cast (SNC)

Swiss needle cast (SNC) is an economically and ecologically important disease of Douglas-fir (*Pseudotsuga menziesii* (Mirb.) Franco) caused by the ascomycete *Nothophaeocryptopus (=Phaeocryptopus) gaeumannii* (T. Rohde) Videira, C. Nakash., U. Braun & Crous. Several key symptoms characterize the disease, the most prominent of which are chlorosis (the progressive yellowing of foliage) and defoliation that results in sparse canopies (Figure 1.1). Occlusion of stomata by the pseudothecia of *N. gaeumannii* results in inhibition of gas exchange and CO_2 assimilation in the needle, causing premature needle abscission (Manter et al., 2000, 2003). The loss of foliage severely reduces the photosynthetic capacity of the tree resulting in reduced height and diameter growth (Maguire et al., 2002, 2011; Manter et al., 2003). The physiological stress and defoliation caused by SNC does not usually kill the host tree, as even the most severely diseased trees still possess the current year's foliage (Hansen et al., 2000; Maguire et al., 2002).

1.1.1 Global distribution

The current distribution of *N. gaeumannii* in Eurasia, Australasia, and South America, is a product of the desirability of Douglas-fir as a timber species. Wherever Douglas-fir has been introduced around the world, reports of SNC have followed (Watt et al., 2011). In the decades following the first report of SNC in Switzerland in 1925 (Gaeumann, 1930), the spread of *N. gaeumannii* across Europe was well documented. The fungus was reported from England and Ireland in 1927 and 1928, respectively (Boyce, 1940; Liese, 1939; Wilson and Waldie, 1928). In 1939, it was reported that 20-

to 30-year-old Douglas-fir trees of the coastal variety that were planted in Ireland had been infected for at least 10 years and were "…badly attacked by the fungus" (Liese 1939). These trees were so severely diseased that the future development of the stands was questioned (Liese, 1939). Douglas-fir needle cast phenomena were later reported from Germany in 1931 (Rhode, 1937), Austria in 1937, and Denmark in 1939 (Boyce, 1940). These outbreaks were presumably caused by the same pathogen as that responsible for the disease reported from Switzerland in 1925. It was suspected that the fungus was spread to these locations from Switzerland via windblown spores that dispersed in the spring and summer when strong southwest winds were known to occur in this region (Boyce, 1940). In addition to these early reports of SNC in Europe, a more recent compilation of disease records indicated that the presence of *N. gaeumannii* has been confirmed in Belgium, Bulgaria, Czech Republic, Finland, Hungary, Italy, Latvia, Netherlands, Portugal, Romania, Scotland, Slovenia, Sweden and Wales (Watt et al., 2011).

The earliest known presence of *N. gaeumannii* in the United States was reported by Boyce (1940) who examined Douglas-fir foliage he had collected in Oregon from Josephine and Lane Counties in 1916 and 1921, respectively, and Shasta County, California in 1923. On these Douglas-fir needles he found pseudothecia of *N. gaeumannii* that had previously gone unnoticed due to the presence of *Rhabdocline pseudotsugae* on the same foliage. This finding serves as the strongest evidence that *N. gaeumannii* was present in North America prior to the first reports of disease from Europe, suggesting that it existed in this region long before the recognition of SNC as a damaging forest

pathogen. Boyce (1940) concluded that *N. gaeumannii* was likely native to western North America and proposed that the fungus had been introduced along with Douglas-fir to the northeastern U.S. and Europe where it became a damaging pathogen due to a combination of conducive climate and increased susceptibility of the host in non-native plantings.

Swiss needle cast was first reported in the United States in 1938 at a plantation of Douglas-fir trees in Connecticut, where trees were described as being badly damaged and nearly dead (McCormick, 1939). However, *N. gaeumannii* was apparently present in this area before 1929, because the fungus was present on needles from the 1928 cohort in the original collection from this plantation (McCormick, 1939). Later reports confirmed the presence of the fungus in Rhode Island, Massachusetts, Vermont, New Hampshire, and Maine (Boyce, 1940). It was also reported that "…a very scant infection…" had been found on the 1936, 1937, and 1938 needle cohorts in a Douglas-fir plantation in New York state in 1940 (Hahn, 1941).

There was a reported outbreak of SNC in Michigan and Wisconsin in 1969, where trees exhibited defoliation and foliage discoloration that was attributed to the presence of *N. gaeumannii* (Morton and Patton, 1970). Though the extent of the disease in this area was not known at the time, it would prove to be insignificant given that Douglas-fir was only grown infrequently as a Christmas tree or nursery ornamental (Morton and Patton, 1970). In 1973, SNC was reported for the first time in Pennsylvania where Douglas-fir Christmas trees had pseudothecia of *N. gaeumannii* on 1- and 2-year-old needles, and most of the 2-year-old needles had been shed (Merrill and Longnecker, 1973). At the

time, this was the southernmost known distribution of SNC in the eastern United States (Merrill and Longnecker, 1973).

The first systematic survey for *N. gaeumannii* along the west coast of the United States occurred in 1939 (Meinecke, 1939). The Swiss needle cast fungus was not found along the western coast of California but was abundant at many of the sites surveyed west of the Cascades in Oregon, and was also found in abundance at Port Angeles, Washington and on Vancouver Island, B.C. (Meinecke, 1939). The distribution of the fungus in this region was not accompanied by any appreciable damage to the host, an observation interpreted as evidence that the fungus was indigenous to the coastal northwestern United States (Boyce, 1940; Meinecke, 1939). There were also several unpublished reports of the disease occurring in the southwestern states including New Mexico, where defoliation due to SNC was reported, and Arizona where the fungus was observed but no defoliation had occurred (Hahn, 1941).

The first report of *N. gaeumannii* in New Zealand occurred in 1959 near Taupo in the central North Island (Hood and Kershaw, 1975; Hood et al., 1990). An intensive survey of the Douglas-fir plantations in the area found that the distribution of the fungus was confined to a radius of approximately 80 miles around the site where it was initially detected (Hood and Kershaw, 1975). At that time, no symptoms of SNC were observed (Hood and Kershaw, 1975). Although the first records of *N. gaeumannii* in New Zealand were not associated with disease, over the following decades the spread of *N. gaeumannii* throughout New Zealand, and the intensification of SNC severity, was monitored closely (Hood et al., 1990; Hood and Kershaw, 1975; Hood and Sandberg, 1979; Kimberley et

al., 2011; Stone et al., 2007; Watt et al., 2011, 2010). By 1989, the fungus and its associated disease symptoms had been observed throughout the Douglas-fir growing regions in the North and South Islands in New Zealand (Kimberley et al., 2011).

In 1974, SNC was reported from Australia where Douglas-fir plantations northeast of Melbourne exhibited severe defoliation and the author noted that pseudothecia of *N. gaeumannii* were very abundant (Marks, 1975). It is unclear whether this represented the first report for Australia, as there were some prior reports of the presence of *N. gaeumannii* in Tasmania that could not be verified (Marks, 1975). The initial outbreak of SNC was considered quite significant, given that Douglas-fir was the second-most widely planted and highly valued timber species in Australia (Marks, 1975).

SNC has been reported recently from eastern Turkey, where Douglas-fir is grown in timber plantations, nurseries, and arboreta (Temel et al., 2003). In Chile, where Douglas-fir is an economically important timber plantation species along with radiata pine (*Pinus radiata*), Swiss needle cast was apparently not observed until 2006 (Osorio, 2007). Recently, an outbreak of the disease was reported from Spain where Douglas-fir is grown as a plantation timber species in the mountainous regions in the northeast (Castaño et al., 2014). In each of these locations, moderate to severe symptoms of SNC were reported. In Spain, the presence of the fungus was apparently reported as early as 2003, but there was no apparent disease prior to the most recent report (Castaño et al., 2014).

1.1.2 Emergence in western Oregon and Washington

Since the surveys for *N. gaeumannii* in the early 20th century, SNC has emerged as a significant forest health problem in western Oregon and Washington. Prior to the late

1970's SNC had not caused any serious damage in Pacific Northwest forests (Hansen et al., 2000). In Oregon and Washington the first serious outbreaks of disease associated with *N. gaeumannii* were reported from Christmas tree plantations (Hadfield and Douglass, 1982; Michaels and Chastagner, 1984). At that time there was apparently a stark contrast between Christmas tree plantations and forestry plantations, as *N. gaeumannii* caused severe defoliation in the former and was considered innocuous in the latter (Hadfield and Douglass, 1982; Hansen et al., 2000). However, in the 1980s symptoms of SNC began to emerge in young forest plantations in western Washington and further south in Oregon, where particularly severe disease was observed near Tillamook, Newport, and Waldport (Hansen et al., 2000). About a decade later, it became clear that SNC was emerging as a significant disease in these young coastal Douglas-fir plantations. Its abundant proliferation and subsequent emergence as a threat to Douglas-fir forest health and productivity in western North America is thought to have been perpetuated by the widespread planting of Douglas-fir where the climate is particularly conducive to disease in a narrow band of low-elevation coastal forests along the western slopes of the Coast Ranges in Oregon and Washington that has historically been considered the *Picea sitchensis* vegetation zone (Franklin and Dyrness, 1973; Hansen et al., 2000) (Figure 1.2). As of 2016, nearly 221,000 ha of Douglas-fir forest in Oregon, and an additional 100,000 ha in Washington, showed moderate or severe symptoms of SNC (Navarro and Norlander, 2016; Ramsey et al., 2015). Given that SNC can cause volume growth losses in excess of 50% annual increment (Maguire et al., 2002), it could result in an estimated loss of up to 190 million board feet of timber per year in the

Oregon Coast Range (Kanaskie et al. 2014). Lost productivity due to SNC in managed Douglas-fir forests is estimated to have resulted in annual losses of $128 million in tax, labor, and job revenue in Oregon alone (Kanaskie et al. 2014).

1.1.3 Measurement of SNC severity

Because disease severity is proportional to the percentage of stomata occluded by pseudothecia of *N. gaeumannii*, quantification of SNC generally includes estimates of incidence (the proportion of needles with stomata occluded by pseudothecia), pseudothecia density (the proportion of stomata occluded by pseudothecia) and foliage retention (the proportion of needles remaining across several needle age-classes on a given Douglas-fir branch) (Hansen et al., 2000; Ritóková et al., 2016; Shaw et al., 2014; Watt et al., 2011, 2010). Foliage retention is often reported as the number of years of foliage remaining (Maguire et al., 2011; Ritóková et al., 2016; Shaw et al., 2014; Weiskittel et al., 2006), but may also be reported as the average percentage of foliage remaining across several needle age classes (Manter et al., 2003b; Temel et al., 2004; Watt et al., 2010, 2011). A colonization index (*CI*), which is an estimate of the average percentage of stomata occluded by pseudothecia in a given needle cohort, is also often used as an SNC severity metric (Manter et al., 2003; Watt et al., 2010). Attempts to correlate the proportion of stomata occluded by pseudothecia with foliage retention (Manter et al., 2003a, Temel et al., 2004) have varied in their success, as these relationships are complex due to the differential abilities of different Douglas-fir genotypes to tolerate stomatal occlusion (Temel et al. 2004, Zhao et al. 2015). Because of

this variation in tolerance, the abundance of pseudothecia may not have a direct negative linear relationship with foliage retention.

Because the proportion of occluded stomata in needles increases annually until needles are shed, defoliation due to SNC occurs primarily in needles in older age classes (Hansen et al., 2000). Typically, healthy Douglas-fir of the coastal variety in western Oregon retain needles for four years (Hansen et al., 2000; Maguire et al., 2002). It has been estimated that severely diseased trees may lose 56% of 4-year old foliage, and up to 99% of the foliage aged 5 years or greater (Weiskittel et al., 2006). A tree with severe SNC experienced an average reduction in total foliage mass of 27% when compared to a tree with less severe disease (Weiskittel et al., 2006).

Major reductions in height and diameter growth of diseased trees have been attributed to the SNC-associated loss of photosynthetic leaf area and the impairment of gas exchange and CO_2 assimilation in retained foliage. Needle retention is the most widely used index for the projection of growth losses (Black et al., 2010; Maguire et al., 2011; Manter et al., 2003b). By some estimates, reductions in foliage retention of 50 to 75% would equate to growth losses of as much as 25 to 50% net periodic annual increment (PAI; m^3 ha^{-1} yr^{-1}) (Maguire et al., 2011). Severely diseased trees may lose as much as 25% of their expected top-height growth, and up to 52% of their potential cubic volume growth (a combination of height and radial growth estimates) relative to trees with little to no SNC (Maguire et al., 2002). In the most severely diseased stands, basal area growth may be as much as 35% less than that expected in the absence of disease (Maguire et al., 2002). In a study of Douglas-fir growth in New Zealand during the 30

years after *N. gaeumannii* was first detected, similar values of height, diameter, and volume growth losses were reported. Growth rates declined steadily for 20 years with cumulative estimated growth losses of 25% in height, 27% in basal area, and 32% in volume (Kimberley et al., 2011). Volume annual increment growth was reduced from around 40 m^3 ha^{-1} yr^{-1} prior to detection of *N. gaeumannii,* to 30 m^3 ha^{-1} yr^{-1} twenty years later (Kimberley et al., 2011).

Although concern about SNC in natural forests in western North America is relatively recent, dendrochronological analyses suggest that growth reductions due to SNC have been ongoing for centuries, but have been intensifying particularly in the area of Tillamook, Oregon since ca. 1984 (Black et al., 2010; Lee et al., 2013, 2016, 2017). Black et al. (2010) assessed growth of SNC Douglas-fir and compared ring widths to western hemlock (*Tsuga heterophylla*) and found radial growth reductions of up to 85% in severely diseased trees when compared to the non-host species. Many trees near Tillamook, OR experienced locally absent rings, suggesting annual growth rates near 0 for the years with the most severe disease (Black et al., 2010). Relative growth reductions at the lower-elevation Tillamook sites were nearly 90% for the period of 1996-2007 (Black et al., 2010). De-trended chronological growth projections indicate that the impacts of this disease have been increasing in magnitude over the past 50 years (Black et al., 2010).

Dendrochronologies have recently been combined with climate modeling in an attempt to attribute historic growth losses to climate conditions that were conducive for *N. gaeumannii* dispersal and infection. Lee et al. (2013) applied time-series intervention

analysis (TSIA) to assess growth impacts in late-successional Douglas-fir trees. That analysis identified cyclical periods of growth impacts and release dating back as far as the 1590's. In contrast to the assessments of Boyce (1940), and other researchers, that study indicated that the impacts of SNC in native forests were not negligible in the years prior to the current epidemic outbreak in Oregon. Lee et al. (2013) showed that an SNC-induced reduction in annual tree-ring width increment was evident in cores from Douglas-firs in the Cascades, where the fungus is present but disease is generally considered negligible. This suggested that not only is the disease not restricted to the western slopes of the Coast Range, but that mature trees in natural stands are equally susceptible to disease as young trees in coastal plantations (Lee et al., 2013). The cyclical nature of the disease impacts, as observed in these dendrochronologies, strongly suggests that climate is the primary agent influencing disease severity. Both the above studies of tree ring chronologies by Black et al. (2010), and Lee et al. (2013, 2017), describe severe growth suppressions in western Oregon Douglas-fir in the years from 1984-1986. This coincides with reports of foliar damage in plantations near Tillamook, and is widely recognized as the beginning of the SNC epidemic in western Oregon. Trees in the Coast Range as well as the Cascades experienced peak growth reductions of 30-100% during that time period (Black et al., 2010; Lee et al., 2013, 2016, 2017).

1.1.4 Climate and SNC

One aspect of SNC that was particularly puzzling to researchers was that the pathogen appeared to be widely distributed and could be found nearly everywhere that Douglas-fir grew but the abundance of *N. gaeumannii*, and thus disease severity, varied

across the landscape. It has long been suggested that spatial variation in local climate influences SNC severity (Hansen and Stone, 2005). Boyce (1940) suggested that this pathogen that is relatively harmless in its native range may have emerged in the eastern U.S. and Europe because the climates in those locales are more favorable for the development of the fungus. His hypotheses about the relationships between SNC and climate were based on the observation that SNC was more severe in regions where precipitation was generally high during the late spring/early summer spore dispersal period (Boyce, 1940). Hood (1982) noted higher levels of *N. gaeumannii* infection on the western slope of the Coast Range in northwestern Washington and Vancouver Island than on the eastern slope, and found a significant correlation between infection and May-July rainfall in that region. In the Pacific Northwest, the severity of SNC symptoms has a strong geographic trend, with the most severe SNC nearest the coast at low-mid elevations (< 150 m) and on south-facing slopes, and visible symptoms steadily diminishing eastward (Stone et al., 2008b; Rosso and Hansen, 2003; Manter et al., 2005; Hansen et al., 2000).

The spatial variation in *N. gaeumannii* abundance and SNC severity can be attributed, at least in part, to a few specific climatic variables that influence key stages in the development of *N. gaeumannii* or in the infection cycle. The variables that have had the greatest statistical support in SNC severity models are related to winter temperature, spring/summer moisture availability, and summer maximum temperature (Lee et al., 2017; Manter et al., 2005; Rosso and Hansen, 2003; Stone et al., 2008b; Stone et al., 2007; Watt et al., 2011, 2010; Zhao et al., 2012). While Rosso and Hansen (2003)

developed a model that explained geographic variation in SNC severity based on a composite disease rating that included foliage retention, growth reduction, and foliage discoloration, and Zhao et al. (2012) modeled foliage retention as a function of climate, most of the modeling efforts have focused on direct correlations between climate and the abundance of *N. gaeumannii* pseudothecia (Table 1.1). The abundance of the pathogen may be a more direct measure of disease given that quantification of pseudothecia is less subjective than visual estimates of crown sparseness and foliage coloration, and because pathogen abundance is directly correlated with SNC severity.

Mean winter temperature is strongly correlated with disease severity, presumably due to the influence of temperature on fungal growth rates (Capitano, 1999; Manter et al., 2005; Stone et al., 2008a). Cold winter temperatures are likely to inhibit the development of pseudothecia (Manter et al., 2005), thereby decreasing the severity of SNC symptoms in the following year (Lee et al., 2017; Stone et al., 2008b, 2007; Zhao et al., 2012, 2011). Models that included a winter temperature variable have explained approximately 57–80% of the observed variation in pseudothecia abundance, when combined with spring/early summer moisture variables and/or summer maximum temperatures (Coop and Stone, 2010; Manter et al., 2005; Stone et al., 2007; Watt et al., 2010).

Variables relating to spring and summer moisture availability that have been used in predictive SNC modeling include precipitation, dew point deficit, vapor pressure deficit, and fog occurrence (Table 1.1). Spring and early summer moisture is required for the dispersal of ascospores from pseudothecia, and moisture is necessary for the adherence and germination of ascospores on the surfaces of needles (Lee et al., 2017;

Manter et al., 2005; Stone et al., 2008b; Watt et al., 2011). Summer temperatures are important components of SNC models because high temperatures likely inhibit fungal growth (Capitano, 1999; Rosso and Hansen, 2003). On the other hand, cooler summer temperatures in coastal Pacific Northwest forests, where fog is prevalent during the summer months, are likely to promote the growth of *N. gaeumannii* (Rosso and Hansen, 2003).

Recent climatic shifts have made the coastal Douglas-fir forests of the Pacific Northwest more favorable for *N. gaeumannii* colonization and proliferation (Lee et al., 2017; Stone et al., 2008b). This change in climate, along with changes in forest management, may have contributed to the recent intensification of SNC in this region (Hansen et al., 2000; Lee et al., 2017; Stone et al., 2008b). Local increases in winter temperature and spring precipitation due to climate change are likely to result in an expansion in the area affected by SNC, and lead to an intensification of SNC in affected areas (Coop and Stone, 2010; Lee et al., 2017; Stone et al., 2008b).

1.1.5 Ecological Interactions

Franklin and Dyrness (1973) recognized a distinct forest community type, the *Picea sitchensis* vegetation zone, that exists in a narrow band from northern California to southern Alaska. It is in this narrow band of temperate coastal forest along the western slopes of the Oregon Coast Range that defoliation due to SNC has been most pronounced (Figure 1.2). This vegetation zone consists primarily of *Tsuga heterophylla* and *Picea sitchensis* as dominant early seral species, with Douglas-fir as a much less common component of the natural forest composition (Franklin and Hemstrom, 1981; Franklin and

Dyrness, 1973). This zone merges into the adjacent *Tsuga heterophylla* zone further inland, where Douglas-fir is the dominant early seral species of the natural vegetation community (Franklin and Hemstrom, 1981). In recent decades, forest managers have increasingly established commercial forest plantations composed predominantly of young Douglas-fir, due to its higher value and normally fast growth, on sites within in the *Picea sitchensis* vegetation zone (Hansen et al., 2000). The current SNC epidemic is likely a result of increased abundance of *N. gaeumannii* far above endemic levels due to increased density of the susceptible host in an environment that is highly conducive to SNC (Hansen et al., 2000; Shaw et al., 2011; Stone et al., 2008b).

The needle loss and reduced growth caused by this fungus can have profound impacts on forest ecology. Where foliage retention is particularly low, net carbon assimilation in the Douglas-fir canopy is reduced, thus limiting primary productivity (Manter et al., 2003). The impacts of SNC also alters carbon dynamics at the stand-level due to its effects on litterfall dynamics and nutrient cycling (Weiskittel and Maguire, 2007). Though it is generally accepted that Douglas-fir has the ability to out-compete western hemlock (*Tsuga heterophylla*) due to faster growth rate in coastal northwest forests, reductions in Douglas-fir foliage retention and growth rate due to SNC make it a poor competitor where the disease is severe (Lee et al., 2017; Stone et al., 2008b; Zhao et al., 2014). In the coastal *Picea sitchensis* vegetative zone, where environmental conditions are most favorable for growth and reproduction of *N. gaeumannii*, Douglas-fir may be at a competitive disadvantage due to the effects of defoliation due to SNC on growth (Lee et al., 2017; Stone et al., 2008b). In fact, Stone et al. (2008b) hypothesized

that SNC may be responsible for the scarcity of naturally-occurring dominant Douglas-fir stands in this region.

The reduction in whole-canopy carbon assimilation due to *N. gaeumannii* colonization could also contribute to the ever-increasing atmospheric concentration of CO_2, an important greenhouse gas that contributes to climate change. Based on the estimates of growth losses of 23-50% due to SNC reported by (Maguire et al., 2002), Manter et al. (2003a) estimated that whole canopy A_{net} could be reduced by as much as 34.6 kg/CO_2/tree/year compared to a healthy tree. With approximately 364,000 ha of symptomatic Douglas-fir forest in Washington and Oregon, this could potentially result in a total regional reduction in carbon assimilation totaling 3 million metric tons, assuming 250 trees/ha (Manter et al., 2003). This suggests that a microscopic fungus, *N. gaeumannii*, is capable of causing a major disruption of forest carbon dynamics that could contribute to climate change (Manter et al., 2003). A feedback mechanism may exist by which climate change leads to an increase in SNC incidence and severity, thus causing further climate warming by diminishing the capacity of Douglas-fir forests to assimilate carbon from the atmosphere.

1.1.6 SNC Management

The adverse effects of *N. gaeumannii* infection on needle retention and growth rate can be temporarily suppressed with the use of chemical fungicides such as chlorothalonil, which is the standard practice for disease management in Christmas tree farms, and also reduces the abundance of the pathogen in young forest stands (Chastagner and Stone, 2001; Manter and Kavanagh, 2003; Stone et al., 2007). In one study of its

effectiveness as a treatment for SNC, severely infected trees were treated with chlorothalonil for five consecutive years and showed significantly higher foliage retention and lower pseudothecia abundance than the untreated controls (Stone et al., 2007). This effect was short-lived, however, and the SNC severity returned to pretreatment levels just two years after the cessation of fungicide treatment (Stone et al., 2007). While fungicidal suppression of SNC impacts with chlorothalonil or elemental sulfur may be a viable option for small-scale Douglas-fir Christmas tree farms and young timber plantations, managing SNC at larger scales with this method is not economically feasible (Stone et al., 2007).

The effects of silvicultural strategies, including thinning and fertilization, on the development and severity of SNC have been the foci of several disease management studies. According to Hood and Sandberg (1979), there was some evidence to suggest that Douglas-fir stands with SNC in New Zealand would respond well to thinning, though their study found that there was little effect on the abundance of pseudothecia in the foliage of the remaining trees (Hood and Sandberg, 1979). Later studies in the U.S. also found that there was no association between thinning and SNC severity (Mainwaring et al., 2005). One study that examined the relationship between SNC severity and fertilization seemed to suggest that the increased foliar nitrogen content resulting from the application of nitrogenous fertilizers was associated with increased abundance of pseudothecia (El-Hajj et al., 2004), but a later study that included larger sample sizes and applied nitrogen fertilizers at rates that were more practical for Douglas-fir management

found little effect on foliar nitrogen and no association between fertilization and SNC severity (Mulvey et al., 2013).

Still the least studied and most promising SNC management strategy is the development of resistant or tolerant seed stock. Significant variation in the host response to infection has been noted by many authors (Boyce, 1940; Mcdermott and Robinson, 1989; Nelson et al., 1989; Temel, 2002; Temel et al., 2004). Although there is no resistance to fungal colonization of needles (i.e. all Douglas-fir trees are susceptible), there is some genetic variation in tolerance, whereby some Douglas-fir seed sources are able to retain their foliage despite their stomata being occluded by pseudothecia (Temel et al., 2004). The most tolerant individuals in many studies are sourced from populations growing in environments that are very conducive to SNC, and have presumably co-evolved with *N. gaeumannii*. Breeding for SNC tolerance should be explored further as a method of cultural control for SNC.

1.2 The Douglas-fir Swiss Needle Cast Fungus *Nothophaeocryptopus gaeumannii* (T. Rohde) Videira, C. Nakash., U. Braun & Crous

The ascomycete *Nothophaeocryptopus gaeumannii* (Dothideomycetes, Mycosphaerellaceae) is an obligate parasite of Douglas-fir and is the causal agent of Swiss needle cast. This fungus produces darkly-pigmented melanized hyphae and black globose ascocarps (pseudothecia) that emerge through stomata (Stone et al., 2008a) (Figure 1.3). The ascopores are two-celled, hyaline and ellipsoidal, approximately 13µm long, and disperse via rain splash and wind to adjacent trees or to foliage lower in the canopy on the same tree. Germination occurs via the formation of two hyaline polar germ

tubes that become melanized shortly after germination (Stone et al., 2008a). Sporulation has not been observed in cultures of *N. gaeumannii*, and asexual (conidial) reproduction is not known to occur in this species (Stone et al., 2008a).

1.2.1 Infection biology

Ascospores are likely the sole source of inoculum for new infections, as there is no known anamorph, or conidial morph, of *N. gaeumannii* (Stone et al., 2008a). The spore dispersal period begins when the pseudothecia mature in late spring and continues until mid-summer. This process coincides with bud break and shoot elongation in the host, as infection occurs only in the first growing season during needle emergence and expansion (Chastagner and Byther, 1983; Hood and Kershaw, 1975). Ascopores are dispersed by wind and rain splash to the surfaces of Douglas-fir needles where, following germination, appressoria are formed near the openings of stomata (Stone et al., 2008a). An elongated hyphal cell, or penetration peg, extends through the guard cells and enters the stomatal chamber (Stone et al., 2008a). Vegetative hyphae colonize the intercellular spaces between mesophyll cells but have not been observed penetrating cell walls (Stone et al., 2008a). Although this fungus does not form haustoria, the specialized structures with which many biotrophic fungal plant pathogens interface with host cells, some hyphae are closely appressed to the surfaces of mesophyll and palisade cells and likely serve as the site of nutrient exchange between host and fungus (Stone et al., 2008a).

The processes of intercellular and epiphytic colonization continue through fall and winter following infection. Pseudothecial initials also begin to form in the sub-stomatal chambers during this time and emerge through stomata in the spring and early summer of

the year following infection (Stone et al., 2008a). Hyphae associated with the developing pseudothecia may emerge from the periphery of stomatal openings to form epiphytic hyphal networks and secondary appressoria with which to penetrate additional stomata (Manter et al., 2003; Stone et al., 2008a). Colonization of the needle may continue for several years with successive rounds of pseudothecia formed each year, thus increasing the proportion of stomata occluded each year after initial infection until the needle is abscised (Manter et al., 2005). Due to the perennial and cumulative nature of the infection, the incidence and severity of SNC in current-year foliage is likely a function of disease severity in the previous year (Manter et al., 2005).

1.2.2 Mechanisms of pathogenicity

While *N. gaeumannii* can remain asymptomatic in Douglas-fir foliage for several years, it can also cause severe damage to its host under environmental conditions that favor its growth and sporulation (Manter et al., 2003). However, the presence of *N. gaeumannii* seems inconsequential when it is present at low abundance (Boyce, 1940; Hansen et al., 2000; Stone et al., 2008a). This fungus grows and reproduces only on live foliage, obtaining its carbon from sugars present in the apoplastic fluid around the mesophyll cells (Capitano, 1999; Hansen et al., 2000; Stone et al., 2008a). Although it often behaves like an obligate biotroph, *N. gaeumannii* does not invade host cells or produce haustoria, a signature cellular structure of biotrophic parasites (Stone et al., 2008a). Instead, physiological damage to its host is a consequence of a proliferation of ascocarps, which emerge from stomata on the undersides of needles thereby impeding gas exchange (Manter et al., 2000, 2003; Stone et al., 2008a).

Physical blockage of the stomata by the pseudothecia of *N. gaeumannii*, and the resulting decrease in stomatal conductance is the primary cause of SNC symptoms (Manter et al., 2000, 2003). The inhibition of gas exchange results in reduced rates of carbon assimilation and subsequent disequilibrium in the carbon balance of a needle (Manter et al., 2000, 2003). Carbon assimilation decreases proportionally as the percentage of occluded stomata increases, and heavily colonized needles cannot produce sufficient photosynthates to meet cell metabolic requirements (Manter et al., 2003). Instead of serving as a source of carbon from which the tree could construct sugars and structural carbohydrates, needles with high proportions of occluded stomata become carbon sinks to which the tree must allocate photosynthates to maintain cellular functions (Manter et al., 2003). Consequently, heavily colonized needles are abscised prematurely.

The physiological model described by Manter (2003) suggested that needle abscission should begin when the infected foliage has approximately 25% of its stomata blocked by pseudothecia (the threshold at which carbon assimilation was reduced to 0, based on an estimated annual carbon budget). Hansen et al. (2000) observed that attached needles rarely had more than 51% of the stomata occluded, and suggested this may be the maximum proportion of stomatal occlusion before needle abscission occurs. In a simulation of long-term needle carbon balance, Manter et al. (2003) found an inverse relationship between carbon assimilation and foliage retention when assimilation was greater than 0, and suggested that needle retention declined precipitously in all needle age classes in which the needles were carbon sinks. When gas exchange is impaired over an

extended period, the more common symptoms of SNC such as chlorosis, needle abscission, and growth reduction begin to manifest (Manter et al., 2003).

1.2.4 Taxonomy

Much confusion about the taxonomic placement of the fungus that causes Swiss needle cast has existed since the original genus name for the pathogen, *Adelopus*, was applied to *Asterina nuda* Peck in 1885 (Hahn, 1947). The fungus now known as *N. gaeumannii*, associated with severe defoliation of planted Douglas-fir in Switzerland and Germany, was first named *Adelopus gaeumannii* Rohde (1936). The genus name *Phaeocryptopus* was introduced by Naumov (1914) for a fungus on foliage of *Abies sibirica*. Although Naumov's type specimen apparently has been lost, the illustration of the fungus was accepted by Petrak as evidence that *Adelopus*, including the species *A. nudus* and *A. gaeumannii*, should be considered a synonym of *Phaeocryptous* (Petrak, 1938), which had priority. Hahn (1947), however, disputed the synonymy, noting that the species on Douglas-fir (*N. gaeumannii*) produced only hyaline ascospores, whereas those illustrated by Naumov were slightly pigmented. Furthermore, Naumov's illustrations of *P. abietis* clearly show paraphyses, which are lacking both in *P. nudus* and *N. gaeumannii*. In synonymizing *Adelopus* under *Phaeocryptopus*, Petrak had not examined either the Peck types nor Naumov's material. Although the genus name *Phaeocryptopus* was applied to the fungi on both *Abies* and Douglas-fir foliage, the question of whether they were actually congeneric was not critically evaluated until the late 1990s.

Modern phylogenetic approaches have provided a taxonomic placement of *N. gaeumannii* within the fungal tree of life that more accurately reflects its evolutionary

relationships to other fungi. Winton et al. (2007b) presented two phylogenetic trees- one with the combined small (SSU) and large (LSU) subunits of the nuclear ribosomal DNA (Figure 1.4), and one with the internal transcribed spacer (ITS) region. These trees provided the first evidence that what was then known as *P. gaeumannii* belonged to a different lineage than that of *P. nudus*, and therefore the two should not be considered congeneric (Winton et al., 2007). Furthermore, neither species is closely related to *Venturia inaequalis*, the type species of Venturiaceae, the family in which *N. gaeumannii* was classified at the time (Figure 1.4) (Winton et al., 2007).

Later phylogenetic analyses using sequence data from the (rDNA) SSU and LSU regions, translation elongation factor-1 alpha (TEF1), and the largest and second largest subunit of the RNA polymerase II gene (RPB1 and RPB2) provided further support for its placement in the Capnodiales together with members of the genus *Mycosphaerella s.l.* (Figure 1.5) (Schoch et al., 2009). The latest phylogenetic assessment of this taxonomic grouping was based on combined sequence data from LSU, ITS, and RPB2, and yielded a similar result as the previous analyses, placing this fungus in the Mycosphaerellaceae (Capnodiales) in a clade with the genus *Pallidocercospora* (Figure 1.6) (Videira et al., 2017). These authors proposed the novel genus name, *Nothophaeocryptopus* (with *N. gaeumannii* as the type) to reflect the fact that this fungus is not closely related to other members of the genus *Phaeocryptopus* (Videira et al., 2017).

1.3 Douglas-fir (*Pseudotsuga menziesii* (Mirb.) Franco)

Douglas-fir (*Pseudotsuga menziesii* (Mirb.) Franco) is a major component of native temperate conifer forests in western North America. It is the single most important

commercial tree species in North America, and is more widely planted outside of its native range than any other American tree besides radiata pine (*Pinus radiata*) (Lavender and Hermann, 2014). It is not a "true" fir (i.e. the genus *Abies*), as its common name implies, nor is it closely related to hemlock (*Tsuga spp.*), as its latin name suggests.

The genus *Pseudotsuga* and its closest relative, *Larix*, are divergent lineages in Pinaceae. They are likely the result of a radiation that occurred in this family approximately 135 million years ago during the lower Cretaceous (Lavender and Hermann, 2014). Genetic evidence suggests that this genus first arose in North America where two distinct varieties of *P. menziesii* now occur together with *P. macrocarpa* ("bigcone Douglas-fir), and subsequently migrated around the Pacific Rim to east Asia where several derived species, including *P. gausseni*, *P. japonica,* and *P. sinensis*, occur (Lavender and Hermann, 2014). Although the fossil record suggests that the North American Douglas-fir species *P. menziesii* did not become dominant in western forests until the middle or late Pleistocene, its first appearance in the fossil record was during the Tertiary, approximately 50 mya (Lavender and Hermann, 2014). The two recognized *P. menziesii* varities, *P. menziesii var. menziesii* (coastal Douglas-fir) and *P. menziesii var. glauca* (Beissn.) Franco (interior or Rocky Mountain Douglas-fir), that are found in western North America today are likely the result of a more recent divergence that occurred during the long periods of geographic and genetic isolation imposed by glaciation (Lavender and Hermann, 2014). Fossil evidence suggests that these infraspecific varieties may have evolved as early as the Oligocene, and they are found

together in deposits from Idaho, British Columbia, and Washington from 7,000 ya (Lavender and Hermann, 2014).

The Swiss needle cast fungus, *Nothophaeocryptopus gaeumannii* (T. Rohde) Videira, C. Nakash., U. Braun & Crous), has been reported from *P. macrocarpa* (Vasey) Mayr (bigcone Douglas-fir) and *P. menziesii* (Gadgil, 2005; Hood, 1982; Stone et al., 2008a). However, the occurrence of SNC on *P. macrocarpa* has not been observed in natural stands (Stone et al., 2008a). The two infraspecific varieties of *P. menziesii, P. menziesii var. glauca*, and *P. menziesii var. menziesii* (coastal Douglas-fir) are considered to be the most susceptible.

The current distribution occupied by the two infraspecific varieties reflects their separation during glaciation and expansion following the glacial recession. The ranges of these two varieties overlaps throughout central and western British Columbia, and may exist as far north as the 55th parallel (Lavender and Hermann, 2014). The western half of this distribution represents the range of *P. menziesii var. menziesii,* and forms a contiguous band throughout the low-elevation forests of western Oregon and Washington, with the Cascade Range as its eastern boundary (Lavender and Hermann, 2014). In northern California, the range of *P. menziesii var. menziesii* forks again to produce a western leg that continues as far south as Sonoma County before becoming discontinuous, and an eastern leg that stretches south through the Sierra Nevada region and the Yosemite Valley (Lavender and Hermann, 2014). The interior form, *P. menziesii var. glauca*, generally exists at much higher elevations, with a range that extends contiguously throughout the Rocky Mountains in Canada and the United States, reaching

eastern Oregon to the west. To the east, its range is contiguous through Idaho, western Montana, northwestern Wyoming, Utah, Colorado, New Mexico, and into Arizona where it becomes discontinuous (Lavender and Hermann, 2014). Isolated natural stands of *P. menziesii var. glauca* have been reported in west Texas, and scattered throughout the inland mountains of Mexico as far south as the 16th parallel in Oaxaca (Lavender and Hermann, 2014).

In the low- to mid-elevation forests along the western slopes of the Coast Ranges in western Oregon and Washington, Douglas-fir (*Pseudotsuga menziesii var. menziesii*) is a major component of the stand composition at the early stages of succession, and its dominance is often perpetuated where disturbances such as fire occur regularly or where plantation forestry is practiced (Franklin and Dyrness, 1973). The shade-tolerant western hemlock (*Tsuga heterophylla*) occupies the understory of this shade-intolerant Douglas-fir canopy (Franklin and Hemstrom, 1981). In the late stages of forest succession, western hemlock is generally dominant (Franklin and Hemstrom, 1981). This late-seral dominance of western hemlock is often purely hypothetical, as the long-lived and decay-resistant Douglas-fir can persist for centuries (Franklin and Dyrness, 1973). In the coastal *Picea sitchensis* zone, Sitka spruce and western hemlock are early seral dominant species that slowly give way to nearly monodominant stands of hemlock in the absence of disturbance (Franklin and Hemstrom, 1981). Here, Douglas-fir is generally a minor component of the stand structure (Franklin and Dyrness, 1973). In recent decades, however, the dominance of young Douglas-fir in this coastal *Picea sitchensis* zone has been maintained due to the conversion of land to commercial forestry use (Hansen et al.,

2000). Forest ecology and succession in these coastal vegetation zones in the northwestern United States have been drastically altered by anthropogenic activities over the last century with the advent of Douglas-fir cultivation for timber production.

1.4 Population Genetics of Fungal Plant Pathogens

Population genetics is a branch of evolutionary biology and ecology that is concerned with the origin and distribution of genetic variation in populations, and the forces contributing to changes in this distribution over time (Hartl and Clark, 2007). The fundamental processes of recombination, migration, mutation, and genetic drift are the mechanisms leading to the introduction and maintenance of genetic variation in populations, and provide the "substrate" on which natural selection may act (Hartl and Clark, 2007). The theories and techniques of population genetics are often applied in plant pathology in an effort to better understand the mechanisms underlying pathogen emergence, adaptation, and evolution. Studies of the genetic structure of plant pathogen populations also provides insights into the effects of anthropogenic activities, such as the movement of infected plant material (Barnes et al., 2014; Linde et al., 2009). An understanding of these processes is essential for the effective mitigation and treatment of plant disease in natural and agricultural systems.

1.4.1 Factors Influencing the Genetic Structure of Pathogen Populations

Genetic structure is used to describe subdivision within populations that may be due to geography, ecology, assortative mating, or some combination of factors that contribute to a non-random spatial distribution of organisms (Hartl and Clark, 2007). The processes by which genetic variation might be introduced into a population are

recombination due to crossing-over during meiosis, the heritable alteration of a nucleotide sequence (mutation), and the movement of new individuals into a population (migration). Random changes in allele frequencies over multiple generations (genetic drift) and the differential survival and reproduction of individuals that possess advantageous phenotypic traits (natural selection) are processes that act upon existing genetic variation leading to changes in allele frequencies, and thus population structure, over time (Hartl and Jones, 1998). These processes are fundamental to our understanding of plant pathogen population structure and evolution. Changes in allele frequencies over time can be measured and analyzed to gain insight into evolutionary processes that contribute to the ability of plant pathogens to infect their hosts and adapt to new or changing environments.

A major factor contributing to genetic diversity and structure within populations or subpopulations of fungal plant pathogens is their reproductive mode(s). In haploid organisms, self-fertilization (homothallism) results in progeny that are genetically identical to the progenitor and therefore is indistinguishable from asexual (clonal) reproduction (Kohn, 2005; Taylor et al., 1999). Sexual recombination via outcrossing results in the formation of novel genotypes that may have increased fitness in a given habitat. Factors that increase genetic variation can contribute to the evolutionary potential of pathogen populations (McDonald and Linde, 2002). Phytopathogenic fungi that have large effective population sizes, high rates of gene flow between populations, high genetic diversity due to sexual or mixed modes of reproduction, and high mutation rates are much more likely to adapt under strong selective pressures such as major gene

resistance, fungicides, and antibiotics (McDonald and Linde, 2002). An understanding of the fundamental evolutionary processes of adaptation to environment and plant host is often a major motivation for the application of population genetics in plant pathology.

Invasive populations of plant pathogens generally have very low genetic diversity compared to populations in the native range of the pathogen due to genetic bottlenecks resulting from founder events, whereby a small number of individuals are introduced and subsequently colonize the new habitat (Dlugosch and Parker, 2008; Linde et al., 2009). These populations often have a diminished capacity for adaptation (McDonald and Linde, 2002). Genetic drift is also much stronger when the organism has a small effective population size and low genetic diversity, and results in the loss or fixation of alleles at random (Hartl and Clark, 2007). The consequences of this can limit the success of invasive populations in new territories. These limitations can be overcome, however, if there are multiple introduction events from a relatively diverse source population (Dlugosch and Parker, 2008). Comparisons of genetic structure and diversity among native and invasive populations of plant pathogens allows for the origins and migration routes to be traced such that future introductions can be mitigated.

1.4.2 Fungal Speciation

Defining species in the kingdom Fungi is often a seemingly intractable endeavor. For decades, mycologists used a morphological species concept (MSC) to define them. This system often relied heavily upon analyses of microscopic and macroscopic characteristics that were misleading in terms of evolutionary relationships. Many seemingly distinctive morphologies evolved multiple times in distantly related groups,

and are thus not phylogenetically informative on their own. Many species have also been designated on the basis of the biological species concept (BSC), which is based on reproductive compatibility. The BSC was used to define many cryptic species within previously described morphological species (Giraud et al., 2008), but a definitive demonstration of reproductive isolation is only possible for species that mate in culture. For species delineations in the kingdom Fungi the phylogenetic species concept (PSC), which defines species based upon concordance among multiple genealogies of the nucleotide sequences of unlinked genes, has become the gold standard because it can discriminate at very fine scales species that would otherwise be indistinguishable by the MSC or BSC criteria (Giraud et al., 2008; Kohn, 2005; Taylor et al., 1999). It is often desirable to examine or interpret the factors that resulted in the observed species divergence. For this, there are two major categories of speciation events to consider: those that occur due to geographic isolation (allopatric), and those that are driven by ecological factors other than geographic isolation (sympatric).

Barriers to gene flow can occur at different stages of development depending on the life cycle of the organism, and may differ depending on the mode(s) of reproduction (Restrepo et al., 2014). Pre-zygotic barriers are generally ecological in nature, and are often due to assortative mating. This can occur due to allopatry, if species range becomes fractured, or as a result of a host shift where microallopatry develops between closely related fungi due to affinities for different sympatric hosts (Giraud et al., 2008; Restrepo et al., 2014). Post-zygotic genetic barriers can occur due to sterility or inviability of hybrids, where the meiotic spores (basidiospores or ascospores) may fail to germinate

due to mating between two incompatible isolates (Giraud and Gourbiere, 2012; Restrepo et al., 2014). Spores resulting from incompatible matings may be able to germinate, but the resulting dikaryon (basidiomycetes) or haploid mycelium (ascomycetes) may be inviable (Giraud and Gourbiere, 2012).

Speciation between plant pathogens is primarily reported as being due to allopatry or microallopatry (i.e. where two or more host species are sympatric but there is no gene flow between their associated plant pathogens) (Restrepo et al., 2014). Geographic barriers are obvious impediments to gene flow between subpopulations, even for microbes that can produce spores that disperse over long distances (Giraud et al., 2008). Prolonged geographic and genetic isolation leads to local adaptation, an accumulation of genetic mutations, and genetic divergence from a common ancestor. The result of this is the formation of genetically distinct evolutionary lineages (de Quieroz, 1998).

Sympatric speciation, however, is often dismissed as a theoretical impossibility for most sexual populations of fungi (Giraud et al., 2008). This is due to the fact that reproductive isolation or assortative mating must exist in some form for lineages to diverge. It is often difficult to provide evidence that speciation has occurred in sympatry because there must also be evidence that the populations were not allopatric at some point in history (Giraud et al., 2008). The reproductive isolation and assortative mating needed for this lineage divergence is often observed in the form of adaptation to ecological niches such that species are not technically allopatric, but exhibit some form of microallopatry in which mating between them does not occur across niche boundaries that may occur in the same habitat (Restrepo et al., 2014). While a lack of gene flow

between incipient species is the primary driver of speciation, complete reproductive isolation is most often the result (Giraud et al., 2008; Kohn, 2005). When genetically isolated groups remain as such over long periods of time, they diverge due to genetic drift, selection, random mutation, or changes in chromosome number, and are eventually rendered reproductively incompatible (Kohn, 2005).

1.4.3 Population structure of N. gaeumannii

What little we know about the population genetics of *N. gaeumannii* was provided by Winton et al. (2006), who described the presence of two lineages of *N. gaeumannii* that appeared to be reproductively isolated but sympatric in coastal Oregon stands. The existence of these lineages was determined on the basis of variation in single-strand conformation polymorphisms (SSCPs) of nuclear and mitochondrial DNA markers. Lineage 1 was found to be widely distributed across North America, New Zealand, and Europe, while Lineage 2 was only found in the western Oregon Coast Range (Winton et al., 2006). The fine-scale distributions of these lineages within sites, trees, or individual Douglas-fir needles, was not assessed at this time. Later, short sequence repeats (SSRs), or microsatellites, were developed to increase the resolution of these types of studies (Winton et al., 2007). Although there is evidence for reproductive isolation between the two sympatric lineages, currently there is insufficient evidence to describe them as separate phylogenetic species within *Nothophaeocryptopus* (Bennett and Stone, 2016; Winton et al., 2006).

A naturally existing variation in aggressiveness between strains of *N. gaeumannii* was first proposed by Boyce (1940) as one potential explanation for the variation in SNC

severity observed between Europe and N. America. Later studies addressing this issue suggested that one of two reproductively isolated cryptic lineages, Lineage 2, might be more aggressive (Winton et al., 2006). This lineage seemed to be restricted to the low-elevation forests on the western slopes of the Oregon Coast Range where SNC had recently emerged, and was abundant in the vicinity of Tillamook, Oregon where SNC was most severe (Winton et al., 2006). The abundance of Lineage 2 relative to Lineage 1 was also correlated with SNC symptoms within Douglas-fir stands in coastal Oregon. Higher Lineage 2: Lineage 1 ratios were correlated with lower canopy density and more severe foliage discoloration, two visual assessments of SNC symptom severity (Winton et al., 2006). However, it appeared that Lineage 2 did not cause more severe defoliation in controlled inoculation trials. Rather, defoliation caused by the Lineage 1 isolates was significantly greater than that caused by Lineage 2 (Winton and Stone, 2004). These seemingly contradictory results suggested that there be some interaction between genotype, environment, and disease (Winton and Stone, 2004). The coastal environment seems to be more conducive to SNC, and may also be more favorable for the growth and reproduction of Lineage 2 (Winton and Stone, 2004).

1.5 Dissertation Outline

The following dissertation provides insights into the factors contributing to the emergence of the fungus *Nothophaeocryptopus gaeumannii* as a serious damage agent in the native range of Douglas-fir. This work expands upon previous studies of the population genetics of *N. gaeumannii* by sampling SSR genotypes from isolates collected using a hierarchical sampling strategy in an effort to gain a better understanding of the

spatial distribution of genetic variation in populations of this fungus. Chapter two examines the genetic structure of native fungal populations in western Oregon and Washington and investigates factors influencing the spatial structure of populations including dispersal and reproductive biology. In Chapter three, similar assessments are presented for a large dataset of *N. gaeumannii* isolates from New Zealand, where the fungus is invasive. Chapter four considers the factors influencing the genetic structure of the global *N. gaeumannii* population with an analysis of the relationships among *N. gaeumannii* genotypes from the U.S.A., New Zealand, Australia, Europe, and Chile, and an inference of the introduction pathways of *N. gaeumannii* into these countries. Chapter five examines relationships between *N. gaeumannii* population structure and SNC severity in its native range, and identifies correlations between these variables and pertinent environmental variables. The final chapter summarizes the results from previous chapters, provides additional context for their interpretation, and discusses the broader implications of the results presented in other chapters. All of these lines of inquiry were performed with the intent of developing a better understanding of the factors influencing the genetic structure of *N. gaeumannii* populations and the relationships between *N. gaeumannii* population structure and SNC severity.

1.6 Literature Cited

Barnes, I., Wingfield, M.J., Carbone, I., Kirisits, T., and Wingfield, B.D. 2014. Population structure and diversity of an invasive pine needle pathogen reflects anthropogenic activity. *Ecology and Evolution* 4, 3642–3661. doi: 10.1002/ece3.1200.

Bennett, P., and Stone, J. 2016. Assessments of population structure, diversity, and phylogeography of the Swiss needle cast fungus (*Phaeocryptopus gaeumannii*) in the U.S. Pacific Northwest. *Forests* 7, 14. doi:10.3390/f7010014.

Black, B.A., Shaw, D.C., and Stone, J.K. 2010. Impacts of Swiss needle cast on overstory Douglas-fir forests of the western Oregon Coast Range. *Forest Ecology and Management* 259, 1673–1680.

Boyce, J.S. 1940. A needle-cast of Douglas-fir associated with *Adelopus gaumanni*. *Phytopathology* 30, 649–659.

Capitano, B.R. 1999. The infection and colonization of Douglas-fir needles by the Swiss needle cast pathogen, *Phaeocryptopus gaeumannii* (Rhode) Petrak. MS Thesis. Oregon State University, Corvallis, OR, USA.

Castaño, C., Colinas, C., Gómez, M., and Oliva, J. 2014. Outbreak of Swiss needle cast caused by the fungus *Phaeocryptopus gaeumannii* on Douglas-fir in Spain. *New Disease Reports* 29, 19. doi: 10.5197/j.2044-0588.2014.029.019.

Chastagner, G.A., and Byther, R.S. 1983. Infection period of *Phaeocryptopus gaeumannii* on Douglas-fir needles in western Washington. *Plant Disease* 67, 811–813.

Chastagner, G.A., and Stone, J.K., 2001. Fungicidal control of Swiss needle cast in stands of Douglas-fir timber. pp. 89–95 in Swiss Needle Cast Cooperative Annual Report 2001. Filip, G. (ed.). College of Forestry, Oregon State University, Corvallis, OR. http://sncc.forestry.oregonstate.edu/annual-reports

Coop, L.B., and Stone, J.K., 2010. Climate models for predicting distribution and severity of Swiss needle cast. pp. 66–80 in *Swiss Needle Cast Cooperative Annual Report 2010*. Mulvey, R., and Shaw, D. (eds.). College of Forestry, Oregon State University, Corvallis, OR. http://sncc.forestry.oregonstate.edu/annual-reports

Dlugosch, K.M., and Parker, I.M. 2008. Founding events in species invasions: genetic variation, adaptive evolution, and the role of multiple introductions. *Molecular Ecology* 17, 431–449. doi: 10.1111/j.1365-294X.2007.03538.x.

El-Hajj, Z., Kavanagh, K., Rose, C., and Kanaan-Atallah, Z. 2004. Nitrogen and carbon dynamics of a foliar biotrophic fungal parasite in fertilized Douglas-fir. *New Phytologist* 163, 139–147. doi: 10.1011/j.1469-8137.2004.01102.x.

Franklin, J.F., and Dyrness, C.T. 1973. Natural vegetation of Oregon and Washington Corvallis, Oregon: Oregon State University Press.

Franklin, J.F.; Hemstrom, M.A. 1981. Aspects of succession in the coniferous forests of the Pacific Northwest. In: West, D.C.; Shugart, H.H.; Botkin, D.B. (eds.). Forest succession: concepts and application. Springer-Verlag, pp. 212–229.

Gaeumann, E. 1930. Über eine neue krankheit der Dougalsien. *Schweiz. Z. Forstwes* 81, 63–67.

Giraud, T., and Gourbiere, S. 2012. The tempo and modes of evolution of reproductive isolation in fungi. *Heredity* 109, 204. doi:10.1038/hdy.2012.30.

Giraud, T., Refrégier, G., Le Gac, M., de Vienne, D.M., and Hood, M.E. 2008. Speciation in fungi. *Fungal Genetics and Biology* 45, 791–802. doi:10.1016/j.fgb.2008.02.001.

Hadfield, J., and Douglass, B.S. 1982. Protection of Douglas-fir Christmas trees from Swiss needle cast in Oregon. *American Christmas Tree Journal* 26, 31–33.

Hahn, G.G. 1941. New reports on *Adelopus gaeumanni* on Douglas fir in the United States. *Plant Disease Reporter* 25, 115–117.

Hahn, G.G. 1947. Analysis of Peck's types of *Meliola balsamicola* and *Asterina nuda*. *Mycologia* 39, 479.

Hansen, E.M., and Stone, J.K. 2005. Impacts of plant pathogenic fungi on plant communities. In: Dighton, J.; White, J.F.; Oudemans, P. (eds.). The fungal community: its organization and role in the ecosystem, CRC Press, Taylor and Francis Group, pp. 461–474.

Hansen, E.M., Stone, J.K., Capitano, B.R., Rosso, P., Sutton, W., Winton, L., Kanaskie, A., and McWilliams, M.G. 2000. Incidence and impact of Swiss needle cast in forest plantations of Douglas-fir in coastal Oregon. *Plant Disease* 84, 773–778.

Hartl, D.L., and Clark, A.G. 2007. Principles of population genetics. Sunderland, Mass: Sinauer Associates.

Hartl, D.L., and Jones, E.W. 1998. Genetics: principles and analysis. Sudbury, Mass: Jones and Bartlett Publishers.

Hood, I.A. 1982. *Phaeocryptopus gaeumannii* on *Pseudotsuga menziesii* in southern British Columbia. *New Zealand Journal of Forestry Science* 12, 415–424.

Hood, I.A., and Kershaw, D.J. 1975. Distribution and infection period of *Phaeocryptopus gaeumannii* in New Zealand. *New Zealand Journal of Forestry Science* 5, 201–208.

Hood, I.A., and Sandberg, C.J. 1979. Changes within tree crowns following thinning of young Douglas-fir infected by *Phaeocryptopus gaeumannii*. *New Zealand Journal of Forestry Science* 9, 177–184.

Hood, I.A., Sandberg, C.J., Barr, C.W., Holloway, W.A., and Bradbury, P.M. 1990. Changes in needle retention associated with the spread and establishment of *Phaeocryptopus gaeumannii* in planted Douglas-fir. *European Journal of Forest Pathology* 20, 418–429.

Kanaskie, A., Kaetzel, B., and Herstrom, A., 2014. Economic impact of Swiss needle cast in Oregon forests. pp. 15–19 in *Swiss Needle Cast Cooperative Annual Report 2014*. Ritóková, G., and Shaw, D. (eds.). College of Forestry, Oregon State University, Corvallis, OR. http://sncc.forestry.oregonstate.edu/annual-reports

Kimberley, M.O., Hood, I.A., and Knowles, R.L. 2011. Impact of Swiss needle cast on growth of Douglas-fir. *Phytopathology* 101, 583–593. doi:10.1094/PHYTO-05-10-0129.

Kohn, L.M. 2005. Mechanisms of fungal speciation. *Annual Review of Phytopathology* 43, 279–308. doi: 10.1146/annurev.phyto.43.040204.135958.

Lavender, D.P., and Hermann, R.K. 2014. Douglas-fir: the genus *Pseudotsuga*. Oregon Forest Research Laboratory, Oregon State University, Corvallis, OR, USA.

Lee, E.H., Beedlow, P.A., Waschmann, R.S., Burdick, C.A., and Shaw, D.C. 2013. Tree-ring analysis of the fungal disease Swiss needle cast in western Oregon coastal forests. *Canadian Journal of Forest Research* 43, 677–690. doi: 10.1139/cjfr-2013-0062.

Lee, E.H., Beedlow, P.A., Waschmann, R.S., Tingey, D.T., Wickham, C., Cline, S., Bollman, M., and Carlile, C. 2016. Douglas-fir displays a range of growth responses to temperature, water, and Swiss needle cast in western Oregon, USA. *Agricultural and Forest Meteorology* 221, 176–188. doi: 10.1016/j.agrformet.2016.02.009.

Lee, E.H., Beedlow, P.A., Waschmann, R.S., Tingey, D.T., Cline, S., Bollman, M., Wickham, C., and Carlile, C. 2017. Regional patterns of increasing Swiss needle cast impacts on Douglas-fir growth with warming temperatures. *Ecology and Evolution* 00, 1–30. doi: 10.1002/ece3.3573.

Liese, J. 1939. The occurrence in the British Isles of the *Adelopus* disease of Douglas Fir. *Quarterly Journal of Forestry* 33, 247–252.

Linde, C.C., Zala, M., and McDonald, B.A. 2009. Molecular evidence for recent founder populations and human-mediated migration in the barley scald pathogen *Rhynchosporium secalis*. *Molecular Phylogenetics and Evolution* 51, 454–464. doi:10.1016/j.ympev.2009.03.002.

Maguire, D.A., Kanaskie, A., Voelker, W., Johnson, R., and Johnson, G. 2002. Growth of young Douglas-fir plantations across a gradient in Swiss needle cast severity. *Western Journal of Applied Forestry* 17, 86–95.

Maguire, D.A., Mainwaring, D.B., and Kanaskie, A. 2011. Ten-year growth and mortality in young Douglas-fir stands experiencing a range in Swiss needle cast severity. *Canadian Journal of Forest Research* 41, 2064–2076. doi:10.1139/X11-114.

Mainwaring, D.B., Maguire, D.A., Kanaskie, A., and Brandt, J. 2005. Growth responses to commercial thinning in Douglas-fir stands with varying severity of Swiss needle cast in Oregon, USA. *Canadian Journal of Forest Research* 35, 2394–2402. doi: 10.1139/X05-164.

Manter, D.K., and Kavanagh, K.L. 2003. Stomatal regulation in Douglas fir following a fungal-mediated chronic reduction in leaf area. *Trees* 17, 485–491. doi: 10.1007/s00468-003-0262-2.

Manter, D.K., Bond, B.J., Kavanagh, K.L., Rosso, P.H., and Filip, G.M. 2000. Pseudothecia of Swiss needle cast fungus, *Phaeocryptopus gaeumannii*, physically block stomata of Douglas fir, reducing CO_2 assimilation. *The New Phytologist* 148, 481–491.

Manter, D.K., Winton, L.M., Filip, G.M., and Stone, J.K. 2003a. Assessment of Swiss needle cast disease: temporal and spatial investigations of fungal colonization and symptom severity. *Journal of Phytopathology* 151, 344–351.

Manter, D.K., Bond, B.J., Kavanagh, K.L., Stone, J.K., and Filip, G.M. 2003b. Modelling the impacts of the foliar pathogen, *Phaeocryptopus gaeumannii*, on Douglas-fir

physiology: net canopy carbon assimilation, needle abscission and growth. *Ecological Modelling* 164, 211–226. doi:10.1016/S0304-3800(03)00026-7.

Manter, D.K., Reeser, P.W., and Stone, J.K. 2005. A climate-based model for predicting geographic variation in Swiss needle cast severity in the Oregon Coast Range. *Phytopathology* 95, 1256–1265. doi: 10.1094/PHYTO-95-1256.

Marks, G.C. 1975. Swiss needle cast of Douglas fir. *Australasian Plant Pathology* 4, 24–24.

McCormick, F.A. 1939. *Phaeocryptopus gaeumanni* on Douglas Fir in Connecticut. *Plant Disease Reporter* 23, 368–369.

Mcdermott, J.M., and Robinson, R.A. 1989. Provenance variation for disease resistance in *Pseudotsuga menziesii* to the Swiss needle-cast pathogen, *Phaeocryptopus gaeumanni*. *Canadian Journal of Forest Research* 19, 244–246.

McDonald, B.A., and Linde, C. 2002. Pathogen population genetics, evolutionary potential, and durable resistance. *Annual Review of Phytopathology* 40, 349–379. doi: 10.1146/annurev.phyto.40.120501.101443.

Meinecke, E.P. 1939. The *Adelopus* needle cast of Douglas Fir on the Pacific coast. Sacramento, California: Dept. of Natural Resources, Division of Forestry.

Merrill, W., and Longnecker, J. 1973. Swiss needle cast of Douglas-fir in Pennsylvania. *Plant Disease Reporter* 57, 984–984.

Michaels, E., and Chastagner, G.A. 1984. Distribution, severity, and impact of Swiss needle cast in Douglas-fir Christmas trees in western Washington and Oregon. *Plant Disease* 68, 939–942.

Morton, H.L., and Patton, R.F. 1970. Swiss needle cast of Douglas-fir in the Lake States. *Plant Disease Reporter* 54, 612–616.

Mulvey, R.L., Shaw, D.C., and Maguire, D.A. 2013. Fertilization impacts on Swiss needle cast disease severity in western Oregon. *Forest Ecology and Management* 287, 147–158. doi: 10.1016/j.foreco.2012.08.050.

Naumov, M.N. 1914. Travaux de l'Institut de pathologie végétale de Saint-Pétersbourg. *Bulletin de La Société Mycologique de France* 30, 423–432.

Navarro, S., and Norlander, D., 2016. Swiss needle cast aerial survey. pp. 7–11 in *Swiss Needle Cast Cooperative Annual Report 2016*, Ritóková, G., and Shaw, D. (eds.). College of Forestry, Oregon State University, Corvallis, OR. http://sncc.forestry.oregonstate.edu/annual-reports; http://www.oregon.gov/ODF/ForestBenefits/Pages/ForestHealth.aspx

Nelson, E.E., Silen, R.R., and Mandel, N.L. 1989. Effects of Douglas-fir parentage on Swiss needle cast expression. *Forest Pathology* 19, 1–6.

Osorio, M. 2007. Detección del hongo defoliador *Phaeocryptopus gaeumannii* en plantaciones de *Pseudotsuga* menziesii de Valdivia, Chile. *Bosque* 28, 69–74.

Petrak, F. 1938. Beiträge zur systematik und phylogenie der gattung *Phaeocryptopus* Naoumov. *Annales Mycologici* 36, 9–26.

de Quieroz, K. 1998. The general lineage concept of species, and the process of speciation. In: Howard, D.J. and Belocher, S.H. (eds.). Endless Forms: Species and Speciation, Oxford University Press, pp. 57–75.

Ramsey, A., Omdal, D., Dozic, A., Kohler, G., and Boderck, M., 2015. Swiss needle cast aerial and ground survey coastal Washington. pp. 12-18 in *Swiss Needle Cast Cooperative Annual Report 2015*. Ritóková, G., and Shaw, D. (eds.). College of Forestry, Oregon State University, Corvallis, OR. http://sncc.forestry.oregonstate.edu/annual-reports

Restrepo, S., Tabima, J.F., Mideros, M.F., Grünwald, N.J., Matute, D.R., 2014. Speciation in Fungal and Oomycete Plant Pathogens. *Annual Review of Phytopathology* 52, 289–316. doi: 10.1146/annurev-phyto-102313-050056.

Ritóková, G., Shaw, D., Filip, G., Kanaskie, A., Browning, J., and Norlander, D. 2016. Swiss needle cast in western Oregon Douglas-fir plantations: 20-year monitoring results. *Forests* 7, 155. doi: 10.3390/f7080155.

Rohde, T. 1936. *Adelopus gaeumannii* n. sp. und die von ihm hervorgerufene "Schweizer" Douglasienschütte. *Forstliche Wochenschrift Silva.* 24, 420–422.

Rosso, P.H., and Hansen, E.M. 2003. Predicting Swiss needle cast disease distribution and severity in young Douglas-fir plantations in coastal Oregon. *Phytopathology* 93, 790–798.

Schoch, C.L., Crous, P.W., Groenewald, J.Z., Boehm, E.W.A., Burgess, T.I., de Gruyter, J., de Hoog, G.S., Dixon, L.J., Grube, M., Gueidan, C., et al. 2009. A class-wide phylogenetic assessment of Dothideomycetes. *Studies in Mycology* 64, 1–15. doi:10.3114/sim.2009.64.01.

Shaw, D.C., Filip, G.M., Kanaskie, A., Maguire, D.A., and Littke, W.A. 2011. Managing an epidemic of Swiss needle cast in the Douglas-fir region of Oregon: the role of the Swiss needle cast cooperative. *Journal of Forestry* 109, 109–119.

Shaw, D.C., Woolley, T., and Kanaskie, A. 2014. Vertical foliage retention in Douglas-fir across environmental gradients of the western Oregon Coast Range influenced by Swiss needle cast. *Northwest Science* 88, 23–32. doi: 10.3955/046.088.0105.

Stone, J.K., Hood, I.A., Watt, M.S., and Kerrigan, J.L. 2007a. Distribution of Swiss needle cast in New Zealand in relation to winter temperature. *Australasian Plant Pathology* 36, 445. doi: 10.1071/AP07049.

Stone, J.K., Reeser, P.W., and Kanaskie, A. 2007b. Fungicidal suppression of Swiss needle cast and pathogen reinvasion in a 20-year-old Douglas-fir stand in Oregon. *Western Journal of Applied Forestry* 22, 248–252.

Stone, J.K., Capitano, B.R., and Kerrigan, J.L. 2008a. The histopathology of *Phaeocryptopus gaeumannii* on Douglas-fir needles. *Mycologia* 100, 431–444. doi: 10.3852/06-170R1.

Stone, J.K., Coop, L.B., and Manter, D.K. 2008b. Predicting effects of climate change on Swiss needle cast disease severity in Pacific Northwest forests. *Canadian Journal of Plant Pathology* 30, 169–176.

Taylor, J.W., Jacobson, D.J., and Fisher, M.C. 1999. The evolution of asexual fungi: reproduction, speciation and classification. *Annual Review of Phytopathology* 37, 197–246.

Temel, F. 2002. Early testing of Douglas-fir *Pseudotsuga* menziesii var. menziesii Mirb. Franco for Swiss needle cast tolerance. PhD Dissertation. Oregon State University, Corvallis, OR, U.S.A.

Temel, F., Stone, J.K., and Johnson, G.R. 2003. First report of Swiss needle cast caused by *Phaeocryptopus gaeumannii* on Douglas-fir in Turkey. *Plant Disease* 87, 1536–1536. doi: 10.1094/PDIS.2003.87.12.1536B.

Temel, F., Johnson, G.R., and Stone, J.K. 2004. The relationship between Swiss needle cast symptom severity and level of *Phaeocryptopus gaeumannii* colonization in coastal Douglas-fir *Pseudotsuga menziesii* var. *menziesii*. *Forest Pathology* 34, 383–394.

Videira, S.I.R., Groenewald, J.Z., Nakashima, C., Braun, U., Barreto, R.W., de Wit, P.J., and Crous, P.W. 2017. Mycosphaerellaceae– chaos or clarity? *Studies in Mycology* 87, 257–421. doi: 10.1016/j.simyco.2017.09.003.

Watt, M.S., Stone, J.K., Hood, I.A., and Palmer, D.J. 2010. Predicting the severity of Swiss needle cast on Douglas-fir under current and future climate in New Zealand. *Forest Ecology and Management* 260, 2232–2240. doi: 10.1016/j.foreco.2010.09.034.

Watt, M.S., Stone, J.K., Hood, I.A., and Manning, L.K. 2011. Using a climatic niche model to predict the direct and indirect impacts of climate change on the distribution of Douglas-fir in New Zealand. *Global Change Biology* 17, 3608–3619. doi: 10.1111/j.1365-2486.2011.02486.x.

Weiskittel, A.R., and Maguire, D.A. 2007. Response of Douglas-fir leaf area index and litterfall dynamics to Swiss needle cast in north coastal Oregon, USA. *Annals of Forest Science* 64, 121–132. doi: 10.1051/forest:2006096.

Weiskittel, A.R., Maguire, D.A., Garber, S.M., and Kanaskie, A. 2006. Influence of Swiss needle cast on foliage age-class structure and vertical foliage distribution in Douglas-fir plantations in north coastal Oregon. *Canadian Journal of Forest Research* 36, 1497–1508. doi: 10.1139/x06-044

Wilson, M., and Waldie, J.S.L. 1928. Notes on new or rare forest fungi. *Transactions of the British Mycological Society* 13, 151–156.

Winton, L.M. 2001. Phylogenetics, population genetics, molecular epidemiology, and pathogenicity of the Douglas-fir Swiss needle cast pathogen *Phaeocryptopus gaeumannii*. PhD Dissertation. Oregon State University, Corvallis, OR, USA.

Winton, L.M., and Stone, J.K. 2004. Microsatellite population structure of *Phaeocryptopus gaeumannii* and pathogenicity of *P. gaeumannii* genotypes/lineages. pp. 42-48 in *Swiss Needle Cast Cooperative Annual Report 2004*, Mainwaring, D. (ed.). College of Forestry, Oregon State University, Corvallis, OR. http://sncc.forestry.oregonstate.edu/annual-reports

Winton, L.M., Hansen, E.M., and Stone, J.K. 2006. Population structure suggests reproductively isolated lineages of *Phaeocryptopus gaeumannii*. *Mycologia* 98, 781–791.

Winton, L.M., Stone, J.K., and Hansen, E.M. 2007a. Polymorphic microsatellite markers for the Douglas-fir pathogen *Phaeocryptopus gaeumannii*, causal agent of Swiss Needle Cast disease. *Molecular Ecology Notes* 7, 1125–1128. doi: 10.1111/j.1471-8286.2007.01802.x.

Winton, L.M., Stone, J.K., Hansen, E.M., and Shoemaker, R.A. 2007b. The systematic position of *Phaeocryptopus gaeumannii*. *Mycologia* 99, 240–252.

Zhao, J., Mainwaring, D.B., Maguire, D.A., and Kanaskie, A. 2011. Regional and annual trends in Douglas-fir foliage retention: Correlations with climatic variables. *Forest Ecology and Management* 262, 1872–1886. doi:10.1016/j.foreco.2011.08.008

Zhao, J., Maguire, D.A., Mainwaring, D.B., and Kanaskie, A. 2012. Climatic influences on needle cohort survival mediated by Swiss needle cast in coastal Douglas-fir. *Trees* 26, 1361–1371. doi: 10.1007/s00468-012-0711-x

Zhao, J., Maguire, D.A., Mainwaring, D.B., and Kanaskie, A. 2014. Western hemlock growth response to increasing intensity of Swiss needle cast on Douglas-fir: changes in the dynamics of mixed-species stands. *Forestry* 87, 697–704. doi: 10.1093/forestry/cpu030.

Zhao, J., Maguire, D.A., Mainwaring, D.B., and Kanaskie, A. 2015. The effect of within-stand variation in Swiss needle cast intensity on Douglas-fir stand dynamics. *Forest Ecology and Management* 347, 75–82. doi: 10.1016/j.foreco.2015.03.010

1.7 Figures and Tables

Figure 1.1: Douglas-fir trees exhibiting symptoms of Swiss needle cast including chlorosis (yellow-brown foliage), and thin crowns resulting from premature foliage loss. Photo credits: J. K. Stone, Oregon State University.

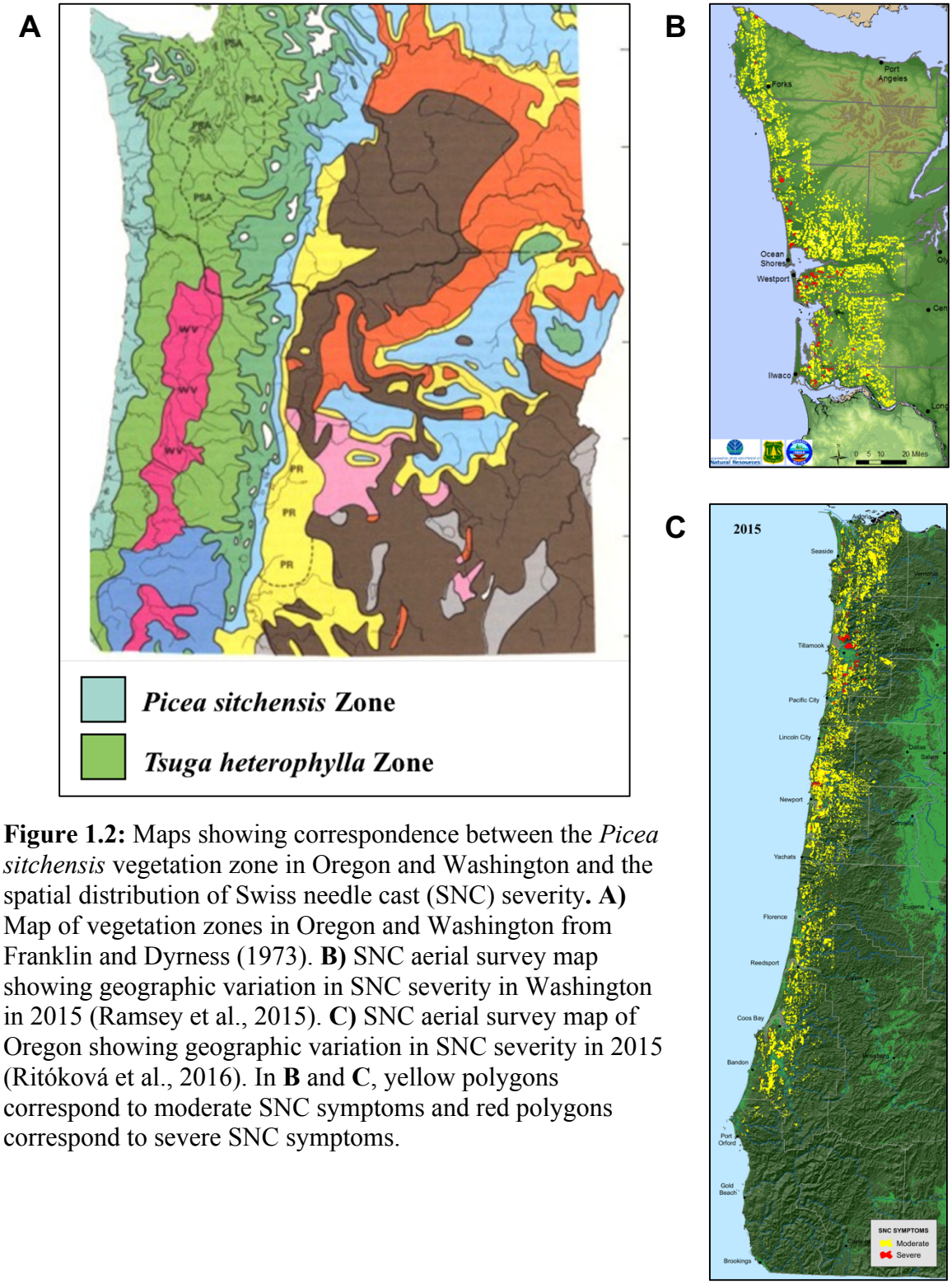

Figure 1.2: Maps showing correspondence between the *Picea sitchensis* vegetation zone in Oregon and Washington and the spatial distribution of Swiss needle cast (SNC) severity**. A)** Map of vegetation zones in Oregon and Washington from Franklin and Dyrness (1973). **B)** SNC aerial survey map showing geographic variation in SNC severity in Washington in 2015 (Ramsey et al., 2015). **C)** SNC aerial survey map of Oregon showing geographic variation in SNC severity in 2015 (Ritóková et al., 2016). In **B** and **C**, yellow polygons correspond to moderate SNC symptoms and red polygons correspond to severe SNC symptoms.

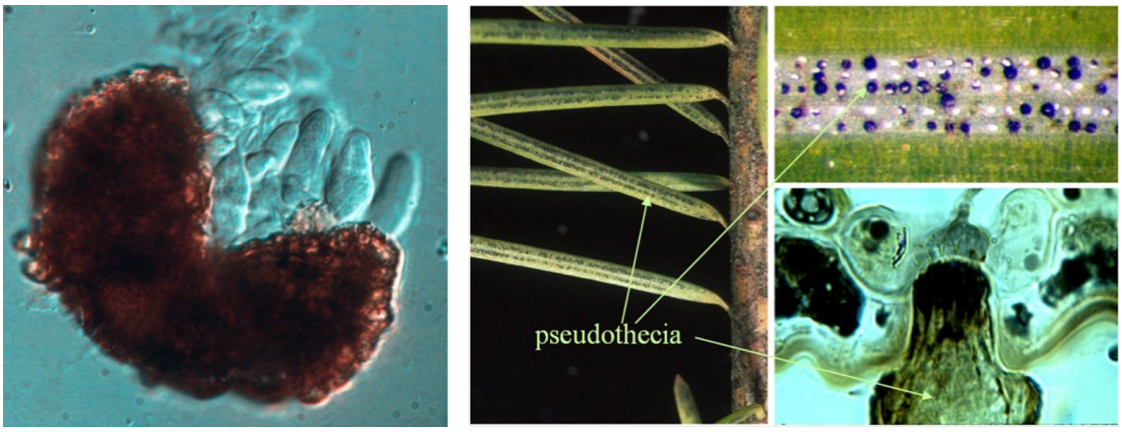

Figure 1.3: Ascocarps (pseudothecia) of *Nothophaeocryptopus gaeumannii* cause Swiss Needle Cast (SNC) by blocking the stomata in Douglas-fir needles. A) A pseudothecium of *N. gaeumannii*, showing the asci. B) The undersides of Douglas-fir needles infected with *N. gaeumannii* showing pseudothecia protruding from the stomata. C) close-up of pseudothecia protruding from stomata on a Douglas-fir needle. D) Micrograph image of a pseudothecium growing to occlude a stomate. Photo credits: J. K. Stone, Oregon State University.

Figure 1.4: Phylogenetic tree from Winton et al. (2007b) based on combined SSU and LSU sequences placing *Phaeocryptopus gaeumannii* (marked with a star) in the Mycosphaerellaceae and *P. nudus* in Dothideales.

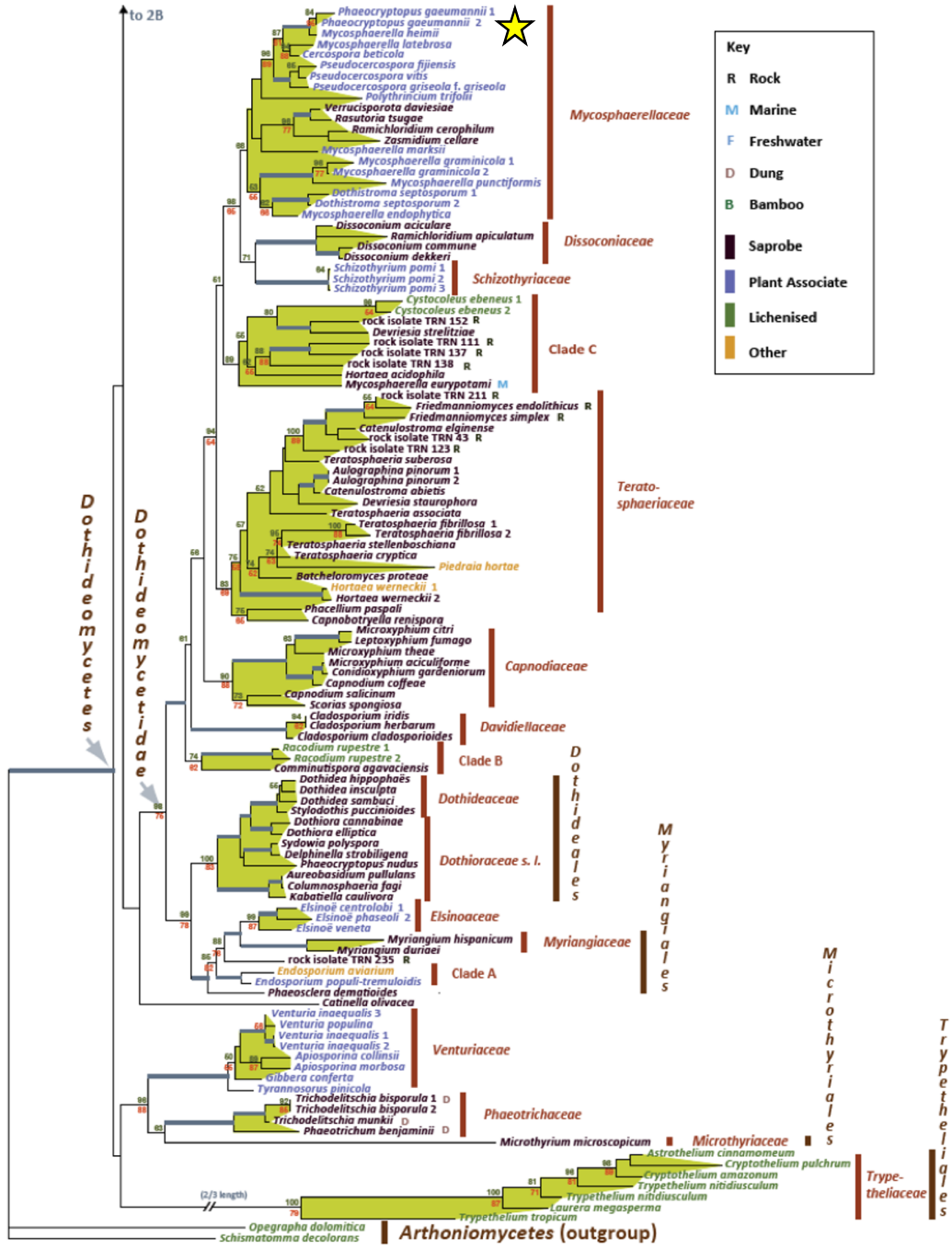

Figure 1.5: A portion of the phylogenetic tree from Schoch et al. (2009) based on a combined LSU, SSU, TEF1, RPB1 and RPB2 sequence dataset showing placement of *P. gaeumannii* (marked with a star) in the Mycosphaerellaceae, supporting the findings of Winton et al. (2007b).

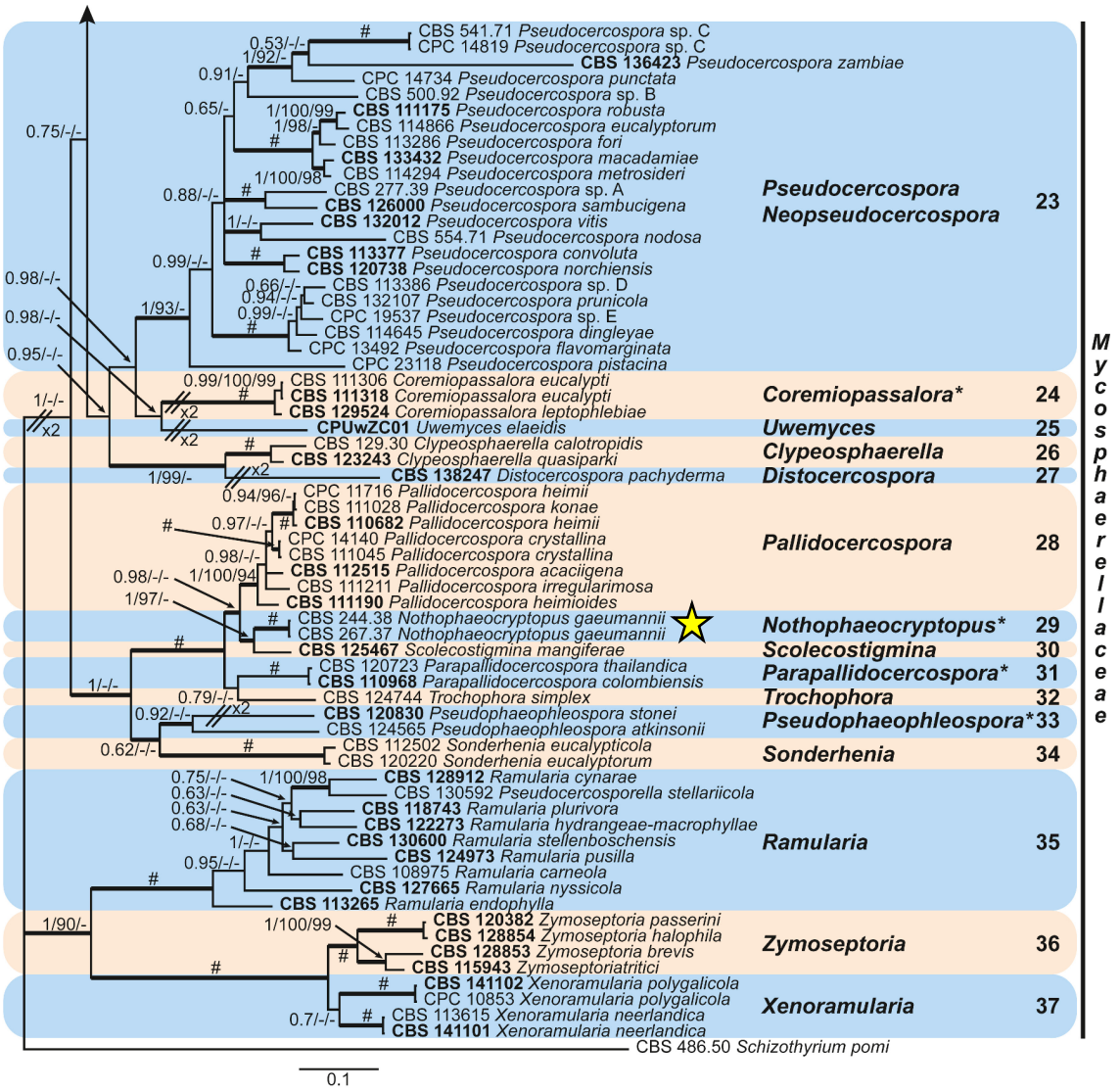

Figure 1.6: A portion of the phylogenetic tree presented in Videira et al. (2017) based on an alignment of LSU, RPB2, and ITS, which placed the former *P. gaeumannii* in the new genus *Nothophaeocryptopus* (marked with a star).

Table 1.1: Summary of studies that have investigated the relationships between Swiss needle cast (SNC) and climate.

Table 1.1

Study	Region	Method	Response variable	Explanatory variable	Relationship with response
Rosso & Hansen 2003	western OR	Linear regression	SNC severity rating (foliage retention, height growth, foliage color)	July precipitation	+
				July fog	+
				July temperature (maximum)	-
Manter et al. 2005	western OR	Linear regression	pseudothecia abundance	Winter temperature (daily)	+
				Spring leaf wetness	+
Stone et al. 2007	New Zealand	Linear regression	pseudothecia abundance	Winter temperature (average)	+
				August temperature (maximum)	+
Watt et al. 2010	New Zealand	Linear regression	pseudothecia abundance	June temperature (average)	+
				November precipitation	+
Coop & Stone 2010	western OR & WA	Linear regression	pseudothecia abundance	Winter temperature (average)	+
				June-July dew point deficit	-
				Jun-July precipitation	+
Zhao et al. 2011	western OR & WA	Linear regression	foliage retention	August temperature (average)	+
				June temperature (average)	-
				December temperature (minimum)	-
				August precipitation	-
Watt et al. 2011	worldwide	climatic niche CLIMEX	pseudothecia abundance, foliage retention	T_{min} 10 °C, T_{max} 28 °C, T_{opt} 20 °C	N/A
				Soil moisture 11% to 170% field capacity	

Table 1.1 (Continued)

Lee et al. 2013	western OR	Time-series intervention analysis (TSIA)	reduction in growth (%) calculated from tree ring width data	Winter temperature (mean)	+
				Summer temperature (mean)	+ at humid coastal sites, - at warmer drier sites
				Winter precipitation (mean)	+
				Spring precipitation (mean)	+
				Summer precipitation (mean)	+
				June-July dew point deficit	-
Lee et al. 2017	western OR	TSIA	reduction in growth (%) calculated from tree ring width data	Winter temperature	+
				June-July precipitation	+
				June-July temperature	-

Chapter 2. Hierarchical Genetic Structure in Populations of the Douglas-fir Swiss Needle Cast Fungus *Nothophaeocryptopus gaeumannii* in Coastal Oregon and Washington Forests

2.1 Abstract

The incidence and severity of Swiss needle cast (SNC), a Douglas-fir foliage disease caused by the fungus *Nothophaeocryptopus gaeumannii*, has increased in recent decades in the low-elevation forests along the western slopes of the Coast Ranges in Oregon and Washington. This recent intensification has prompted numerous investigations into factors that might influence disease severity such as climate, forest management, and the dynamics of the pathogen population. Among these factors, the genetic structure of the *N. gaeumannii* population is still the least understood. This study analyzed multilocus genotypes (MLGs) consisting of alleles from nine polymorphic SSR markers to assess the genetic diversity and population structure of native *N. gaeumannii* populations as a way to better understand the biology of *N. gaeumannii* in relation to SNC severity. A total of 1,061 *N. gaeumannii* isolates were collected from 35 sites in western Oregon and Washington between 2014 and 2016. Genotypic clustering provided support for the presence of two distinct lineages, and strong genetic differentiation between the lineages supports previous observations that suggested that they are reproductively isolated. This apparent reproductive isolation has been maintained despite the fact that the lineages were sympatric within Douglas-fir stands, within trees, and within Douglas-fir needles. The two lineages were admixed in stands in the low elevation forests along the western slopes of the Coast Ranges in northwestern Oregon and Washington where the most severe SNC symptoms have been observed. Lineage 2 was more abundant relative to Lineage 1 in coastal sites, and decreased in abundance relative to Lineage 1 with increasing distance inland. We observed significant linkage

disequilibrium that was due to the presence of repeated MLGs and reproductively-isolated subpopulations (i.e. the two non-interbreeding lineages). The presence of repeated MLGs supports the inference that the reproductive mode of this fungus is homothallic. The spatial distributions of shared MLGs across sites in Oregon and Washington may provide a reasonable assessment of the effective dispersal distance, or may indicate that human-mediated dispersal has occurred between sites across Oregon and Washington. Our results suggest that a given tree may host many distinct *N. gaeumannii* MLGs, and that an infected needle may be a mosaic of different fungal genotypes including both lineages.

2.2 Introduction

Examining the genetic structures of pathogen populations can improve our understanding their origins and life histories, and allow for the estimation of their potential for evolutionary adaptation (McDonald and Linde, 2002). Molecular genetic techniques are often utilized to infer population dynamics of microbial pathogens whose life histories are not readily observable. The field of population genetics has provided essential tools for inferring biological traits from molecular data including diversity, reproductive mode(s), and genetic differentiation. In the field of plant pathology, population genetics has proven useful for detecting changes in population structure in relation to disease intensification or emergence, and has also allowed for the detection and identification of virulent genotypes, pathogen races, and genetic lineages (Grünwald et al., 2016; McDonald and Linde, 2002; Rieux et al., 2011; Smith et al., 1993). These types of studies also can inform management strategies that aim to prevent the spread of

pathogens and minimize the ecological and economic impacts of plant disease in natural and agricultural systems.

Swiss needle cast of Douglas-fir (*Pseudotsuga menziesii* (Mirb.) Franco) is a foliar disease caused by the ascomycete *Nothophaeocryptopus gaeumannii* (T. Rohde) Videira, C. Nakash., U. Braun & Crous. The inhibition of carbon assimilation caused by the blockage of stomata by the ascocarps (pseudothecia) of *N. gaeumannii* results in premature needle abscission, which further reduces photosynthetic capacity leading to growth impacts (Black et al., 2010; Maguire et al., 2011; Manter et al., 2003b, 2000; Stone et al., 2008). Although the disease was first described in Europe, its widespread presence in western North America was later recognized (Boyce, 1940; Hood, 1982; Meinecke, 1939). The fact that this fungus was widespread, but caused little disease in the native range of its host, together with the discovery of *N. gaeumannii* pseudothecia on Douglas-fir herbarium specimens that pre-date its emergence in Europe, suggest that it is endemic in the native range of Douglas-fir in western North America (Boyce, 1940; Meinecke, 1939). In the early 1980s, *N. gaeumannii* began to cause serious damage in Douglas-fir Christmas tree plantations in western Oregon and Washington (Hadfield and Douglass, 1982; Michaels and Chastagner, 1984) where its aggressiveness was apparently contrasted with its benign presence in nearby forest plantations and natural stands (Hadfield and Douglass, 1982). Particularly severe symptoms began to manifest in timber plantations in the vicinity of Tillamook, Oregon beginning in the mid 1980s and intensified over the following two decades, prompting increased interest in understanding the factors contributing to disease (Hansen et al., 2000; Shaw et al., 2011). Since then, the

disease has continued to intensify, and the affected area has expanded to include approximately 223,000 ha of symptomatic Douglas-fir forest in Oregon, and approximately 100,000 ha in Washington (Ramsey et al., 2015; Ritóková et al., 2016).

The possible existence of an aggressive race or genotype of *N. gauemannii* was first proposed by Boyce (1940) in his consideration of the various factors that might explain the emergence of SNC as a damaging disease in Europe. More recently, evidence from single-strand conformation polymorphisms (SSCPs) revealed that the *N. gaeumannii* population in the U.S. Pacific Northwest consisted of two distinct subpopulations (i.e. lineages) that appeared to be reproductively isolated (Winton et al., 2006). The spatial distribution of Lineage 2 seemed to coincide with variation in disease severity across the landscape, as it was most abundant near the coast where SNC was most severe, and was often absent from sites east of the Coast Ranges in Oregon and Washington where SNC was generally less severe. Compared to Lineage 1, Lineage 2 was twice as likely to be recovered from sites with severe SNC symptoms, and only half as likely to be recovered from healthier stands (Winton et al., 2006). Furthermore, stands having higher Lineage 2: Lineage 1 ratios had more sparse canopies and more severe foliage discoloration (Winton et al., 2006). These findings suggested that Lineage 2 may be more aggressive and may be an indication that selection for aggressive *N. gaeumannii* genotypes occurred where SNC symptoms were most severe (Winton et al., 2006). It is unclear from these observations whether this apparent aggressiveness of Lineage 2 may have contributed to the emergence or intensification of SNC in northwestern Oregon.

Although it has not been experimentally demonstrated, there is evidence to suggest that *N. gaeumannii* is capable of reproducing via selfing (i.e. homothallism) (Stone et al., 2008; Winton et al., 2006). Along with these observations, the assumption that ascospore deposition is more likely to occur within the same canopy in which the ascocarps were produced led Winton et al. (2006) to suggest that a single tree may, over time, become dominated by a single genotype. Those authors also suggested that finer-scale spatial analyses of genetic structure should be performed to further explore these phenomena.

This study was designed to address the following hypotheses 1) The two *N. gaeumannii* lineages are admixed within Douglas-fir stands in the Coast Range in northwestern Oregon where SNC has been most severe, 2) the two *N. gaeumannii* lineages are highly differentiated because they are reproductively isolated, 3) the genetic structure of the native *N. gaeumannii* population is influenced by homothallic reproduction, and 4) the spatial distributions of shared multilocus genotypes (MLGs) reflect the effective dispersal/migration distance of *N. gaeumannii*.

To address these goals, variation among 663 multilocus SSR genotypes representing 1,061 isolates of *N. gaeumannii* collected from 35 sites in western Oregon and Washington was analyzed. Samples were collected from multiple spatial scales ranging from several millimeters (within a single needle) to hundreds of kilometers (between Oregon and Washington). Analytical tools such as genotypic clustering, analysis of molecular variance (AMOVA), and bootstrap analysis of Nei's genetic

distance were employed to examine spatial genetic structure and differentiation among levels of a population hierarchy.

2.3 Materials and Methods

2.3.1 Foliage Sampling

Douglas-fir foliage was collected from long-term study sites arranged in a gridded plot network of privately-owned plantations in the western Coast Range in Oregon managed by the Oregon State University Swiss Needle Cast Cooperative (SNCC) (Ritóková et al. 2016). Samples were also collected from study sites in western Washington managed by the Washington Department of Natural Resources (Figure 2.1). Foliage samples were collected from 35 sites across five sampling blocks in Oregon and three sampling blocks in Washington. In 2014, samples were collected from nine sites in the Tillamook block in northwestern Oregon, three sites in the Florence block in central western Oregon, and two sites in the DNR block in southwestern Washington (Figure 2.1). In 2015, foliage was collected from four sites in the Newport block in northwestern Oregon, two additional sites in the Florence block, four sites in the Coos Bay block, and one site in the Gold Beach block on the southern Oregon coast (Figure 2.1). Also in 2015, samples were collected from the western Washington, with four sites in the southern Olympic Peninsula and five sites in the northern Olympic Peninsula (Figure 2.1). One additional site in the Gold Beach block was sampled in 2016. In Oregon, the sites within sampling blocks were stratified by distance from the coast. The sites ranged from 2 km from the shore to approximately 58 km inland, and from the southern border of Oregon to the northern Olympic Peninsula in Washington. The only exceptions were the Gold

Beach block, in which both sites were within a few km of the shoreline, and the DNR block in southwest Washington, where the sites were 48 and 57 km inland. In total, Douglas-fir foliage was collected from 35 sites for isolation of *N. gaeumannii*. Sampling in Oregon and southwest Washington was performed by researchers with the SNCC, while the sites in the Olympic Peninsula were sampled by the authors of this study. At each site, foliage was collected from second- and third-year internodes on secondary branches in the upper crowns of five randomly selected 10–30-year-old Douglas-fir trees. From one of the five trees sampled at each of the SNCC sites, foliage samples were also collected from the lower, mid, and upper crowns to capture within-tree diversity. The foliage was stored on ice and promptly returned to the campus of Oregon State University, and stored in a cold room for no longer than 5 days prior to processing.

2.3.2 Isolation of N. gaeumannii from Infected Foliage

Two-year-old needles bearing pseudothecia of *N. gaeumannii* were chosen arbitrarily for ascospore isolations. Double-sided adhesive tape was used to attach needles to the lids of 100 mm plastic Petri dishes. The needles were then suspended above water agar to allow ascospore discharge onto the agar surface below. After incubating at room temperature for 48–72 hours, individual germinating ascospores were excised from the agar with the aid of flame-sterilized forceps and transferred onto 2% malt agar (MA) (Difco Laboratories, Detroit, MI). Cultures were incubated at 17 °C for a minimum of 2–6 months to allow sufficient growth for DNA extraction and permanent storage.

2.3.3 DNA Extraction, Multiplex PCR, and SSR Genotyping

The DNeasy Plant Mini Kit (Qiagen, Hilden, Germany) was used to extract genomic DNA from vegetative mycelium. The manufacturer's protocol was modified with the addition of an initial maceration procedure. Agar plugs extracted from *N. gaeumannii* cultures were added to cryogenic vials along with sterile 3mm glass beads. The vials were briefly submerged in liquid nitrogen to freeze the agar plugs prior to shaking at 5000 rpm for 60 seconds with either a Mini-Beadbeater-1 (BioSpec Products, Bartlesville, OK, USA) or MP Bio FastPrep-24 (MP Biomedicals, Santa Ana, CA, USA).

For each isolate, ten SSR microsatellite loci (Winton et al. 2007b) were amplified in three multiplexed PCR reactions. The multiplexed reactions contained 2, 3, and 5 primer sets, each with a fluorescent dye label on the reverse primer to allow for the separation of overlapping alleles. The sequences of the primers were identical to those described in Winton et al. (2007b), but without the 18 bp M13 universal primer tails. The resulting amplicons were approximately 36 bp shorter than those produced using those primers. The Qiagen Type-It Microsatellite kit was used for PCR amplification. The PCR reactions were performed as recommended by the manufacturer, but with reaction volumes of 12.5 µl. A PTC-200 thermal cycler (MJ Research, Inc. Waltham, MA, USA) was used for the amplification, and was programmed as follows: 95 °C for 15 min, 30 cycles of 94 °C for 30 s, 57 °C for 90 s, and 72°C for 30 s, with a final extension at 60 °C for 30 min.

Each of the multiplexed PCR reactions was diluted by a factor of 10 in deionized water and submitted to the Center for Genome Research and Biocomputing (CGRB, Oregon State University, Corvallis, OR USA) for genotyping via capillary

electrophoresis on an ABI 3730 DNA Analyzer (Applied Biosystems, ThermoFisher Scientific Corporation, Waltham, MA USA) with the GS-500ROX size standard. The ABI GeneMapper 4.1 software (Applied Biosystems, ThermoFisher Scientific Corporation, Waltham, MA USA) was used to assign alleles and genotypes. Microsatellite alleles were called using a custom analysis method in the GeneMapper software, and were also validated visually for each locus and isolate. A positive control isolate was included to ensure that each independent PCR amplification and genotyping run resulted in consistent allele sizing. One of the loci, Pgdi5, did not amplify consistently across all isolates and was omitted from subsequent analyses.

2.3.4 Data Analysis

The multilocus genotypes (MLGs) consisting of alleles for the 9 SSR loci were formatted in Microsoft Excel 2016 with GenAlEx 6.503 (Peakall and Smouse, 2012, 2006), and imported into R version 3.4.1 (R Core Team 2017) for use with the R packages *poppr* version 2.5.0 (Kamvar et al., 2015, 2014), *adegenet* 2.0.1 (Jombart, 2008), and *ade4* 1.7-8 (Dray and Dufour, 2007). Analyses were performed with a population hierarchy that included levels for lineages, states within lineages, sites within states, and trees within sites. Implementation and interpretation of *poppr* graphics, as well as source code for modifying *poppr* output, was adapted from http://grunwaldlab.github.io/Population_Genetics_in_R/ (Grünwald et al., 2016). Maps were constructed with the R packages *ggplot2*, *ggsn, mapplots*, and *shapefiles* (Baquero, 2017; Gerritsen, 2014; Stabler, 2013; Wickham, 2016).

The membership of each isolate in either Lineage 1 or Lineage 2 was determined by genotypic clustering with a UPGMA dendrogram based on 10,000 bootstrap replicates of Nei's genetic distance (Nei, 1978) performed with the aboot function in the *poppr* R package (Kamvar et al., 2015, 2014). The dendrogram was visualized with the R package *ggtree* version 1.12.0 (Yu et al., 2017).

Estimates of genetic diversity were calculated with the R package *poppr* (Kamvar et al., 2015, 2014), and included genotypic diversity (Shannon-Weiner index, H) and Nei's unbiased gene diversity (H_e) (Nei, 1978). Because genotypic diversity estimates are sensitive to differences in sample size, H was estimated from 1,000 iterations of a bootstrap analysis with rarefaction. This function sub-sampled the data such that the number of samples in each group was equal to the sample size of the group with the fewest samples, with a minimum rarefaction sample size of $n \geq 10$. Thus, the genotypic diversity estimates could be directly compared among lineages, states, and sites with unequal sample sizes. Genotypic richness was estimated as the number of expected multilocus genotypes (eMLG) with a rarefaction sample size of $n \geq 10$.

A genotype accumulation curve indicating the ability to discriminate between individuals given the number of loci sampled, was calculated in the *poppr* R package (Kamvar et al., 2015, 2014). This curve was constructed by estimating the number of MLGs in 1,000 random samples across n-1 loci. Rarefaction curves depicting the expected genotypic richness for a given sample size were produced with the R package *vegan* (Oksanen et al., 2017).

The effect of the reproductive mode and population subdivision on the genetic structure of the populations was inferred by examining linkage disequilibrium. The standardized multilocus index of association, $\bar{r}_d$ (Agapow and Burt, 2001), was calculated with the R package *poppr* (Kamvar et al., 2015, 2014). Analyses were performed with the full dataset, on a clone-censored dataset (to eliminate the influences of repeated MLGs), and on the two lineages separately (to eliminate the influence of reproductively-isolated subpopulations). The observed values of $\bar{r}_d$ were plotted in relation to those obtained from simulated populations in linkage equilibrium. The probability of obtaining the observed value of $\bar{r}_d$, or more extreme, under the null hypothesis of no linkage among loci (H_0: $\bar{r}_d = 0$) was calculated from 999 permutations of the data.

Genetic structure due to differentiation among subpopulations was evaluated with analysis of molecular variance (AMOVA) (Excoffier et al., 1992), implemented with the R package *poppr* (Kamvar et al., 2015, 2014) utilizing the *ade4* implementation (Dray and Dufour, 2007). This method partitioned the genetic variance within and among populations and subpopulations at all levels of the population hierarchy, which was clone-censored with respect to the lowest hierarchical level (i.e. tree). Fixation indices (ϕ statistics) were interpreted as measures of subpopulation differentiation (Excoffier et al., 1992). The probability of obtaining the observed ϕ, or more extreme, under the null hypothesis of no differentiation between subpopulations (H_0: $\phi = 0$) was obtained with 1,000 permutations of the data, as implemented in the R package *ade4* (Dray and Dufour, 2007).

An additional metric, G'_{ST} (Hedrick, 2005), was used to estimate genetic differentiation between the two *N. gaeumannii* lineages. This measure is scaled such that the value for two populations that do not share any alleles is one, and the value for population pairs that do not have any unique alleles (i.e. all alleles are shared), is equal to zero (Hedrick, 2005). Statistics such as G'_{ST} are directly linked to the effective number of migrants (N_m) when the rate of gene flow between populations is higher than the mutation rate within populations (Balloux and Lugon-Moulin, 2002; Hedrick, 2005). Because they incorporate both migration and mutation, the genetic structuring estimated from differentiation statistics reflects both the rate of exchange of alleles between populations and the time since divergence (Balloux and Lugon-Moulin, 2002).

The genetic differentiation among sites within each state (OR, WA) was further examined with discriminant analysis of principal components (DAPC), a multivariate analysis of genetic clustering among genotypes (Jombart et al., 2010). The function *xvaldapc* from the R package *adegenet* (Jombart, 2008) was utilized to select the appropriate number of principal components (PCs) corresponding to the lowest Mean Squared Error, with a training set consisting of 90% of the data (Jombart and Collins, 2015). The function scatter.dapc from the R package *adegenet* (Jombart, 2008) was used to visualize the results. This function produced a 2-dimensional scatterplot with axes for each of the first two discriminant functions and each isolate represented as a point. In this analysis, variations in allele frequencies were partitioned among groups within an analysis of variance (ANOVA) framework. Here, the separation between groups in the DAPC plot is proportional to the *F*-statistic, which represents the ratio of between-group

variances to within-group variances. DAPC results in linear combinations of principal components (equivalent to linear combinations of alleles) that best describe the differentiation between groups by maximizing *F*, and thus maximizing between-group variance (Jombart et al., 2010).

To assess isolation by distance, Mantel's test (Mantel, 1967) was performed with the R package *ade4* (Dray and Dufour, 2007). This test utilized a regression approach to test for a statistical correlation between a matrix containing pairwise Euclidean geographic distances between each of the 35 sample sites and a matrix containing pairwise genetic distances between the sites. A Euclidean genetic distance measure, Roger's distance (Rogers, 1972), was calculated with the R package *adegenet* (Jombart, 2008). A randomization test with 10,000 permutations was employed to test the null hypothesis of no correlation between genetic distance and geographic distance (H_0: $r = 0$). Multilocus genotypes that were shared across populations were identified using the function mlg.crosspop from the R package *poppr*. For estimating the distances between sites with shared MLGs, the geodesic distances between sites were calculated in R using the *Imap* package (Wallace, 2012).

2.4 Results

2.4.1 Genetic diversity

This study included a total of 1,061 isolates collected from 35 sites in western Oregon and Washington from 2014 to 2016. Of the total, 646 isolates had MLGs indicative of Lineage 1, and 415 isolates had MLGs characteristic of Lineage 2 (Table 2.1). In total, 403 Lineage 1 isolates had distinct MLGs, while 260 Lineage 2 isolates had

distinct MLGs (Table 2.1). Of the 657 isolates collected in Oregon, 384 had distinct MLGs, and of the 404 isolates collected in Washington, 282 had distinct MLGs (Table 2.2). Total gene diversity (H_e) for the 1,061 isolates was 0.82 (Table 2.2). Overall, Lineage 1 had higher genotypic diversity, genotypic richness, and gene diversity than Lineage 2, even after correction for the difference in sample sizes via rarefaction (Table 2.2). The isolates collected in Oregon had higher gene diversity than those collected in Washington (Table 2.2).

A genotype accumulation curve began to plateau at eight loci, indicating that nine SSR loci would be adequate to discriminate between individuals and capture most of the genotypic diversity (Figure S2.1). A rarefaction curve depicting genotypic richness (i.e. the number of observed MLGs) indicated that we did not capture all of the genotypic richness expected in the two lineages, and that we would expect to discover new MLGs with continued sampling (Figure S2.2).

2.4.2 Spatial distributions of multilocus genotypes

The MLGs corresponding to the two *N. gaeumannii* lineages varied in their relative abundances across the 35 sites sampled in the Oregon and Washington Coast Ranges (Figure 2.2). Sites containing Lineage 2 exclusively occurred within a few kilometers of the coast, ranging in latitude from the California border (42º N) to just north of Newport, Oregon (~45 º N; Figure 2.1A). From Tillamook to the northern border of Oregon, the lineages were recovered in roughly equal proportions from sites nearest the coast. At the southern end of the sampling range, Lineage 2 was present at sites as far as 57 km inland, but from Newport north, Lineage 2 was absent from the furthest inland

sites (Figure 2.1A). The lineages exhibited similar distributions in Washington. The southwestern Washington sites were approximately 48–58 km inland, but consisted of both lineages. Along the southern end of the Olympic Peninsula Lineage 2 was present in very high relative abundances at the coast (WDNRQ), but was absent from the easternmost site (WDNR32) (Figure 2.1B). At the northern Olympic Peninsula sites, Lineage 2 was more abundant in sites near the coast, and less abundant further inland even though the furthest inland sites were near the Strait of Juan de Fuca (Figure 2.1B).

There were 27 MLGs recovered from more than one site, three of which were recovered from both Oregon and Washington sites (Table 2.2). The distances between sites with shared MLGs ranged from 1.4 km to 307 km, with a mean of 83 km (Table 2.3). The most common genotype (MLG 548) was shared by 19 isolates recovered from seven sites in both Oregon and Washington (Figure 2.3 A, C). A total of 50 MLGs were recovered from more than one tree, 23 of which were shared among trees within the same site, and 27 of which contributed to the MLGs shared among sites (Figure 2.3 B, C). Mantel's test revealed a weak, but significant, positive correlation between the geographic distance matrix and the genetic distance matrix ($r = 0.139$, $P = 0.039$), and thus only a very small proportion of the genetic divergence among sites could be explained by the geographic distance between them.

2.4.3 Population structure and differentiation

The hierarchical analysis of molecular variance (AMOVA) allowed for the estimation of genetic differentiation between the *N. gaeumannii* subpopulations represented by lineages, states, blocks, sites, and trees. Most of the genetic variance was

partitioned to the within-tree component (61.27%, Table 2.4). Approximately 30% of the total genetic variance was partitioned to the between-lineages component, 0.35% between states, 0.26% between blocks within states, and 3.95% between sites within blocks (Table 2.4). The remaining genetic variance (4.74%) occurred among trees within sites (Table 2.4). Although the AMOVA revealed significant subpopulation differentiation at all levels except for blocks within states, the subpopulations that were most strongly differentiated were the two lineages ($G'_{ST} = 0.942$; $\phi_{LT} = 0.294$, $P < 0.001$) (Table 2.4). There was weak, but significant, genetic differentiation between Oregon and Washington ($\phi_{SL} = 0.005$, P= 0.033) (Table 2.4). Moderate genetic differentiation was detected among sites within blocks, and among trees within sites ($\phi_{SB} = 0.056$, $P < 0.001$; $\phi_{TS} = 0.072$, $P < 0.001$) (Table 2.4).

When all 1,061 isolates were analyzed, estimates of the standardized index of association ($\bar{r}_d$) (Agapow and Burt, 2001) were significantly higher than those from 999 simulated populations in linkage equilibrium ($\bar{r}_d = 0.165$, $P = 0.001$) (Figure 2.4A). When the clones (i.e. repeated MLGs) were removed, the index of association decreased ($\bar{r}_d = 0.146$, $P = 0.001$) (Figure 2.4B). The values were still significantly greater than 0 when the lineages were analyzed separately ($\bar{r}_d = 0.035$, $P = 0.001$; $\bar{r}_d = 0.029$, $P = 0.001$ for Lineage 1 and Lineage 2, respectively) (Figure 2.4C, D).

The DAPC bar plots representing the probability of membership of each isolate in clusters representing Oregon and Washington suggested that each of the genotypes had some probability of membership in both clusters (Figure 2.5A). When groups of sites corresponding to the sampling blocks (Figure 2.2, Table 2.2) were analyzed individually

with DAPC, it appeared that the isolates collected from coastal sites were differentiated from those at sites further inland (Figure 2.5B-G). For example, when DAPC was performed with only the sites in the Newport block, isolates collected from the two sites nearest the coast (N0-1 and N5-2) clustered together, but were separated from the clusters representing the isolates collected from sites further inland (N15-3 and N25-5) (Figure 2.5C). There was also considerable separation between the clusters representing the isolates from inland sites N15-3 and N25-5 (Figure 2.5C). The same general trend was observed when the sites in the Florence block were analyzed with DAPC. Isolates collected from the sites closest to the coast (F0-2 and F5-1) clustered together, but were separated from the isolates collected at sites further inland (F15-1, F15-3, and F25-2). Here, the sites further inland clustered together with considerable overlap (Figure 2.5D). Similar trends were observed for isolates collected from sites in the Tillamook (Figure 2.5B), Coos Bay (Figure 2.5E), and Olympic Peninsula blocks (Figure 2.5F, G).

In the UPGMA dendrogram constructed from a bootstrap analysis of Nei's distance, isolates from the two lineages clustered into two distinct groups separated by large genetic distances (Figure 2.6). There appeared to be some genetic structure within Lineage 1, as evidenced by the presence of several internal clusters. The within-tree sampling strategy implemented in this study indicated that the two lineages co-occurred within trees, and that a given tree may be occupied by as many as 20 distinct MLGs (Figure 2.7). Several distinct MLGs were also detected in collections of isolates from individual Douglas-fir needles. In one needle collected from WDNR66, five distinct MLGs were detected and all clustered with Lineage 1 (Figure 2.8A). A collection of

isolates from an individual needle from WDNRQ revealed the presence of both Lineages 1 and 2, with three distinct Lineage 2 MLGs and one Lineage 1 MLG (Figure 2.8B).

2.5 Discussion

The genetic structure of *N. gaeumannii* in Oregon and Washington reflects the presence of two strongly differentiated non-interbreeding lineages (Table 2.2, Figure 2.5) (Bennett and Stone, 2016; Winton et al., 2006). The geographic distributions of these two lineages in Oregon, assessed here with multilocus SSR genotypes, support and expand upon the findings of Winton et al. (2006) where the distributions of the lineages were assessed on the basis of single-strand conformation polymorphisms (SSCPs). However, that study did not detect Lineage 2 in Washington. The analyses presented here indicate that Lineage 2 has similar geographic distributions in Oregon and Washington. The relative abundances of the lineages varied across a west-east gradient, with Lineage 2 most abundant relative to Lineage 1 in sites near the coast and decreasing in relative abundance away from the coast. At sites approximately 40–56 km inland, Lineage 2 was supplanted entirely by Lineage 1 in some cases. One site near Coos Bay, Oregon (CB5-2) did not fit this trend, as it was within 25 km of the coast, but all of the isolates sampled from two separate trees at this site were Lineage 1 (Table 2.1, Figure 2.2A). This was anomalous, considering that the isolates sampled from a site just a few kilometers to the west were all Lineage 2, and both lineages were recovered from the closest sites to the northeast (Figure 2A). This suggests that little gene flow is occurring between these sites, even though they are only a few kilometers apart. Considering its location and the fact that Lineage 2 was present at nearby sites, site CB5-2 may have harbored both lineages,

but Lineage 2 might not have been detected due to sampling bias (this site had the smallest sample size, N = 8 isolates), or the trees planted at that site (a commercial forest plantation) may have been sourced from an infected plantation or nursery further east, where Lineage 2 is generally less abundant or absent.

These results seem to be in agreement with the findings of Winton et al. (2006), which suggested that the contemporary distributions of the two lineages reflects their evolutionary origins. The findings of Winton et al. (2006) and the current study are in agreement that the contemporary distributions suggest that Lineage 2 is native the southern Oregon coast, and that Lineage 1 is native to the Douglas-fir region further north and inland. The fact that they are now sympatric in the western Oregon Coast Range suggests that they may have experienced a recent range expansion.

Lineage 1 had higher genotypic diversity, genotypic richness, and gene diversity than Lineage 2. The two lineages accounted for the majority of between-population genetic variance (Table 2.4). There was also strong genetic differentiation between the two lineages, as evidenced by the results of the AMOVA (Table 2.4) and the value of G'_{ST}. Further evidence for the strong differentiation between lineages was shown in the UPGMA dendrogram constructed from a bootstrap analysis of Nei's genetic distance. That analysis resolved two distinct clusters representing the isolates from the two lineages, and these clusters were separated by large genetic distances reflecting their divergence (Figure 2.6). This is in agreement with the results of previous analyses that suggested that the lineages were reproductively isolated (Bennett and Stone, 2016; Winton et al., 2006). This apparent lack of recombination between lineages influenced

our estimates of linkage disequilibrium, as linkage was considerably higher in the analyses where both lineages were included (Figure 2.4A, B) compared to those where the lineages were analyzed separately (Figure 2.4C, D). All of these results provide evidence that there is a lack of interbreeding between the two lineages, and bolster previous findings that suggested that they are separate species by the biological and phylogenetic species concepts (Winton et al., 2001).

The presence of repeated MLGs within the two lineages also contributed to this genetic structure, as lower values of $\bar{r}_{\mathrm{d}}$ resulted when the data were clone-corrected (Figure 2.3B). These values were nevertheless still significantly greater than zero ($P < 0.001$) (Figure 2.3B) suggesting that the population structure is clonal, even though *N. gaeumannii* is not known to reproduce asexually. Homothallism (i.e. self-fertilization) could result in the repeated MLGs observed here. Although this reproductive mode likely contributes to the genetic structure of *N. gaeumannii*, the level of genetic variation observed suggests that outcrossing also occurs.

Genetic diversity did not differ between the *N. gaeumannii* isolates collected in Oregon and Washington, and the AMOVA indicated very weak genetic differentiation between the *N. gaeumannii* isolates from these two states (Tables 2.2, 2.4). This was supported by the DAPC analysis which showed shared membership probabilities among genotypes from Oregon and Washington (Figure 2.4A). The results of the AMOVA and DAPC, along with the fact that there were shared *N. gaeumannii* genotypes between the isolates collected in the two states, suggest that either there has been contemporary gene flow between them, or that they have shared ancestry. Along with the fact that genetic

diversity did not differ between the *N. gaeumannii* isolates collected in Oregon and Washington, these observations are consistent with assertions that Douglas-fir and *N. gaeumannii* are native to this region and both the fungus and the host have a contiguous range throughout Oregon and Washington.

The *N. gaeumannii* isolates collected in Oregon and Washington were not differentiated, but the isolates collected from sites within sampling blocks in the two states were moderately differentiated (Table 2.4). The DAPC provided additional support for this, and suggested that there was some genetic differentiation between the isolates collected at coastal sites (those that were within 16 km of the shore) and those that were collected at inland sites (those that were 40-60 km from the shore), but that neither were differentiated from the sites in between (Figure 2.4B-G). This likely reflects the differentiation between lineages, as Lineage 2 generally makes up a larger proportion of the populations at coastal sites, and a much lower proportion of the populations at inland sites. Whether the observed distribution of MLGs is the result of dispersal distance limitations, or some selective factor (e.g. climate) that limits the survival of the coastal Lineage 2 isolates at sites further inland, is not clear. It is also possible that the observed spatial distributions of the two lineages are influenced by the human-mediated movement of infected Douglas-fir seedlings.

The *N. gaeumannii* isolates collected from trees within sites were moderately differentiated, but most of the genetic variation in the population occurred within trees, suggesting that *N. gaeumannii* isolates migrate between trees (Table 2.4). The observed differentiation could result from autocthonous dispersal, where *N. gaeumannii* spores are

deposited on foliage within the same tree. That would be consistent with previous assertions that dispersal between trees might be limited (Winton et al., 2006), except that those authors posited that a given tree might be predominately infected by a single *N. gaeumannii* genotype. If this were the case, we might expect to see stronger genetic differentiation between the isolates collected from trees within each site, and little genetic variance partitioned to the within-tree component. It was particularly interesting to discover that several distinct genotypes could be isolated from a single tree (Figure 2.7). This, along with the results of the AMOVA (Table 2.4) and the observed spatial distributions of shared MLGs (Figure 2.3, Table 2.3), suggest that gene flow occurs between trees in the same site.

There was a very weak, but significant, relationship between the geographic and genetic distance matrices ($r = 0.139$, $P = 0.039$), indicating that isolates collected from sites that were more distant from one another were more dissimilar than those collected from sites closer together, but that only a small proportion of the genetic divergence could be explained by distance. The spatial distributions of shared *N. gaeumannii* MLGs in Oregon and Washington may provide a reasonable estimate of dispersal distance only if we assume that identical MLGs occurring across states and across sites are identical by descent (i.e. are not the result of homoplasy), and are the result of aerial ascospore dispersal rather than human-mediated dispersal. Although our sampling distribution covered a contiguous range of approximately 684 km along the coast from the southern Oregon border to the northern Olympic Peninsula in Washington (Figure 2.1), the furthest distance between sites with shared MLGs was only 307 km (Table 2.3). We

cannot be certain whether this reflects long distance aerial ascospore dispersal between sites, or whether distant sites might be linked by ascospore dispersal that occurs over shorter distances, as was suggested for another plant-pathogenic ascomycete *Mycosphaerella graminicola* (Linde et al., 2002).

Our assessments of within-needle diversity suggested that a single Douglas-fir needle may be colonized by multiple *N. gaeumannii* genotypes, including genotypes from both lineages (Figure 2.8). As many as five distinct genotypes were present in a single needle (Figure 2.8B). This demonstrates that each needle may be independently infected by multiple ascospores, and that the pseudothecia on a given needle represent a mosaic of fungal genotypes. This mosaic of genotypes in a single infection is not uncommon for plant pathogens, as multiple genotypes of *M. graminicola* are known to occur in a single lesion (Linde et al., 2002). Those authors also suggested that the different pathogen genotypes within a lesion may compete with one another (Linde et al., 2002). This idea is relevant in the present study as well, as the region where SNC is most severe (Navarro and Norlander, 2016; Ramsey et al., 2015; Ritóková et al., 2016) corresponds to the region where populations are admixed (i.e. the lineages co-occur) (Figure 2.2). This could be investigated further by performing controlled inoculation trials where some trees are inoculated with genotypes from both lineages. The presence of both lineages within a given needle also supports the assertion that the lineages are reproductively isolated due to genetic incompatibility, as it would be unlikely that they could maintain such a high degree of genetic differentiation if they were reproductively compatible and sympatric at such minute spatial scales.

The sampling strategies implemented here allowed for a fine-scale assessment of population structure. However, differences in sample sizes among the levels of our population hierarchy may have contributed to some bias in our analyses. Although the total sample size was quite large, there was unequal sampling among states, sites, and trees within sites. Our assessment of the geographic distributions of the two *N. gaeumannii* lineages would have benefited from larger samples of isolates from some sites. Genotypic diversity and richness are also very sensitive to differences in sample sizes among the groups that are being compared (Grünwald et al., 2003). We attempted to account for this by performing these calculations with rarefied samples, but there still may have been some downward bias in our estimates of diversity and richness for sites from which there were few samples. A rarefaction genotypic richness curve suggested that we did not capture all of the expected genetic variation in the two lineages with the numbers of samples in our dataset (Figure S2.2). This suggests that we would have continued to discover new genotypes had we continued to sample additional isolates. One of the SSR loci, Pgdi5 (Winton et al., 2007) proved to be particularly problematic in that it did not amplify consistently across samples, even when higher concentrations of the primer were added and other modifications were made to the PCR protocol. This was curious, given that there was very successful and consistent amplification of the other loci, regardless of modifications to the PCR protocol. Consequently, this locus was omitted from the analyses, and its omission may have diminished our ability to distinguish between some individuals. However, the genotype accumulation curve (Figure S2.1) indicated that 97% of the observed MLGs could be discriminated with only

eight loci, and thus we can infer that the loci used here were adequate to describe the majority of the genotypic variation in our data.

These analyses have provided a case study for some of the factors influencing the genetic structure of a native fungal plant pathogen population. Given that there may be an association between the spatial distributions of MLGs and SNC severity, some knowledge of the genetic structure of *N. gaeumannii* populations in a region with high SNC severity may be useful for informing future management strategies. For instance, the spatial distribution of Lineage 2 may be a good predictor of SNC severity, and thus land managers may choose to survey the *N. gaeumannii* population as part of an SNC risk assessment process. Future studies should assess the relative aggressiveness of the two lineages, as well as genotypes that are abundant where SNC is most severe. Modern genomic techniques such as genome-wide association studies (GWAS) may provide better resolution in future investigations of the factors influencing *N. gaeumannii* population structure, and may allow for an examination of the genomic variation associated with SNC disease severity, the environment, and Douglas-fir timber management strategies.

2.6 Acknowledgements

The authors thank Michelle Agne, Gabriela Ritóková, and Dave Shaw who helped coordinate the sampling efforts in the Swiss Needle Cast Cooperative (SNCC) plot network in Oregon and provided foliage samples for this study. Thanks to Dan Omdal and Amy Ramsey for coordinating the sampling in Washington, and assisting with field collections. Thank you to the many landowners who allowed access to their lands. W. Sutton and P. Reeser provided invaluable assistance in the laboratory, and J. Tabima and Z. Kamvar provided technical support and assisted in the interpretation of *poppr* and *adegenet* analyses. The authors would also like to express their sincere gratitude and appreciation for the work performed by L. Winton without which these studies would not have been possible. Funding was provided by the Oregon State University Swiss Needle Cast Cooperative (SNCC), the Portland Garden Club, the Cascade Mycological Society, Oregon Mycological Society, Puget Sound Mycological Society, the USDA Forest Service, the Oregon Lottery Graduate Student Scholarship, the Washington Department of Natural Resources and the Quinault Indian Nation.

2.7 Literature Cited

Agapow, P., Burt, A., 2001. Indices of multilocus linkage disequilibrium. *Molecular Ecology Notes* 1, 101–102.

Balloux, F., Lugon-Moulin, N., 2002. The estimation of population differentiation with microsatellite markers. *Molecular Ecology* 11, 155–165.

Baquero, O.S., 2017. ggsn: North symbols and scale bars for maps created with "ggplot2" or "ggmap". R package version 0.4.0. https://CRAN.R-project.org/package=ggsn

Bennett, P., Stone, J., 2016. Assessments of population structure, diversity, and phylogeography of the Swiss needle cast fungus (*Phaeocryptopus gaeumannii*) in the U.S. Pacific Northwest. *Forests* 7, 14. doi: 10.3390/f7010014.

Black, B.A., Shaw, D.C., Stone, J.K., 2010. Impacts of Swiss needle cast on overstory Douglas-fir forests of the western Oregon Coast Range. *Forest Ecology and Management* 259, 1673–1680. doi: 10.1016/j.foreco.2010.01.047

Boyce, J.S., 1940. A needle-cast of Douglas fir associated with *Adelopus gaumanni*. *Phytopathology* 30, 649–659.

Dray, S., Dufour, A.B., 2007. The *ade4* package: implementing the duality diagram for ecologists. *Journal of Statistical Software* 22, 1–20.

Excoffier, L., Smouse, P.E., Quattro, J.M., 1992. Analysis of molecular variance inferred from metric distances among dna haplotypes: application to human mitochondrial DNA restriction data. *Genetics Society of America* 131, 479–491.

Gerritsen, H., 2014. mapplots: Data Visualization on Maps. R package version 1.5. https://CRAN.R-project.org/package=mapplots

Grünwald, N.J., Goodwin, S.B., Milgroom, M.G., Fry, W.E., 2003. Analysis of genotypic diversity data for populations of microorganisms. *Phytopathology* 93, 738–746.

Grünwald, N.J., McDonald, B.A., Milgroom, M.G., 2016. Population genomics of fungal and Oomycete pathogens. *Annual Review of Phytopathology* 54, 323–346. doi: 10.1146/annurev-phyto-080614-115913

Hadfield, J., Douglass, B.S., 1982. Protection of Douglas-fir Christmas trees from Swiss needle cast in Oregon. *American Christmas Tree Journal* 26, 31–33.

Hansen, E.M., Stone, J.K., Capitano, B.R., Rosso, P., Sutton, W., Winton, L., Kanaskie, A., McWilliams, M.G., 2000. Incidence and impact of Swiss needle cast in forest plantations of Douglas-fir in coastal Oregon. *Plant Disease* 84, 773–778.

Hedrick, P.W., 2005. A standardized genetic differentiation measure. *Evolution* 59, 1633–1638.

Hood, I.A., 1982. *Phaeocryptopus gaeumannii* on *Pseudotsuga menziesii* in southern British Columbia. *New Zealand Journal of Forestry Science* 12, 415–24.

Jombart, T., 2008. adegenet: a R package for the multivariate analysis of genetic markers. *Bioinformatics* 24, 1403–1405. doi: 10.1093/bioinformatics/btn129

Jombart, T., Collins, C., 2015. A tutorial for discriminant analysis of principal components (DAPC) using *adegenet* 2.0.0. London: Imperial College London, MRC Centre for Outbreak Analysis and Modelling.

Jombart, T., Devillard, S., Balloux, F., 2010. Discriminant analysis of principal components: a new method for the analysis of genetically structured populations. *BMC Genetics* 11, 1. doi:10.1186/1471-2156-11-94.

Kamvar, Z.N., Brooks, J.C., Grunwald, N.J., 2015. Novel R tools for analysis of genome-wide population genetic data with emphasis on clonality. *Frontiers in Genetics* 6. doi: 10.3389/fgene.2015.00208

Kamvar, Z.N., Tabima, J.F., Grünwald, N.J., 2014. *Poppr*: an R package for genetic analysis of populations with clonal, partially clonal, and/or sexual reproduction. *PeerJ* 2, e281. doi: 10.7717/peerj.281.

Linde, C.C., Zhan, J., McDonald, B.A., 2002. Population structure of *Mycosphaerella graminicola*: from lesions to continents. *Phytopathology* 92, 946–955.

Maguire, D.A., Mainwaring, D.B., Kanaskie, A., 2011. Ten-year growth and mortality in young Douglas-fir stands experiencing a range in Swiss needle cast severity. *Canadian Journal of Forest Research* 41, 2064–2076. doi: 10.1139/x11-114.

Mantel, N., 1967. The detection of disease clustering and a generalized regression approach. *Cancer Research* 27, 209–220.

Manter, D.K., Bond, B.J., Kavanagh, K.L., Rosso, P.H., Filip, G.M., 2000. Pseudothecia of Swiss needle cast fungus, *Phaeocryptopus gaeumannii*, physically block stomata of Douglas fir, reducing CO_2 assimilation. *The New Phytologist* 148, 481–491.

Manter, D.K., Bond, B.J., Kavanagh, K.L., Stone, J.K., Filip, G.M., 2003. Modelling the impacts of the foliar pathogen, *Phaeocryptopus gaeumannii*, on Douglas-fir physiology: net canopy carbon assimilation, needle abscission and growth. *Ecological Modelling* 164, 211–226. doi: 10.1016/S0304-3800(03)00026-7.

McDonald, B.A., Linde, C., 2002. Pathogen population genetics, evolutionary potential, and durable resistance. *Annual Review of Phytopathology* 40, 349–379. doi: 10.1146/annurev.phyto.40.120501.101443.

Meinecke, E.P., 1939. The *Adelopus* needle cast of Douglas fir on the Pacific Coast. Dept. of Natural Resources, Division of Forestry, Sacramento, California.

Michaels, E., Chastagner, G.A., 1984. Distribution, severity, and impact of Swiss needle cast in Douglas-fir Christmas trees in western Washington and Oregon. *Plant Disease* 68, 939–942.

Navarro, S., and Norlander, D., 2016. Swiss needle cast aerial survey. pp. 7–11 in *Swiss Needle Cast Cooperative Annual Report 2016*, Ritóková, G., and Shaw, D. (eds.). College of Forestry, Oregon State University, Corvallis, OR. http://sncc.forestry.oregonstate.edu/annual-reports http://www.oregon.gov/ODF/ForestBenefits/Pages/ForestHealth.aspx

Nei, M., 1978. Estimation of average heterozygosity and genetic distance from a small number of individuals. *Genetics* 89, 583–590.

Oksanen, J., Guillaume, B., Friendly, M., Kindt, R., Legendre, P., McGlinn, D., Minchin, P.R., O'Hara, R.B., Simpson, G.L., Solymos, P., Stevens, M.H.H., Szoecs, E., Wagner, H., 2017. vegan: community ecology package. R package version 2.4-5. https://CRAN.R-project.org/package=vegan

Peakall, R., Smouse, P.E., 2012. GenAlEx 6.5: genetic analysis in Excel. Population genetic software for teaching and research--an update. *Bioinformatics* 28, 2537–2539. doi: 10.1093/bioinformatics/bts460.

Peakall, R., Smouse, P.E., 2006. GenAlEx 6: genetic analysis in Excel. Population genetic software for teaching and research. *Molecular Ecology Notes* 6, 288–295. doi: 10.1111/j.1471-8286.2005.01155.x

R Core Team. 2017. R: A language and environment for statistical computing. R Foundation for Statistical Computing, Vienna, Austria. https://www.R-project.org.

Ramsey, A., Omdal, D., Dozic, A., Kohler, G., and Boderck, M., 2015. Swiss needle cast aerial and ground survey coastal Washington. pp. 12-18 in *Swiss Needle Cast Cooperative Annual Report 2015*. Ritóková, G., and Shaw, D. (eds.). College of Forestry, Oregon State University, Corvallis, OR. http://sncc.forestry.oregonstate.edu/annual-reports

Rieux, A., Halkett, F., De Lapeyre de Bellaire, L., Zapater, M.-F., Rousset, F., Ravigne, V., Carlier, J., 2011. Inferences on pathogenic fungus population structures from microsatellite data: new insights from spatial genetics approaches. *Molecular Ecology* 20, 1661–1674. doi: 10.1111/j.1365-294X.2011.05053.x.

Ritóková, G., Shaw, D., Filip, G., Kanaskie, A., Browning, J., Norlander, D., 2016. Swiss needle cast in western Oregon Douglas-fir plantations: 20-year monitoring results. *Forests* 7, 155. doi: 10.3390/f7080155.

Rogers, J.S., 1972. Measures of genetic similarity and genetic distances. In: Studies in Genetics. University of Texas Publishers, pp. 145–153.

Shaw, D.C., Filip, G.M., Kanaskie, A., Maguire, D.A., Littke, W.A., 2011. Managing an epidemic of Swiss needle cast in the Douglas-fir region of Oregon: the role of the Swiss needle cast cooperative. *Journal of Forestry* 109, 109–119.

Smith, J.M., Smith, N.H., O'Rourke, M., Spratt, B.G., 1993. How clonal are bacteria? *Proceedings of the National Academy of Sciences* 90, 4384–4388.

Stabler, B., 2013. shapefiles: Read and write ESRI shapefiles. R package version 0.7. https://CRAN.R-project.org/package=shapefiles

Stone, J.K., Capitano, B.R., Kerrigan, J.L., 2008. The histopathology of *Phaeocryptopus gaeumannii* on Douglas-fir needles. *Mycologia* 100, 431–444.

Wallace, J.R., 2012. Imap: interactive mapping. R package version 1.3.2. https://CRAN.R-project.org/package=Imap

Wickham, H., 2016. ggplot2: Elegant graphics for data analysis. Springer-Verlag, New York. http://ggplot2.org

Winton, L.M., 2001. Phylogenetics, population genetics, molecular epidemiology, and pathogenicity of the Douglas-fir Swiss needle cast pathogen *Phaeocryptopus gaeumannii*. PhD dissertation. Oregon State University, Corvallis, Oregon.

Winton, L.M., Hansen, E.M., Stone, J.K., 2006. Population structure suggests reproductively isolated lineages of *Phaeocryptopus gaeumannii*. *Mycologia* 98, 781–791.

Winton, L.M., Stone, J.K., Hansen, E.M., 2007. Polymorphic microsatellite markers for the Douglas-fir pathogen *Phaeocryptopus gaeumannii*, causal agent of Swiss

needle cast disease. *Molecular Ecology Notes* 7, 1125–1128. doi: 10.1111/j.1471-8286.2007.01802.x

Yu, G., Smith, D.K., Zhu, H., Guan, Y., Lam, T.T.-Y., 2017. ggtree: an R package for visualization and annotation of phylogenetic trees with their covariates and other associated data. *Methods in Ecology and Evolution* 8, 28–36. doi: 10.1111/2041-210X.12628.

2.8 Figures and Tables

Table 2.1: Sample sizes and diversity estimates for the two *Nothophaeocryptopus gaeumannii* lineages.

	N_{sites}	$N_{isolates}$	MLG[a]	eMLG[b]	SE[c]	H^{d*}	H_e^{e}
Lineage 1	28	646	403	290	5.66	5.48	0.70
Lineage 2	31	415	260	260	0.00	5.35	0.63
Total	35	1061	663	323	6.74	5.66	0.82

[a] MLG= number of multilocus genotypes, [b] eMLG = expected number of multilocus genotypes in rarefied sample ($n \geq 10$), [c] SE = standard error of eMLG estimate, [d] H= Shannon-Weiner diversity index, [e] H_e = Nei's unbiased gene diversity. * = estimated genotypic diversity from 1,000 bootstrap replicates with rarefaction ($n \geq 10$).

Table 2.2: Sample sizes and diversity estimates for the 35 sites in Oregon and Washington from which *Nothophaeocryptopus gaeumannii* isolates were collected for this study.

Population Level	Year	N_{trees}	$N_{isolates}$	MLG	eMLG	SE	H^*	H_e	L1	L2
State										
Oregon		95	657	384	273.64	5.75	5.44	0.82	394	263
Washington		55	404	282	282.00	0.00	5.44	0.80	252	152
Total State		150	1,061	663**	316.12	6.67	5.64	0.82	646	415
Site										
Oregon										
Tillamook										
T0-1	2014	9	53	36	9.26	0.78	2.20	0.79	26	27
T0-2	2014	5	16	8	5.96	0.91	1.61	0.55	3	13
T0-3	2014	5	26	19	8.79	0.90	2.13	0.75	13	13
T5-3	2014	5	28	24	9.44	0.67	2.23	0.75	22	6
T5-5	2014	5	24	18	8.92	0.83	2.15	0.73	19	5
T15-1	2014	4	49	37	9.27	0.79	2.19	0.75	27	22
T15-2	2014	5	31	25	9.35	0.71	2.21	0.79	17	14
T25-2	2014	5	101	40	8.56	1.03	2.09	0.60	101	0
T25-3	2014	5	63	38	8.93	0.93	2.14	0.67	62	1
Newport										
N0-1	2015	4	28	9	5.85	1.01	1.59	0.56	0	28
N5-2	2015	3	23	17	8.71	0.89	2.12	0.59	0	23
N15-3	2015	3	13	6	5.30	0.66	1.54	0.66	6	7
N25-5	2015	2	10	6	6.00	0.00	1.61	0.65	10	0
Florence										
F0-2	2015	5	11	11	10.00	0.00	2.30	0.56	0	11
F5-1	2015	3	13	4	3.73	0.45	1.16	0.49	0	13
F15-1	2014	5	32	21	8.57	0.97	2.09	0.75	28	4
F15-3	2014	2	15	11	8.12	0.83	2.03	0.68	4	11
F25-2	2014	5	38	22	8.07	1.11	2.00	0.74	25	13

Table 2.2 (continued)

Coos Bay										
CB0-1	2015	2	11	5	4.73	0.45	1.34	0.32	0	11
CB5-2	2015	2	8	3	3.00	0.00	0.97	0.42	8	0
CB15-2	2015	5	12	9	7.82	0.65	1.97	0.82	7	5
CB25-2	2015	1	23	12	7.32	1.01	1.90	0.75	16	7
Gold Beach										
G0-1	2015	3	19	8	6.00	0.90	1.62	0.58	0	19
G0-2	2016	2	10	6	6.00	0.00	1.70	0.52	0	10
Washington										
N Olympic Pensinsula										
WDNR70	2015	5	37	29	9.05	0.91	2.16	0.78	20	17
WDNR71	2015	5	39	28	9.04	0.87	2.17	0.81	21	18
WDNR49	2015	5	41	32	9.38	0.72	2.21	0.78	30	11
WDNR68	2015	5	31	27	9.61	0.56	2.25	0.65	29	2
WDNR66	2015	5	53	36	8.93	0.94	2.15	0.60	52	1
S Olympic Peninsula										
WDNRQ	2015	5	31	24	9.18	0.79	2.19	0.65	2	29
WDNR64	2015	5	38	26	8.99	0.86	2.16	0.64	2	36
WDNR63	2015	5	40	28	9.13	0.82	2.18	0.76	17	23
WDNR32	2015	5	46	33	9.10	0.87	2.17	0.64	46	0
SW Washington										
DNRL25-2	2014	5	25	24	9.85	0.36	2.28	0.74	19	6
DNRS25-1	2014	5	23	15	8.07	1.01	2.02	0.73	14	9
Total Site		150	1061	663**	9.92	0.28	2.29	0.82	646	415

[a]L1, abundance of Lineage 1; [b]L2, abundance of Lineage 2; **, total MLG not equal to sum of population totals due to shared MLGs.

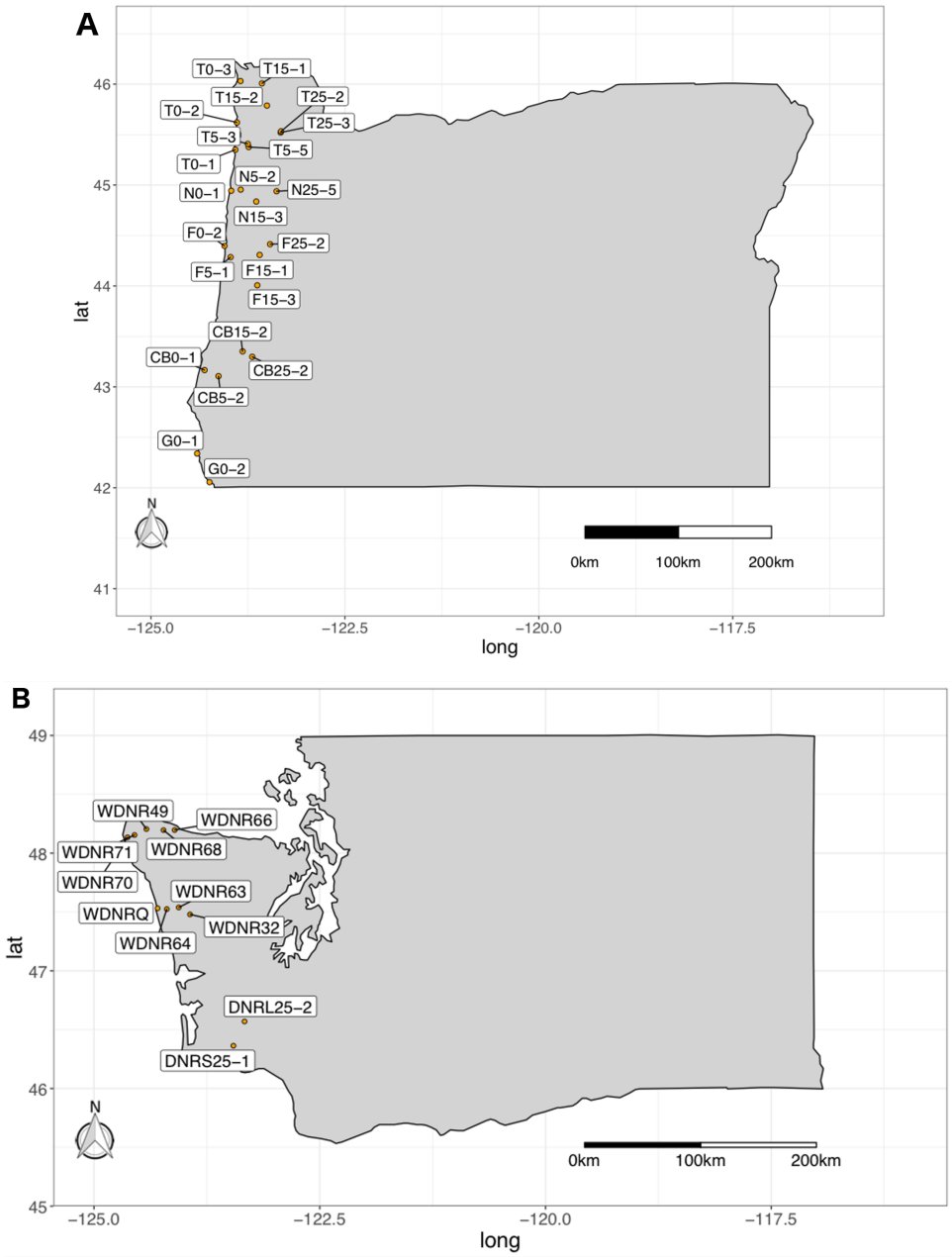

Figure 2.1: Maps showing the geographic locations of each site from which Douglas-fir foliage was sampled for isolation of *Nothophaeocryptopus gaeumannii*. A) 24 sites in western Oregon. B) 11 sites in western Washington. Site labels correspond to those shown in the maps in Figure 2.2 and described in Table 2.2. T, Tillamook; N, Newport; F, Florence; CB, Coos Bay; G, Gold Beach; WDNR, Washington Department of Natural Resources.

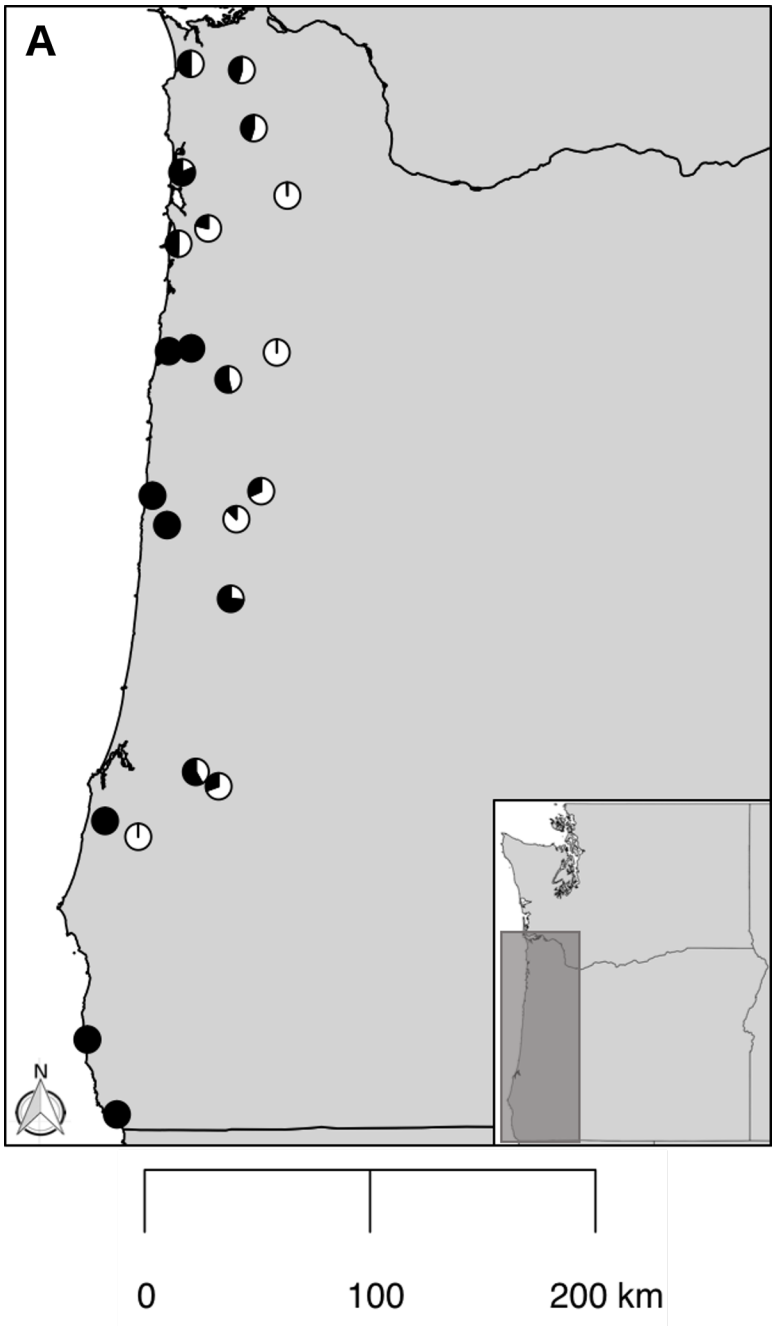
A
N
0
100
200 km

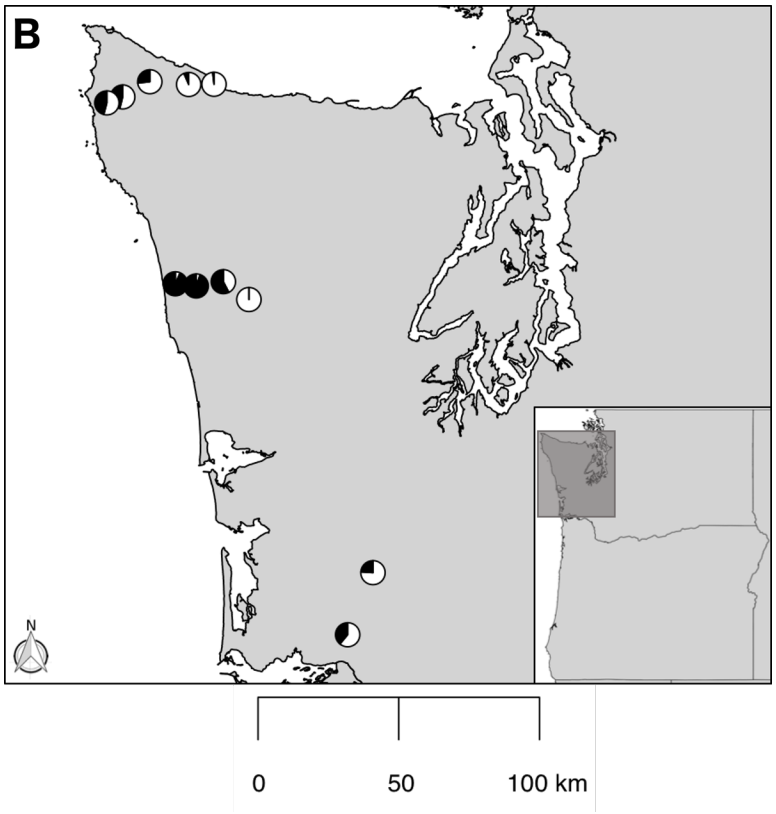

Figure 2.2: Distributions of two *Nothophaeocryptopus gaeumannii* lineages in **A)** 24 sites in western Oregon (overlapping pie charts were pooled for two sites), **B)** 11 sites in western Washington. Pie charts represent the relative proportions of Lineage 1 (white) and Lineage 2 (black) at each site.

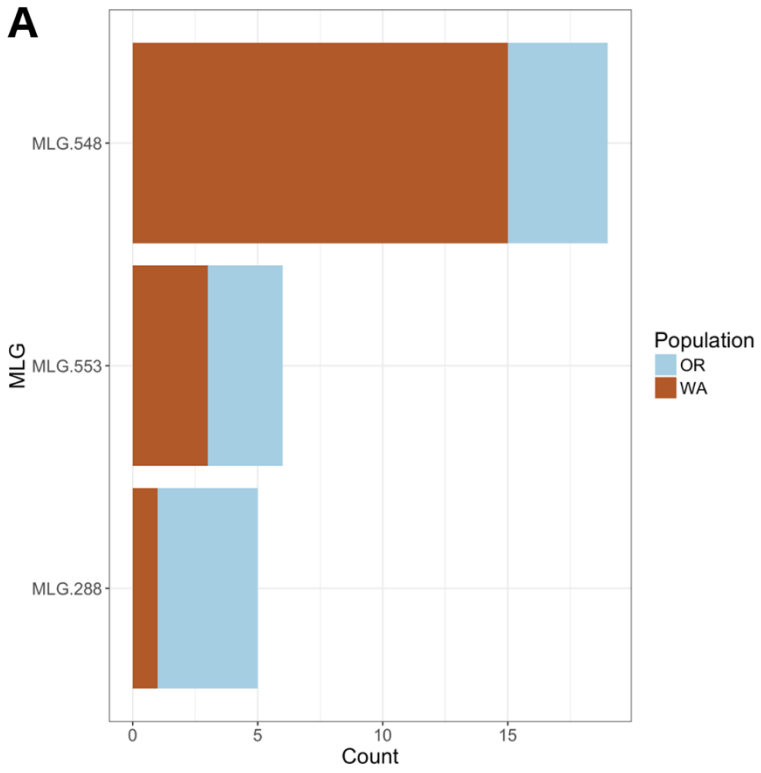
A
MLG.548
MLG.553
MLG.288
MLG
0
5
10
15
Count
Population
OR
WA

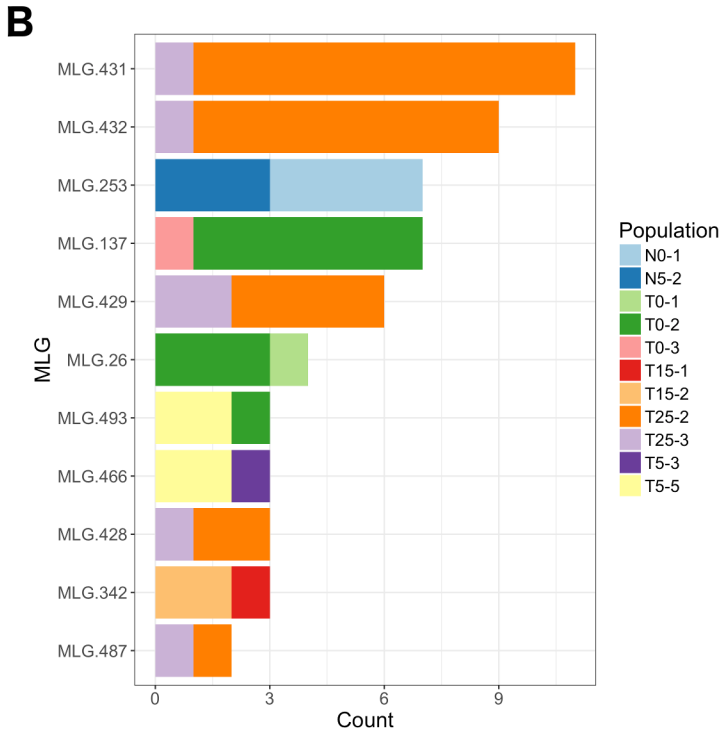
B
MLG.431
MLG.432
MLG.253
MLG.137
MLG.429
MLG.26
MLG.493
MLG.466
MLG.428
MLG.342
MLG.487
MLG
0
3
6
9
Count
Population
N0-1
N5-2
T0-1
T0-2
T0-3
T15-1
T15-2
T25-2
T25-3
T5-3
T5-5

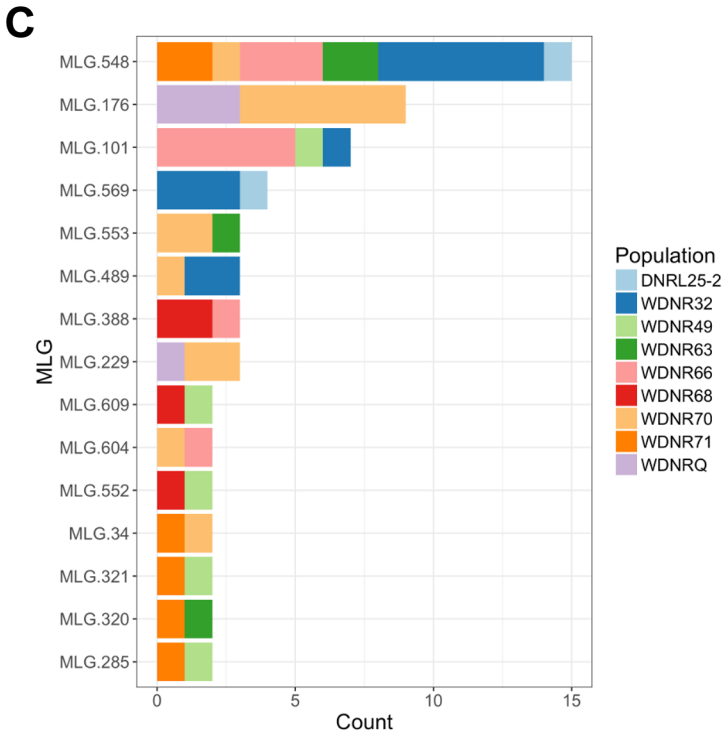

Figure 2.3: Bar plots showing the abundances of *Nothophaeocryptopus gaeumannii* SSR genotypes (MLGs) that were shared between **A)** Oregon and Washington, **B)** sites within Oregon, **C)** sites in Washington. Each bar corresponds to a distinct MLG with the length of the bar representing the numbers of isolates with that MLG, and colors corresponding to each of the populations listed in the legend.

Table 2.3: Pairwise geodesic distances between sites in Oregon and Washington with shared *Nothophaeocryptopus gaeumannii* multilocus genotypes (MLGs).

Table 2.3

Genotype	Sites		Distance (km)
MLG 26	T0-1	T0-2	30.05
MLG 34	WDNR70	WDNR71	6.15
MLG 101	WDNR66	WDNR49	23.25
	WDNR66	WDNR32	80.73
	WDNR32	WDNR49	88.36
MLG 137	T0-2	T0-3	45.77
MLG 176	WDNR70	WDNRQ	71.47
MLG 229	WDNR70	WDNRQ	71.47
MLG 253	N0-1	N5-2	9.72
MLG 284	WDNR49	WDNR71	11.31
MLG 287	N15-3	DNRL25-2	194.17
MLG 320	WDNR63	WDNR71	77.61
MLG 321	WDNR49	WDNR71	11.31
MLG 342	T15-1	T15-2	24.98
MLG 388	WDNR66	WDNR68	9.17
MLG 428	T25-2	T25-3	1.37
MLG 429	T25-2	T25-3	1.37
MLG 431	T25-2	T25-3	1.37
MLG 432	T25-2	T25-3	1.37
MLG 466	T5-3	T5-5	3.60
MLG 487	T25-2	T25-3	1.37
MLG 489	WDNR32	WDNR70	89.36
MLG 493	T0-2	T5-5	29.55
MLG 548	WDNR70	WDNR71	6.15
	WDNR32	WDNR63	11.48
	WDNR66	WDNR71	33.40
	WDNR66	WDNR70	39.42
	T15-1	DNRL25-2	65.13
	WDNR63	WDNR66	73.18
	WDNR63	WDNR71	77.61
	WDNR63	WDNR70	78.64
	WDNR32	WDNR66	80.73
	WDNR32	WDNR71	88.01
	WDNR32	WDNR70	89.36
	DNRL25-2	WDNR32	111.05
	DNRL25-2	WDNR63	121.11
	T15-1	WDNR32	166.03
	T15-1	WDNR63	174.35
	DNRL25-2	WDNR66	190.04
	DNRL25-2	WDNR71	198.72
	DNRL25-2	WDNR70	199.57
	T15-1	WDNR66	246.75
	T15-1	WDNR70	249.75
	T15-1	WDNR71	250.03
MLG 552	WDNR49	WDNR68	14.10
MLG 553	WDNR63	WDNR70	78.64
	T25-3	WDNR63	231.30
	T25-3	WDNR70	307.01
MLG 569	DNRL25-2	WDNR32	111.05
MLG 604	WDNR66	WDNR70	39.42
MLG 609	WDNR49	WDNR68	14.1
Mean			82.96

Table 2.4: Analysis of molecular variance (AMOVA) showing the partitioning of genetic variance and estimates of differentiation among *Nothophaeocryptopus gaeumannii* subpopulations. Isolates clone-censored, $N_{isolates}$ = 663.

Hierarchical level	**Variance (%)**	ϕ	**P***
ϕ_{LT} (between lineages)	29.432	0.294	< 0.001
ϕ_{SL} (between states within lineages)	0.345	0.005	0.033
ϕ_{BS} (between blocks within states)	0.260	0.004	0.248
ϕ_{SB} (between sites within blocks)	3.950	0.056	< 0.001
ϕ_{TS} (between trees within sites)	4.740	0.072	< 0.001
ϕ_{TT} (within trees)	61.272	0.387	< 0.001

*P-value was obtained for the ϕ statistic from 1,000 permutations of the data.

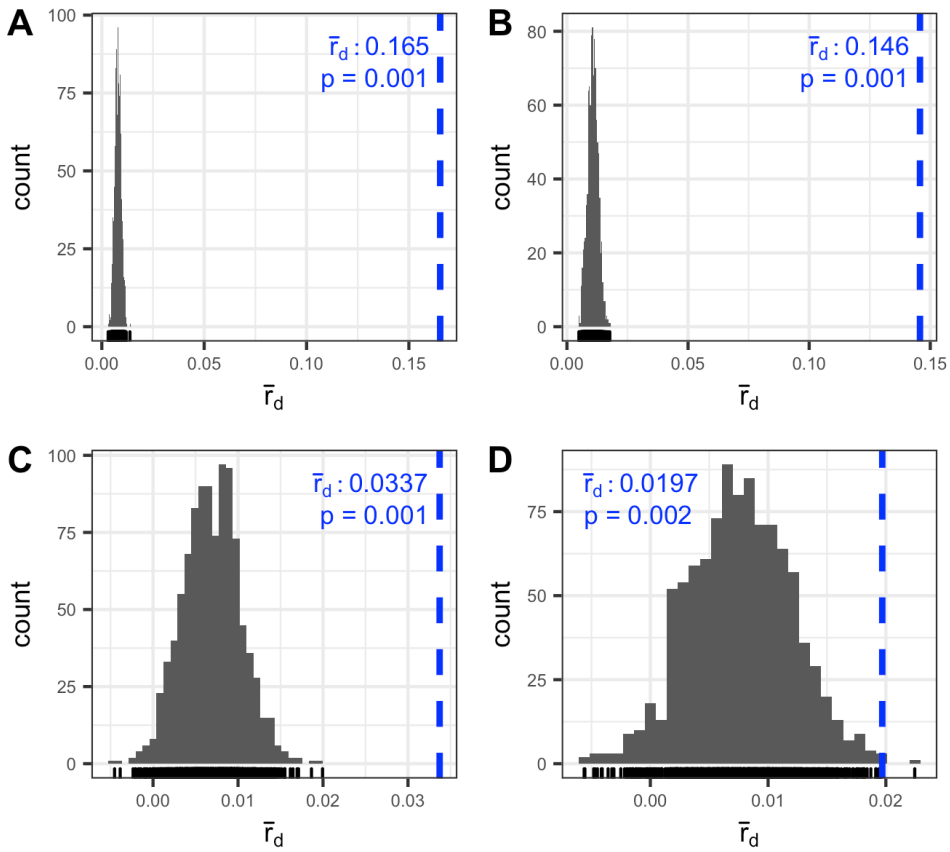

Figure 2.4: Estimates of the standardized multilocus index of association ($\bar{r}_d$) (Agapow and Burt, 2001) based on SSR genotypes from *Nothophaeocryptopus gaeumannii* isolates collected in Oregon and Washington. Histograms show the distributions of $\bar{r}_d$ values from 999 populations simulated with no linkage among loci. Values of 0 reflect linkage equilibrium, while those significantly greater than 0 indicate linkage disequilibrium. P-values reflect the chances of obtaining the observed value, or more extreme, under the null hypothesis of no linkage among loci. A) all isolates, including Lineages 1 and 2 (N = 1,061). B) Clone-censored, including lineages 1 and 2 (N = 663). C) Clone-censored, Lineage 1 isolates only (N = 403). D) Clone-censored, Lineage 2 isolates only (N = 260).

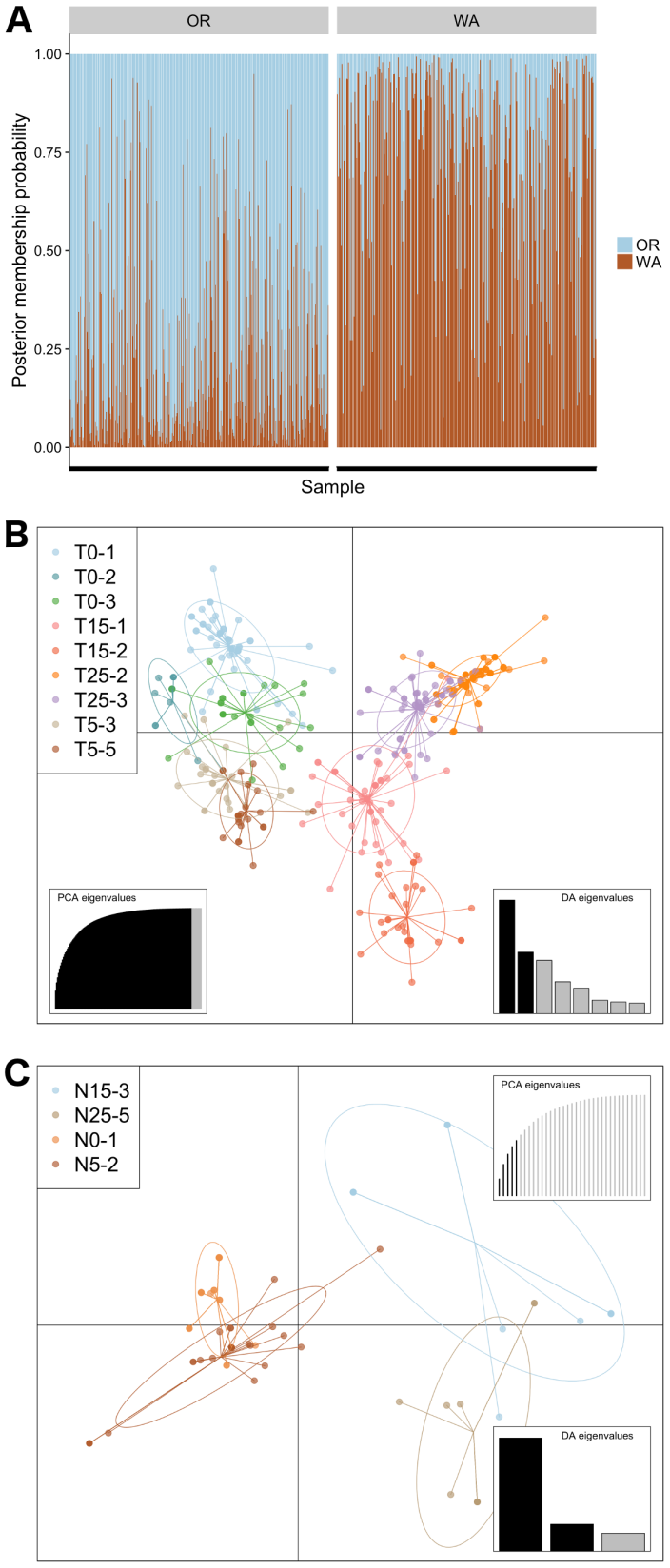
A
OR
WA
1.00
0.75
0.50
0.25
0.00
Posterior membership probability
Sample
OR
WA
B
T0-1
T0-2
T0-3
T15-1
T15-2
T25-2
T25-3
T5-3
T5-5
PCA eigenvalues
DA eigenvalues
C
N15-3
N25-5
N0-1
N5-2
PCA eigenvalues
DA eigenvalues

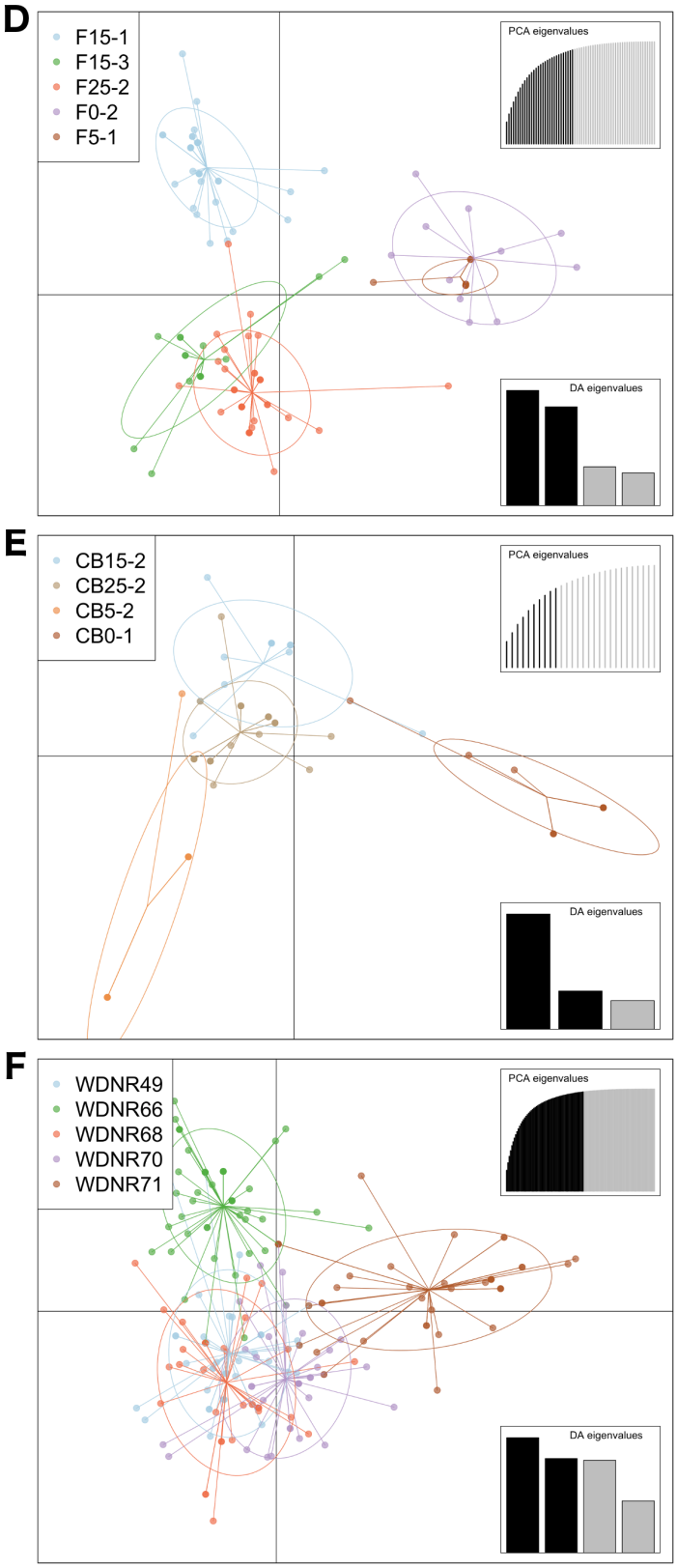
D
F15-1
F15-3
F25-2
F0-2
F5-1
PCA eigenvalues
DA eigenvalues
E
CB15-2
CB25-2
CB5-2
CB0-1
PCA eigenvalues
DA eigenvalues
F
WDNR49
WDNR66
WDNR68
WDNR70
WDNR71
PCA eigenvalues
DA eigenvalues

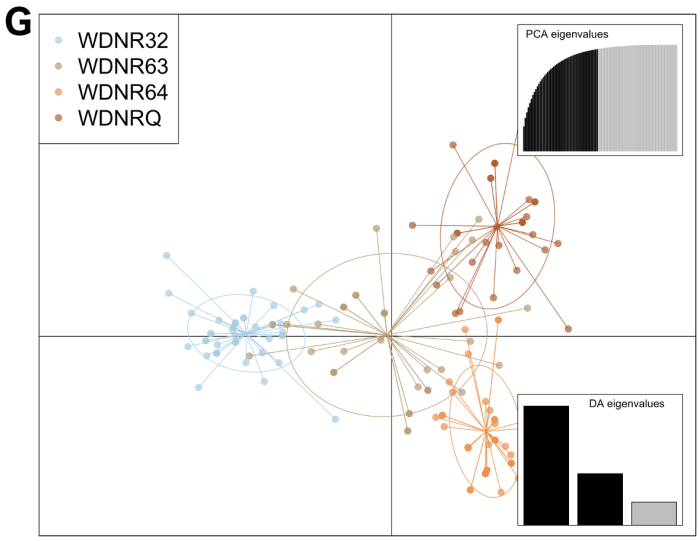

Figure 2.5: A) Bar plot from discriminant analysis of principal components (DAPC) showing posterior membership probabilities of 663 *Nothophaeocryptopus gaeumannii* genotypes (MLGs) in clusters representing Oregon (OR) and Washington (WA), from a clone-censored dataset including MLGs from 35 sites. Each bar represents one MLG, and the colors represent the probability of membership of that MLG in the Oregon and Washington clusters. B-G) DAPC scatterplots showing differentiation among the coastal and inland sites within each sampling block B) Tillamook (N = 391 isolates), C) Newport (N = 74 isolates), D) Florence (N = 109 isolates), E) Coos Bay (N = 54 isolates), F) Northern Olympic Peninsula (N = 201 isolates), and G) Southern Olympic Peninsula (N = 155 isolates). The axes represent the first and second discriminant functions. The color of each cluster corresponds to a sample sites listed in the legend (Table 2.2, Figure 2.1), and each point represents an MLG from a given site. Overlapping points represent identical MLGs. Inertia ellipses are drawn around 2/3 of the isolates in a given cluster. The insets indicate the principal components and discriminant functions retained in each analysis.

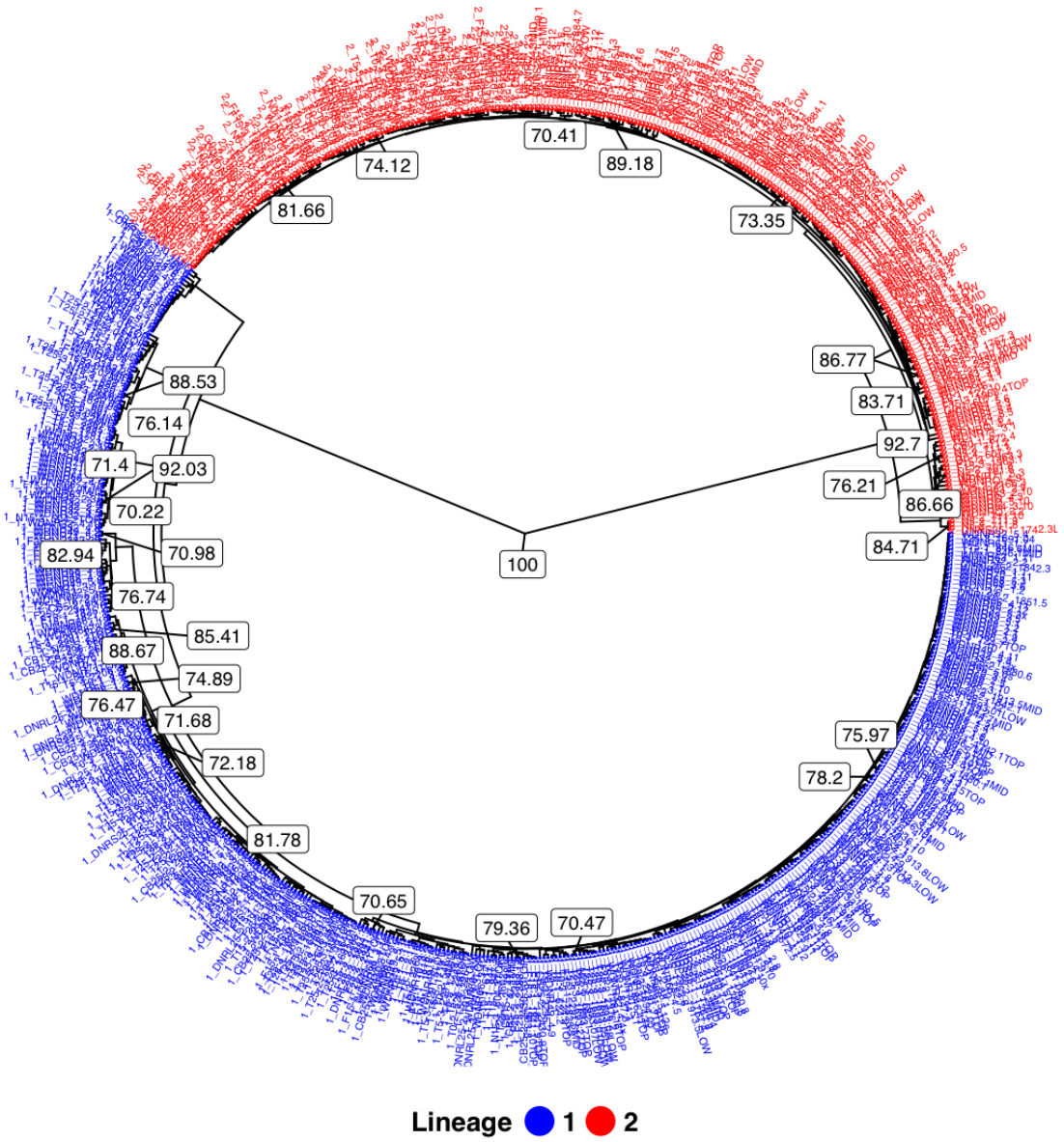

Figure 2.6: UPGMA dendrogram from bootstrap analysis of Nei's genetic distance showing divergence between genotypes corresponding to two *Nothophaeocryptopus gaeumannii* lineages from Oregon and Washington (clone-censored, N = 663). Node labels represent bootstrap statistics (≥ 70%) from 10,000 replicate trees.

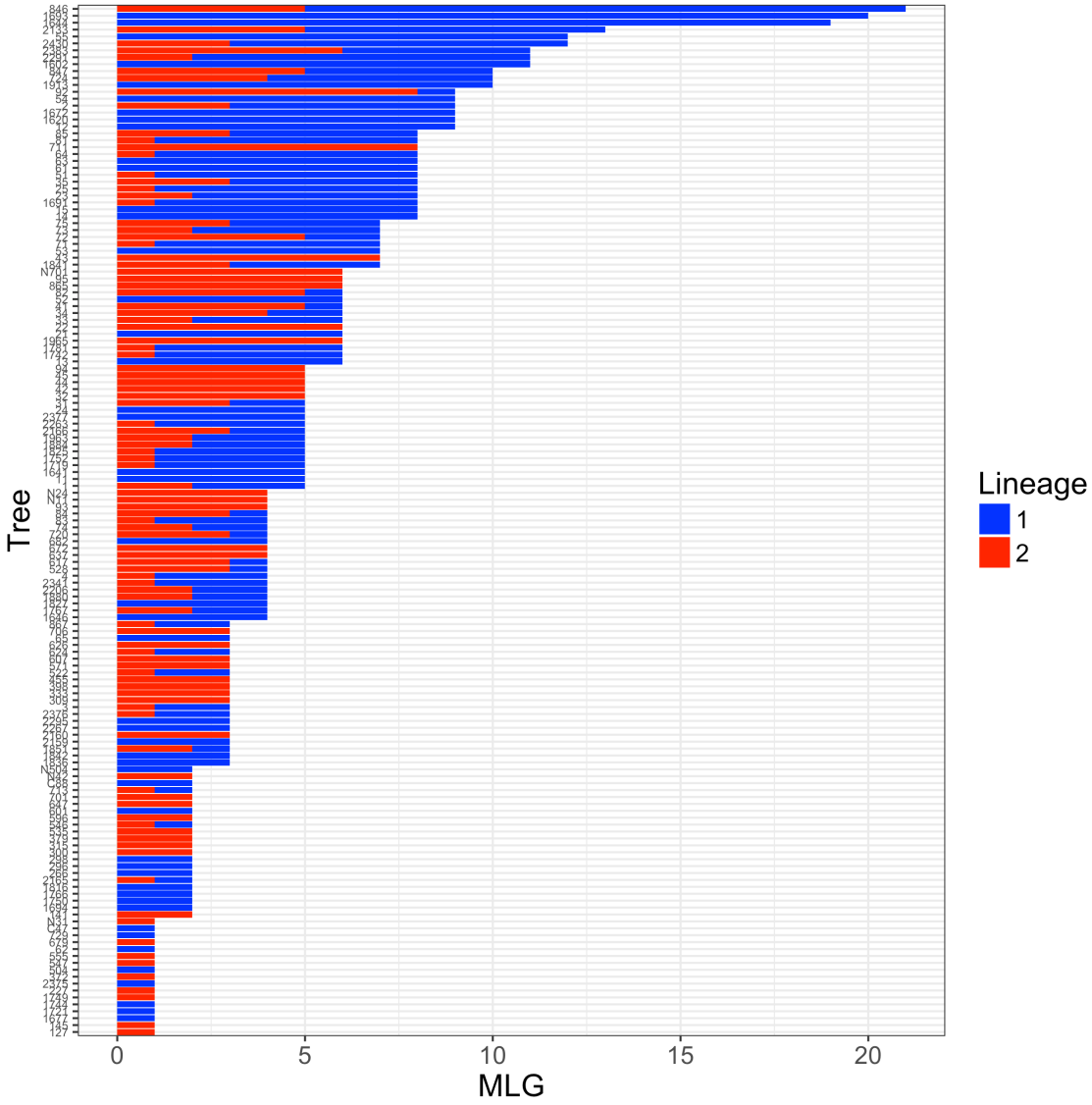

Figure 2.7: Bar plot showing the numbers of SSR multilocus genotypes of *Nothophaeocryptopus gaeumannii* recovered from 150 Douglas-fir trees in Oregon and Washington. Each bar represents the total number of multilocus genotypes (MLG) from one tree, with colors indicating the numbers of genotypes corresponding to each *N. gaeumannii* lineage.

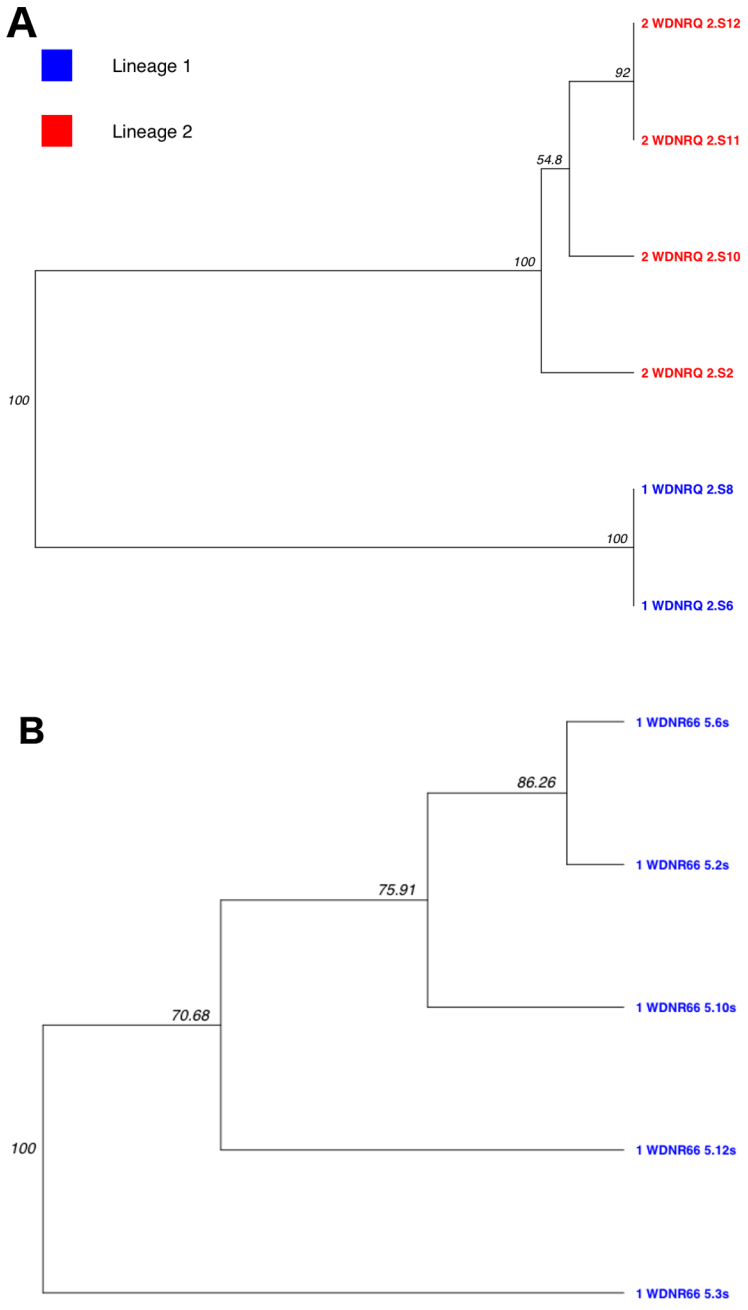

Figure 2.8: UPGMA dendrograms from bootstrap analyses of Nei's genetic distance for *Nothophaeocryptopus gaeumannii* genotypes isolated from individual Douglas-fir needles from western Washington sites. A) Four distinct genotypes recovered from a single needle, one from Lineage 1 and three from Lineage 2. B) Five distinct Lineage 1 genotypes recovered from a single needle.

2.9 Supplementary Figures

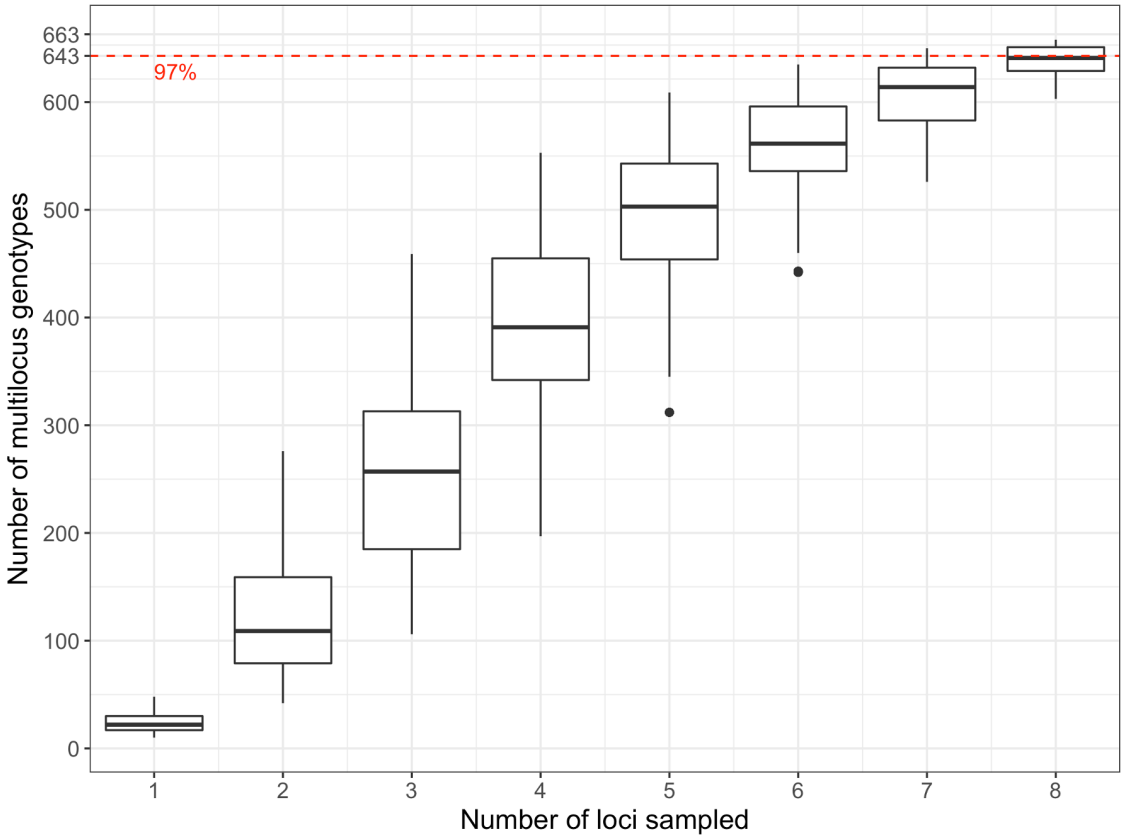

Figure S2.1: Genotype accumulation curve showing the number of *Nothophaeocryptopus gaeumannii* multilocus SSR genotypes (MLGs) from the Oregon and Washington dataset observed in 1,000 random samples with numbers of loci ranging from 1 to *n*-1.

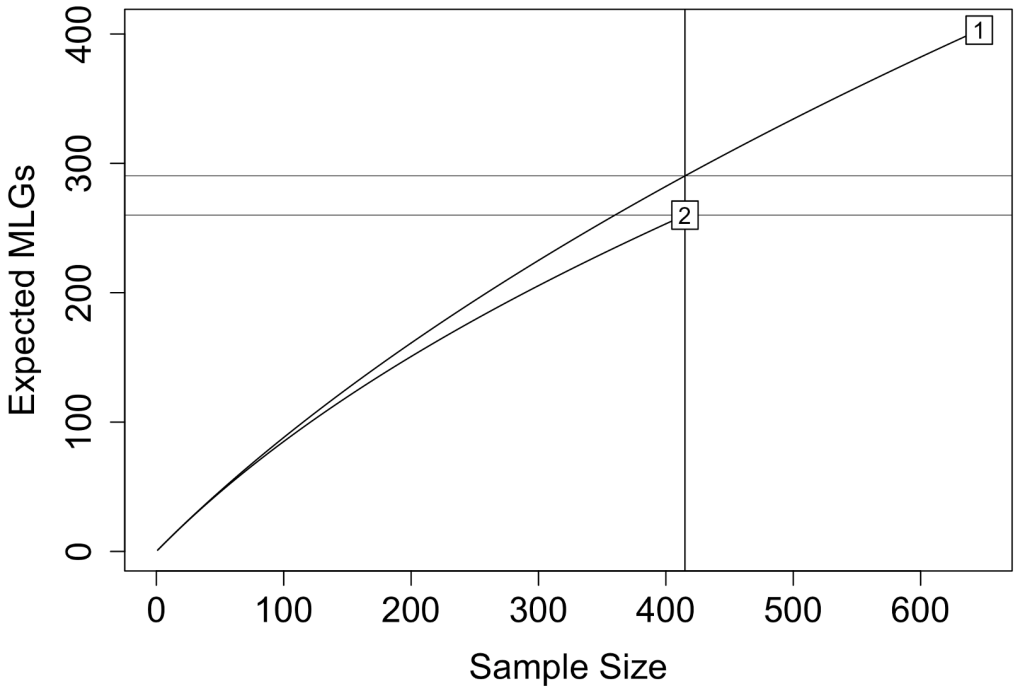

Figure S2.2: Rarefaction curve showing the observed genotypic richness in *Nothophaeocryptopus gaeumannii* Lineages 1 and 2 from Oregon and Washington samples. The vertical line represents the rarefaction sample size (minimum shared sample size between the two lineages), while the horizontal lines represent the genotypic richness of the two lineages at that sample size.

Chapter 3. The Genetic Structure of Populations of the Douglas-fir Swiss Needle Cast Fungus *Nothophaeocryptopus gaeumannii* in New Zealand

Patrick I. Bennett, Ian A. Hood, Jeffrey K. Stone

Target Journal: *Phytopathology*

3.1 Abstract

Swiss needle cast is a foliar disease of Douglas-fir that results in premature foliage loss and results in reduced growth. The causal fungus, *Nothophaeocryptopus gaeumannii,* was first detected in New Zealand in 1959 and spread throughout the North and South Islands over the following decades. The contemporary genetic structure of the *N. gaeumannii* population in New Zealand was assessed by analyzing 468 multilocus SSR genotypes (MLGs) from 2,085 *N. gaeumannii* isolates collected from 32 sites in in the North and South Islands. Overall diversity was lower than that reported from native *N. gaeumannii* populations in the northwestern U.S., which was expected given that *N. gaeumannii* is introduced in New Zealand. Linkage disequilibrium was significantly higher than expected under random mating, suggesting that population structure is clonal. Populations of *N. gaeumannii* in the North and South Island were weakly differentiated, and the isolates collected from sites within the islands were moderately differentiated. This suggests that gene flow has occurred between the *N. gaeumannii* populations in the North and South Islands, and between the local *N. gaeumannii* populations within each island. Eighteen isolates of *N. gaeumannii* Lineage 2, which has previously been reported only from western Oregon, were recovered from two sites in the North Island and four sites in the South Island. The most likely explanation for the contemporary distribution of *N. gaeumannii* in New Zealand is that it was introduced on infected live seedlings through the forestry or ornamental nursery trade, as the fungus is neither seed borne nor saprobic, and the observed population structure is not consistent with a stochastic intercontinental dispersal event.

3.2 Introduction

The foliar disease Swiss needle cast (SNC) is specific to Douglas-fir (*Pseudotsuga menziesii* (Mirb.) Franco), and results from cumulative occlusion of needle stomata by the ascocarps of *Nothophaeocryptopus gaeumannii* (T. Rohde) Videira, C. Nakash., U. Braun & Crous (Manter et al., 2000; Stone et al., 2008a). The disease was first described from a Douglas-fir plantation in Switzerland in 1925 and became established throughout central Europe and the U.K. in the following decades (Boyce, 1940; Liese, 1939; Peace, 1962; Rohde, 1936; Wilson and Waldie, 1928). However, there is ample evidence to suggest that the fungus is endemic in the native range of its host in western North America (Boyce, 1940; Hood, 1982; Meinecke, 1939). The pathogen has since accompanied its host worldwide as exotic Douglas-fir plantings have been established for timber production. The presence of this fungus has been confirmed in Douglas-fir plantations in the northeastern United States (McCormick, 1939; Morton and Patton, 1970), Australia (Marks, 1975), New Zealand (Hood et al., 1990; Hood and Kershaw, 1975), Turkey (Temel et al., 2003), Chile (Osorio, 2007), and Spain (Castaño et al., 2014). A severe outbreak of SNC that started in mid 1980s continues to intensify in the low-elevation forests along western slopes of the Coast Ranges in Oregon and Washington where both host and pathogen are native (Hansen et al., 2000; Ritóková et al., 2016; Stone et al., 2008b).

Douglas-fir has been cultivated as a commercial timber species in New Zealand since the early 20th century, but accounts for only a small fraction of the total forest land area and timber production (Ministry for Primary Industries, 2016). The origins of

Douglas-fir seed imported into New Zealand before 1926 are unknown, but plantations were established thereafter from seed sources in the Coast Ranges of Oregon, Washington, and British Columbia, with the majority of seed stock coming from southern Washington (Weston, 1957). The first reported presence of *N. gaeumannii* in New Zealand was in 1959 in the North Island near Taupo, where it was initially restricted to an area with a radius of approximately 130 km (Hood and Kershaw, 1975). However, symptoms of SNC, such as chlorosis and needle loss, were not reported in the region until 1962 (Hood and Kershaw, 1975). Over the following 10 years, the fungus was found in most of the Douglas-fir plantations in the North Island, and was detected for the first time in the South Island in 1969 (Hood and Kershaw, 1975). By 1974, the fungus had been found throughout the Douglas-fir growing region in the northern part of the South Island, and sporadically at sites farther south (Hood and Kershaw, 1975). It has been suggested that the spread of the disease to the South Island may have been due to the movement of infected seedlings from the North Island (Hood and Kershaw, 1973). In total, it took approximately 30 years for *N. gaeumannii* to become established in all but a few of the most remote Douglas-fir plantations in New Zealand (Hood et al., 1990).

A comparison of the genetic structures of *N. gaeumannii* populations in New Zealand, Europe, and the U.S. revealed that the populations in western Oregon, where SNC symptoms had become increasingly more severe in many natural Douglas-fir stands and timber plantations, consisted of two reproductively isolated lineages (Winton et al., 2006). Lineage 1 was found to be widespread, occurring throughout the native range of Douglas-fir (except for the extreme southern coast of Oregon) and wherever its host was

grown abroad as an exotic, including Europe and New Zealand. Lineage 2 was found to be much less common, occurring in pure (i.e. non-admixed) populations along the southern Oregon coast and in admixed populations with Lineage 1 in the central and northwestern Oregon Coast Range. Lineage 2 was not detected in collections from Washington, the eastern United States, Europe, or New Zealand (Winton et al., 2006). At the time of this discovery, it was suggested that Lineage 2 may be responsible for the recent emergence of SNC in western Oregon, as it was found in high abundance in severely diseased stands near the coast and was often not detected in healthier stands further east (Winton et al., 2006).

The aims of this study were to i) examine the effects of the introduction and spread of *N. gaeumannii* in New Zealand on the genetic structure of its populations, and ii) determine whether *N. gaeumannii* Lineage 2 is present in New Zealand. There is evidence to suggest that this fungus is capable of homothallic reproduction, i.e. fertile asci arise from self-fertilization (asexual conidial reproduction is not known in *N. gaeumannii*) (Bennett and Stone, 2016; Winton, 2001). Thus, we hypothesized that the introduction of *N. gaeumannii* to New Zealand would have resulted in a founder event, and successive generations of self-fertilization along with genetic drift would result in a bottleneck. We also considered several hypotheses about the expected spatial genetic structure of the *N. gaeumannii* population in New Zealand, and considered two possible scenarios that might explain the current extent of colonization: i) *N. gaeumannii* spread from an initial site of introduction in the North Island to its current distribution by the anthropogenic movement of infected Douglas-fir seedlings (or foliage) or long-distance

aerial spore dispersal, ii) *N. gaeumannii* spread from the site of initial introduction via local ascospore dispersal and colonized the South Island gradually as described in Hood and Kershaw (1973). The first scenario would likely result in a relatively homogeneous distribution of *N. gaeumannii* genotypes and an abundance of shared multilocus genotypes (MLGs) between islands and sites. We might also expect the first scenario to result in a lack of isolation by distance, where genetic dissimilarity between sites is not related to geographic distance between sites. On the other hand, the second scenario should result in a more heterogeneous spatial distribution of MLGs and an abundance of regionally specific genotypes resulting from selection or genetic drift. The second scenario would be expected to result in isolation by distance.

3.3 Materials and Methods

3.3.1 Field Sampling, Isolations, and Culturing

The isolates included in these analyses were collected from Douglas-fir plantations in New Zealand in 2005 and 2007 (Stone et al., 2007; Watt et al., 2010). Foliage was sampled from 13 sites in the North Island and 19 in the South Island (Figure 3.1). Samples were collected from secondary branches in the upper crowns of 10 Douglas-fir trees of the coastal variety (*P. menziesii var. menziesii*) at each site. Double-sided adhesive tape was used to affix two-year-old needles bearing pseudothecia to the lids of Petri dishes. These plates were then incubated at room temperature for approximately 24–48 h, during which time the ascospores discharged onto the agar surface below. Individual ascospores were then transferred onto 2% malt agar and incubated for a minimum of 2–6 mo. to allow adequate growth for DNA extraction.

3.3.2 Molecular techniques

DNA was extracted with the procedure described in Winton et al. (2006). Briefly, mycelium was scraped from the agar surface and macerated by shaking in a mini-beadbeater with glass beads and CTAB (cetyltrimethylammonium bromide) extraction buffer. The samples were then incubated at 65 ºC for 2 hrs and precipitated in 24:1 chloroform: isoamyl alcohol. A QIAAmp Spin Column (Qiagen, Hilden, Germany) was then used to purify the DNA and reduce PCR inhibitors (Winton et al., 2006). Ten microsatellite loci were amplified in three multiplexed PCR reactions with fluorescently-labeled reverse primers (Winton et al., 2007). Genotyping was performed via capillary electrophoresis at the Oregon State University Center for Genome Research and Biocomputing (CGRB) with the parameters described in Winton et al. (2007) and Bennett and Stone (2016). Allele scoring was performed as described in Bennett and Stone (2016). A positive control isolate was included to ensure that each independent PCR amplification and genotyping run resulted in consistent allele sizing. One of the loci, Pgdi5, did not amplify consistently for all isolates and was omitted from subsequent analyses.

3.3.3 Data analysis

The map of sampling sites in New Zealand was created in R version 3.4.1 (R Core Team, 2017) with the R packages *ggplot2* (Wickham, 2016), *ggrepel* (Slowikowski, 2017), and *ggsn* (Baquero, 2017). The multilocus SSR genotypes for the *N. gaeumannii* isolates collected in New Zealand were formatted in Microsoft Excel 2016 with GenAlEx 6.503 (Peakall and Smouse, 2012, 2006), and imported into R version 3.4.1 (R Core

Team, 2017) for use with the R packages *poppr* version 2.5.0 (Kamvar et al., 2015a, 2014), *adegenet* 2.0.1 (Jombart, 2008), and *ade4* 1.7-8 (Dray and Dufour, 2007). Analyses were performed with a population hierarchy that included levels for Lineage, Island, and Site. Implementation and interpretation of *poppr* graphics, as well as source code for modifying *poppr* output, was adapted from http://grunwaldlab.github.io/Population_Genetics_in_R/ (Grünwald et al., 2016).

Genotypic and gene diversity estimates were calculated with the R package *poppr* (Kamvar et al., 2015a, 2014), including Shannon-Weiner diversity (H) (Shannon, 2001) and Nei's unbiased gene diversity (H_e) (Nei, 1978). Genotypic richness was estimated as the number of expected multilocus genotypes (eMLG) in a minimum shared sample size of 10 isolates. Because these analyses are sensitive to differences in sample size between groups (Grünwald et al., 2003), H was estimated from 1,000 iterations of a bootstrap analysis with rarefaction. Random sub-samples of the data were selected such that the number of samples in each group was equal to the sample size of the group with the smallest number of samples, with a minimum rarefaction sample size of 10. This allowed for the direct comparison of diversity estimates among lineages, islands, and sites. Rarefaction genotypic richness curves were constructed using the *vegan* package in R (Oksanen et al., 2017), and a genotype accumulation curve was produced with the R package *poppr* (Kamvar et al., 2015a, 2014).

The effect of the reproductive mode of the fungus on the genetic structure of the New Zealand population was examined by estimating linkage disequilibrium. The standardized multilocus index of association, $\bar{r}_{\mathrm{d}}$ (Agapow and Burt, 2001), was calculated

with the R package *poppr* (Kamvar et al., 2015a, 2014). Analyses were performed with the full dataset, on a clone-censored dataset (to eliminate the influences of repeated MLGs), and on the two lineages separately (to eliminate the influence of reproductively-isolated subpopulations). The observed values of $\bar{r}_d$ were plotted in relation to a simulated population in linkage equilibrium. The probability of obtaining the observed value of $\bar{r}_d$, or more extreme, under the null hypothesis of no linkage among loci (H_0: $\bar{r}_d = 0$) was calculated with 999 permutations of the data.

Genetic structure due to differentiation among subpopulations was evaluated with a hierarchical analysis of molecular variance (AMOVA) (Excoffier et al., 1992) in the R package *poppr* (Kamvar et al., 2015a, 2014), and utilized the *ade4* implementation (Dray and Dufour, 2007). This method partitioned the genetic variance within and among populations and subpopulations across all levels of the population hierarchy, which was clone-censored with respect to hierarchical level. Fixation indices (ϕ statistics) were interpreted as measures of subpopulation differentiation (Excoffier et al., 1992). The probability of obtaining the observed ϕ, or more extreme, under the null hypothesis of no differentiation between subpopulations (H_0: $\phi = 0$) was obtained from 1,000 iterations of a permutation test implemented with the R package *ade4* (Dray and Dufour, 2007).

Subpopulation differentiation between islands and sites within islands was further explored with discriminant analysis of principal components (DAPC), a multivariate analysis of genetic clustering among isolates (Jombart et al., 2010). The function xvaldapc from the R package *adegenet* (Jombart, 2008) was utilized with a dataset that was clone-censored with respect to the hierarchical level of interest. In this analysis,

variations in allele frequencies are partitioned within an analysis of variance (ANOVA) framework (Jombart et al., 2010). *F*-statistics, which represent the ratio of between-group variances to within-group variances, are used as a measure of separation between groups, with larger values of *F* corresponding to greater separation (Jombart et al., 2010). DAPC results in linear combinations of principal components (equivalent to linear combinations of alleles) that best describe the differentiation between groups by maximizing *F* (Jombart et al., 2010). For the DAPC analyses presented here, the number of principal components (PCs) corresponding to the lowest Mean Squared Error was selected via cross-validation, with a training set consisting of 90% of the data (Jombart and Collins, 2015). The R package *adegenet* (Jombart, 2008) was also used to visualize the results of the DAPC.

Our assessment of population genetic structure was aided by a bootstrap analysis of Nei's genetic distance (Nei, 1978, 1972), performed with 10,000 replicates and visualized as a UPGMA dendrogram. This analysis was performed with the aboot function in the R package *poppr* (Kamvar et al., 2015*a*, 2014), and the dendrogram was visualized with the R package *ggtree* version 1.12.0 (Yu et al., 2017).

Repeated MLGs occurring across the subpopulations within each level of the population hierarchy were identified with the R package *poppr* (Kamvar et al., 2015a, 2014). The four unique MLGs corresponding to *N. gaeumannii* Lineage 2 isolates were displayed in a bar plot in which each unique MLG was represented by a bar with the length corresponding to the abundance of that MLG, and the colored portions of each bar corresponding to the site(s) from which that MLG was recovered.

Mantel's test (Mantel, 1967) was performed with the R package *ade4* (Dray and Dufour, 2007). This test utilized a regression approach to test for a statistical correlation between a matrix containing pairwise Euclidean geographic distances among the 32 sample sites, and a matrix containing pairwise values for Roger's genetic distance (Rogers, 1972) among the sites. Genetic distance was calculated with the function dist.genpop from the R package *adegenet* (Jombart, 2008). A randomization test with 10,000 permutations was employed to test the null hypothesis of no correlation between genetic distance and geographic distance (H_0: $r = 0$).

3.4 Results

3.4.1 Genetic diversity

Of the 2,085 total isolates analyzed for this study, 468 unique multilocus genotypes (MLGs) were detected. The genotype accumulation curve showed that 90% of the MLGs could be distinguished on the basis of eight SSR loci (Figure S3.1). A total of 2,067 of the isolates were associated to Lineage 1, while 18 isolates were associated to Lineage 2 (Table 3.1). Even with a large sample size, we did not capture all of the expected genetic variation in Lineage 1 (Figure S3.2A). However, the four MLGs from the 18 Lineage 2 isolates were sufficient to represent the expected genetic variation within Lineage 2 (Figure S3.2B). Lineage 2 had lower genetic diversity than Lineage 1 after accounting for differences in sample size via rarefaction (Lineage 1: $H = 2.56$, $H_e = 0.649$; Lineage 2: $H = 1.24$, $H_e = 0.425$) (Table 3.1).

Overall, genotypic diversity and richness were higher for the North Island populations, but gene diversity did not differ considerably between the *N. geaumannii*

populations in the North and South islands (Table 3.1). Isolates sampled from Tauhara (TAU), near Taupo in the central part of the North Island, had the highest genotypic diversity of all sites in New Zealand (H = 2.23), the highest genotypic richness (eMLG = 9.49), and the second highest gene diversity (H_e = 0.652). The lowest diversity was observed for the *N. gaeumannii* isolates collected at the South Island site Mawhera (eMLG = 2.00, H= 0.500, H_e = 0.198) (Table 3.1).

3.4.2 Population structure and differentiation

The observed value of the multilocus index of association ($\bar{r}_d$; Agapow and Burt, 2001), an estimate of linkage disequilibrium, for the total New Zealand population (N = 2,085 isolates) was significantly larger than expected for the simulated population in which there was no linkage among loci ($\bar{r}_d$ = 0.307, P = 0.001) (Figure 3.2A). This indicates that alleles do not pair randomly in MLGs, and thus the population is not panmictic. This linkage disequilibrium was also detected, though to a lesser extent, when the repeated MLGs (i.e. clones) were removed from the data (N = 468 isolates) ($\bar{r}_d$ = 0.130, P = 0.001) (Figure 3.2B). Linkage disequilibrium was slightly less when the analysis was performed with only the unique Lineage 1 MLGs (N = 464 isolates) ($\bar{r}_d$ = 0.126, P = 0.001) (Figure 3.2C). Linkage disequilibrium was not detected when the unique Lineage 2 MLGs were analyzed alone (N = 4) ($\bar{r}_d$ = -0.0148, P = 0.567) (Figure 3.2D).

The partitioning of molecular variance within and among the levels of a clone-corrected population hierarchy indicated that most of the genetic variation was within sites (est. var. = 57.9%, ϕ_{SS} = 0.421, P < 0.001) (Table 3.2). Strong genetic differentiation

was detected between the two *N. gaeumannii* lineages (est. var. = 33.5%, ϕ_{LT} = 0.335, P < 0.001) (Table 3.2). Moderate genetic differentiation was detected between sample sites within the islands (est. var. = 8.26%, ϕ_{SI} = 0.126, P < 0.001), but there little genetic differentiation between the North and South Island populations (est. var. = 0.245%, ϕ_{IL} = 0.004, P = 0.222) (Table 3.2).

Many isolates had a high probability of being assigned to the North Island cluster, even if they had been collected in the South Island, and vice versa. The bar plot produced from the DAPC with clusters representing the North and South Islands showed a high degree of admixture, as the bars representing each genotype had high probabilities of membership in both clusters (Figure 3.3 A). The DAPC scatterplot depicting the relationships among isolates collected from each of the sites in New Zealand showed considerable overlap among sites, with few isolates lying outside of the central cluster of points (Figure 3.3B). The isolates that appeared to be the most highly differentiated in this plot are the *N. gaeumannii* Lineage 2 isolates from South Kaingaroa (North Island), Mawhera (South Island), and Golden Downs (South Island) (Figure 3.3B).

The isolates corresponding to Lineages 1 and 2 clustered into distinct groups In the UPGMA dendrogram based on Nei's genetic distance. These clusters were separated at the basal node with strong bootstrap support (Figure 3.4). The isolates did not cluster regularly based on the site or island from which they were collected (Figure 3.4).

3.4.3 Spatial distributions of multilocus genotypes

A total of 104 MLGs occurred at more than one site, 60 of which were recovered from both islands (Table 3.1, Figure S3.3). The most common genotype (MLG 261) was

shared among 291 individuals across 17 sites in the North and South Islands (Figure S3.3). There was no isolation by distance detected, as no significant correlation was found between the geographic and genetic distance matrices (r = -0.013, P = 0.562). The 18 Lineage 2 isolates comprised only four distinct MLGs (Table 3.1, Figure 3.5). Two of these MLGs were collected from sites in the North Island: Kaingaroa (KGA) and South Kaingaroa (SKGA), while the other two Lineage 2 MLGs were present at four sites in the South Island: Golden Downs (GD-SS and GD-P), Mawhera (MAW), and Forest Creek (FC). The most common Lineage 2 genotype (MLG 9) occurred at both Mawhera and Forest Creek (Figure 3.5). The second Lineage 2 genotype that occurred at Mawhera (MLG 10) was also present at a Golden Downs site (GD-P) (Figure 3.5).

3.5 Discussion

Populations of *Nothophaeocryptopus gaeumannii* in New Zealand exhibit characteristics that are typical of an introduced population. Estimates of both Shannon diversity and Nei's gene diversity were lower for the total New Zealand population compared to the U.S. population (4.59 vs. 6.09 and 0.655 vs. 0.820 for H and H_e, respectively) (Bennett and Stone, 2016). This, along with the high linkage disequilibrium observed, may indicate a population bottleneck whereby a small group of individuals was introduced in one or more discrete events, and a founder effect due to subsequent genetic drift in the introduced population. Isolates from Tauhara (TAU), a site in the central part of the North Island near Taupo where *N. gaeumannii* was first reported in 1959, had the highest genotypic diversity and richness. This is consistent with the central North Island being the locus of initial introduction of *N. gaeumannii* into the country, as suggested by

Hood and Kershaw (1975). However, isolates recovered from this site consisted of Lineage 1 genotypes exclusively. Isolates of Lineage 2 were recovered nearby at Kaingaroa, but their MLGs were not similar to the Lineage 2 isolates collected from the South Island sites Mawhera, Forest Creek, and Golden Downs (Figure 3.5). These Lineage 2 isolates from the South Island exhibited combinations of alleles in MLGs that, until now, have only been detected in the coastal low-elevation forests in the western Oregon Coast Range (Bennett and Stone, 2016; Winton et al., 2006). This strongly suggests that the New Zealand *N. gaeumannii* population originated from a source in the coastal Douglas-fir forests of western North America.

The reproductive biology of *N. gaeumannii* appears to have had a strong influence on the contemporary structure of the introduced New Zealand population. Estimates of the multilocus index of association suggested that alleles in this population do not associate randomly in multilocus genotypes, as would be expected in a random-mating population (Agapow and Burt, 2001). Here it is important to consider the differences between reproductive mode (i.e. heterothallism vs. homothallism) and reproductive morphology (i.e. ascospores vs. conidia), as self-fertilization via meiospores and asexual reproduction via mitospores both can result in clonal population structures (Taylor et al., 1999; Winton et al., 2006). The clonal population structure we observed might be expected to result from asexual reproduction via mitospores (conidia), except that conidial reproduction has not been observed in *N. gaeumannii*, despite considerable scrutiny (Stone et al., 2008a). One possible explanation for this population structure is that *N. gaeumannii* is homothallic, and is reproducing primarily via self-fertilization,

resulting in progeny that are genetically identical to the parent. Another potential explanation is that *N. gaeumannii* is outcrossing, but recombination occurs between individuals with similar or identical MLGs and thus does not lead to significant change in genetic diversity. In theory, this population genetic structure indicates a diminished capacity for adaptation, as recombination between individuals with dissimilar MLGs would be rare and new combinations of alleles occur infrequently (McDonald and Linde, 2002).

Significant linkage disequilibrium was also detected, albeit to a lesser degree, when repeated MLGs were removed (Figure 3.2B), suggesting that the population structure of *N. gaeumannii* is strongly influenced by its reproductive mode. High linkage disequilibrium due to the presence of clones is often interpreted as evidence of an "epidemic" population structure in pathogenic microbes, whereby natural selection results in an abundance of certain genotypes that have superior fitness (often due to greater virulence or aggressiveness) relative to the rest of the population (Smith et al., 1993). In addition to the observation that a few genotypes were particularly abundant in this invasive population, the high linkage disequilibrium due to large numbers of clones could be an indication of such an epidemic population structure in New Zealand. However, the relative aggressiveness of the overrepresented genotypes has not been examined experimentally, and disease severity does not appear to coincide with the distribution of Lineage 2 or the overrepresented genotypes (discussed below). The apparent linkage disequilibrium was also due, at least in part, to the presence of reproductively-isolated subpopulations (i.e. Lineages 1 and 2). When the two lineages

were analyzed separately, $\bar{r}_d$ for the Lineage 1 subpopulation was reduced further, and that of the Lineage 2 isolates did not differ significantly from that expected under panmixia (Figure 3.2 C, D). After removal of duplicate MLGs from the dataset, linkage disequilibrium for the Lineage 1 subpopulation was still much higher than would be expected with random mating. High linkage disequilibrium in the absence of repeated MLGs and reproductively isolated subpopulations may have resulted from a bottleneck due to the introduction of a small founding population in which allele frequencies were subsequently altered by genetic drift (Hartl and Clark, 2007).

The AMOVA and bootstrap analyses revealed that the lineages were strongly differentiated, as they accounted for a large proportion of the between-population variation, and were separated at a basal node into distinct clusters on the UPGMA dendrogram with strong statistical support. These results are consistent with the findings of Winton et al. (2006), who provided evidence that the two *N. gaeumannii* lineages are reproductively isolated in endemic populations in the northwestern United States. Whether they should be recognized as separate species should be examined by comparing nucleotide sequence data from multiple genes (or genomes) among isolates from both lineages.

Given that the Douglas-fir production regions in the North and South Islands are very patchy and do not form a contiguous distribution, we expected that spread via aerial ascospore dispersal would result in some genetic differentiation between the islands, and between sites within the islands, due to dispersal limitations. However, only a very small proportion of the overall genetic variation occurred between islands (Table 3.2), and there

was little genetic differentiation between them (Table 3.2, Figure 3.3A). The lack of genetic differentiation between the North and South Islands is further supported by the fact that there were 60 shared MLGs between them (Figure S3.3).

A moderate, but significant, degree of genetic differentiation was identified among the isolates collected from sites within the islands, but the DAPC scatterplot showed little differentiation among the clusters representing the 32 sites. Several Lineage 2 isolates with distinct genotypes fell outside of the central cluster of points, suggesting that some of the genetic variation among sites is due to the presence of Lineage 2. Still, the majority of the genetic variation was partitioned to the within-site component, suggesting that gene flow occurs between sites (Table 3.2). There were 104 MLGs that occurred at more than one site, and the most common MLG was shared by 271 individuals across 17 sites. This MLG was present at both Wairangi (N. Island) and Gowan Hills (S. Island), which are nearly 1,000 km apart (Figure 3.1).

There was no isolation by distance in the New Zealand *N. gaeumannii* populations, as no correlation between the genetic distances and geographic distances among sites was detected. These results suggest a relatively homogeneous distribution of Lineage 1 MLGs across New Zealand with few genetic barriers or dispersal limitations. Hood and Kershaw (1975) and Hood (1990) documented the gradual spread of *N. gaeumannii* from a single introduction locus near Taupo to the rest of the North Island, and subsequently throughout the South Island, over a period of approximately 30 years. A gradual spread and colonization via the aerial dispersal of ascospores over short distances would be expected to result in some genetic differentiation between the islands,

or between sites within each island. The effects of random dispersal, local adaptation, mutation, natural selection, and genetic drift would presumably lead to genetic variation across sites over time. Unless long-distance ascospore dispersal occurs regularly, the gradual expansion from a single source would also be expected to result in an isolation by distance phenomenon whereby genetic dissimilarity increases with the geographic distance between sites. A similar line of reasoning was used to test hypotheses about the introduction and spread of the sudden oak death pathogen, *Phytophthora ramorum*, in Oregon. Kamvar et al. (2015b) described the spread of *P. ramorum* populations from two points of introduction. Those authors suggested that it was the accumulation of mutations during the spread of these clonal populations that resulted in isolation by distance, and that this pattern would not be expected to occur if the spread had occurred via long distance dispersal (Kamvar et al., 2015b). Since we did not observe isolation by distance associated with the introduction and spread of *N. gaeumannii* in New Zealand, we can infer that either mutation rates are low, or that migration rates are high. Other potential explanations for the lack of differentiation between islands, and between sites within islands, include a "stepping-stone" hypothesis in which connectivity between distant patches of a host plant may be attained by ascospore dispersal over shorter distances (Linde et al., 2002), the colonization of isolated Douglas-fir plantations via human-mediated dispersal by movement of infected plant material, or long-distance aerial ascospore dispersal among sites within and between islands. The aerial dispersal of ascospores over 1,000 km would be exceedingly rare (Brown and Hovmøller, 2002; Rivas et al., 2004). The observed distribution of MLGs also could have resulted from the

establishment of Douglas-fir plantations in the North and South Islands with infected seedlings from a single source population such as a nursery.

Given that there has apparently been gene flow between the Douglas-fir plantations in the North and South Islands, the fact that there were Lineage 2 MLGs that were relatively abundant in the South Island but were not detected in the North Island suggests that there may have been a separate introduction to the South Island from a coastal Oregon or Washington source. However, the possibilities that the observed distribution of Lineage 2 genotypes resulted from a single introduction near Taupo and our sampling either did not recover Lineage 2 MLGs that were present, or that Lineage 2 genotypes initially present in the North Island spread to the South Island but subsequently went extinct in the North Island cannot be excluded, but is a much less parsimonious explanation. Nevertheless, the 4 MLGs we detected from 18 Lineage 2 isolates seemed to account for all of the expected genotypic richness in Lineage 2 (Figure S3.2B). It is also possible that differentiation of local populations where Lineage 2 was abundant in the South Island, i.e. at Golden Downs and Mawhera, has occurred via natural selection, or is due to processes such as genetic drift, which is particularly influential in small populations such as these (Hartl and Clark, 2007).

One major question that remains largely unanswered is whether the genetic variation in *N. gaeumannii* is related to SNC severity. Winton et al. (2006) suggested that Lineage 2 may have contributed to the emergence of SNC in the native range of Douglas-fir, as they found that a higher Lineage 2 to Lineage 1 ratio was associated with lower canopy density and increased foliage discoloration in some stands in coastal northwestern

Oregon. The distribution of Lineage 2 in the northwestern Coast Ranges in Oregon and Washington generally corresponds to the region where SNC is most severe (Bennett and Stone, 2016; Winton et al., 2006). This suggests that there is some variation in aggressiveness between strains of this fungus. In New Zealand, however, the geographic distribution of Lineage 2 was very limited and was not restricted to severely diseased sites (data not shown). Much of the variation in SNC severity among sites occurred where *N. gaeumannii* Lineage 2 was absent. The fact that disease severity seemed to vary among sites in New Zealand despite the fact that the Lineage 1 genotypes were relatively uniformly distributed across sites in both the North and South Islands suggests that there is no clear association between specific genotypes or lineages and disease. The observed spatial variation in SNC severity in New Zealand is much more likely to be a function of climate, as areas with warmer winter temperatures and more precipitation in spring and early summer generally have more severe SNC symptoms (Stone et al., 2007; Watt et al., 2010).

The records of the introduction of Douglas-fir into New Zealand for use as a plantation forestry species imply that plantations were established using seed obtained from western North America, rather than planting stock, and were locally propagated thereafter (Hood and Kershaw, 1975; Weston, 1957). However, *N. gaeumannii* must have been introduced on infected live seedlings through the forestry or ornamental nursery trade because *N. gaeumannii* can only be vectored on live or recently abscised foliage. It is highly unlikely that *N. gaeumannii* migrated to New Zealand naturally via passive ascospore dispersal, given that major dispersal barriers and vast distances exist between

New Zealand and the nearest known *N. gaeumannii* populations in Europe and North America. The SNC fungus was present in Europe long before it was detected in New Zealand, but Lineage 2 has only been found in coastal northwestern North America and New Zealand, which strongly suggests North America as the source.

One potential limitation of the sampling design for this study is that there was unequal sampling among the levels of the population hierarchy. Although foliage was collected from 10 trees at each site, the number of isolates collected from each of the trees was not uniform. This was due to variation in infection levels, as well as sample loss due to culture contamination and the inhibition of PCR amplification by impurities such as fungal melanin. Another factor that contributed to unequal sample sizes among populations was the fact that only some of the sites were sampled in both years. Those that were sampled in only 2005 or 2007 generally had fewer isolates. We attempted to account for unequal sample sizes in many analyses by using rarefaction. This technique was used to select random sub-samples of the data such that all sample sizes included in the analyses were equal to the number of samples in the group with the fewest samples. This allowed for direct comparisons to be made among groups with unequal sample sizes. There were also fewer loci available than anticipated due to inconsistent amplification and genotyping of the Pgdi5 locus. Removal of this locus did not seem to diminish our ability to distinguish among individuals, as the genotype accumulation curve suggested that we would be able to adequately discriminate between 90% of the MLGs with only eight loci (Figure S3.1). However, even with the large number of samples genotyped, the genotypic richness curve indicated that we were not able to capture all of the expected

genetic variation in Lineage 1, given the genotypic richness observed (Figure S3.2A). This suggests that had we continued to genotype more Lineage 1 isolates from New Zealand, we would have continued to discover new genotypes. The richness curve for Lineage 2 plateaued with only four MLGs (Figure S3.2B), indicating that our sample size was sufficient for describing most of the genotypic richness for Lineage 2 in New Zealand.

3.6 Acknowledgements

We thank the following for field and laboratory assistance: J. Britt, J. F. Gardner, R. J. Hood, and W. Sutton. Z. Kamvar and J. Tabima assisted in the implementation and interpretation of analyses performed with the R packages *poppr* and *adegenet*. The authors would also like to thank N. Grünwald for helpful comments on an earlier version of the manuscript. Major funding, laboratory, technical, and logistic support provided by Scion is gratefully acknowledged. Additional funding was provided from the New Zealand Ministry of Business, Innovation and Employment Strategic Science Investment Fund. We also thank the many forest landowners in New Zealand who generously provided access to their lands.

3.7 Literature Cited

Agapow, P., Burt, A., 2001. Indices of multilocus linkage disequilibrium. *Molecular Ecology Notes* 1, 101–102.

Baquero, O.S., 2017. ggsn: north symbols and scale bars for maps created with 'ggplot2' or 'ggmap'. R package version 0.4.0. https://CRAN.R-project.org/package=ggsn

Bennett, P., Stone, J., 2016. Assessments of population structure, diversity, and phylogeography of the Swiss needle cast fungus (*Phaeocryptopus gaeumannii*) in the U.S. Pacific Northwest. *Forests* 7, 14. doi: 10.3390/f7010014

Black, B.A., Shaw, D.C., Stone, J.K., 2010. Impacts of Swiss needle cast on overstory Douglas-fir forests of the western Oregon Coast Range. *Forest Ecology and Management* 259, 1673–1680. doi: 10.1016/j.foreco.2010.01.047

Boyce, J.S., 1940. A Needle-Cast of Douglas fir Associated with *Adelopus gaumanni*. *Phytopathology* 30, 649–659.

Brown, J.K.M., Hovmøller, M.S., 2002. Aerial dispersal of pathogens on the global and continental scales and its impact on plant disease. *Science* 297, 537–541.

Castaño, C., Colinas, C., Gómez, M., Oliva, J., 2014. Outbreak of Swiss needle cast caused by the fungus *Phaeocryptopus gaeumannii* on Douglas-fir in Spain. *New Disease Reports* 29, 19. doi: 10.5197/j.2044-0588.2014.029.019

Dray, S., Dufour, A.-B., 2007. The ade4 package: implementing the duality diagram for ecologists. *Journal of Statistical Software* 22, 1–20.

Excoffier, L., Smouse, P.E., Quattro, J.M., 1992. Analysis of Molecular Variance Inferred from Metric Distances Among DNA Haplotypes: Application to Human Mitochondrial DNA Restriction Data. *Genetics Society of America* 131, 479–491.

Grünwald, N.J., Hoheisel, G.A., 2006. Hierarchical analysis of diversity, selfing, and genetic differentiation in populations of the oomycete *Aphanomyces euteiches*. *Phytopathology* 96, 1134–1141. doi: 10.1094/PHYTO-96-1134.

Grünwald N., Kamvar Z.N., Everhart S.E., 2016. grunwaldlab/Population_Genetics_in_R: First release [Dataset]. Zenodo. doi: 10.5281/zenodo.160588

Hansen, E.M., Stone, J.K., Capitano, B.R., Rosso, P., Sutton, W., Winton, L., Kanaskie, A., McWilliams, M.G., 2000. Incidence and impact of Swiss needle cast in forest plantations of Douglas-fir in coastal Oregon. *Plant Disease* 84, 773–778.

Hartl, D.L., Clark, A.G., 2007. Principles of population genetics, 4th ed. Sinauer Associates, Sunderland, Mass.

Hood, I.A., Kershaw, D.J., 1975. Distribution and infection period of *Phaeocryptopus gaeumannii* in New Zealand. *New Zealand Journal of Forestry Science* 5, 201–208.

Hood, I.A., Kershaw, D.J., 1973. Distribution and life history of *Phaeocryptopus gaeumannii* on Douglas Fir in New Zealand (Forest Pathology Report No. 37 (unpublished)). New Zealand Forest Service, Forest Research Institute.

Hood, I.A., Kimberley, M.O., 2005. Douglas fir provenance susceptibility to Swiss needle cast in New Zealand. *Australasian Plant Pathology* 34, 57. doi: 10.1071/AP04080.

Hood, I.A., Sandberg, C.J., Barr, C.W., Holloway, W.A., Bradbury, P.M., 1990. Changes in needle retention associated with the spread and establishment of *Phaeocryptopus gaeumannii* in planted Douglas fir. *European Journal of Forest Pathology* 20, 418–429.

Jombart, T., 2008. adegenet: a R package for the multivariate analysis of genetic markers. *Bioinformatics* 24, 1403–1405. doi: 10.1093/bioinformatics/btn129.

Jombart, T., Devillard, S., Balloux, F., 2010. Discriminant analysis of principal components: a new method for the analysis of genetically structured populations. *BMC Genetics* 11, 1.

Jombart, T., Collins, C., 2015. A tutorial for discriminant analysis of principal components (DAPC) using adegenet 2.0.0. London: Imperial College London, MRC Centre for Outbreak Analysis and Modelling.

Kamvar, Z.N., Brooks, J.C., Grünwald, N.J., 2015a. Novel R tools for analysis of genome-wide population genetic data with emphasis on clonality. *Frontiers in Genetics* 6. doi: 10.3389/fgene.2015.00208.

Kamvar, Z.N., Larsen, M.M., Kanaskie, A.M., Hansen, E.M., Grünwald, N.J., 2015b. Spatial and temporal analysis of populations of the sudden oak death pathogen in Oregon forests. *Phytopathology* 105, 982–989. doi: 10.1094/PHYTO-12-14-0350-FI.

Kamvar, Z.N., Tabima, J.F., Grünwald, N.J., 2014. *Poppr*: an R package for genetic analysis of populations with clonal, partially clonal, and/or sexual reproduction. *PeerJ* 2, e281. doi: 10.7717/peerj.281

Kimberley, M.O., Hood, I.A., Knowles, R.L., 2011. Impact of Swiss needle-cast on growth of Douglas-fir. *Phytopathology* 101, 583–593. doi:10.1094/PHYTO-05-10-0129.

Lavender, D.P., Hermann, R.K., 2014. Douglas-fir: the genus *Pseudotsuga*. Oregon Forest Research Laboratory, Oregon State University, Corvallis, OR, USA.

Liese, J., 1939. The occurrence in the British Isles of the Adelopus disease of Douglas fir. *Quarterly Journal of Forestry* 33, 247–252.

Linde, C.C., Zhan, J., McDonald, B.A., 2002. Population structure of *Mycosphaerella graminicola*: from lesions to continents. *Phytopathology* 92, 946–955.

Mantel, N., 1967. The detection of disease clustering and a generalized regression approach. *Cancer Research* 27, 209–220.

Maguire, D.A., Mainwaring, D.B., Kanaskie, A., 2011. Ten-year growth and mortality in young Douglas-fir stands experiencing a range in Swiss needle cast severity. *Canadian Journal of Forest Research* 41, 2064–2076. doi: 10.1139/x11-114

Manter, D.K., Bond, B.J., Kavanagh, K.L., Rosso, P.H., Filip, G.M., 2000. Pseudothecia of Swiss needle cast fungus, *Phaeocryptopus gaeumannii*, physically block stomata of Douglas fir, reducing CO_2 assimilation. *The New Phytologist* 148, 481–491.

Marks, G.C., 1975. Swiss needle cast of Douglas fir. *Australasian Plant Pathology* 4, 24–24.

McCormick, F.A., 1939. *Phaeocryptopus gaeumannii* on Douglas Fir in Connecticut. *Plant Disease Reporter* 23, 368–369.

McDonald, B.A., Linde, C., 2002. Pathogen population genetics, evolutionary potential, and durable resistance. *Annual Review of Phytopathology* 40, 349–379. doi: 10.1146/annurev.phyto.40.120501.101443.

Meinecke, E.P., 1939. The *Adelopus* needle cast of Douglas Fir on the Pacific Coast. Dept. of Natural Resources, Division of Forestry, Sacramento, California.

Ministry for Primary Industries, 2016. National Exotic Forest Description as at 1 April 2016. New Zealand.

Morton, H.L., Patton, R.F., 1970. Swiss needle cast of Douglas-fir in the Lake States. *Plant Disease Reporter* 54, 612–616.

Nei, M., 1972. Genetic distance between populations. *The American Naturalist* 106, 283–292.

Nei, M., 1978. Estimation of average heterozygosity and genetic distance from a small number of individuals. *Genetics* 89, 583–590.

Oksanen, J., Guillaume, B., Friendly, M., Kindt, R., Legendre, P., McGlinn, D., Minchin, P.R., O'Hara, R.B., Simpson, G.L., Solymos, P., Stevens, M.H.H., Szoecs, E., Wagner, H., 2017. vegan: Community Ecology Package. R package version 2.4-5. https://CRAN.R-project.org/package=vegan

Osorio, M., 2007. Detección del hongo defoliador *Phaeocryptopus gaeumannii* en plantaciones de *Pseudotsuga menziesii* de Valdivia, Chile. *Bosque* 28, 69–74.

Peace, T.R., 1962. Pathology of Trees and Shrubs with Special Reference to Britain. Clarendon Press, Oxford.

Peakall, R., Smouse, P.E., 2012. GenAlEx 6.5: genetic analysis in Excel. Population genetic software for teaching and research--an update. *Bioinformatics* 28, 2537–2539. doi: 10.1093/bioinformatics/bts460.

Peakall, R., Smouse, P.E., 2006. GenAlEx 6: genetic analysis in Excel. Population genetic software for teaching and research. *Molecular Ecology Notes* 6, 288–295. doi: 10.1111/j.1471-8286.2005.01155.x

R Core Team. 2017. R: A language and environment for statistical computing. R Foundation for Statistical Computing, Vienna, Austria. https://www.R-project.org.

Ritóková, G., Shaw, D., Filip, G., Kanaskie, A., Browning, J., Norlander, D., 2016. Swiss needle cast in western Oregon Douglas-fir plantations: 20-year monitoring results. *Forests* 7, 155. doi: 10.3390/f7080155.

Rivas, G.G., Zapater, M.F., Abadie, C., Carlier, J., 2004. Founder effects and stochastic dispersal at the continental scale of the fungal pathogen of bananas *Mycosphaerella fijiensis*. *Molecular Ecology* 13, 471–482. doi: 10.1046/j.1365-294X.2003.02043.x.

Rogers, J.S., 1972. Measures of genetic similarity and genetic distances. In: Studies in Genetics. University of Texas Publishers, pp. 145–153.

Rohde, T., 1936. *Adelopus gaeumannii* n. sp. und die von ihm hervorgerufene "Schweizer" Douglasienschütte. *Forstliche Wochenschrift Silva*. 24, 420–422.

Shannon, C.E., 2001. A mathematical theory of communication. *ACM SIGMOBILE Mobile Computing and Communications Review* 5, 3–55.

Slowikowski, K., 2017. ggrepel: repulsive text and label geoms for 'ggplot2'. R package version 0.7.0. https://CRAN.R-project.org/package=ggrepel

Smith, J.M., Smith, N.H., O'Rourke, M., Spratt, B.G., 1993. How clonal are bacteria? *Proceedings of the National Academy of Sciences* 90, 4384–4388.

Stone, J.K., Capitano, B.R., Kerrigan, J.L., 2008a. The histopathology of *Phaeocryptopus gaeumannii* on Douglas-fir needles. *Mycologia* 100, 431–444.

Stone, J.K., Coop, L.B., Manter, D.K., 2008b. Predicting effects of climate change on Swiss needle cast disease severity in Pacific Northwest forests. *Canadian Journal of Plant Pathology* 30, 169–176.

Stone, J.K., Hood, I.A., Watt, M.S., Kerrigan, J.L., 2007. Distribution of Swiss needle cast in New Zealand in relation to winter temperature. *Australasian Plant Pathology* 36, 445. doi: 10.1071/AP07049

Taylor, J.W., Jacobson, D.J., Fisher, M.C., 1999. The evolution of asexual fungi: reproduction, speciation and classification. *Annual Review of Phytopathology* 37, 197–246.

Temel, F., Stone, J.K., Johnson, G.R., 2003. First report of Swiss needle cast caused by *Phaeocryptopus gaeumannii* on Douglas-fir in Turkey. *Plant Disease* 87, 1536–1536. doi: 10.1094/PDIS.2003.87.12.1536B.

Watt, M.S., Stone, J.K., Hood, I.A., Palmer, D.J., 2010. Predicting the severity of Swiss needle cast on Douglas-fir under current and future climate in New Zealand. *Forest Ecology and Management* 260, 2232–2240. doi: 10.1016/j.foreco.2010.09.034.

Weston, G.C., 1957. Exotic forest trees in New Zealand. Statement prepared for the 7th British Commonwealth Forestry Conference, Australia and New Zealand No. 13. New Zealand Forest Service, Wellington, New Zealand.

Wickham, H. 2016. ggplot2: elegant graphics for data analysis. New York: Springer-Verlag. http://ggplot2.org.

Wilson, M., Waldie, J.S.L., 1928. Notes on new or rare forest fungi. *Transactions of the British Mycological Society* 13, 151–156.

Winton, L.M., 2001. Phylogenetics, population genetics, molecular epidemiology, and pathogenicity of the Douglas-fir Swiss needle cast pathogen *Phaeocryptopus gaeumannii*. PhD dissertation. Oregon State University, Corvallis, OR, USA.

Winton, L.M., Hansen, E.M., Stone, J.K., 2006. Population structure suggests reproductively isolated lineages of *Phaeocryptopus gaeumannii*. *Mycologia* 98, 781–791.

Winton, L.M., Stone, J.K., Hansen, E.M., 2007. Polymorphic microsatellite markers for the Douglas-fir pathogen *Phaeocryptopus gaeumannii*, causal agent of Swiss needle cast disease. Molecular Ecology Notes 7, 1125–1128. doi: 10.1111/j.1471-8286.2007.01802.x.

Yu, G., Smith, D.K., Zhu, H., Guan, Y., Lam, T.T.-Y., 2017. ggtree: an R package for visualization and annotation of phylogenetic trees with their covariates and other associated data. *Methods in Ecology and Evolution* 8, 28–36. doi: 10.1111/2041-210X.12628.

3.8 Figures and Tables

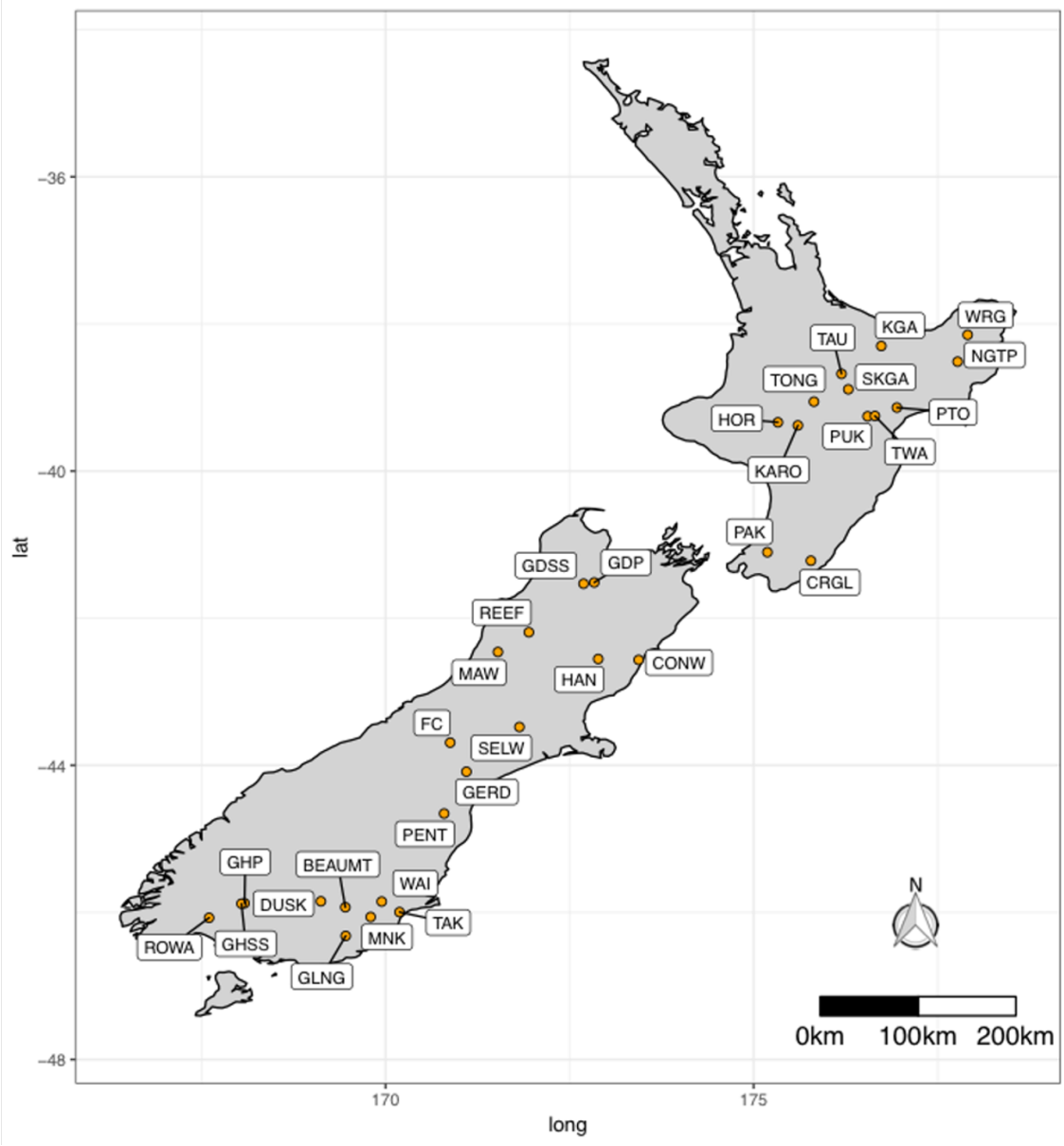

Figure 3.1: Locations of 32 sampling sites from which foliage was collected for isolation of *Nothophaeocryptopus gaeumannii* in New Zealand. Site labels correspond to abbreviated names shown in Table 3.1.

Table 3.1: Sample sizes and diversity estimates for the *Nothophaeocryptopus gaeumannii* isolates collected from 32 sites in the North and South Islands of New Zealand.

Population Level	$N_{isolates}$[a]	MLG[b]	eMLG[c]	SE[d]	H^*[e]	H_e[f]
Lineage						
L1	2067	464	14.4	1.68	2.56	0.65
L2	18	4	4	0	1.24	0.43
Total Lineage	2085	468	14.4	1.67	2.57	0.66
North Island						
Craigie Lea (CRGL)	47	25	7.70	1.21	1.93	0.55
Horopito (HOR)	25	15	7.59	1.11	1.92	0.46
Karioi (KAR)	168	64	8.51	1.08	2.08	0.64
Kaingaroa (KGA)	176	56	7.10	1.36	1.78	0.48
Ngatapa (NGTP)	49	21	7.36	1.19	1.89	0.53
Pakuratahi (PAK)	46	21	7.57	1.16	1.94	0.41
Putorino (PTO)	18	10	6.52	1.02	1.68	0.31
Puketitiri (PUK)	60	33	8.30	1.13	2.02	0.52
South Kaingaroa (SKGA)	46	27	8.76	0.94	2.13	0.60
Tauhara (TAU)	177	112	9.49	0.70	2.23	0.65
Tongariro (TONG)	24	15	7.62	1.10	1.93	0.44
Te Waka (TWA)	64	31	7.79	1.21	1.96	0.37
Wairangi (WRG)	53	35	8.59	1.07	2.08	0.54
Total North Island	953	335**	-	-	-	0.64
South Island						
Beaumont (BEAUMT)	154	48	8.10	1.14	2.02	0.53
Conway Hills (CONW)	12	7	6.00	0.67	1.50	0.44
Dusky (DUSK)	29	12	5.66	1.21	1.54	0.25
Forest Creek (FC)	25	10	6.08	1.05	1.65	0.23
Golden Downs (Progeny) (GD-P)	127	28	5.37	1.35	1.36	0.23
Golden Downs (Seed Source) (GD-SS)	71	26	7.37	1.22	1.88	0.54
Geraldine (GERD)	15	7	6.02	0.72	1.69	0.34
Gowan Hills (Progeny) (GH-P)	170	49	7.64	1.23	1.93	0.68
Gowan Hills (Seed Source) (GH-SS)	91	21	6.03	1.28	1.60	0.62
Glenelg (GLNG)	22	10	6.83	0.96	1.82	0.39

Table 3.1 (Continued)

Hanmer (HAN)	138	39	7.16	1.31	1.82	0.59
Mawhera (MAW)	10	2	2.00	0.00	0.50	0.20
Manuka Awa (MNK)	48	12	4.99	1.22	1.30	0.30
Pentland Hills (PENT)	12	9	7.82	0.65	1.98	0.31
Reefton (REEF)	18	7	5.65	0.80	1.61	0.50
Rowallen (ROWA)	38	14	6.94	1.09	1.82	0.48
Selwyn (SELW)	12	11	9.32	0.47	2.21	0.41
Takitoa (TAK)	17	11	7.24	1.01	1.85	0.47
Waipori (WAI)	123	30	5.89	1.35	1.55	0.44
Total South Island	1132	193**	–	–	–	0.64
Total	2085	468**	8.73	1.06	2.12	0.66

[a]$N_{isolates}$ = number of *N. gaeumannii* isolates, [b]MLG = number of multilocus genotypes, [c]eMLG = expected number of multilocus genotypes in rarefied sample equal to the number of samples in the group with the smallest number of samples (N = 10 isolates for pooled sites), [d]SE = standard error of eMLG estimate, [e]H = Shannon- Weiner diversity index (Shannon, 2001), [f]H_e = Nei's unbiased gene diversity (expected heterozygosity) (Nei, 1978). *estimated genotypic diversity from 1,000 bootstrap replicates with rarefaction sample sizes equal to the number of samples in the group with the smallest number of samples (N = 10 isolates for pooled sites). – data not calculated.
**Total MLG not equal to the sum of population totals due to shared MLGs.

Table 3.2: Hierarchical analysis of molecular variance (AMOVA) performed with clone-corrected dataset including unique SSR multilocus genotypes from 468 *Nothophaeocryptopus gaeumannii* isolates collected from 32 sites in the North and South Islands of New Zealand.

Hierarchical level	Variance (%)	ϕ	*P**
ϕ_{LT} (between lineages)	33.546	0.335	< 0.001
ϕ_{IL} (between islands within lineages)	0.245	0.004	0.222
ϕ_{SI} (between sites within islands)	8.264	0.125	< 0.001
ϕ_{SS} (within sites)	57.945	0.421	< 0.001

*P-value was obtained for the ϕ statistic with 1,000 permutations of the data.

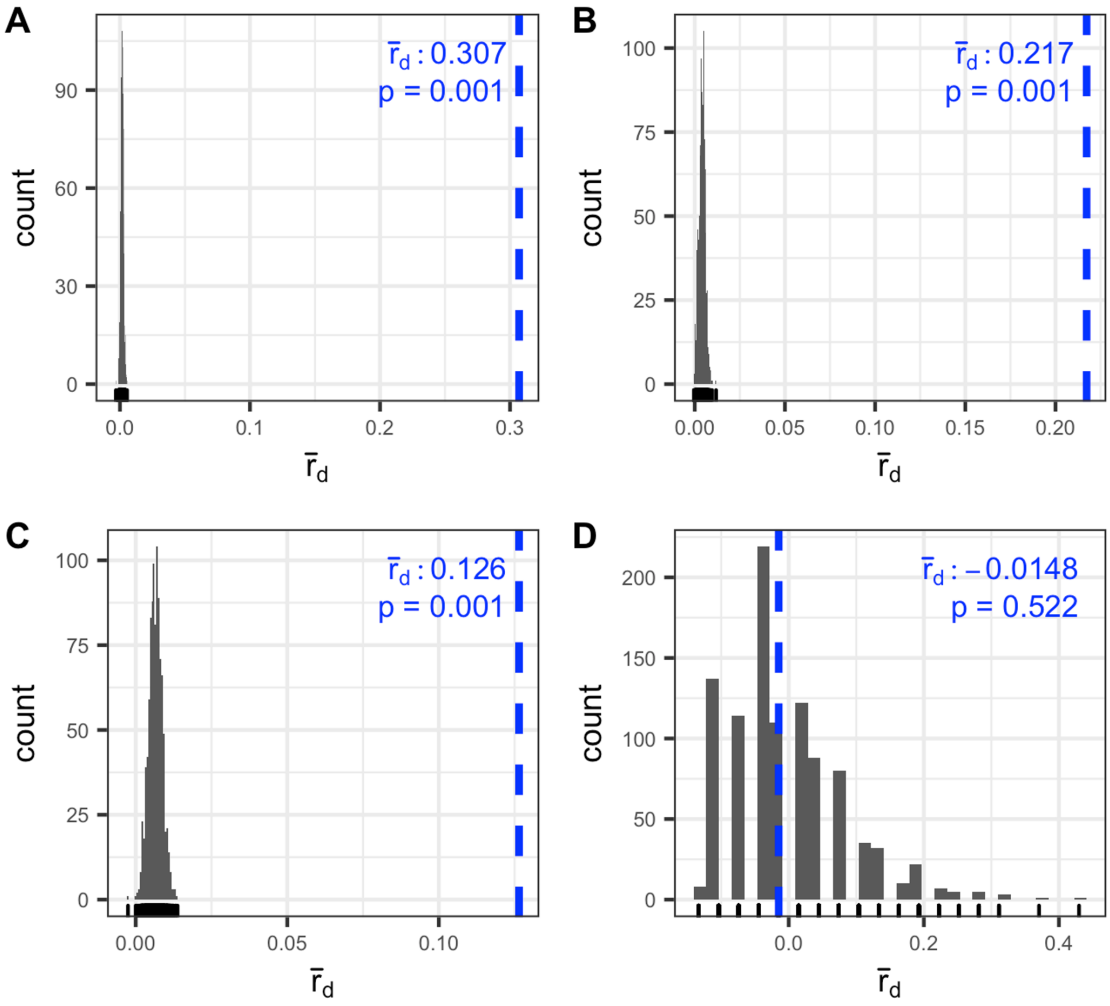

Figure 3.2: Estimates of the unbiased index of association ($\bar{r}_d$) (Agapow and Burt, 2001) based on SSR genotypes from *Nothophaeocryptopus gaeumannii* isolates collected in New Zealand. Histograms show the distributions of $\bar{r}_d$ values from 999 simulated populations with no linkage among loci ($\bar{r}_d = 0$ reflects linkage equilibrium). P-values reflect the chances of obtaining the observed value, or more extreme, under the null hypothesis of no linkage among loci. **A)** All isolates, including Lineages 1 and 2 (N = 2,085). **B)** Clone-censored, including Lineages 1 and 2 (N = 468). **C)** Clone-censored, Lineage 1 isolates only (N = 464). D, Clone-censored, Lineage 2 isolates only (N = 4).

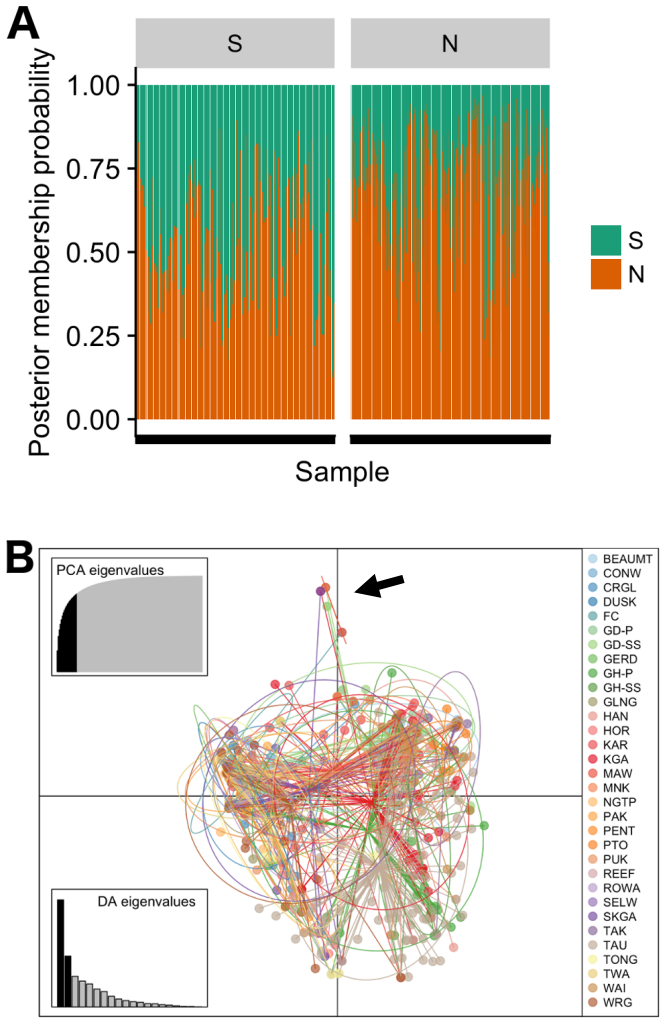

Figure 3.3: A) Bar plot from discriminant analysis of principal components (DAPC) showing posterior membership probabilities of 468 *Nothophaeocryptopus gaeumannii* genotypes (MLGs) in clusters representing the North (N) and South (S) Islands of New Zealand. Each bar represents one MLG, and the colored portion of each bar represents the probability of membership of that MLG in the North and/or South Island clusters. **B)** DAPC scatterplot showing clustering among multilocus genotypes (MLGs) from 32 sites. Each color represents a cluster (here, a site), and each point represents an MLG. Overlapping points represent identical MLGs. Inertia ellipses are drawn around 2/3 of the isolates in each cluster. The inset at top left indicates the proportion of principal components retained, while the graph at lower left indicates the number of discriminant functions retained. The legend at right shows the site name abbreviations corresponding to each cluster (Table 3.1, Figure 3.1). The black arrow in **B** points to the divergent genotypes (Lineage 2) from Mawhera (MAW), South Kaingaroa (SKGA), and Golden Downs (GD).

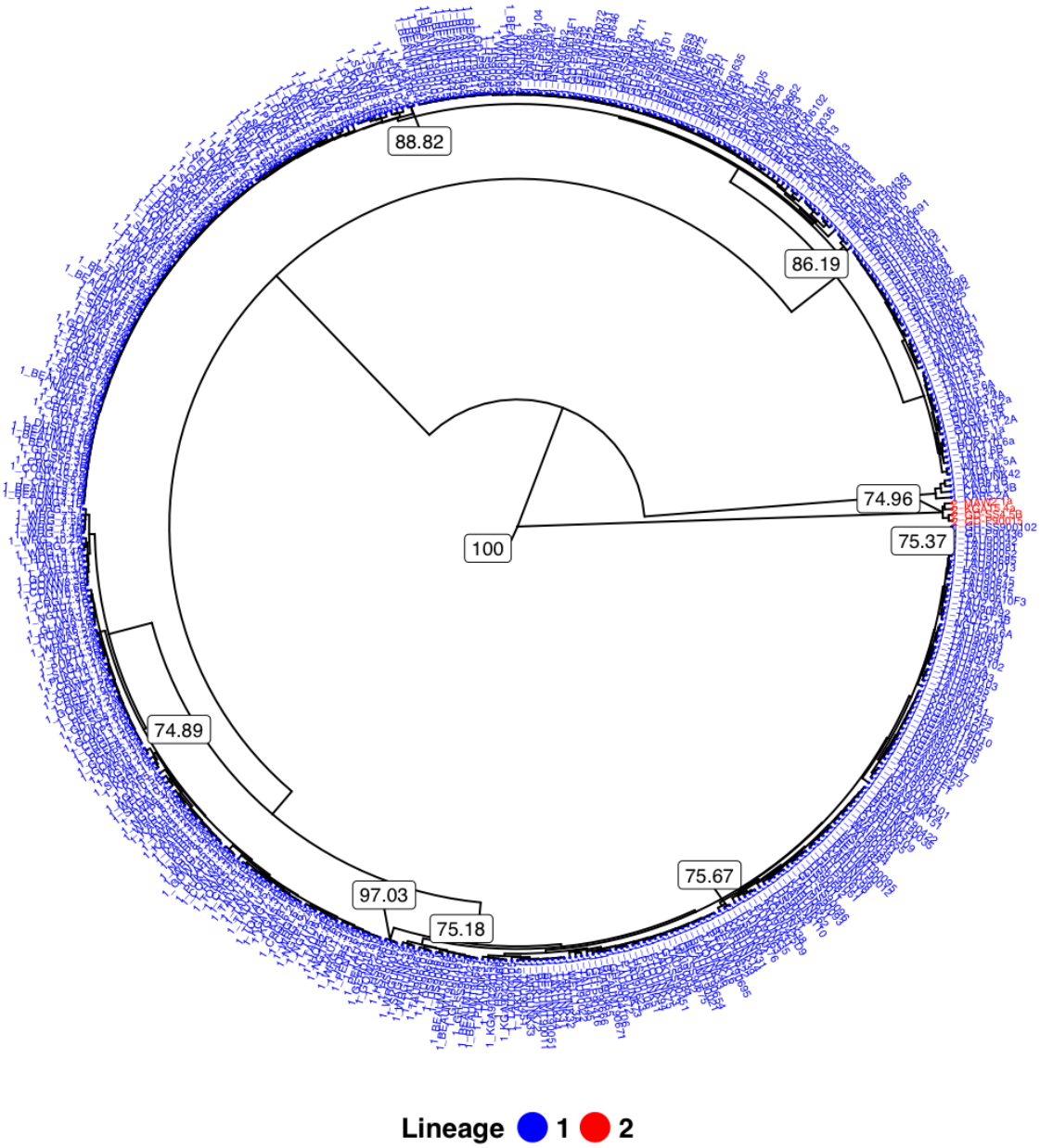

Figure 3.4: UPGMA dendrogram from a bootstrap analysis of Nei's genetic distance showing divergence among *Nothophaeocryptopus gaeumannii* multilocus genotypes (MLGs) corresponding to two lineages from New Zealand (clone-censored, $N = 468$). Node labels represent bootstrap statistics (≥ 70%) from 10,000 replicate trees.

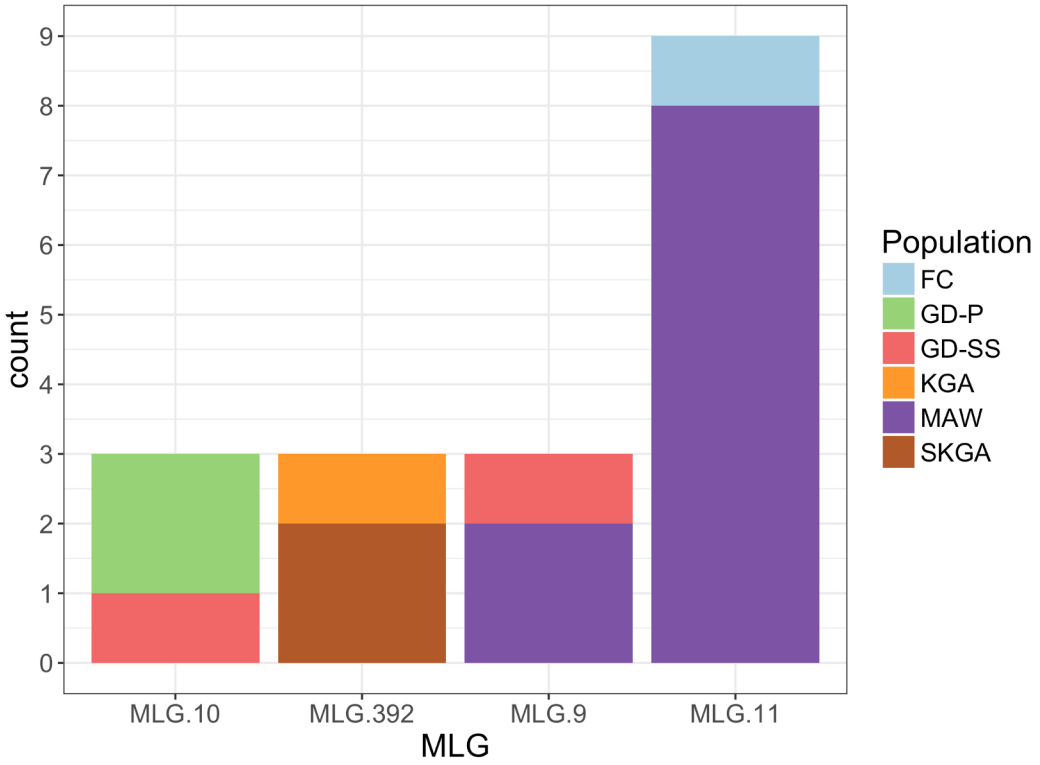

Figure 3.5: Bar plot showing the abundances of four *Nothophaeocryptopus gaeumannii* Lineage 2 SSR genotypes (MLGs) at six sites in the North and South Islands of New Zealand. Each bar represents a unique Lineage 2 MLG, with the colored portions of the bars corresponding to the number of isolates with that MLG at each of the sites listed in the legend (site locations shown in Figures 3.1 and 3.2).

3.9 Supplementary Figures

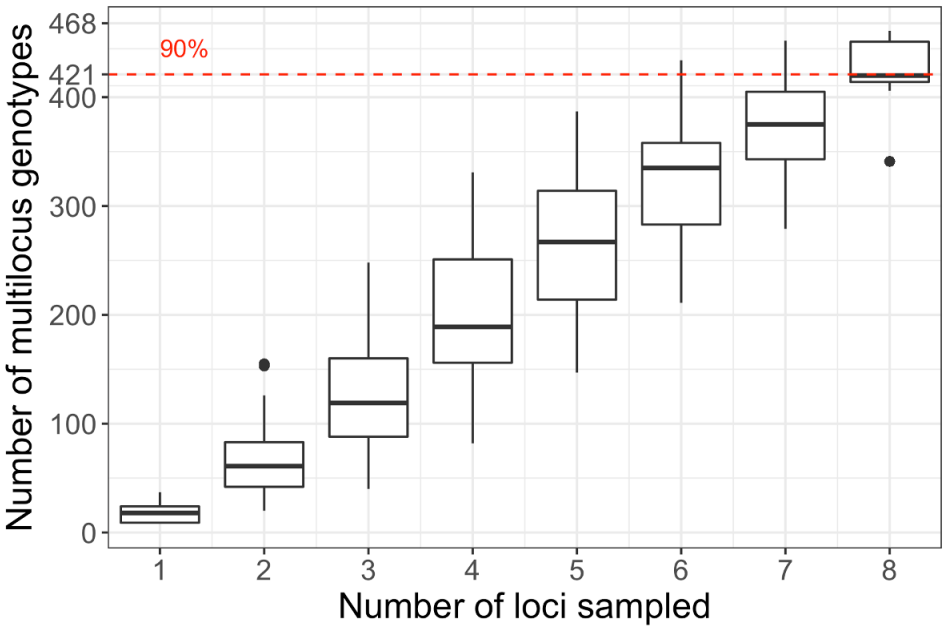

Figure S3.1: Genotype accumulation curve for *Nothophaeocryptopus gaeumannii* in New Zealand, with the vertical axis showing the observed number of multilocus genotypes (MLGs), and the horizontal axis showing the numbers of SSR loci for which 1,000 random samples were selected without replacement. The horizontal dashed line shows that eight loci provided enough resolution to discriminate between 90% of the MLGs.

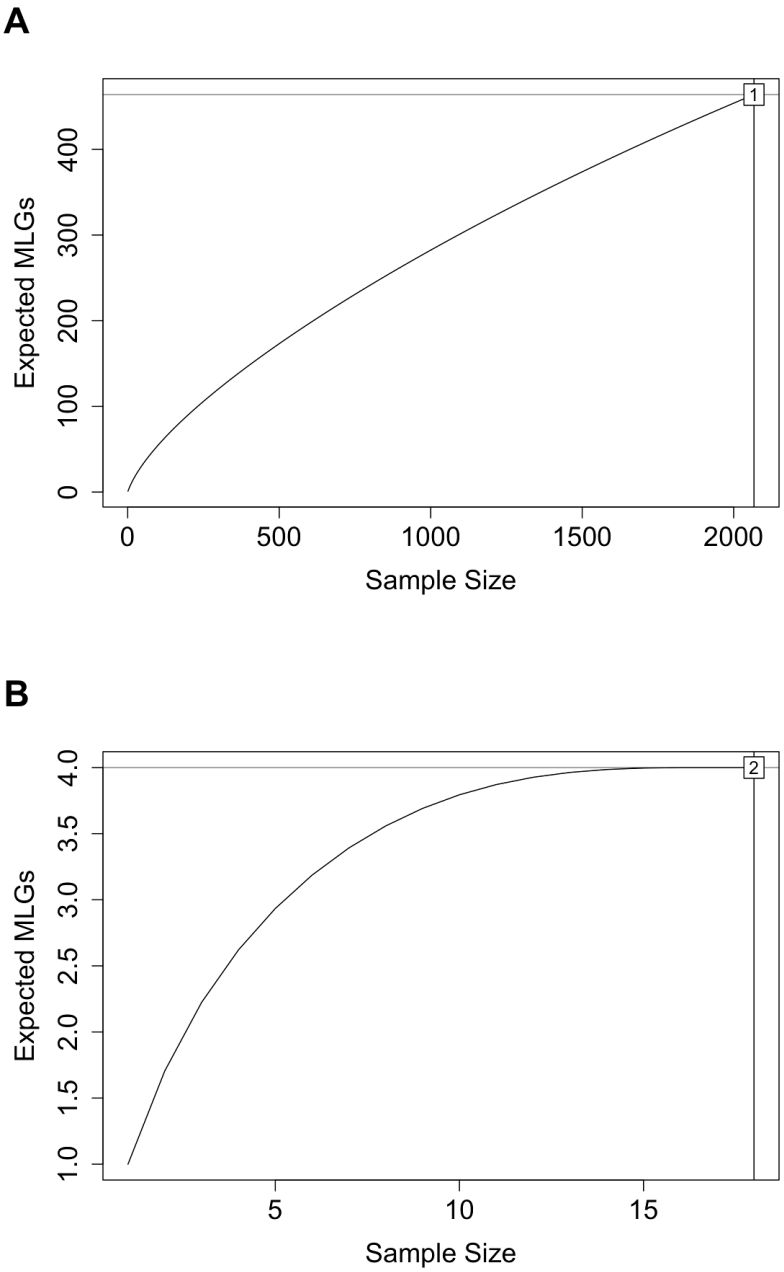

Figure S3.2: Genotypic richness curves with horizontal axes showing the numbers of *N. gaeumannii* isolates, and vertical axes showing the numbers of expected MLGs from **A)** Lineage 1, and **B)** Lineage 2.

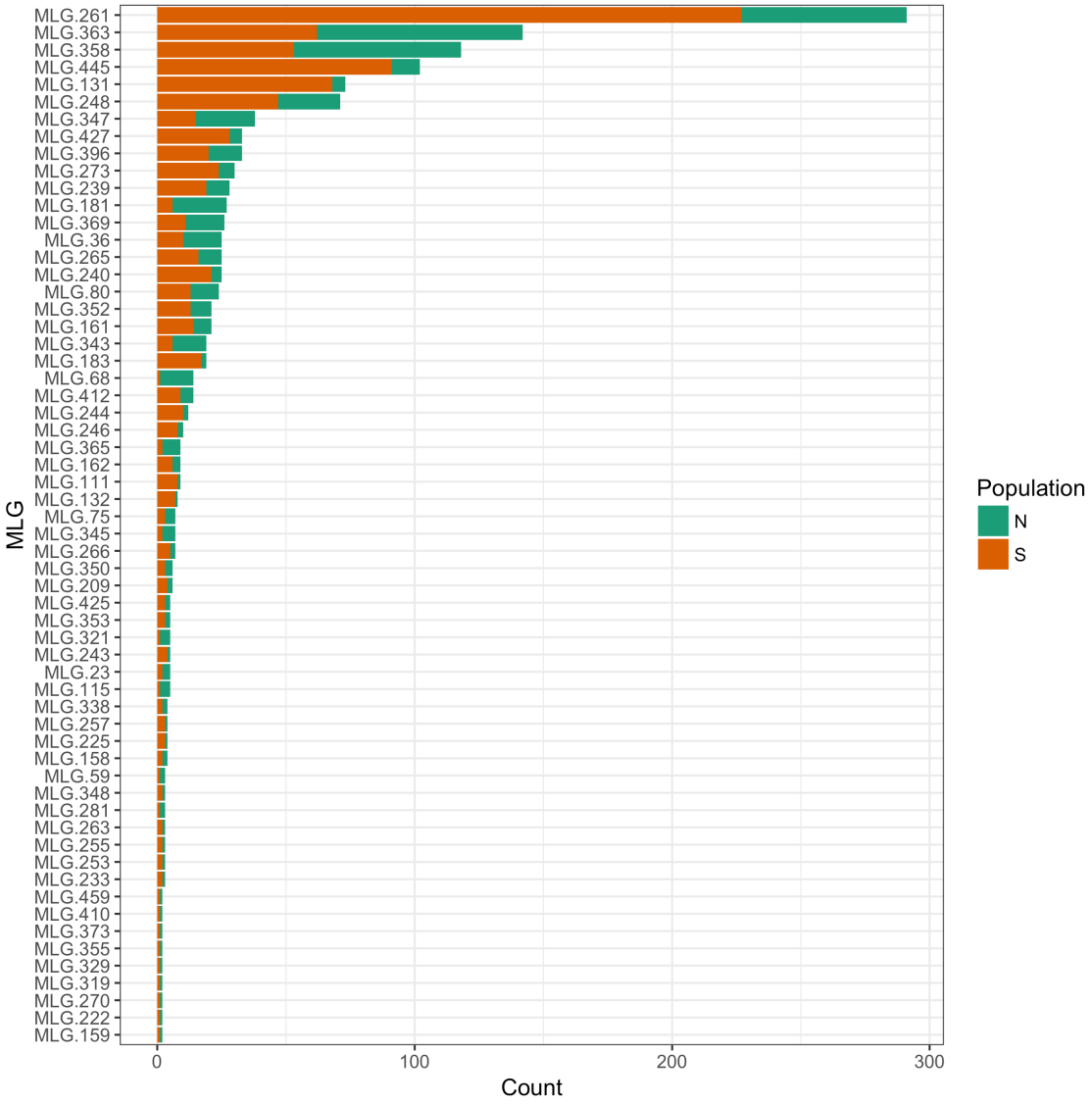

Figure S3.3: Abundances of the 60 *Nothophaeocryptopus gaeumannii* SSR genotypes (MLGs) shared between the North (N) and South (S) Islands of New Zealand. Each bar represents a unique MLG, with the colored portions of each bar corresponding to the number of isolates with that MLG on each island.

Chapter 4. Global Population Structure, Diversity and Introduction Pathways of the Douglas-fir Swiss Needle Cast Fungus *Nothophaeocryptopus gaeumannii*

4.1 Abstract

The Douglas–fir Swiss needle cast fungus, *Nothophaeocryptopus gaeumannii*, was first described from Switzerland in 1925. It was later determined to be widespread in western North America, and several lines of evidence suggest that it is native there. The goals of this study were to examine genetic diversity and population structure of *N. gaeumannii* populations globally to identify the most likely sources of each of four introduced populations and infer their demographic histories. For this study, a total of 1,591 multilocus SSR genotypes from 3,829 *N. gaeumannii* isolates collected from 9 countries were analyzed. Various demographic scenarios were examined using approximate Bayesian computation (ABC). The results provided support for previous studies that suggest that *N. gaeumannii* is endemic in western North America, and suggested that populations of the fungus in Europe and New Zealand were introduced directly from native populations, while those in Australia were introduced from Europe. The results also suggested that the *N. gaeumannii* populations in Chile and New Zealand were established from a common source population in western North America. The *N. gaeumannii* populations in New Zealand and Chile were either established in multiple independent introduction events, or were established with a diverse sample of migrants. The population in Australia appears to have been established with a single introduction from a source in Europe. The most parsimonious explanation for the introductions of *N. gaeumannii* from North America to these disparate geographic locations is the human-mediated transfer of infected plant material, as the fungus is not saprotrophic, nor seed

borne, and the genetic structure observed in introduced populations is not consistent with a stochastic transcontinental dispersal of ascospores.

4.2 Introduction

The invasion of new habitats by plant pathogenic microbes has increased due to intercontinental travel and trade (Barnes et al., 2014). Severe outbreaks of introduced fungal and oomycete pathogens often have devastating consequences for agriculture and forestry, as evidenced by the recent introduction of the sudden oak death pathogen, *Phytopthora ramorum*, to the western United States (Rizzo et al., 2005), and the establishment of *Cronartium ribicola* in native pine-dominated ecosystems in North America (Kinloch, 2003). Invasive species are expected to exhibit low diversity and richness due to founder events in which a small fraction of the variants in a source population are introduced to new territory, resulting in a genetic bottleneck (Nei et al., 1975). These genetic bottlenecks often result in reduced adaptive potential, though this effect may be overcome if gene flow occurs via multiple repeated introductions (Dlugosch and Parker, 2008). Analyses of genetic structure and population differentiation within introduced populations can allow for the inference of gene flow via long-distance aerial dispersal, gradual expansion, or human-mediated migration (Barnes et al., 2014; Brown and Hovmøller, 2002; Rivas et al., 2004).

A new needle cast disease of Douglas-fir (*Pseudotsuga menziesii* (Mirb.) Franco) was reported in Switzerland in 1925, and was named Swiss needle cast to distinguish it from the more common foliage disease of Douglas-fir caused by *Rhabdocline* spp. This disease was later reported from England and Ireland in 1927 and 1928, respectively

(Liese, 1939; Peace, 1962), and from southern Germany and Austria in the 1930s (Boyce, 1940). By 1940, *N. gaeumannii* was widespread throughout Switzerland and southern Germany (Boyce, 1940). A compilation of global SNC reports indicated that the presence of *N. gaeumannii* has been confirmed in Belgium, Bulgaria, Czech Republic, Finland, Hungary, Italy, Latvia, Netherlands, Portugal, Romania, Scotland, Slovenia, Sweden and Wales (Watt et al., 2011). Recently, SNC has been reported from Spain (Castaño et al., 2014).

In 1959, the presence of *N. gaeumannii* was reported for the first time in New Zealand (Hood et al., 1990; Hood and Kershaw, 1975). A single introduction locus was identified at that time, and the spread of the fungus throughout the North and South Islands was observed over the following three decades (Hood et al., 1990; Hood and Kershaw, 1975). Although there was an earlier report of *N. gaeumannii* in Tasmania that could not be confirmed, the fungus was present in Australia as early as 1975 (Marks, 1975). Currently, the only known occurrence of *N. gaeumannii* in South America is in Chile (Osorio, 2007).

Boyce (1940) reported the presence of *N. gaeumannii* pseudothecia on Douglas-fir foliage he collected in Oregon in 1916 that had gone unnoticed, due to the presence of a *Rhabdocline* sp. on the same foliage. This finding suggested that the fungus was present in North America before the reported outbreak of SNC in Europe. Subsequent surveys in California, Oregon, Washington, and British Columbia established that the fungus was widespread in the native range of Douglas-fir, but at this time there was no apparent disease in native forests associated with the presence of the fungus (Meinecke, 1939).

Boyce (1940) suggested that this apparent lack of severe disease, along with the fact that the only host of the fungus, Douglas-fir, is native to western North America, constituted evidence that the fungus was also endemic to this region. Although it has now emerged as a serious threat to forest health in coastal Oregon and Washington, *N. gaeumanii* was considered by most forest pathologists at the time to be innocuous in its native range (Boyce, 1940; Peace, 1962). Prior to the 1990s, it was only considered a serious pathogen in Christmas tree plantations in the PNW and Midwestern states, and in forest plantings outside of the native range of Douglas-fir where young trees were planted in environments conducive to disease (Morton and Patton, 1970; Hadfield and Douglass, 1982).

For this study, multilocus SSR genotypes (MLGs) were analyzed to test hypothesis that the current distribution of *N. gaeumannii* in Europe, New Zealand, Australia, and Chile resulted from independent introduction events from the native range of Douglas-fir in western North America, and to examine the influence of these introduction events on the diversity and genetic structures of each of the invasive populations. Our approach was to rank several putative introduction scenarios that explain the contemporary distribution of *N. gaeumannii* globally, identify the most probable origin of each invasive population, and make inferences as to whether they were established with a single discrete introduction event or with repeated introductions from their source population. The influence of population bottlenecks on the contemporary genetic structure of the invasive populations was also assessed by examining genetic

diversity, allelic richness, and population structure within and between five regional populations and 14 sub-regional populations representing nine countries.

4.3 Materials and Methods

4.3.1 Field Sampling, Isolations, and Culturing

The isolates analyzed here were a combination of those described in Chapter 2, which included 1,061 isolates from Oregon and Washington, those described in Chapter 3, which consisted of 2,085 isolates from 32 sites on the North and South Islands of New Zealand (Stone et al., 2007; Watt et al., 2010), and those described in Winton et al. (2006) and Winton and Stone (2004), which were collected from U.S. states including Oregon, Washington, Idaho, New Mexico, Vermont, and New York, from countries in Europe including Switzerland, France, Italy, Germany, and the U.K., and from 2 sites in New Zealand. Additional isolates analyzed here included 38 isolates from five sites in Chile as well as 63 isolates collected from a single site in Australia. At each location, foliage samples were collected from Douglas–fir trees of the coastal variety (*Pseudotsuga menziesii var. menziesii*), except in Idaho and New Mexico where the interior variety of Douglas–fir (*P. menziesii var. glauca*) was sampled (Winton et al., 2006). The isolation and culturing methods are described in detail in Bennett and Stone (2016) and Winton et al. (2006). Briefly, double-sided tape was used to attach two-year-old needles bearing pseudothecia of *N. gaeumannii* to the lids of Petri dishes to allow ascospores to discharge onto the agar below. These were incubated for approximately 24–48 h before transferring individual ascospores onto 2% potato dextrose agar (PDA) or malt agar (MA). These

cultures were then incubated for a minimum of 2–6 mo. to allow adequate growth for DNA extraction.

4.3.2 Molecular techniques

DNA was extracted following either the methods described in Winton et al. (2006) (for isolates collected (2001–2007) or those described in Bennett and Stone (2016) (for isolates collected 2014–2016). For the methods from Winton et al (2006), mycelium was scraped from the agar surface and macerated by shaking in a Mini-Beadbeater (BioSpec Products, Bartlesville, OK, USA) with glass beads and CTAB (cetyltrimethylammonium bromide) extraction buffer. The samples were then incubated at 65 ºC for 2 hrs and precipitated in 24:1 chloroform:isoamyl alcohol. Genomic DNA was purified with a QIAamp spin column to reduce PCR inhibitors. The method from Bennett and Stone (2016) utilized the DNeasy Plant Mini Kit (Qiagen, Hilden, Germany), and followed the manufacturer's instructions with the addition of an initial maceration procedure. Agar plugs extracted from *N. gaeumannii* cultures were added to cryogenic vials along with sterile glass beads. The vials were briefly submerged in liquid nitrogen to freeze the agar plugs prior to being shaken at 5000 rpm for 60 seconds with either a Mini-Beadbeater (BioSpec Products, Bartlesville, OK, USA) or MP Bio FastPrep (MP Biomedicals, LLC, Santa Ana, CA, USA).

Ten SSR loci (Winton et al., 2007) were amplified in three multiplexed PCR reactions, each with a fluorescently-labeled reverse primer to allow for the separation of overlapping allele sizes. Genotyping was performed via capillary electrophoresis at the Oregon State University Center for Genome Research and Biocomputing (CGRB) with

the parameters described in Winton et al. (2007) and Bennett and Stone (2016). Allele scoring was performed as described in Bennett and Stone (2016). The locus Pgdi5 did not amplify consistently across samples, and was omitted from subsequent analyses.

The resulting MLGs were then combined with a dataset of genotypes from isolates collected in 1997 and genotyped between 2007 and 2010 with primers that included 18 bp universal M13 primer tails (Winton et al., 2007). To combine the genotypes from the 1997 and 2014–2016 isolates into a single dataset, allele sizes from the 1997 samples were first adjusted by subtracting 36 bp from each allele to account for the absence of the M13 tails. These allele sizes were then compared to a validation set (N= 90 isolates) representing samples from the 1997 isolates that were genotyped without the M13 primer tails. Some discrepancies between the two datasets remained after adjustment. For the locus Pgdi4 an additional 4 bp was removed from the 1997 isolates to match the validation set. Alleles of other loci were adjusted in 1–2 bp increments to match allele sizes observed in the validation set. Further processing and validation was performed to reconcile the two datasets and to optimize agreement between the two genotyping methods. A positive control isolate that was included with each of the genotyping runs from 2014–2016 was also present in the validation dataset, and ensured the reproducibility and accuracy of the allele calls performed by different researchers.

4.3.3 Data Analysis

The SSR genotypes were formatted in Microsoft Excel 2016 with GenAlEx 6.503 (Peakall and Smouse, 2012, 2006), prior to being imported into R version 3.4.1 (R Core Team 2017) for use with the R packages *poppr* version 2.5.0 (Kamvar et al., 2015, 2014),

adegenet 2.0.1 (Jombart, 2008), and *ade4* 1.7–8 (Dray and Dufour, 2007). The interpretation of *poppr* output, as well as the source code for producing graphics from *poppr* and *adegenet* output, was adapted from http://grunwaldlab.github.io/Population_Genetics_in_R/ (Grünwald et al., 2016). For this study, the data were stratified in a population hierarchy with the most inclusive level corresponding to the five regions from which Douglas-fir foliage was sampled (i.e. North America, Europe, New Zealand, Australia, and South America). The regions were then divided into sub-regional populations (for instance, six states in the U.S. and five countries in Europe), and within these sub-regional populations was a level corresponding to the sampling sites (Table 4.1). The map of sampling sites (Figure 4.1) was constructed with the R packages *ggplot2* and *ggsn* (Baquero, 2017; Wickham, 2016).

Genotypic diversity estimates were calculated with the R package *poppr* (Kamvar et al., 2015, 2014), and included Shannon-Weiner diversity (H), Nei's unbiased gene diversity (H_e) (Nei 1978), and evenness (E_5). Genotypic richness was estimated as the number of expected multilocus genotypes (eMLG) in a rarefied sample size (n). Allelic richness was calculated with the R package *hierfstat* (Goudet and Jombart, 2015). Because these parameters are dependent upon the number of individuals in the populations, and thus are sensitive to differences in sample sizes, a rarefaction method was used to select random sub-samples of the data that corresponded to the sample size of the population with the fewest samples ($n \geq 10$), allowing the estimates of diversity and richness to be compared among groups for which sampling was unequal. Genotypic

diversity and evenness were estimated from 1,000 iterations of a bootstrap analysis with rarefaction, as implemented in the R package *poppr* (Kamvar et al., 2015, 2014).

Linkage disequilibrium was estimated for each of the populations with a standardized index of association, $\bar{r}_d$ (Agapow and Burt, 2001), which was calculated in R with *poppr* (Kamvar et al., 2015, 2014). These calculations were performed with a clone–censored dataset to remove the influence of duplicate MLGs. The probabilities of obtaining the observed values of $\bar{r}_d$, or more extreme, under the null hypothesis of no linkage among loci (H_0: $\bar{r}_d = 0$) were calculated with 999 permutations of the data.

The genetic variance in the total population was partitioned within and among the regions, among sub-regional populations, and among the sampling sites in each of those populations, using analysis of molecular variance (AMOVA), implemented in R with *poppr* (Kamvar et al., 2015, 2014). This technique also allowed for the genetic differentiation among each of the hierarchical subpopulation levels to be estimated with a fixation index, phi (ϕ) (Excoffier et al., 1992). The probability of obtaining the observed ϕ, or more extreme, under the null hypothesis of no differentiation between subpopulations (H_0: $\phi = 0$) was obtained with 1,000 permutations of the data, as implemented in the R package *ade4* (Dray and Dufour, 2007).

Clustering among the genotypes from each population was analyzed with 10,000 bootstrap replicates of Nei's genetic distance, which was visualized as a UPGMA dendrogram. This analysis was performed in R with the aboot function from *poppr* (Kamvar et al., 2015, 2014). The dendrogram was visualized with the R package *ggtree* version 1.12.0 (Yu et al., 2017).

The degree of genetic differentiation between populations was examined by calculating G'_{ST} (Hedrick, 2005). This measure is scaled such that the value for two populations that do not share any alleles is one, and the value for population pairs that do not have any unique alleles (i.e. all alleles are shared), is equal to zero (Hedrick, 2005). Statistics such as G'_{ST} are directly linked to the effective number of migrants (N_m) when the rate of gene flow between populations is higher than the mutation rate within populations (Balloux and Lugon-Moulin, 2002; Hedrick, 2005). Because they incorporate both migration and mutation, the genetic structuring estimated from differentiation statistics reflects both the rate of exchange of alleles between populations and the time since divergence (Balloux and Lugon-Moulin, 2002).

Genetic differentiation across levels of the population hierarchy was examined more closely with discriminant analysis of principal components (DAPC), a multivariate analysis of genetic clustering among isolates (Jombart et al., 2010), implemented with the R package *adegenet* (Jombart, 2008). The number of principal components (PCs) corresponding to the lowest Mean Squared Error was selected via cross-validation, with a training set consisting of 90% of the observations in each subpopulation.

Approximate Bayesian computation (ABC) was performed with the software *DIYABC* version 2.1.0 (Cornuet et al., 2008). This coalescence-based analysis provided estimates of the posterior probabilities of complex demographic scenarios that aimed to describe the evolutionary and geographic origins of sampled populations (Cornuet et al., 2010, 2008; Guillemaud et al., 2010). We applied this analytical framework to infer the routes of introduction of *N. gaeumannii* into Europe, New Zealand, Australia, and Chile.

Preliminary analyses included 15 demographic scenarios that were aimed at examining the relationships between the four oldest populations: North America, Europe, New Zealand, and Australia (Figure S4.1). These scenarios were evaluated by comparing summary statistics calculated from a clone-censored dataset consisting of 1,237 MLGs from *N. gaeumannii* Lineage 1 to those calculated from a simulated reference table consisting of 2 x 10^6 "pseudo-observed" datasets. An additional 16 demographic scenarios were built around the framework of the scenario that yielded the highest posterior probability in the preliminary analysis, and were designed to test hypotheses regarding the evolutionary and geographic origins of the invasive *N. gaeumannii* population in Chile (Figure S4.2). This analysis included a total of 1,260 distinct MLGs from the four populations used in the preliminary analyses (North America, Europe, New Zealand, and Australia) in addition to 23 MLGs from *N. gaeumannii* isolates collected in Chile. Some of the scenarios examined here considered the possibility that some origins of the endemic and introduced populations had not been sampled (Figure S4.2). Other scenarios included population admixture events, or population size reductions associated with founder events (Figure S4.2, Table S4.4). Because the estimation of coalescence times in these simulations relies explicitly upon the generalized stepwise mutation model (GSM) (Cornuet et al., 2008), one of the SSR loci, Pgtri2, which was presumed not to adhere to this model given its complex structure (Table S4.1), was omitted from the dataset prior to analysis. Genotypes of Lineage 2 were not included in these analyses, as this lineage was only detected in Oregon, Washington, and New Zealand. The reference datasets were constructed with priors such as the observed allele size ranges and mutation

models for the eight microsatellite loci, and summary statistics included mean number of alleles, genetic diversity, and shared allele distance. It was assumed that all scenarios had equal probabilities prior to the analyses. Parameters such as the effective population size (N_e) and coalescence times were given uniform prior distributions with a range of 10–10,000 (Tables S4.2, S4.4). We also provided priors regarding the relative effective population sizes of the regional populations, given historical documentation of the introduction events, and considering the associated population bottlenecks following founder events (Table S4.2, S4.4).

4.4 Results

4.4.1 Diversity and Richness

The MLGs analyzed here consisted of alleles from nine SSR loci (Winton et al., 2007). The 3,829 isolates from 115 sites in nine countries yielded 1,591 distinct MLGs (Table 4.1). A genotype accumulation curve suggested that eight loci would have been adequate to resolve 95% of the MLGs (Figure S4.1). At the regional scale, diversity and richness were lowest in the Australia population, and highest in the North American population (Table 4.1). Among the states in the U.S., Oregon had the highest diversity and richness, while New York had the lowest gene diversity and the lowest genotypic diversity, along with New Mexico (Table 4.1). Among the European countries sampled, Italy had the lowest diversity and richness (Table 4.1). Germany had the highest genotypic diversity and richness, but Switzerland had higher gene diversity (Table 4.1). The genetic diversity of the Chile population was comparable to some of the other introduced populations in Eastern North America and Europe (Table 4.1). The New York

population has strong linkage disequilibrium, even after removing duplicate MLGs ($\bar{r}_d$ = 0.43, P = 0.01), while those in New Mexico, Germany, France, and Australia were in linkage equilibrium (Table 4.1).

Mean allelic richness across the nine loci, in a rarefied sample of 10 isolates from each of the nine countries, ranged from 1.2 for Italy to 6.0 for the United States (Table 4.2). New Zealand had the second highest allelic richness with 4.0 alleles observed in a sample of 10 isolates (Table 4.2).

4.4.2 Population Structure and Differentiation

Of the total genetic variation in the global population, the AMOVA analysis partitioned the highest proportion to the within-sites component (76%) (Table 4.3). Approximately 11.46% of the genetic variation was partitioned to the between-sites component, 5.86% to the between-subpopulations component and the remaining 6.56% to the between-regions component (Table 4.3). The between-sites component yielded the strongest genetic differentiation (ϕ = 0.131). Overall, the broad geographic regions (i.e. North America, Europe, New Zealand, Australia, and South America) were not significantly differentiated from one another (ϕ_{RT} = 0.066, P = 0.054), but the subpopulations within those regions (i.e. states within the U.S. and countries within Europe) were moderately differentiated (ϕ_{SR} = 0.063, P < 0.001) (Table 4.3).

The pattern of clustering in the UPGMA dendrogram (Figure 4.2) reflected the similarity between the genotypes sampled within each of the regions. Genotypes from North America, New Zealand, and South America clustered together, but were diverse and intermixed throughout the dendrogram. All of the genotypes from Australia, and

many of those from Europe, were less diverse and clustered together in a terminal node that was subtended by a cluster of North American genotypes (Figure 4.2).

At the regional level, genetic differentiation was weakest between North America and New Zealand ($G'_{ST} = 0.30$) and strongest between the populations from Australia and South America, which were almost entirely fixed for separate alleles ($G'_{ST} = 0.97$) (Table 4.4). Pairwise estimates of differentiation between each of the sub-regional populations ranged from 0.10 for Washington and Oregon to 0.97 between Australia and Chile (Table 4.5). Among the European countries, France and Switzerland were the least differentiated ($G'_{ST} = 0.17$), while Germany and Italy showed the strongest differentiation ($G'_{ST} = 0.92$) (Table 4.5). Among the U.S. states, Oregon and Washington showed the weakest differentiation, and the strongest differentiation was between Washington and New York ($G'_{ST} = 0.90$) (Table 4.5). The sub-regional population that was most strongly differentiated from the Australia population was Chile, while the population least differentiated from Australia was Germany ($G'_{ST} = 0.52$) (Table 4.5). The sub-regional population most strongly differentiated from the New Zealand population was New York ($G'_{ST} = 0.92$), while that with the weakest differentiation from the New Zealand population was Oregon ($G'_{ST} = 0.31$). The *N. gaeumannii* population in Chile was completely differentiated from the population in New York ($G'_{ST} = 1.00$), and was least differentiated from New Zealand ($G'_{ST} = 0.47$) (Table 4.5).

Analyses of genetic differentiation among regions with DAPC revealed considerable overlap between the clusters representing North America, Europe, New Zealand, and Chile, but showed no overlap between those clusters and the cluster

representing Australia (Figure 4.3). Among the countries in Europe, a single cluster representing populations from Italy, Switzerland, and France, and separate clusters representing populations from Germany and the United Kingdom were resolved. One of the genotypes from the U.K. cluster appeared to be similar to a genotype from the Germany cluster, but the inertia ellipses for these clusters did not overlap (Figure 4.4A). To examine these relationships more closely, the same DAPC analysis was reconfigured as a bar plot showing the probability of membership of each genotypes in each cluster (Figure 4.4B). While the genotypes from the Italy-Switzerland-France cluster were highly admixed, the genotypes in the clusters representing Germany and the U.K. were not admixed (Figure 4.4B). These genotypes had a high probability of assignment in their respective clusters (representing the countries from which they were collected), except for one genotype from the U.K. that was assigned to the Germany cluster (Figure 4.4B).

Within the U.S. population, there were three distinct clusters– one represented by the genotypes from Oregon and Washington, one with the genotypes from Idaho and New Mexico, and one with the genotypes from New York and Vermont (Figure 4.5). While the cluster represented by the New York and Vermont populations appeared to be strongly differentiated from the other two clusters, there were some isolates that were similar between the cluster represented by the *N. gaeumannii* genotypes from Oregon and Washington and the cluster represented by those from Idaho and New Mexico (Figure 4.5).

4.4.3 Demographic History and Routes of Introduction

In our preliminary investigations, the demographic scenarios with the highest posterior probabilities were those that depicted the *N. gaeumannii* populations in New Zealand and Australia as having different source populations. In these scenarios, the populations in New Zealand originated from the native *N. gaeumannii* population in North America, while the population in Australia originated from the introduced population of *N. gaeumannii* in Europe (Figure 4.6). The most highly supported of these two scenarios, Scenario 15 (posterior probability = 0.794, 95% CI [0.717, 0.872]), was that which depicted the introduction events as having occurred at the same time (Figure 4.6, Table S4.3). The scenario in which the introduction to New Zealand occurred prior to the introduction to Australia had less support (Scenario 12: posterior probability = 0.157, 95% CI [0.086, 0.228]) (Figure S4.2, Table S4.3).

Of the 16 scenarios that included the South America population, Scenario 13 had the strongest statistical support (posterior probability = 0.500, 95% CI [0.389, 0.610]) (Figure S4.4). This scenario depicted the South American population as being introduced from the North American population at the same time as the introduction of *N. gaeumannii* to New Zealand (Figure 4.7). This scenario also included population bottlenecks associated with each of the introduction events (i.e. North America to Europe, North America to New Zealand, North America to Chile, and Europe to Australia) (Figure 4.7). The same scenario that did not include bottlenecks had much lower support (Scenario 11: posterior probability = 0.075, 95% CI [0.000, 0.185]) (Figure S4.4, Table S4.5).

4.5 Discussion

Here, the SSR loci described in Winton et al. (2007a) were employed to genotype over 3,000 *N. gaeumannii* isolates collected from Europe, North America, New Zealand, Australia, and Chile. The resulting MLGs were analyzed to describe the diversity and genetic structure within and between each of these regional populations, and infer the demographic histories and origins of the introduced *N. gaeumannii* populations.

Within North America, the populations of *N. gaeumannii* sampled within the native range of *P. menziesii* in Oregon, Washington, Idaho, and New Mexico were more similar to one another than to the introduced populations in New York and Vermont (Figure 4.5), and had much higher diversity (Table 4.1). The genotypes from Idaho and New Mexico were very similar to one another, and were moderately differentiated from those in the Oregon and Washington populations (Table 4.4, Figure 4.5). Given that the foliage samples from Idaho and New Mexico were collected from the interior form of Douglas-fir (*P. menziesii var. glauca*) (Winton and Stone, 2004), which is native in Idaho and New Mexico (Lavender and Hermann, 2014), it is possible that these locations represent native populations of *N. gaeumannii*.

In the eastern U.S. states, however, both *N. gaeumannii* and its host are introduced. Genetic differentiation was low between the two northeastern U.S. populations ($G'_{ST} = 0.22$) (Table 4.5) and several genotypes were shared between New York and Vermont (Figure 4.5) suggesting that there has been gene flow between them or that they shared a common origin. While the populations in the western and eastern U.S. states appeared to be differentiated (Figure 4.5), the value of G'_{ST} between Idaho and New Mexico was equal to that between Idaho and Vermont ($G'_{ST} = 0.61$) (Table 4.5). If

we assume that these statistics serve as a rough estimate of the connectivity between populations, as suggested by Lowe and Allendorf (2010), then it seems reasonable to conclude that the New York and Vermont populations originated in the western U.S.A. However, these results are not consistent with a recent direct introduction, as that would likely result in much less differentiation and might be expected to result in shared genotypes between the populations. The level of differentiation observed is more consistent with a historical introduction followed by a long period of separation during which these populations have diverged due to mutation, selection, genetic drift, or a combination of these. In fact, historical records indicate that *N. gaeumannii* may have been present in New York as early as 1936 (Hahn, 1941). The eastern U.S. population was almost certainly introduced by anthropogenic activities, as Douglas–fir is not contiguous across this range and the dispersal of spores over that distance (> 3,000 km) would be highly unlikely.

The populations of *N. gaeumannii* from Europe had less diversity than expected, given that the presence of the fungus was reported there before any of the other populations. The genetic differentiation observed between the *N. gaeumannii* isolates collected across countries within Europe was comparable to that observed between the isolates collected across U.S. states (Table 4.3). The DAPC analysis suggested three distinct genetic clusters of *N. gaeumannii* in Europe– one represented by the regional subpopulations in Italy, France, and Switzerland, one represented by the regional subpopulation in Germany, and one represented by the regional subpopulation of *N. gaeumannii* in U.K. This seems to suggest that there may have been multiple

introductions from North America to Europe, as the observed level of differentiation would could have arisen only if these populations had been genetically isolated for a considerable period of time. There were 14 shared MLGs between Italy and France, suggesting either that there has been gene flow between the local *N. gaeumannii* populations in those countries (either through aerial spore dispersal or the human-mediated movement of plant material), or that they were introduced from the same source population. Between the Germany and U.K. genotypes there was strong genetic differentiation, but at least one isolate from the U.K. had a high probability of membership in the cluster of isolates collected from Germany (Figure 4.4B). Given that the first reports of *N. gaeumannii* in Europe were from Switzerland (Boyce, 1940; Gaeumann, 1930), and that isolates from this country were the most diverse of all those sampled in Europe (Tables 4.1, 4.2; Figure 4.4), it is reasonable to conclude that the initial introduction of *N. gaeumannii* into Europe occurred there.

Some of the genotypes from France, Italy, and Switzerland were admixed, as evidenced by the DAPC (Figure 4.4B), suggesting that gene flow has occurred between these regional subpopulations. Switzerland may have served as the source for these subpopulations, or they may have shared a common source. Given the results of that analysis, it seems less likely that *N. gaeumannii* in the U.K. and Germany were introduced from those in Switzerland, France, or Italy (Figure 4.4 B). However, based on the estimated G'_{ST}, the genetic differentiation between Germany and Switzerland is weaker than between other European subpopulations (Table 4.3), suggesting that the *N.*

gaeumannii genotypes from these locations may be more similar than the DAPC suggests.

The *N. gaeumannii* population in New Zealand had much higher diversity and richness than the other introduced populations, suggesting that there may have been multiple introductions from its source population. In the UPGMA dendrogram based on a bootstrap analysis of genetic distance, clusters representing the New Zealand genotypes were spread out among the North American genotypes (Figure 4.2), suggesting that either there were multiple spatial or temporal introductions, or that the founder population was genetically diverse. Another line of evidence to support the idea that multiple spatial or temporal introductions may have occurred in New Zealand, which was discussed in Chapter 3, was that distinctive Lineage 2 genotypes (possessing alleles which had previously only been detected in the western Coast Range in Oregon) were present at sites in the South Island, but not those in the North Island where the first recorded introduction of *N. gaeumannii* occurred. This suggests that a separate introduction from western North America occurred in the South Island.

The *N. gaeumannii* isolates from Australia had the lowest diversity and richness, which could reflect a serial introduction from a source that was itself an introduced population (i.e. Europe). The grouping of the Australian genotypes in a terminal clade in the UPGMA dendrogram along with isolates from Europe reflects this lack of diversity (Figure 4.2). The subpopulation in Europe with the weakest genetic differentiation from the Australia population was Germany ($G'_{ST} = 0.52$). This suggests that among the countries that were sampled in Europe for this study, the genotypes from Germany are

most similar to the Australian genotypes. This could indicate either that Germany was the source of the isolates that were introduced to Australia, or that the isolates in Germany and Australia shared a common source within Europe.

A similar genetic structure to that observed in our Australian population resulted when *Dothistroma septosporum* was introduced to Australasia on infected seedling of radiata pine (*Pinus radiata)* from Europe and/or Africa (Barnes et al., 2014). However, in that case, populations from Australia and New Zealand were very similar, and the distribution of shared genotypes, along with migration analyses, suggested that migrants had either moved between those locations via aerial spore dispersal across the Tasman Sea, or had been transported inadvertently on live plant material used to supply timber production economies in Australia and New Zealand (Barnes et al., 2014). Neither of these phenomena appear to have occurred in the case of *N. gaeumannii* on Douglas–fir in Australasia. In the present study, the *N. gaeumannii* isolates collected in New Zealand were not at all similar to those from Australia (Figures 4.2, 4.3), estimates of G'_{ST} suggested that they were almost entirely fixed for separate alleles (Table 4.4), and the *DIYABC* analyses suggested that they had different source populations (Figures 4.6, 4.7, S4.2, S4.4, Tables S4.3, S4.5).

Along with the analyses of diversity, richness, and genetic differentiation within and among the sub-regional populations, the results from *DIYABC* allowed for the inference of the most likely routes of introduction of *N. gaeumannii* into four disparate regions of the globe. The demographic scenario with the highest posterior probability in the preliminary analysis indicated that *N. gaeumannii* was introduced first to Europe, and

later to New Zealand from a source in North America, and to Australia from a source in Europe. This is in agreement with the clustering observed in the UPGMA dendrogram and the DAPC analyses, and with the estimates of population differentiation based on G'_{ST}. In the UPGMA dendrogram, clusters of European genotypes were always subtended by clusters of North America genotypes, the Australian isolates clustered only with those from Europe, and the New Zealand isolates were dispersed among clusters of the North American genotypes (Figure 4.2). In the DAPC scatterplot (Figure 4.3) the clusters representing genotypes from North America and Europe overlapped, as did those from North America and New Zealand. While the cluster of genotypes from Australia and Europe did not overlap, a large proportion of the genotypes from the European cluster were close to the Australian genotype cluster, suggesting that they were more similar in their allelic compositions (Figure 4.3). The estimated genetic differentiation between these regions provided further support for their putative origins. Among the regional subpopulations, those that were least differentiated from Europe were North America ($G'_{ST} = 0.53$) and Australia ($G'_{ST} = 0.58$), and the population least differentiated from New Zealand was North America ($G'_{ST} = 0.30$) (Table 4.4). The historical record also supports the hypothesized series of introduction events from the preliminary *DIYABC* analysis in that *N. gaeumannii* was first reported from Europe (~ 1925) (Boyce, 1940; Gaeumann, 1930), and the next reported presence outside of North America was New Zealand (~1959) (Hood et al., 1990; Hood and Kershaw, 1975). However, the historical records suggest that *N. gaeumannii* was not present in Australia until the mid 1970s, although *N. gaeumannii* was reported in Tasmania prior to the outbreak on the

mainland (Marks, 1975). The *DIYABC* scenario with the highest support in the preliminary analysis modeled the introductions to New Zealand and Australia as having occurred at approximately the same time, and scenarios with the introduction to New Zealand occurring prior to the introduction to Australia did not have as much statistical support (Figure S4.2, Table S4.3). However, as discussed below, estimating the timing of events in *DIYABC* can be problematic.

Subsequent *DIYABC* scenarios incorporated the regional population from South America into the basic framework that had the highest support in the preliminary analyses. The scenario with the highest support from this second round of analyses suggested that the *N. gaeumannii* populations in New Zealand and Chile shared a common origin in North America, and that their introductions occurred around the same time. This is consistent with our estimates of differentiation between these populations as the DAPC and G'_{ST} analyses both indicated weak differentiation between these populations and their North American source population. In fact, the pairwise genetic differentiation between the regional populations in New Zealand and Chile ($G'_{ST} = 0.47$) suggested that those populations were less differentiated than those in North America and Chile ($G'_{ST} = 0.50$). However, the *DIYABC* scenarios that modeled the New Zealand population as the source of the Chile population (Figure S4.4B Scenario 8), the Chile population as the source of the New Zealand population (Figure S4.4B Scenario 7), or the population in Chile as the product of an admixture between the populations in New Zealand and North America (Figure S4.4B Scenarios 14 and 16) did not have strong statistical support (Table S4.5).

This study provided insights into the genetic diversity and population structure within and between regional *N. gaeumannii* populations worldwide, and tested several hypotheses regarding the introduction routes of this fungal pathogen from its native origin in western North America into Europe, New Zealand, Australia, and Chile where it has invaded and become established in Douglas-fir plantations. The results of the *DIYABC* analyses, along with the high genetic diversity and allelic richness observed in the North American populations provided additional support for western North America as the center of diversity, and likely the evolutionary origin, of *N. gaeumannii.* The comparatively low genetic diversity and allelic richness in each of the invasive populations reflect population bottlenecks due to founding events in which a small number of individuals are introduced in one or more discrete events, leading to a loss of alleles and thus a loss of genetic diversity (Nei et al., 1975). The results presented here suggested that the native populations in western North America served as the source for all of the introduced populations, either directly, as was the case with New Zealand and Europe, or indirectly, as was the case with Australia (which was introduced via Europe). Thus, the populations in New Zealand and Australia, which are spatially very close to one another, do not appear to be similar genetically, and this can be explained by the fact that they have been introduced from separate source populations entirely.

There are several reasons that the results presented here should not be viewed as a definitive determination of the origins of the introduced *N. gaeumannii* populations. Genotypic clustering analyses such as bootstrap analyses and DAPC are based on similarities between genotypes, and do not necessarily reflect evolutionary relationships.

Due to their high mutation rates, the likelihood that a given MLG could occur more than once by chance alone is not negligible, in which case identity in state does not imply identity by descent. This is essentially the same reason why SSR genotypes cannot be used for phylogenetic analyses– they do not reflect evolutionary relationships. Thus, conclusions about the evolutionary origins of introduced *N. gaeumannii* populations cannot be made solely based on the results of a genotypic clustering analyses. These analyses are only suggestive of similarities among the populations, and this similarity may not necessarily be due to shared ancestry.

The utility of fixation indices such as F_{ST} and G_{ST} as estimates of population differentiation has been discussed in depth (Balloux and Lugon-Moulin, 2002; Hedrick, 2005; Jost, 2008; Lowe and Allendorf, 2010; Meirmans and Hedrick, 2011), and some authors have concluded that they should not be used to infer genetic differentiation, migration rates, or gene flow (Jost, 2008). Others concede that they may be viewed as rough estimates of population connectivity (Lowe and Allendorf, 2010). Still, the inferences based on these statistics can be problematic when factors such as within-population differentiation and mutation rates have not been accounted for (Balloux and Lugon-Moulin, 2002). Here, we attempted to avoid some of the problems associated with these statistics by calculating a standardized G_{ST} that has been re-scaled to yield a value of one when the two populations are entirely fixed for different alleles, and zero when no alleles differ between the two populations (Hedrick, 2005; Jost, 2008). This presumably provides a better estimate of the rate of gene flow between populations, but this is apparently very difficult to disentangle from the effects of mutation and genetic drift,

which may cause subpopulations to become differentiated even when some gene flow still occurs (Hartl and Clark 2007). Another drawback to using this standardized statistic is that it does not adhere to the familiar scale with which biological interpretations of fixation indices are generally made. Thus, the recommendations of Hartl and Clark (2007) and others in regards to the interpretation of these values do not apply here.

When comparing the genetic differentiation among the sub-regional populations, it became clear that the hypothesized introduction scenarios from the *DIYABC* analyses (Figures 4.6, 4.7) may be oversimplified. Within the North American population, there is significant genetic differentiation between the eastern and western states. For instance, North America is the most likely source of the *N. gaeumannii* population in Chile according to the *DIYABC* analysis, but the isolates from Chile are entirely fixed for separate alleles, and are thus completely differentiated from those collected in New York (G'_{ST} = 1.00). Thus, to conclude that the population in Chile originated from the North American population as a whole could be misleading because it is completely differentiated from the populations in eastern North America. It would be much more accurate to further refine the putative introduction scenarios to include separate eastern and western North American populations. This could provide a much more precise specification of which North America populations served as the source of the introduction. The same applies to Europe. For instance, even though the *DIYABC* scenario with the highest support suggests that Europe is the source of the introduction to Australia, the *N. gaeumannii* genotypes from Australia and Italy are almost completely differentiated (G'_{ST} = 0.96). They are less differentiated from those in Germany (G'_{ST} =

0.52), however. We must assume that this subpopulation differentiation within the source populations introduced some error and uncertainty into the *DIYABC* analyses because these subpopulations were combined into a single population for those analyses.

There were also some inherent limitations to the study design implemented here. The unequal sampling among populations likely introduced some bias in our estimations of diversity, richness, and population structure. To account for this, analyses that were dependent upon sample size (e.g. genotypic diversity, genotypic richness, allelic richness) were performed with rarefaction sample sizes that were equal to the number of samples in the population with the fewest samples. This presumably removed the bias associated with unequal sampling, and allowed for direct comparisons among populations for which sampling was unequal. Still, some aspects of these analyses may have been negatively influenced by sampling bias.

Another form of bias may have been introduced in the formulation of the *DIYABC* scenarios. For each analysis, we attempted to consider only the scenarios which seemed to be the most biologically relevant. The computationally-intensive nature of calculating millions of datasets necessitates this. It would be nearly impossible to test every imaginable scenario, and would have likely been a waste of time and resources. However, the final scenarios that we chose to implement may have been biased in that some perfectly plausible scenarios could have inadvertently been left out. While all attempts were made to test all of the plausible and biologically relevant scenarios for this study, there is a chance that the “true” scenario was not included.

In addition to those sources of error, the *DIYABC* simulations performed for this study had a high posterior predictive error rate (i.e. the rate at which the wrong scenario was chosen as the top scenario among 1,000 scenarios simulated from the posterior distribution of parameters). For the preliminary *DIYABC* analysis with only four populations, the posterior predictive error calculated from a logistic regression on the top 1,000 scenarios was 0.532. This means that on average, there was a 53% chance that the incorrect scenario was chosen as the top scenario. For the preliminary *DIYABC* analysis, the type 1 error was also quite high for the chosen scenario (Scenario 15) (Figure 4.6, Figure S4.2). The probability of rejecting this particular scenario, even when it was the "true" scenario was 0.674 (data not shown). However, in many cases, the "wrong" scenario that was chosen as the top scenario in error was one that was essentially the same hypothesis (having the same source populations for each of the introductions) but differed in the timing of the events. The combined Type 1 error rates for the three scenarios in which the Australia population was introduced from Europe, and New Zealand population from North America (Scenarios 12, 13, and 15) (Figure S4.2) was only 0.326 (data not shown). This suggests that much of the error associated with this analysis had to do with the estimation of the timing of the introduction events. Although a single scenario was chosen as the most probable, there was uncertainty in distinguishing this scenario from its counterparts that had different coalescence times for the populations of interest. This problem is likely compounded by the fact that SSR markers mutate at such a high rate. This would contribute to the problem by making it much more difficult to calibrate the number of generations corresponding to a given coalescence event. We

also only used eight SSR markers for this analysis, which likely made these coalescence times even more difficult to estimate with a high level of accuracy.

4.6 Acknowledgements

We thank the following for field and laboratory assistance: J. Britt, J. F. Gardner, R. J. Hood, P. Reeser, and W. Sutton. R. Morales and E. Sanfuentes kindly provided DNA from *N. gaeumannii* in Chile, and A. Carnegie kindly provided isolates of *N. gaeumanii* from Australia. Z. Kamvar and J. Tabima assisted in the implementation and interpretation of analyses performed with the R packages *poppr, adegenet,* and *DIYABC*. Most of all, the authors would like to express their sincere gratitude and appreciation for the work performed by L. Winton without which the present study would not have been possible. All of the samples from Europe, and many of those from North America were provided by L. Winton, with contributors acknowledged in Winton et al. (2006). Thanks to all of the concerned plant pathologists around the world who contributed to the sampling effort for this study. Funding for this work was provided by the Oregon State University Swiss Needle Cast Cooperative (SNCC), the Portland Garden Club, the Cascade Mycological Society, Oregon Mycological Society, Puget Sound Mycological Society, the USDA Forest Service, Scion, and the New Zealand Ministry of Business, Innovation and Employment Strategic Science Investment Fund.

4.7 Literature Cited

Agapow, P., Burt, A., 2001. Indices of multilocus linkage disequilibrium. *Molecular Ecology Notes* 1, 101–102.

Balloux, F., Lugon-Moulin, N., 2002. The estimation of population differentiation with microsatellite markers. *Molecular Ecology* 11, 155–165.

Baquero, O.S., 2017. ggsn: north symbols and scale bars for maps created with "ggplot2" or "ggmap". R package version 0.4.0. https://CRAN.R-project.org/package=ggsn

Barnes, I., Wingfield, M.J., Carbone, I., Kirisits, T., Wingfield, B.D., 2014. Population structure and diversity of an invasive pine needle pathogen reflects anthropogenic activity. *Ecology and Evolution* 4, 3642–3661. doi: 10.1002/ece3.1200

Bennett, P., Stone, J., 2016. Assessments of population structure, diversity, and phylogeography of the Swiss needle cast fungus (*Phaeocryptopus gaeumannii*) in the U.S. Pacific Northwest. *Forests* 7, 14. doi: 10.3390/f7010014

Boyce, J.S., 1940. A Needle-cast of Douglas fir associated with *Adelopus gaumanni*. *Phytopathology* 30, 649–659.

Brown, J.K.M., Hovmøller, M.S., 2002. Aerial dispersal of pathogens on the global and continental scales and its impact on plant disease. *Science* 297, 537–541.

Cornuet, J.M., Ravigné, V., Estoup, A., 2010. Inference on population history and model checking using DNA sequence and microsatellite data with the software DIYABC (v1.0). *BMC Bioinformatics* 11, 1. doi: 10.1186/1471-2105-11-401.

Cornuet, J.M., Santos, F., Beaumont, M.A., Robert, C.P., Marin, J.-M., Balding, D.J., Guillemaud, T., Estoup, A., 2008. Inferring population history with DIY ABC: a user-friendly approach to approximate Bayesian computation. *Bioinformatics* 24, 2713–2719. doi: 10.1093/bioinformatics/btn514

Dlugosch, K.M., Parker, I.M., 2008. Founding events in species invasions: genetic variation, adaptive evolution, and the role of multiple introductions. *Molecular Ecology* 17, 431–449. https://doi.org/10.1111/j.1365-294X.2007.03538.x

Dray, S., Dufour, A.B., 2007. The ade4 package: implementing the duality diagram for ecologists. *Journal of Statistical Software* 22, 1–20.

Excoffier, L., Smouse, P.E., Quattro, J.M., 1992. Analysis of molecular variance inferred from metric distances among DNA haplotypes: application to human mitochondrial DNA restriction data. *Genetics Society of America* 131, 479–491.

Gaeumann, E., 1930. Über eine neue krankheit der Douglasien. *Schweiz. Z. Forstwes* 81, 63–67.

Goudet, J., Jombart, T., 2015. hierfstat: estimation and tests of hierarchical F-statistics. R package version 0.04-22. https://CRAN.R-project.org/package=hierfstat

Guillemaud, T., Beaumont, M.A., Ciosi, M., Cornuet, J.-M., Estoup, A., 2010. Inferring introduction routes of invasive species using approximate Bayesian computation on microsatellite data. *Heredity* 104, 88–99. doi: 10.1038/hdy.2009.92.

Hahn, G.G., 1941. New Reports on *Adelopus gaeumanni* on Douglas fir in the United States. *Plant Disease Reporter* 25, 115–117.

Hedrick, P.W., 2005. A standardized genetic differentiation measure. *Evolution* 59, 1633–1638.

Hood, I.A., Kershaw, D.J., 1975. Distribution and infection period of *Phaeocryptopus gaeumannii* in New Zealand. *New Zealand Journal of Forestry Science* 5, 201–208.

Hood, I.A., Sandberg, C.J., Barr, C.W., Holloway, W.A., Bradbury, P.M., 1990. Changes in needle retention associated with the spread and establishment of *Phaeocryptopus gaeumannii* in planted Douglas fir. *European Journal of Forest Pathology* 20, 418–429.

Jombart, T., 2008. adegenet: a R package for the multivariate analysis of genetic markers. *Bioinformatics* 24, 1403–1405. doi: 10.1093/bioinformatics/btn129.

Jombart, T., Devillard, S., Balloux, F., 2010. Discriminant analysis of principal components: a new method for the analysis of genetically structured populations. *BMC Genetics* 11, 1. doi:10.1186/1471-2156-11-94.

Jost, L., 2008. G_{ST} and its relatives do not measure differentiation. *Molecular Ecology* 17, 4015–4026. doi: 10.1111/j.1365-294X.2008.03887.x.

Kamvar, Z.N., Brooks, J.C., Grunwald, N.J., 2015. Novel R tools for analysis of genome-wide population genetic data with emphasis on clonality. *Frontiers in Genetics* 6. doi: 10.3389/fgene.2015.00208.

Kamvar, Z.N., Tabima, J.F., Grünwald, N.J., 2014. *Poppr*: an R package for genetic analysis of populations with clonal, partially clonal, and/or sexual reproduction. *PeerJ* 2, e281. doi: 10.7717/peerj.281.

Kinloch Jr, B.B., 2003. White pine blister rust in North America: past and prognosis. *Phytopathology* 93, 1044–1047.

Lavender, D.P., Hermann, R.K., 2014. Douglas-fir: the genus *Pseudotsuga*. Oregon Forest Research Laboratory, Oregon State University, Corvallis, OR, USA.

Liese, J., 1939. The occurrence in the British Isles of the *Adelopus* disease of Douglas fir. *Quarterly Journal of Forestry* 33, 247–252.

Lowe, W.H., Allendorf, F.W., 2010. What can genetics tell us about population connectivity? *Molecular Ecology* 19, 3038–3051. doi: 10.1111/j.1365-294X.2010.04688.x

Marks, G.C., 1975. Swiss needle cast of Douglas fir. *Australasian Plant Pathology* 4, 24–24.

Meirmans, P.G., Hedrick, P.W., 2011. Assessing population structure: FST and related measures. *Molecular Ecology Resources* 11, 5–18. doi: 10.1111/j.1755-0998.2010.02927.x

Nei, M., Maruyama, T., Chakraborty, R., 1975. The bottleneck effect and genetic variability in populations. *Evolution* 29, 1. doi: 10.2307/2407137

Osorio, M., 2007. Detección del hongo defoliador *Phaeocryptopus gaeumannii* en plantaciones de *Pseudotsuga menziesii* de Valdivia, Chile. *Bosque* 28, 69–74.

Peace, T.R., 1962. Pathology of trees and shrubs with special reference to Britain. Clarendon Press, Oxford.

Peakall, R., Smouse, P.E., 2012. GenAlEx 6.5: genetic analysis in Excel. Population genetic software for teaching and research--an update. *Bioinformatics* 28, 2537–2539. doi: 10.1093/bioinformatics/bts460

Peakall, R., Smouse, P.E., 2006. GenAlEx 6: genetic analysis in Excel. Population genetic software for teaching and research. *Molecular Ecology Notes* 6, 288–295. doi: 10.1111/j.1471-8286.2005.01155.x

Rivas, G.G., Zapater, M.F., Abadie, C., Carlier, J., 2004. Founder effects and stochastic dispersal at the continental scale of the fungal pathogen of bananas Mycosphaerella fijiensis. *Molecular Ecology* 13, 471–482. doi: 10.1046/j.1365-294X.2003.02043.x.

Rizzo, D.M., Garbelotto, M., Hansen, E.M., 2005. *Phytophthora ramorum*: integrative research and management of an emerging pathogen in California and Oregon forests. *Annual Review of Phytopathology* 43, 309–335. doi: 10.1146/annurev.phyto.42.040803.140418

Stone, J.K., Hood, I.A., Watt, M.S., Kerrigan, J.L., 2007. Distribution of Swiss needle cast in New Zealand in relation to winter temperature. *Australasian Plant Pathology* 36, 445. doi: 10.1071/AP07049.

Videira, S.I.R., Groenewald, J.Z., Nakashima, C., Braun, U., Barreto, R.W., de Wit, P.J., Crous, P.W., 2017. Mycosphaerellaceae–chaos or clarity? *Studies in Mycology* 87, 257–421. doi: 10.1016/j.simyco.2017.09.003.

Watt, M.S., Stone, J.K., Hood, I.A., Palmer, D.J., 2010. Predicting the severity of Swiss needle cast on Douglas-fir under current and future climate in New Zealand. *Forest Ecology and Management* 260, 2232–2240. doi: 10.1016/j.foreco.2010.09.034.

Wickham, H., 2016. ggplot2: elegant graphics for data analysis. Springer-Verlag, New York.

Winton, L.M., and Stone, J.K. 2004. Microsatellite population structure of *Phaeocryptopus gaeumannii* and pathogenicity of *P. gaeumannii* genotypes/lineages. pp. 42-48 in *Swiss Needle Cast Cooperative Annual Report 2004*, Mainwaring, D. (ed.). College of Forestry, Oregon State University, Corvallis, OR. http://sncc.forestry.oregonstate.edu/annual-reports

Winton, L.M., Hansen, E.M., Stone, J.K., 2006. Population structure suggests reproductively isolated lineages of *Phaeocryptopus gaeumannii*. *Mycologia* 98, 781–791.

Winton, L.M., Stone, J.K., Hansen, E.M., 2007. Polymorphic microsatellite markers for the Douglas-fir pathogen *Phaeocryptopus gaeumannii*, causal agent of Swiss needle cast disease. *Molecular Ecology Notes* 7, 1125–1128. doi: 10.1111/j.1471-8286.2007.01802.x

Winton, L.M., Stone, J.K., Hansen, E.M., Shoemaker, R.A., 2007. The systematic position of *Phaeocryptopus gaeumannii*. *Mycologia* 99, 240–252.

Yu, G., Smith, D.K., Zhu, H., Guan, Y., Lam, T.T.-Y., 2017. ggtree: an R package for visualization and annotation of phylogenetic trees with their covariates and other associated data. *Methods in Ecology and Evolution* 8, 28–36. doi: 10.1111/2041-210X.12628.

4.8 Figures and Tables

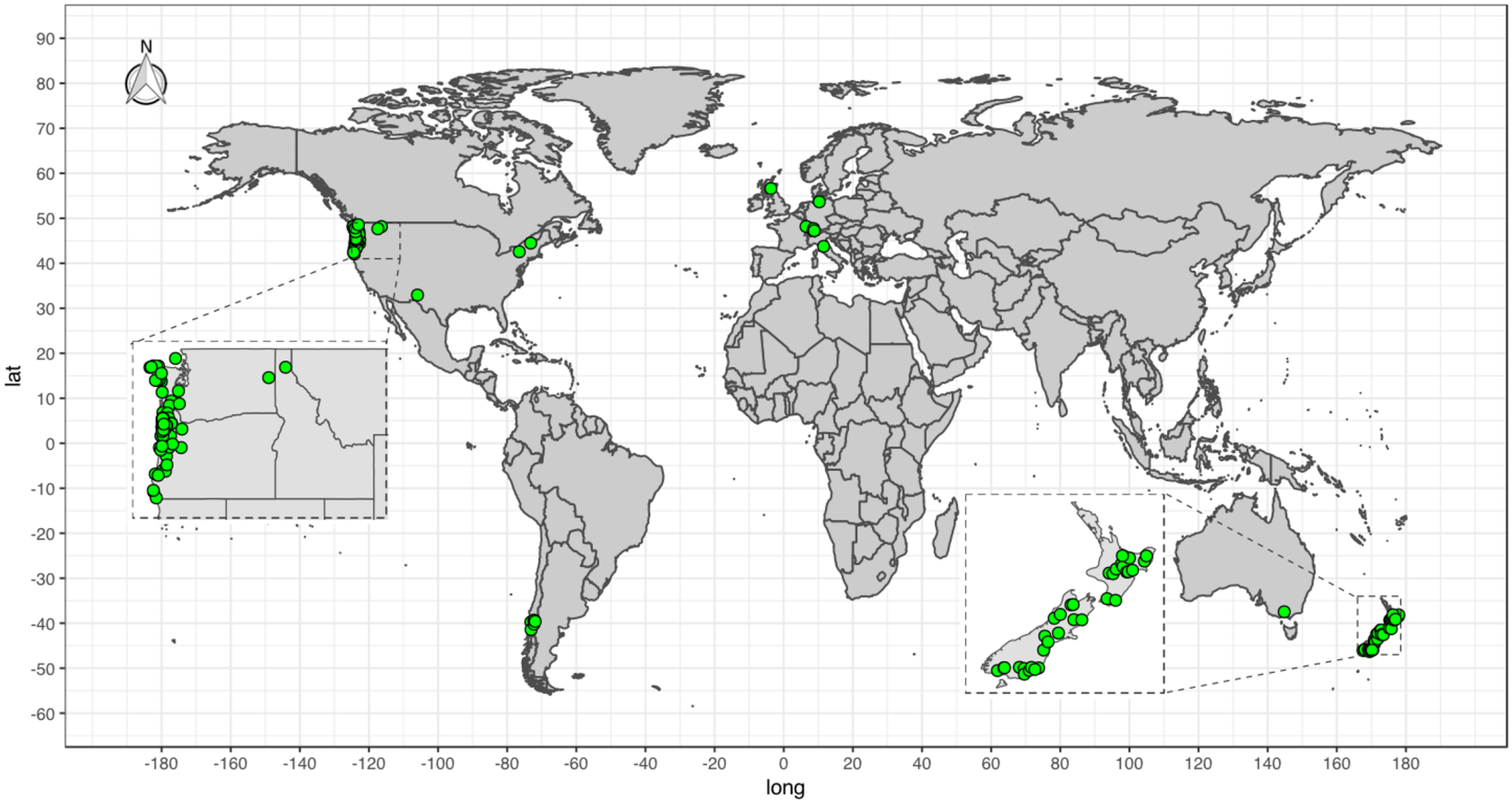

Figure 4.1: Locations from which Douglas–fir foliage was sampled for the isolation of *Nothophaeocryptopus gaeumannii*.

Table 4.1: Estimates of genetic diversity for native and introduced *Nothophaeocryptopus gaeumannnii* populations worldwide.

Population Level	N_{Sites}	$N_{Isolates}$	MLG [a]	eMLG [b]	SE [c]	H [d*]	E_5 [e*]	H_e [f]	$\bar{r}_d$ [g]	P [h]
North America										
Oregon	45	1003	659	9.93	0.26	2.29	1.00	0.84	0.13	0.00
Washington	16	466	330	9.87	0.37	2.28	0.99	0.81	0.15	0.00
Idaho	3	24	23	9.84	0.37	2.28	0.99	0.57	0.04	0.05
New Mexico	1	5	5	5.00	0.00	1.61	1.00	0.60	0.05	0.22
New York	1	10	10	6.00	0.00	1.61	0.79	0.22	0.43	0.01
Vermont	1	15	15	7.00	0.93	1.75	0.76	0.48	0.12	0.00
Total North America	67	1523	1022	9.95	0.22	2.30	1.00	0.84	0.13	0.00
Europe										
France	1	12	9	7.67	0.64	1.90	0.82	0.43	–0.01	0.60
Germany	1	10	8	8.00	0.00	1.97	0.85	0.18	–0.13	0.96
Italy	1	13	3	2.73	0.45	0.65	0.65	0.05	NA	NA
Switzerland	4	39	21	6.41	1.34	1.61	0.75	0.48	0.13	0.00
UK	1	11	4	3.82	0.39	1.02	0.68	0.30	0.40	0.00
Total Europe	8	85	43**	7.78	1.27	1.95	0.89	0.55	0.10	0.00
Australia	1	63	24	6.94	1.32	1.77	0.82	0.13	–0.07	0.73
New Zealand	35	2120	479	8.77	1.05	2.12	0.94	0.66	0.13	0.00
South America										
Chile	5	38	23	8.06	1.14	2.00	0.90	0.39	0.16	0.00
Total	116	3829	1591	9.57	0.67	2.24	0.98	0.79	0.10	0.00

[a] MLG = number of multilocus genotypes, [b] eMLG = expected number of multilocus genotypes in rarefied sample equal to the number of samples in the group with the smallest number of samples (N = 10 isolates), [c] SE = standard error of eMLG estimate, [d] H = Shannon– Weiner diversity index (Shannon, 2001), [e] E_5 = evenness, [f] H_e = Nei's unbiased gene diversity (expected heterozygosity) (Nei, 1978), [g] $\bar{r}_d$ = standardized index of association (Agapow and Burt, 2001) for clone–censored data, [h] P = p–value for $\bar{r}_d$ from 999 permutations, * = estimated from 1,000 bootstrap replicates with rarefaction sample size of 10 isolates, ** = Total MLG not equal to the sum of population totals due to shared MLGs, NA = insufficient data for analysis

.

Table 4.2: Allelic richness for nine microsatellite loci (Winton et al., 2007) across nine countries from which *Nothophaeocryptopus gaeumannii* was sampled for this study. All calculations were performed with rarefaction sample sizes of 10 isolates.

Locus	United States	France	Germany	Italy	Switzerland	United Kingdom	New Zealand	Australia	Chile
PgDi1	4.1	2.0	1.0	1.0	2.0	1.9	1.9	1.0	1.0
PgDi2	6.7	2.0	1.0	1.0	2.6	2.8	4.2	1.0	3.5
PgDi3	3.5	1.8	1.0	1.0	1.0	1.9	2.8	1.0	2.0
PgDi4	5.3	1.8	1.0	1.0	2.0	1.0	2.8	1.2	2.3
PgTri1	7.2	2.0	2.0	1.0	3.3	2.8	4.3	1.0	2.5
PgTri2	7.5	1.8	1.0	1.0	2.0	3.0	4.8	1.0	1.7
PgTri6	8.2	4.5	4.0	2.7	4.4	2.8	6.7	2.9	5.1
PgTri7	4.9	4.5	3.0	1.0	3.6	2.8	3.0	4.3	2.5
PgTet1	6.7	3.8	1.0	1.0	3.6	2.8	5.2	1.0	2.7
Mean	6.0	2.7	1.7	1.2	2.7	2.4	4.0	1.6	2.6

Table 4.3: Analysis of molecular variance (AMOVA) table showing genetic variation and estimates of differentiation among *Nothophaeocryptopus gaeumannii* populations from a hierarchical sampling of 14 subpopulations covering nine countries and five regions. Samples are from a clone-censored dataset.

Hierarchical level	**Variance (%)**	ϕ	**P***
ϕ_{RL} (between regions)	6.557	0.066	0.0539
ϕ_{SR} (between subpopulations within regions)	5.859	0.063	< 0.001
ϕ_{SS} (between sites within subpopulations)	11.461	0.131	< 0.001
ϕ_{SS} (within sites)	76.123	0.239	< 0.001

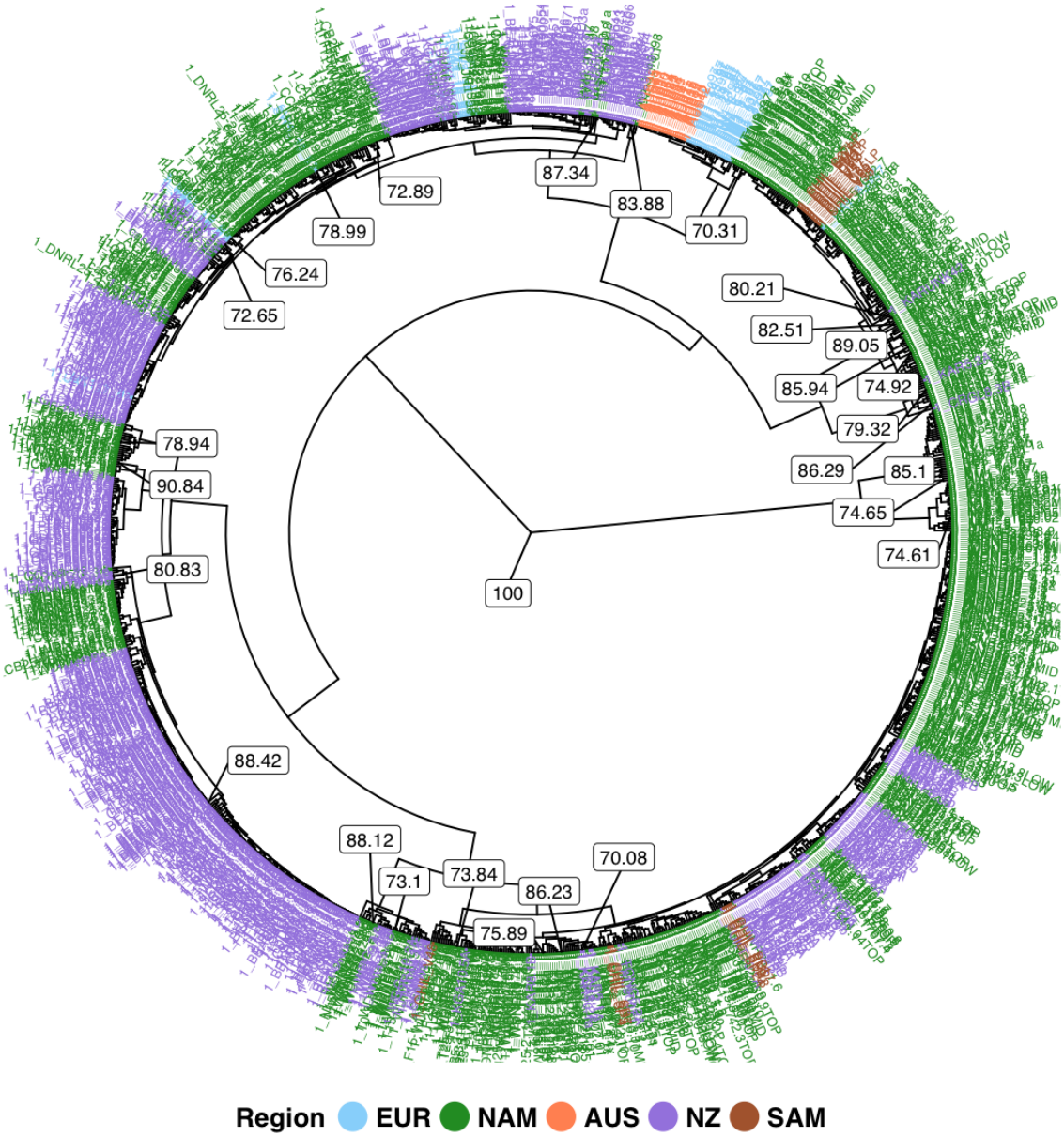

Figure 4.2: UPGMA dendrogram from a bootstrap analysis of Nei's genetic distance among multilocus SSR genotypes from 1,260 *Nothophaeocryptopus gaeumannii* isolates collected from five regions that included nine countries. EUR= Europe (France, Germany, Italy, Switzerland, U.K.), NAM= North America (United States), AUS= Australia, NZ= New Zealand, SAM= South America (Chile). Node labels represent bootstrap statistics (≥ 70%) from 10,000 replicate trees.

Table 4.4: Estimates of population differentiation (G'_{ST}) (Hedrick, 2005) for the five regions from which Douglas–fir foliage was sampled for isolation of *Nothophaeocryptopus gaeumannii.*

	EUR	NAM	AUS	NZ	SAM
EUR	–				
NAM	0.53	–			
AUS	0.58	0.88	–		
NZ	0.60	0.30	0.88	–	
SAM	0.82	0.50	0.97	0.47	–

EUR, Europe; NAM, North America; AUS, Australia; NZ, New Zealand; SAM, South America.

Table 4.5: Estimates of population differentiation (G'_{ST}) (Hedrick, 2005) between each of the fourteen regional *Nothophaeocryptopus gaeumannii* subpopulations.

	FR	GY	IT	SW	UK	ID	NM	NY	OR	VT	WA	AUS	NZ	CHIL
FR	–													
GY	0.55	–												
IT	0.33	0.92	–											
SW	0.17	0.48	0.51	–										
UK	0.31	0.65	0.63	0.26	–									
ID	0.65	0.88	0.71	0.58	0.65	–								
NM	0.84	0.96	0.91	0.83	0.85	0.62	–							
NY	0.90	0.96	0.95	0.82	0.90	0.64	0.83	–						
OR	0.49	0.84	0.62	0.52	0.39	0.62	0.81	0.88	–					
VT	0.81	0.86	0.89	0.73	0.81	0.66	0.64	0.56	0.83	–				
WA	0.60	0.89	0.70	0.62	0.51	0.64	0.86	0.90	0.10	0.87	–			
AUS	0.70	0.52	0.96	0.64	0.75	0.89	0.96	0.96	0.87	0.94	0.90	–		
NZ	0.60	0.87	0.71	0.59	0.41	0.70	0.83	0.92	0.31	0.89	0.33	0.88	–	
CHIL	0.80	0.96	0.87	0.84	0.65	0.87	0.91	1.00	0.49	0.96	0.51	0.97	0.47	–

FR, France; GY, Germany; IT, Italy; SW, Switzerland; UK, United Kingdom; ID, Idaho; NM, New Mexico; NY, New York; OR, Oregon; WA, Washington; AUS, Australia; NZ, New Zealand; CHIL, Chile.

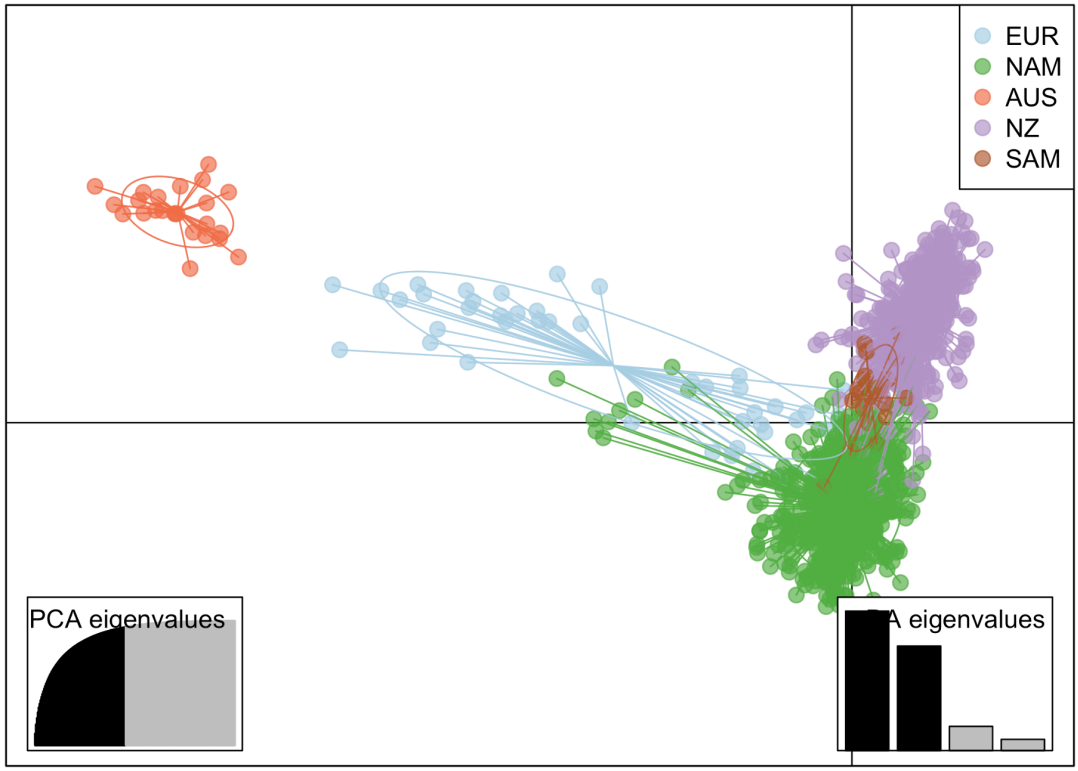

Figure 4.3. Scatterplot from discriminant analysis of principal components (DAPC) showing clustering among *Nothophaeocryptopus gaeumannii* Lineage 1 genotypes from a clone–censored dataset, with clusters representing the five regions from which samples were collected. EUR = Europe, NAM = North America (United States), AUS = Australia, NZ = New Zealand, SAM = South America. Inset at bottom left shows the proportion of principal components retained, inset at bottom right shows the number of discriminant functions retained.

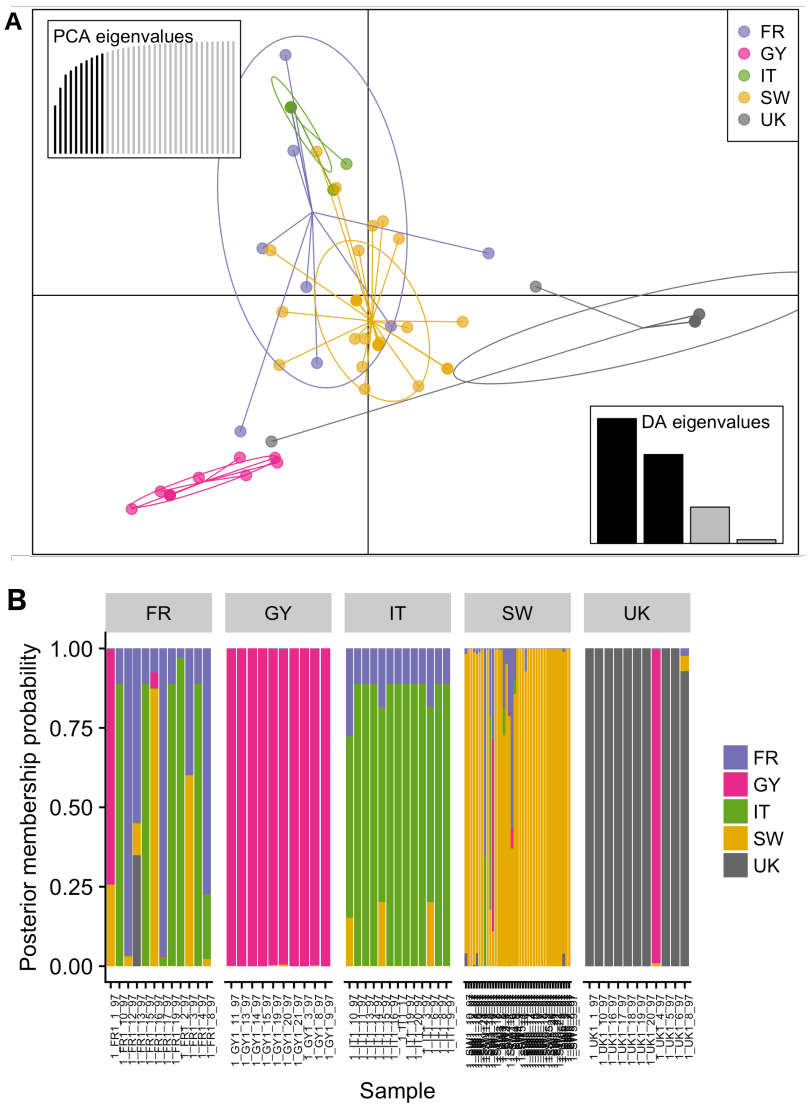

Figure 4.4: A) Scatterplot from discriminant analysis of principal components (DAPC) with clusters representing the five countries in Europe from which *Nothophaeocryptopus gaeumannii* was sampled. Each point represents a mutlilocus genotype (MLG), with overlapping points representing identical MLGs. Inertia ellipses are drawn around 2/3 of the samples in a given cluster. Inset at top left shows the proportion of principal components retained. Inset at bottom right shows the number of discriminant functions retained. B) Bar plot from DAPC showing the probability of membership for each isolate in each of five clusters representing the countries from which *N. gaeumannii* was sampled in Europe. Each bar represents one isolate, and the colors correspond to the probability of membership in each cluster listed in the legend. FR = France, GY = Germany, IT = Italy, SW = Switzerland, UK = United Kingdom. N = 85 isolates, 43 MLGs (Table 4.1).

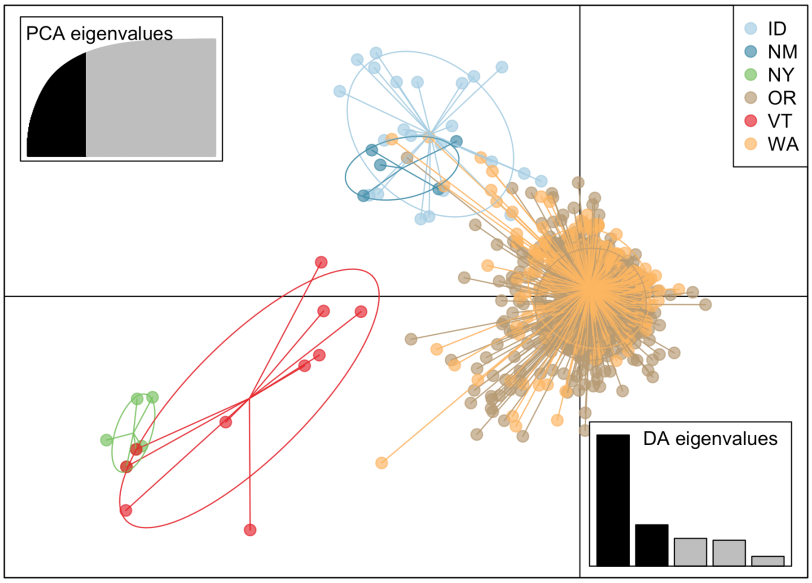

Figure 4.5: Scatterplot from DAPC with clusters representing the six states in the U.S. from which *Nothophaeocryptopus gaeumannii* was sampled. ID, Idaho; NM, New Mexico; NY, New York; OR, Oregon; VT, Vermont; WA, Washington. Here, a clone–corrected dataset was used, and isolates of both Lineages 1 and 2 were included. Inset at top left shows the proportion of principal components retained, inset at bottom right shows the number of discriminant functions retained. N = 1,523 isolates and 1,022 MLGs (Table 4.1).

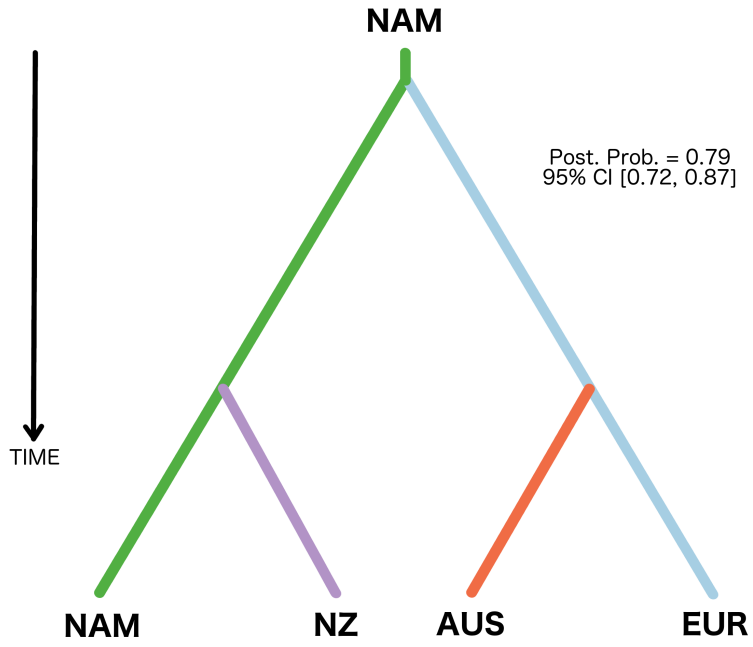

Figure 4.6: Graphical representation of the demographic scenario with the highest posterior probability from the preliminary *DIYABC* analysis. NAM = North America, NZ = New Zealand, EUR = Europe.

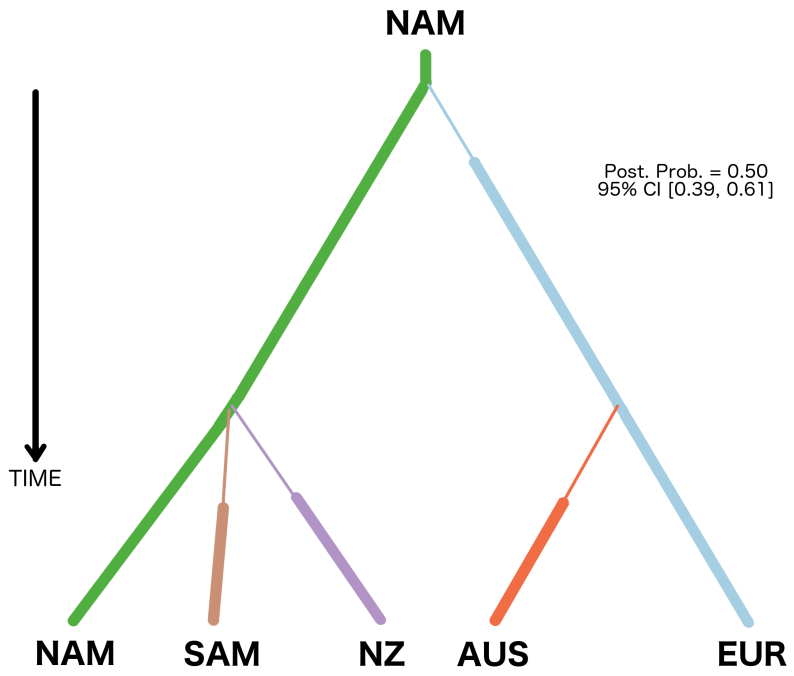

Figure 4.7: Graphical representation of the demographic scenario with the highest posterior probability from the final *DIYABC* analysis. NAM = North America, SAM = South America, NZ = New Zealand, EUR = Europe. Changes in line weight represent reductions in effective population size (N_e).

4.9 Supplementary Figures and Tables

Table S4.1: Summary of locus characteristics for the SSR markers used to genotype *Nothophaeocryptopus gaeumannii* isolates for this study.

					Lineage 1			Lineage 2		
Locus	**Repeat Motif**	**Primer Sequences**	**N_A**	**Range**	**N_A**	**H_e**	**Range**	**N_A**	**H_e**	**Range**
Multiplex 1										
Pgdi1	(CA)18	F: TCCCCGCCTATATTTCTC R: (FAM) CCGAATCGATTTGCTAGG	11	90–114	6	0.34	90–100	10	0.70	92–114
Pgdi2	(AG)26	F: ATTCCAGAGCCATACCGTTG R: (HEX) AGGTGGATGAGGGATGTTTG	21	224–266	15	0.83	226–266	11	0.78	224–250
Pgdi3	(TC)18	F: GGGGATGCTGGAATGTATGT R: (NED) GCACATTGCTCAGTGCTCTC	13	328–366	10	0.65	328–366	6	0.18	334–344
Pgdi4	(GT)17	F: GGCATCGCAGTCAACTTA R: (FAM) CGAGCCGAACCTTTAGTT	26	438–494	11	0.59	438–468	17	0.80	446–494
Multiplex 2										
PgTri1	(CAT)22(CTT)19	F: TGGAGACCATTAACCCTGGA R: (FAM) TTGGGAGGGTATTGAGGTTG	37	274–434	31	0.82	274–434	25	0.88	274–434
PgTri2	(GAC)4[(GAA)3(GAC)3] 9 GAA(GAC)2	F: AGGCAGAGAAGGGAGAGGAG R: (HEX) TCTGCAAGACCGTCATCATC	43	244–425	32	0.88	268–425	16	0.82	244–359
PgTri6	(CAA)24	F: CCCTTCCCAATCACTTCTCA R: (NED) GGACTGCTTTGGGTGATGTT	59	257–431	54	0.93	269–431	34	0.93	257–374
Multiplex 3										
PgTri7	(TTC)8TTT(CTT)7	F: ATGCTATCCCTCCCCAACTC R: (FAM) TGCGAAGCGTGTAAATTCTG	24	373–451	22	0.72	379–451	9	0.63	373–427
PgTet1	(AATC)13	F: CATCCGCTCCATTTCATTCT R: (HEX) TGGCGACGGAGTTGATAATA	52	200–432	49	0.89	200–432	7	0.12	200–264

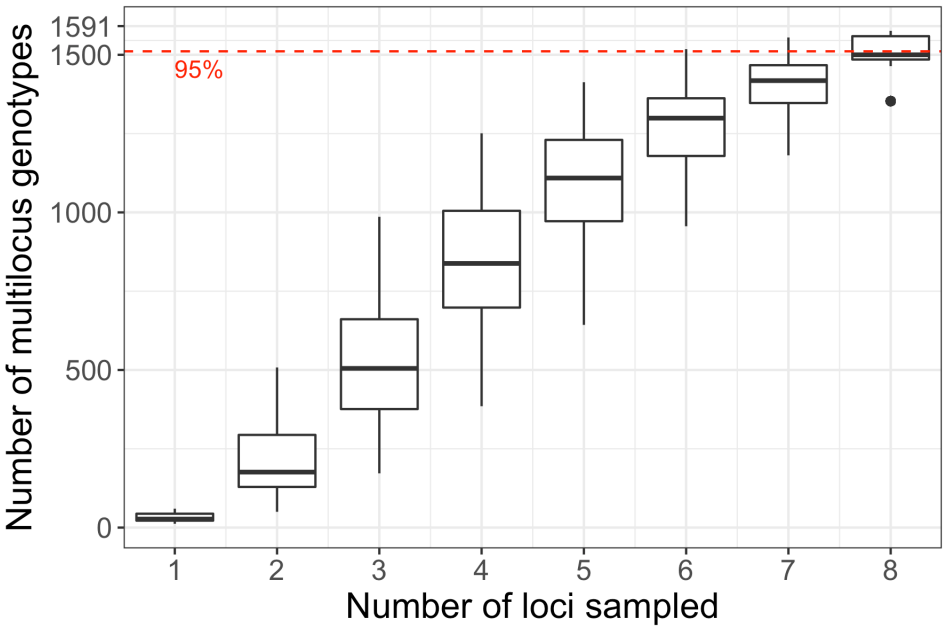

Figure S4.1: Genotype accumulation curve showing the number of *Nothophaeocryptopus gaeumannii* multilocus SSR genotypes (MLGs) from the global dataset observed in 1,000 random samples of *n*-1 loci sampled without replacement.

A

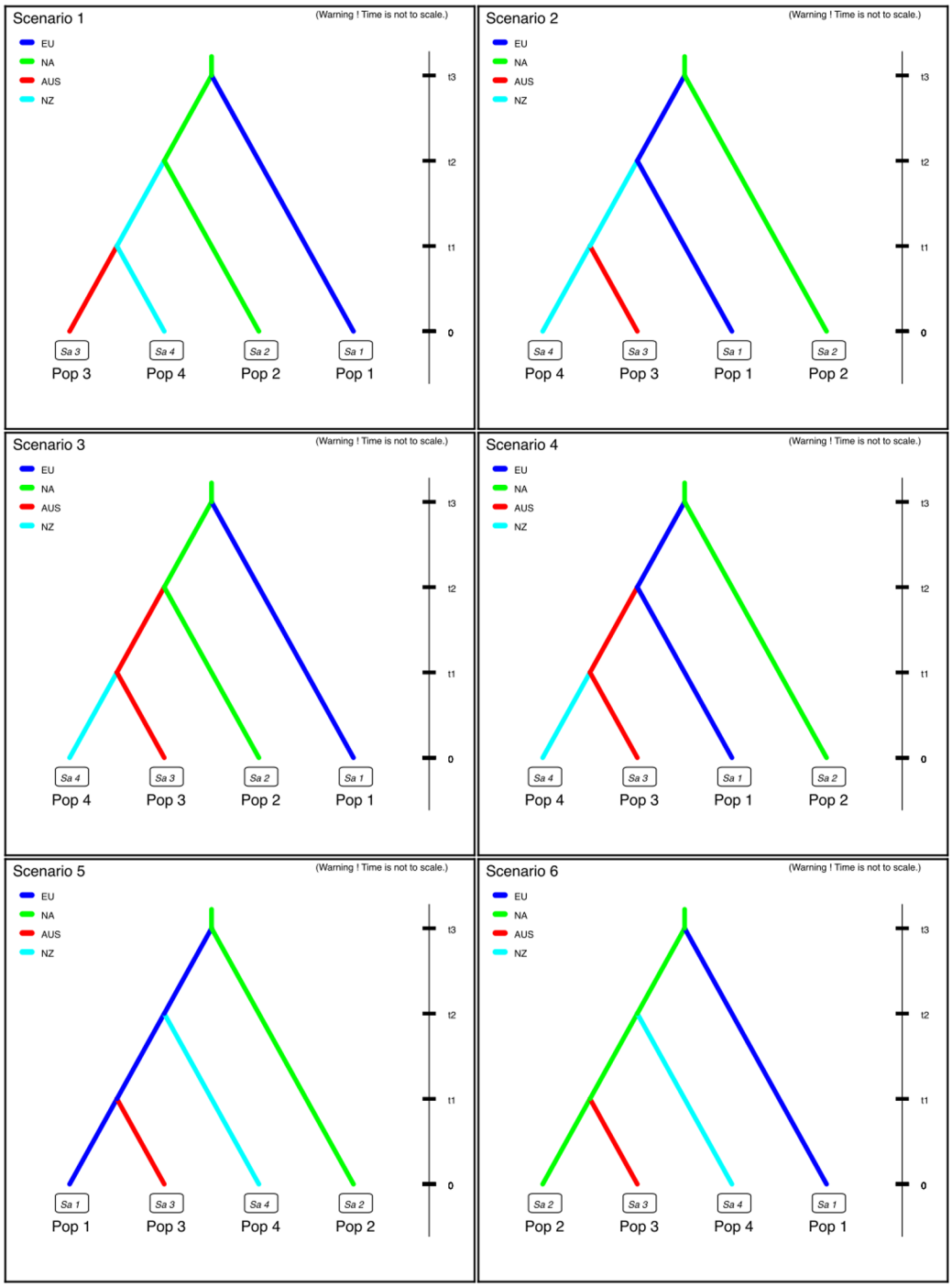
Scenario 1
(Warning ! Time is not to scale.)
EU
NA
AUS
NZ
t3
t2
t1
0
Sa 3
Sa 4
Sa 2
Sa 1
Pop 3
Pop 4
Pop 2
Pop 1
Scenario 2
(Warning ! Time is not to scale.)
EU
NA
AUS
NZ
t3
t2
t1
0
Sa 4
Sa 3
Sa 1
Sa 2
Pop 4
Pop 3
Pop 1
Pop 2
Scenario 3
(Warning ! Time is not to scale.)
EU
NA
AUS
NZ
t3
t2
t1
0
Sa 4
Sa 3
Sa 2
Sa 1
Pop 4
Pop 3
Pop 2
Pop 1
Scenario 4
(Warning ! Time is not to scale.)
EU
NA
AUS
NZ
t3
t2
t1
0
Sa 4
Sa 3
Sa 1
Sa 2
Pop 4
Pop 3
Pop 1
Pop 2
Scenario 5
(Warning ! Time is not to scale.)
EU
NA
AUS
NZ
t3
t2
t1
0
Sa 1
Sa 3
Sa 4
Sa 2
Pop 1
Pop 3
Pop 4
Pop 2
Scenario 6
(Warning ! Time is not to scale.)
EU
NA
AUS
NZ
t3
t2
t1
0
Sa 2
Sa 3
Sa 4
Sa 1
Pop 2
Pop 3
Pop 4
Pop 1

B

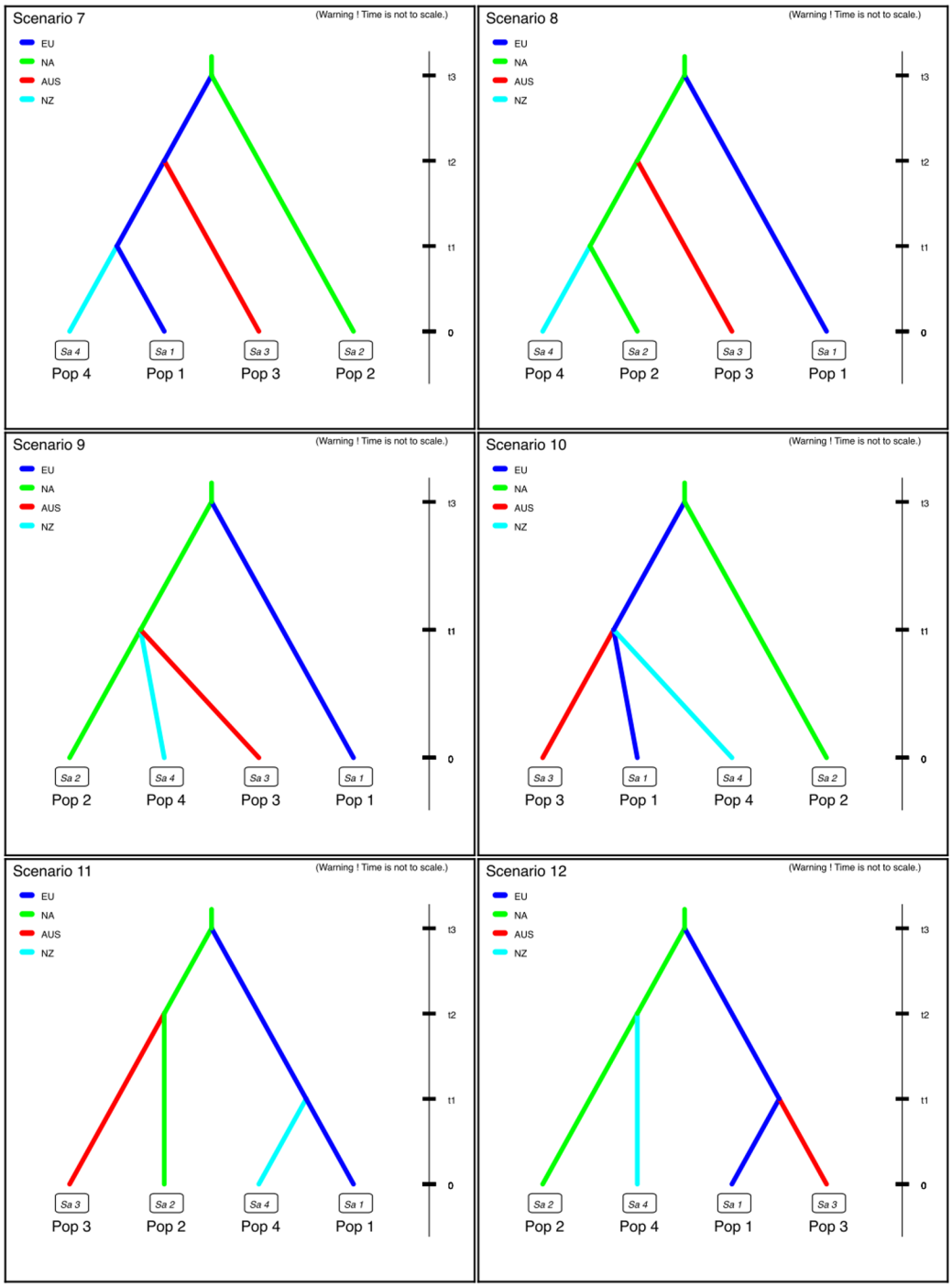
Scenario 7
(Warning ! Time is not to scale.)
EU
NA
AUS
NZ
t3
t2
t1
0
Sa 4
Sa 1
Sa 3
Sa 2
Pop 4
Pop 1
Pop 3
Pop 2
Scenario 8
(Warning ! Time is not to scale.)
EU
NA
AUS
NZ
t3
t2
t1
0
Sa 4
Sa 2
Sa 3
Sa 1
Pop 4
Pop 2
Pop 3
Pop 1
Scenario 9
(Warning ! Time is not to scale.)
EU
NA
AUS
NZ
t3
t1
0
Sa 2
Sa 4
Sa 3
Sa 1
Pop 2
Pop 4
Pop 3
Pop 1
Scenario 10
(Warning ! Time is not to scale.)
EU
NA
AUS
NZ
t3
t1
0
Sa 3
Sa 1
Sa 4
Sa 2
Pop 3
Pop 1
Pop 4
Pop 2
Scenario 11
(Warning ! Time is not to scale.)
EU
NA
AUS
NZ
t3
t2
t1
0
Sa 3
Sa 2
Sa 4
Sa 1
Pop 3
Pop 2
Pop 4
Pop 1
Scenario 12
(Warning ! Time is not to scale.)
EU
NA
AUS
NZ
t3
t2
t1
0
Sa 2
Sa 4
Sa 1
Sa 3
Pop 2
Pop 4
Pop 1
Pop 3

C

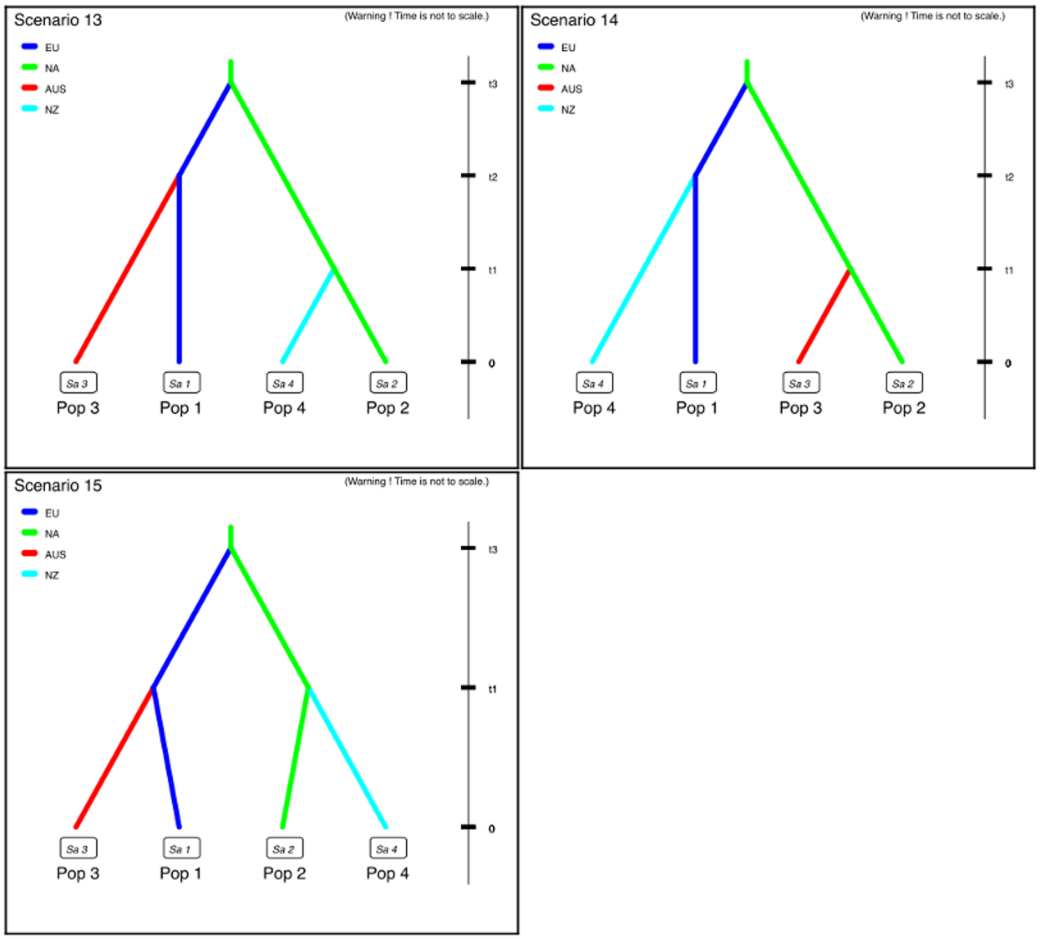

Figure S4.2: Fifteen *DIYABC* scenarios designed to test hypotheses about the evolutionary and geographic origin(s) of the *Nothophaeocryptopus gaeumannii* populations in Europe (EU), North America (NA), Australia (AUS), and New Zealand (NZ). **A)** Scenarios 1–6, **B)** Scenarios 7–12, **C)** Scenarios 13–15.

Table S4.2: Prior distributions and analysis parameters for the preliminary *DIYABC* analysis of *Nothophaeocryptopus gaeumannii* populations in North America, New Zealand, Europe, and Australia (Figures 4.6, S4.2).

Parameter	Distribution	Range (min.–max.)
Effective Population Size[b]	Uniform	10–10,000
EU	Uniform	10–10,000
NA	Uniform	10–10,000
AUS	Uniform	10–10,000
NZ	Uniform	10–10,000
Time to Coalescence[a]		
t1 (time to most recent introduction event)	Uniform	10–10,000
t2 (time to second most recent introduction event)	Uniform	10–10,000
t3 (time to coalescence of the introduced population with the ancestral population)	Uniform	10–10,000
Microsatellite Evolution		
Mean mutation rate	Uniform	1.00×10^{-4}–1.00×10^{-3}
Individual locus mutation rate	Gamma	1.00×10^{-5}–1.00×10^{-2}

[a] additional time constraints were imposed such that t1>t2, t3>t2, t3>t1, [b] priors relating to the relative effective population sizes were also provided, and assumed that the ancestral population (NA) was larger than the introduced populations, and populations that have been established the longest (based on first reports of SNC) would be larger than those introduced more recently: NA > NZ, NA > AUS, NA > EU, AUS < NZ, AUS < EU, NZ ≤ EU.

Table S4.3: Posterior prob. and 95% confidence intervals for the 15 scenarios from the preliminary *DIYABC* analysis of *Nothopaeocryptopus gaeumannii* populations in North America, New Zealand, Europe, and Australia (Figures 4.6, S4.2).

Scenario	Posterior Probability	95% CI
1	0.0000	[0.0000,0.0135]
2	0.0000	[0.0000,0.0135]
3	0.0000	[0.0000,0.0135]
4	0.0000	[0.0000,0.0135]
5	0.0183	[0.0052,0.0315]
6	0.0000	[0.0000,0.0135]
7	0.0000	[0.0000,0.0135]
8	0.0003	[0.0000,0.0137]
9	0.0001	[0.0000,0.0135]
10	0.0003	[0.0000,0.0137]
11	0.0000	[0.0000,0.0135]
12	0.1568	[0.0861,0.2276]
13	0.0296	[0.0117,0.0474]
14	0.0000	[0.0000,0.0135]
15	0.7945	[0.7171,0.8719]

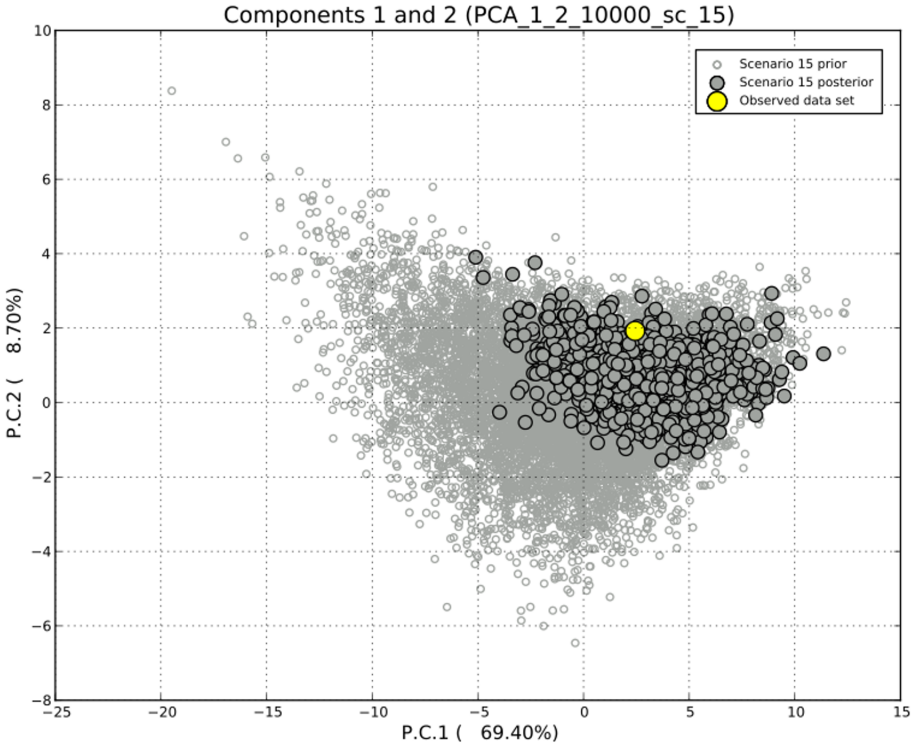

Figure S4.3: Principal components analysis (PCA) from the preliminary *DIYABC* analysis (Figures 4.6, S4.2) showing how well the summary statistics calculated from the observed dataset (yellow point) fit with the summary statistics calculated from simulated datasets. Each of the lighter points represents a dataset simulated from the prior distributions of parameters, while the darker points represent datasets simulated from the posterior distributions of parameters.

A

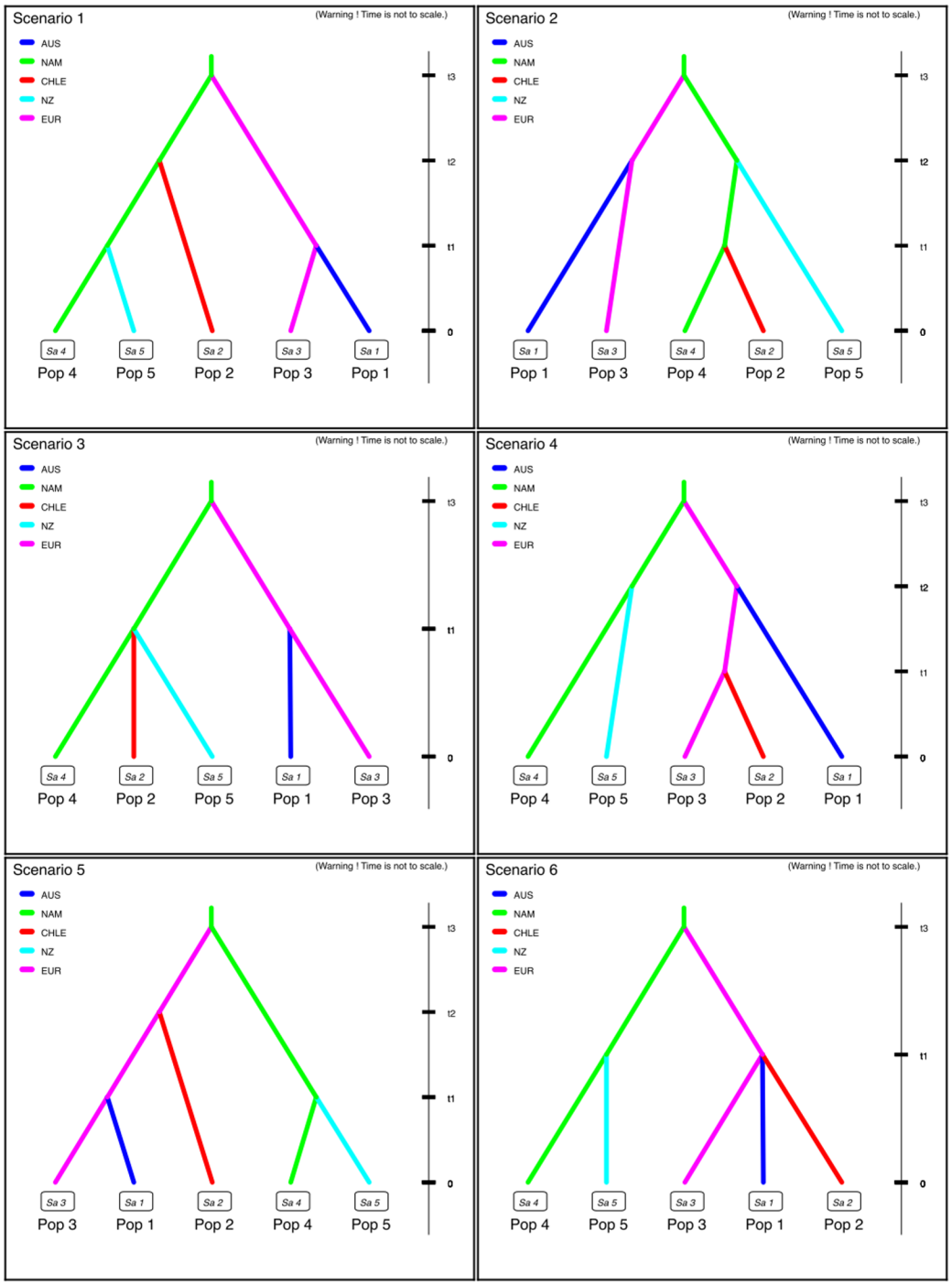
Scenario 1
(Warning ! Time is not to scale.)
AUS
NAM
CHLE
NZ
EUR
t3
t2
t1
0
Sa 4
Sa 5
Sa 2
Sa 3
Sa 1
Pop 4
Pop 5
Pop 2
Pop 3
Pop 1
Scenario 2
(Warning ! Time is not to scale.)
AUS
NAM
CHLE
NZ
EUR
t3
t2
t1
0
Sa 1
Sa 3
Sa 4
Sa 2
Sa 5
Pop 1
Pop 3
Pop 4
Pop 2
Pop 5
Scenario 3
(Warning ! Time is not to scale.)
AUS
NAM
CHLE
NZ
EUR
t3
t1
0
Sa 4
Sa 2
Sa 5
Sa 1
Sa 3
Pop 4
Pop 2
Pop 5
Pop 1
Pop 3
Scenario 4
(Warning ! Time is not to scale.)
AUS
NAM
CHLE
NZ
EUR
t3
t2
t1
0
Sa 4
Sa 5
Sa 3
Sa 2
Sa 1
Pop 4
Pop 5
Pop 3
Pop 2
Pop 1
Scenario 5
(Warning ! Time is not to scale.)
AUS
NAM
CHLE
NZ
EUR
t3
t2
t1
0
Sa 3
Sa 1
Sa 2
Sa 4
Sa 5
Pop 3
Pop 1
Pop 2
Pop 4
Pop 5
Scenario 6
(Warning ! Time is not to scale.)
AUS
NAM
CHLE
NZ
EUR
t3
t1
0
Sa 4
Sa 5
Sa 3
Sa 1
Sa 2
Pop 4
Pop 5
Pop 3
Pop 1
Pop 2

B

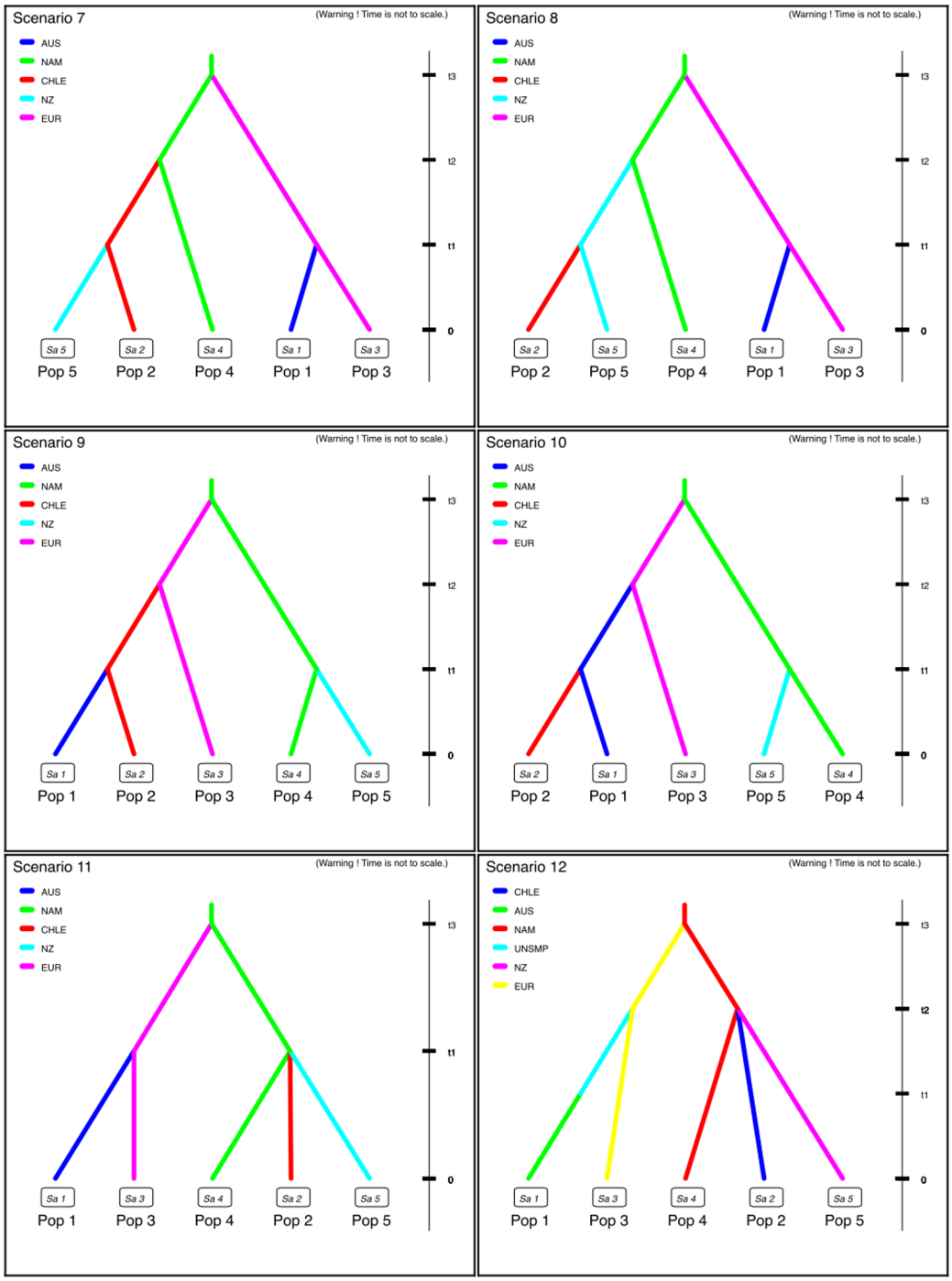
Scenario 7
(Warning ! Time is not to scale.)
AUS
NAM
CHLE
NZ
EUR
t3
t2
t1
0
Sa 5
Sa 2
Sa 4
Sa 1
Sa 3
Pop 5
Pop 2
Pop 4
Pop 1
Pop 3
Scenario 8
(Warning ! Time is not to scale.)
AUS
NAM
CHLE
NZ
EUR
t3
t2
t1
0
Sa 2
Sa 5
Sa 4
Sa 1
Sa 3
Pop 2
Pop 5
Pop 4
Pop 1
Pop 3
Scenario 9
(Warning ! Time is not to scale.)
AUS
NAM
CHLE
NZ
EUR
t3
t2
t1
0
Sa 1
Sa 2
Sa 3
Sa 4
Sa 5
Pop 1
Pop 2
Pop 3
Pop 4
Pop 5
Scenario 10
(Warning ! Time is not to scale.)
AUS
NAM
CHLE
NZ
EUR
t3
t2
t1
0
Sa 2
Sa 1
Sa 3
Sa 5
Sa 4
Pop 2
Pop 1
Pop 3
Pop 5
Pop 4
Scenario 11
(Warning ! Time is not to scale.)
AUS
NAM
CHLE
NZ
EUR
t3
t1
0
Sa 1
Sa 3
Sa 4
Sa 2
Sa 5
Pop 1
Pop 3
Pop 4
Pop 2
Pop 5
Scenario 12
(Warning ! Time is not to scale.)
CHLE
AUS
NAM
UNSMP
NZ
EUR
t3
t2
t1
0
Sa 1
Sa 3
Sa 4
Sa 2
Sa 5
Pop 1
Pop 3
Pop 4
Pop 2
Pop 5

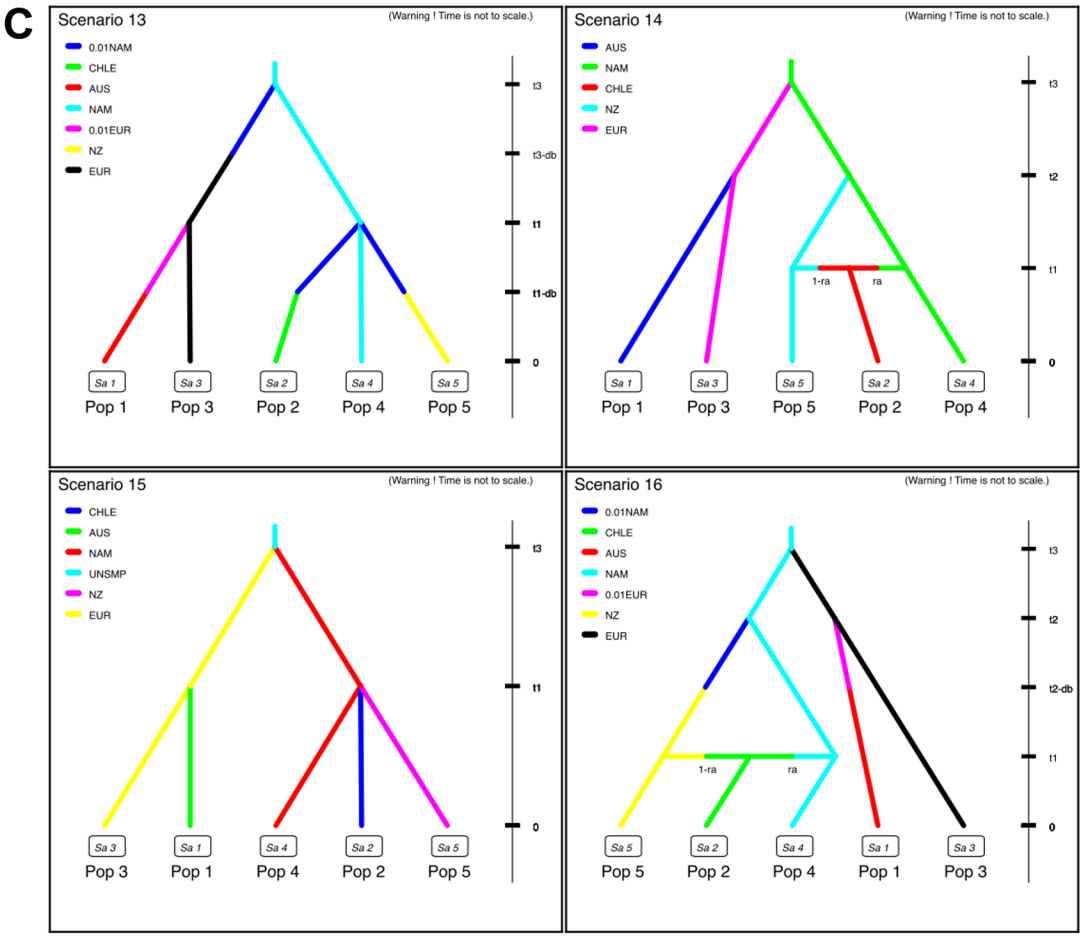

Figure S4.4: Sixteen *DIYABC* scenarios designed to test hypotheses about the evolutionary and geographic origin(s) of the invasive *Nothophaeocryptopus gaeumannii* population in Chile. **A)** Scenarios 1–6, **B)** Scenarios 7–12, **C)** Scenarios 13–16. AUS = Australia, CHLE = Chile, EUR = Europe, NAM = North America, NZ = New Zealand.

Table S4.4: Prior distributions and analysis parameters for the final *DIYABC* analysis (Figures 4.7, S4.4).

Parameter	Distribution	Range (min.–max.)
Population Size	Uniform	10–10,000
AUS	Uniform	10–10,000
CHLE	Uniform	10–10,000
EUR	Uniform	10–10,000
NAM	Uniform	10–10,000
NZ		10–10,000
UNSMP		10–10,000
Admixture Rate		
ra	Uniform	0.001–0.999
Time to Coalescence		
t1	Uniform	10–10,000
t2	Uniform	10–10,000
t3	Uniform	10–10,000
Bottleneck Duration		
db	Uniform	10–10,000
Microsatellite Evolution		
Mean mutation rate	Uniform	1.00×10^{-4}–1.00×10^{-3}
Individual locus mutation rate	Gamma	1.00×10^{-5}–1.00×10^{-2}

[a] additional time constraints were imposed such that t1>t2, t3>t2, t3>t1, [b] priors relating to the relative effective population sizes were also provided, and assumed that the ancestral population (NAM) was larger than the introduced populations, and populations that have been established the longest (based on first reports of SNC) would be larger than those introduced more recently: NAM > NZ, NAM > AUS, NAM > EUR, NZ > AUS, EUR > AUS, NZ ≤ EUR.

Table S4.5: Posterior probabilities and 95% confidence intervals for the 16 scenarios from the final *DIYABC* analysis that included the South American *Nothophaeocryptopus gaeumannii* population (Figures 4.7, S4.4).

Scenario	Posterior Probability	95% CI
1	0.0567	[0.0000,0.1757]
2	0.0082	[0.0000,0.1374]
3	0.0724	[0.0000,0.1837]
4	0.0000	[0.0000,0.1318]
5	0.0092	[0.0000,0.2146]
6	0.0005	[0.0000,0.1322]
7	0.0231	[0.0000,0.1476]
8	0.0602	[0.0000,0.1748]
9	0.0000	[0.0000,0.1318]
10	0.0000	[0.0000,0.1318]
11	0.0746	[0.0000,0.1853]
12	0.0079	[0.0000,0.1373]
13	0.4999	[0.3895,0.6103]
14	0.0062	[0.0000,0.1360]
15	0.0984	[0.0000,0.2039]
16	0.0828	[0.0000,0.1920]

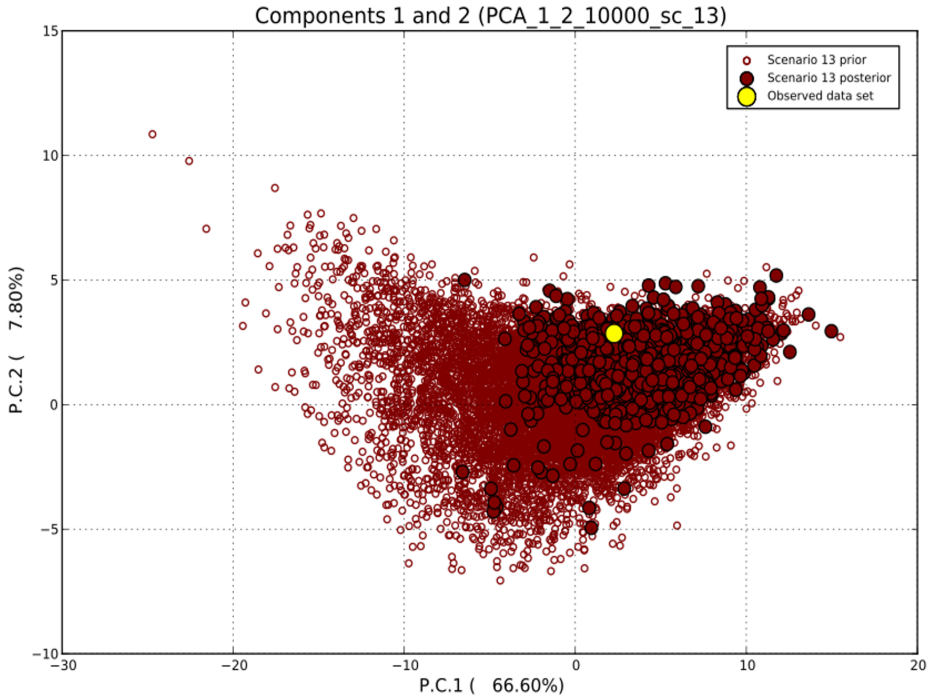

Figure S4.5: Principal components analysis (PCA) from the final *DIYABC* analysis (Figures 4.7, S4.4) showing how well the summary statistics calculated from the observed dataset (yellow point) fit with the summary statistics calculated from simulated datasets. Each of the lighter points represents a dataset simulated from the prior distributions of parameters, while the darker represent datasets simulated from the posterior distributions of parameters.

Chapter 5. Environmental Variables Associated with Swiss Needle Cast Severity and *Nothophaeocryptopus gaeumannii* Population Structure in Western Oregon and Washington

5.1 Abstract

Environmental variables such as seasonal temperatures, precipitation, and relative humidity are important factors influencing the abundance of the Douglas-fir Swiss needle cast (SNC) fungus, *Nothophaeocryptopus gaeumannii,* and are strongly correlated with spatial variation in SNC severity. For this study, non-metric multidimensional scaling (NMDS) and linear models were used to analyze correlations between the genetic structure of *N. gaeumannii* populations, SNC severity, and key environmental variables. Although the geographical distribution of *N. gaeumannii* Lineage 2 in western Oregon and Washington appears to coincide with the geographic distribution of SNC severity, the analyses presented here failed to detect a relationship between the relative abundance of Lineage 2 and disease severity at the stand level, after accounting for a major confounding variable. Lineage 2 was more abundant relative to Lineage 1, and average foliage retention (AFR) was lower, at sites having warmer average winter temperatures but the relative abundance of Lineage 2 was not associated with lower AFR after accounting for distance from the coast, which was strongly correlated with both variables. The colonization index (CI, the average percentage of stomata occupied by *N. gaeumannii* pseudothecia) was correlated with AFR, as foliage loss associated with SNC is caused by inhibition of carbon assimilation due to stomatal occlusion. Higher spring/early summer dew point temperatures were associated with higher CI and lower AFR. Higher summer mean temperatures were associated with lower CI and higher AFR. Our results suggest that the two lineages are adapted to different environments, and the

same environmental factors that favor Lineage 2 are favorable for needle colonization and the development of pseudothecia, and thus are conducive to SNC.

5.2 Introduction

Populations of the Swiss needle cast (SNC) fungus *Nothophaeocryptopus gaeumannii* (T. Rohde) Videira, C. Nakash., U. Braun & Crous (= *Phaeocryptopus gaeumannii* (T. Rohde) Petrak) in western Oregon and Washington comprise two reproductively-isolated lineages (Bennett and Stone, 2016; Winton et al., 2006). Lineage 1 occurs throughout the native range of Douglas-fir, and where Douglas-fir is grown as an exotic, while Lineage 2 is more narrowly distributed. Lineage 2 is most abundant along the western Coast Ranges within a few kilometers of the coast, and its abundance decreases further inland, where it is often supplanted entirely by Lineage 1 (Bennett and Stone, 2016; Winton et al., 2006). The factors influencing the spatial distributions of these lineages are not currently understood.

Because the distribution of Lineage 2 in the western Coast Ranges in Oregon and Washington corresponds to the region where the most severe SNC symptoms (foliage loss, growth reduction) have been observed, a causal relationship between Lineage 2 and the recent intensification and expansion of SNC in this region has been suggested (Winton et al., 2006). Compared to Lineage 1, recovery of Lineage 2 isolates from diseased foliage was twice as likely in severely diseased stands, and only half as likely in healthier stands (Winton et al., 2006). In coastal Oregon, Douglas-fir stands with higher relative proportions of Lineage 2 had more sparse canopies suggesting lower foliage retention due to SNC (Winton et al., 2006). Visual estimates of foliage discoloration as

an indicator of disease severity also suggested a causal relationship with increasing proportion of Lineage 2 isolates recovered from the stand (Winton et al., 2006). Isolates of *N. gaeumannii* collected from severely diseased sites also seemed to cause more severe SNC symptoms in an inoculation study, suggesting that selection for more virulent or aggressive genotypes may have occurred in the low-elevation coastal forests in Oregon and Washington where SNC is most severe (Winton, 2001). These observations informed our hypotheses about the potential relationships between the geographic distribution of *N. gaeumannii* Lineage 2 and SNC severity.

The variation in SNC symptom severity in relation to site-specific climate factors has been well documented (Coop and Stone, 2010; Hansen et al., 2000; Lee et al., 2017, 2013; Manter et al., 2005; Rosso and Hansen, 2003; Stone et al., 2008b, 2007; Watt et al., 2010; Zhao et al., 2012, 2011). Winter temperature has been consistently identified as being strongly correlated with *N. gaeumannii* abundance, and thus SNC severity, given that needle colonization and the development of pseudothecia continue throughout winter following the spring/summer infection period (Capitano, 1999; Manter et al., 2005; Stone et al., 2008a). Low winter temperatures limit the colonization of needles by *N. gaeumannii* (Lee et al., 2017). Leaf wetness and moisture availability (as precipitation, fog, or dew) during the spring and early summer are necessary for spore dispersal, adherence, and germination on the needle surface (Manter et al. 2005; Capitano, 1999; Rosso and Hansen, 2003), and thus are highly influential in predictive spatial models of SNC severity. High temperatures inhibit the growth of *N. gaeumannii*, and thus higher summer temperatures are associated with less severe SNC symptoms (Capitano, 1999;

Lee et al., 2017; Rosso and Hansen, 2003; Zhao et al., 2011). Predictive models based on combinations of these factors can explain a major portion of the geographic variation in SNC severity in western North America (Lee et al., 2017; Manter et al., 2005; Rosso and Hansen, 2003; Stone et al., 2008b; Watt et al., 2011). Climate change projections suggest that the climate in the western Coast Ranges in Oregon and Washington will become increasingly conducive to SNC intensification and expansion in the coming decades, given that winters may become warmer and spring moisture/rainfall is expected to increase (Lee et al., 2017; Mote and Salathé, 2010; Stone et al., 2008b).

Our specific objectives were to 1) assess the spatial distributions of the two *N. gaeumannii* lineages in relation to SNC severity in the OR and WA Coast Ranges, 2) determine whether any relationship exists between SNC severity and the relative abundance of *N. gaeumannii* Lineage 2, and 3) examine the relationships between the genetic structure of *N. gaeumannii* populations, SNC severity, and key environmental variables with a multivariate statistical ordination. Given previous observations of the relationship between the spatial distribution of *N. gaeumannii* Lineage 2 and SNC severity, we aimed to test the hypothesis that the relative abundance of Lineage 2 within sites is correlated with disease severity. The analyses performed here were also designed to test the hypothesis that SNC severity and the spatial distributions of the two lineages (and thus the genetic structure of *N. gaeumannii* populations) are correlated with key environmental variables that have been previously identified has having an influence on the development of *N. gaeumannii*. For this study, we analyzed 663 multilocus genotypes (MLGs) consisting of alleles for nine microsatellite (SSR) markers (Winton et al., 2007)

from 1,061 *N. gaeumannii* individuals collected from a hierarchical spatial sampling of Douglas-fir in western Oregon and Washington.

5.3 Materials and Methods

5.3.1 Foliage Sampling

Douglas-fir foliage was collected from sites in a gridded plot network of privately-owned plantations in the western Coast Range in Oregon managed by the Oregon State University Swiss Needle Cast Cooperative (SNCC) (Ritóková et al. 2016), and from sites managed by the Washington Department of Natural Resources (WA DNR) (Figure 1). In Oregon and Washington, foliage samples were collected from 35 sites with five sampling blocks in Oregon and three sampling blocks in Washington. In 2014, samples were collected from nine sites in the Tillamook block in northwestern Oregon, three sites in the Florence block in central western Oregon, and two sites in the DNR block in southwestern Washington (Figure 5.1). In 2015, foliage was collected from four sites in the Newport block in northwestern Oregon, two additional sites in the Florence block, four sites in the Coos Bay block, and one site in the Gold Beach block on the southern Oregon coast (Figure 5.1). Also in 2015, samples were collected from four sites in the southern Olympic Peninsula and five sites in the northern Olympic Peninsula (Figure 5.1). One additional site in the Gold Beach block was sampled in 2016. Sites within sampling blocks were stratified by distance from the coast, with sites ranging from the shoreline to 56 km inland. The only exceptions were the Gold Beach block, in which both sites were within a few km of the shoreline, and the DNR block in southwest Washington, where the sites were 48 and 57 km inland. Sampling in Oregon and

southwest Washington was performed by researchers with the SNCC, while the sites in the Olympic Peninsula were sampled by the authors of this study. At each site, foliage was collected from second- and third-year internodes on secondary branches in the upper crowns of five randomly selected 10–30-year-old Douglas-fir trees. From one of the five trees sampled at each of the SNCC sites, foliage samples were also collected from the lower, mid, and upper crowns to account for within-tree diversity. The foliage was stored on ice and promptly returned to the campus of Oregon State University for storage in a cold room for no longer than 5 days prior to processing.

5.3.2 Isolation of N. gaeumannii from Infected Foliage

Needles bearing pseudothecia of *N. gaeumannii* were selected for ascospore isolations, and double-sided tape was used to attach the needles to the lid of a 100 mm plastic Petri dish. These were then suspended above the surface of 2% water agar and incubated to allow ascospore discharge. After 48–72 hours, individual germinating ascospores were excised from the agar with the aid of flame-sterilized forceps and transferred onto 2% malt agar (MA) (Difco Laboratories, Detroit, MI). Cultures were incubated at 17 °C for a minimum of 2–6 months to allow sufficient growth for DNA extraction and permanent storage.

5.3.3 DNA Extraction, PCR, and SSR Genotyping

The DNeasy Plant Kit (Qiagen, Hilden, Germany) was used to extract genomic DNA from vegetative mycelium. The manufacturer's protocol was modified with the addition of a maceration procedure. Agar plugs extracted from *N. gaeumannii* cultures were added to cryogenic vials along with sterile glass beads. The vials were briefly

submerged in liquid nitrogen to freeze the agar plugs prior to the addition of the DNeasy extraction buffer. The vials were then shaken at 5000 rpm for 60 seconds with either a Mini-Beadbeater (BioSpec Products, Bartlesville, OK, USA) or MP Bio FastPrep (MP Biomedicals, Santa Ana, CA, USA).

For each isolate, ten SSR loci (Winton et al. 2007b) were amplified in three multiplexed PCR reactions. The multiplexed reactions contained 2, 3, and 5 primer sets, each with a fluorescent dye label on the reverse primer. The sequences of the primers were identical to those described in (Winton et al. (2007b), but without the 18 bp M13 universal tails and therefore resulting amplicons were 36 bp shorter than those produced using those primers. The PCR reactions were performed with the Qiagen Type-It Microsatellite PCR kit. The manufacturer's protocol was followed, but with reaction volumes of 12.5 µl. The amplification was performed on a PTC-200 thermal cycler (MJ Research, Inc. Waltham, MA, USA) programmed as follows: 95 °C for 15 min, 30 repeated cycles of 94 °C for 30 s, 57 °C for 90 s, and 72°C for 30 s, final extension of 60 °C for 30 min.

Each of the multiplexed PCR reactions was diluted in deionized water and submitted to the Center for Genome Research and Biocomputing (CGRB, Oregon State University, Corvallis, OR USA) for genotyping via capillary electrophoresis on an ABI 3730 DNA Analyzer (Applied Biosystems- ThermoFisher Scientific Corporation, Waltham, MA USA) with the GS-500ROX size standard. Allele sizes and genotypes were assigned with the aid of the ABI GeneMapper 4.1 software. Microsatellite alleles were called using a customized analysis method and were also validated visually for each

locus and isolate. A positive control isolate was included to ensure that each independent PCR amplification and genotyping run resulted in consistent allele sizing. One of the loci, Pgdi5, did not amplify reliably for all isolates, and therefore was omitted from the dataset prior to analysis. The actual number of trees per site represented by the SSR dataset was often less than five. This was due to a number of steps that may have resulted in sample loss such as variation in the presence of pseudothecia, contamination during isolations and culturing, and inconsistent amplification during PCR.

5.3.4 Data Analysis

All data formatting and statistical analyses were performed with R version 3.4.1 (R Core Team, 2017) and Microsoft Excel 2016. The microsatellite allele data were formatted in GenAlEx 6.5 (Peakall and Smouse 2006, 2012) and imported to R for use with *poppr* 2.5 (Kamvar et al. 2015). Maps depicting the distributions of the two lineages in this region were constructed with the R packages *mapplots* (Gerritsen, 2014) and *shapefiles* (Stabler, 2013), and were superimposed on SNC aerial survey maps from surveys conducted by the Oregon Department of Forestry (ODF), the USDA Forest Service, and the Washington Department of Natural Resources (Ramsey et al., 2015; Ritóková et al., 2016).

Foliage retention and the abundance of pseudothecia were measured by researchers with the Oregon State University Swiss Needle Cast Cooperative (SNCC) and the Washington Department of Natural Resources using methods similar to those described in Manter et al. (2005) and Watt et al. (2010). For this study, the average foliage retention (AFR) was expressed as the average percentage of foliage remaining

across four needle age-classes from secondary branches collected in the mid-canopies of 10 trees from each site. The colonization index (CI), an estimate of the average percentage of stomata occluded by pseudothecia, was calculated as the product of incidence (the proportion of needles bearing pseudothecia, N = 50 needles) and the percentage of stomata occluded by pseudothecia (N = 10 needles). The percentage of stomata occluded was calculated by averaging the numbers of pseudothecia from 100 stomata in each of three sections per needle (base, middle, and tip) for each sample of ten 2-year-old needles from each of three canopy sections per tree (lower, middle, and upper) for ten trees from each site.

Pearson correlation coefficients, and their associated p-values, were calculated for all pairwise correlations among geographic and disease variables (for the 34 sites for which disease severity data were available) with the R package *Hmisc* (Harrell, 2017). Scatter plots associated with these statistical analyses were constructed with *ggplot2* (Wickham, 2016). Douglas-fir foliage retention, SNC severity, and the relative proportion of *N. gaeumannii* Lineage 2 may vary independently along the west-east sampling gradient due to climate and other spatial geographic factors. Thus, a linear mixed model was utilized to investigate the influence of the proportion of Lineage 2 on foliage retention with the distance from the coast held at its mean value (26 km). Distance from the coast is related to continentality, and encompasses a complex combination of environmental variables (i.e. average temperature, precipitation, RH, dew point deficit, wind speed and other unknown factors) that are expected to influence our explanatory and response variables. The model described below was designed to test the null

hypothesis that the proportion of Lineage 2 had no effect on average foliage retention after accounting for distance from the coast (H_0: $\beta_1 = 0$).

$$Y_i = \beta_0 + \beta_1 X_i + \beta_2 X_i + \varepsilon_i$$

where:

Y_i is the average foliage retention of the ith site,

β_0 is the mean average foliage retention when the relative proportion of Lineage 2 recovered at the site is 0 and the distance from the coast is 0 km,

β_1 is the coefficient for the effect of the relative proportion of Lineage 2 on mean average foliage retention,

X_i is the relative proportion of Lineage 2 recovered from the ith site,

β_2 is the coefficient for the effect of the distance from the coast (km) on mean average foliage retention,

X_i is the distance from the coast (km) of the ith site,

ε_i is the random effect of the ith site on mean average foliage retention, $\varepsilon_i \sim N(0, \sigma^2)$

Non-metric multidimensional scaling (NMDS) ordination was used to visualize genetic differentiation among each of the sample sites. Roger's genetic distance (Rogers, 1972) was calculated pairwise between each of the sampling sites with the R package *adegenet* (Jombart, 2008). The NMDS ordination based on this genetic distance matrix was performed with the function metaMDS in the R package *vegan* version 2.4-5 (Oksanen et al. 2017). This method ranks sample units according to their dissimilarity and then attempts to minimize the stress in the relationship between ordination distances and genetic distances (McCune et al., 2002). Correlations between the ordination, SNC severity, and the environmental/geographic variables associated with each site, were

calculated with the function envfit from the R package *vegan* (Oksanen et al. 2017). The environmental and geographic variables were then displayed as a series of radiating vectors with the direction of the vector corresponding to the direction of increase of the variable, and the length of the vector proportional to the strength of the correlation between the variable and the ordination. Included as vectors on the joint plot were SNC severity (AFR and CI), the relative proportion of Lineage 2, latitude, longitude, elevation, and several environmental variables that have been shown to contribute to SNC disease and *N. gaeumannii* abundance (Lee et al., 2017; Manter et al., 2005; Rosso and Hansen, 2003; Stone et al., 2008b, 2007; Watt et al., 2010; Zhao et al., 2011). Time-series values for the climate variables were obtained for each of the sample sites from the PRISM data explorer (PRISM Climate Group, Oregon State University, http://prism.oregonstate.edu).

5.4 Results

5.4.1 The Spatial Distributions of N. gaeumannii Lineages in Relation to SNC Severity

There was a strong association between the geographic distributions of *N. gaeumannii* Lineage 2 and SNC symptom severity delineated during aerial surveys (Figure 5.1). With few exceptions, the sites nearest the coast had the highest proportions of Lineage 2 and occurred in areas where moderate to severe SNC symptoms were observed in the aerial surveys (Figure 5.1). Sites further inland, where Lineage 2 was generally rare or absent, had less severe SNC or symptoms were not visible (Figure 5.1). However, the aerial survey did not detect visible symptoms of SNC near Gold Beach and

Brookings near the southern Oregon coast, where only Lineage 2 was isolated from foliage samples and Lineage 1 was not recovered (Figure 5.1).

5.4.2 Variations in Disease Severity, Geography, and Environment Across Sites

There was a wide range in SNC severity across the 34 sites for which disease severity data were available. Estimates of average foliage retention (AFR) ranged from 30.5% to 89.2%, with a mean of 65.3% (Tables 5.1, 5.2). The colonization index ranged from 3.7 to 42.8 with a mean of 19.2 (Tables 5.1, 5.2). The most severe SNC symptoms occurred at sites near the coast in the vicinity of Tillamook, OR (Table 5.1). The lowest AFR was at site T0-3 (elevation = 127 m, distance from the coast = 8.3 km), and the highest CI was at T5-3 (elevation = 158 m, distance from the coast = 16.7 km) (Table 5.1). The sites with the least severe SNC symptoms were at higher elevations and further inland. The highest AFR was at site N25-5 (elevation = 251 m, distance from the coast = 51 km), and the lowest CI was at T25-2 (elevation = 591 m, distance from the coast = 49.5 km) (Table 5.1).

The 35 sampling sites in Oregon and Washington covered a latitudinal range from 42˚ N to 48˚ N, and a longitudinal range from -124.6˚ W to -123.3˚ W (Table 5.2). Elevation ranged from 16 m to 595 m, and the sites occupied a range of distances from the coast from 1.8 km to 57.6 km (Table 5.2). There were considerable variations in the environmental variables across the sample sites. Mean average dewpoint temperature (MADT) ranged from 7.3˚ to 10.5˚ (Table 5.2). Mean summer temperature (TmSummer)

ranged from 14.2˚ to 17.8˚, and mean winter temperature (TmWinter) ranged from 4.1˚ to 10.3˚ (Table 5.2).

5.4.3 Correlations Between Environment, Disease, and the Genetic Structure of N. gaeumannii Populations

Pearson's coefficient (*r*) was calculated pairwise between the environmental, geographic, and disease variables in our dataset. CI was negatively correlated with elevation and distance from the coast (Figure 5.2, Table 5.3), and positively correlated with mean average May-July dew point temperature (MADT) (Table 5.3). AFR was negatively correlated with CI, the relative proportion of *N. gaeumannii* Lineage 2 recovered from the site (PL2) (Figure 5.2), and MADT (Table 5.3). AFR was positively correlated with elevation and distance from the coast (Figure 5.2, Table 5.3). The relative proportion of Lineage 2 was negatively correlated with distance from the coast (Figure 5.2) and elevation, and positively correlated with mean winter temperature (TmWinter) (Table 5.3). There was a significant association between AFR and CI, but there was considerable variation in foliage retention for a given level of colonization (Figure 5.4).

The linear model described the site-level average foliage retention as a function of the relative proportion of *N. gaeumannii* Lineage 2 recovered from the site, after accounting for distance from the coast (km) (a variable that is strongly correlated with the relative abundance of *N. gaeumannii* Lineage 2 and SNC severity) (Figure 5.2, Table 5.3). Although it initially appeared that there was a significant correlation between AFR and PL2 (Figure 5.2 D), there was no evidence to support this association between average foliage retention and the relative proportion of Lineage 2 when the distance from

the coast was held at its mean (25.95 km) (t_{31} = -0.01, P = 0.99) (Figure 5.3). This model did not appear to violate the assumption of constant variance, and the residuals from the model did not appear to deviate considerably from a normal distribution (Figure S5.1).

In initial runs of NMDS that included all of the 34 sites for which disease severity data were available, CB5-2 appeared as an outlier in the periphery of the plot, and appeared to repel the other points causing a disproportionate influence on the ordination. For this reason, CB5-2 was removed from subsequent analyses. The results presented here are from the ordination of the 33 remaining sites for which disease severity data were available (Table 5.1). The NMDS ordination had a final stress of 0.095 (Figure 5.5), and there was a strong linear correlation between the ordination distances and the original community distances (i.e. pairwise genetic distance among the sites) (R^2 = 0.96) and a strong non-metric fit (R^2 = 0.99) (Figure S5.2). The relative proportion of *N. gaeumannii* Lineage 2 (PL2) had the strongest relationship with the NMDS ordination (R^2 = 0.947, P = 0.001) (Figure 5.5, Table 5.4). Sites were aligned along NMDS axis 1 according to the relative proportion of the isolates recovered from the site that were identified as *N. gaeumannii* Lineage 2. Disease severity varied along NMDS axis 2 (Figure 5.5), and AFR was most strongly correlated with the ordination of genetic distance between the sites (R^2 = 0.569, P = 0.001) (Figure 5.5, Table 5.4). CI was inversely related to AFR, but was not correlated as strongly with the ordination (R^2 = 0.228, P = 0.016) (Figure 5.5, Table 5.4). Winter temperature (TmWinter) was the environmental variable most strongly correlated with the genetic differentiation among sites (R^2 = 0.513, P = 0.001), and with the relative proportion of Lineage 2 (Figure 5.5, Table 5.4). Mean summer temperature

(TmSummer) (R^2 = 0.284, *P* = 0.012) and average spring/early summer dew point temperature (MADT) (R^2 = 0.247, *P* = 0.015) had much weaker, but nonetheless significant, correlations with the ordination (Figure 5.5, Table 5.4). Latitude was the geographic variable with the strongest correlation with the ordination (R^2 = 0.342, *P* = 0.004), followed by elevation (R^2 = 0.283, P = 0.009), and longtitude (R^2 = 0.253, *P* = 0.017) (Table 5.4). AFR and TmSummer were positively correlated with elevation and longitude, while CI was positively correlated with latitude and MADT (Figure 5.5, Table 5.3). In addition to the genetic differentiation among sites related to the divergence between lineages, there also appeared to be genetic variation among sites that was correlated with environment and SNC severity (Figure 5.5).

5.5 Discussion

The distribution of *N. gaeumannii* Lineage 2 in western Oregon and Washington initially appeared to be correlated with the geographic distribution of SNC severity. At the landscape level, visible symptoms of the disease mapped via aerial survey are most prevalent where the relative abundance of Lineage 2 was high, or where the lineages coexisted within ~ 30 km of the coast (Figure 5.1). This trend was observed in the low-elevation forests along the western slopes of the Coast Ranges in Oregon and Washington from Coos Bay to the northern Olympic Peninsula (Figure 5.1, Table 5.1). Further inland, Lineage 2 was generally less abundant (or absent) and SNC symptoms were generally less severe or not detected (Figure 5.1). Lineage 1 was not isolated from the Douglas-fir foliage samples collected at the two sites in the Gold Beach block, and the aerial survey did not detect any visible symptoms of SNC in that region (Figure 5.1A). Overall, the

observation that the region where the spatial distributions of the lineages overlap is where SNC is most severe is in agreement with the findings of Winton et al. (2006) and Winton and Stone (2004). The apparent association between the relative proportion of Lineage 2 (PL2) and average foliage retention (AFR) when distance from the coast was not taken into account (Figure 5.2D, Table 5.3) also supported those findings, which suggested that stands with higher proportions of Lineage 2 had more severe SNC symptoms (Winton et al., 2006; Winton and Stone, 2004). However, the results of the controlled inoculation experiments presented in Winton and Stone (2004) suggested that Lineage 2 was not more aggressive, as the trees inoculated with Lineage 2 isolates actually had higher foliage retention than those inoculated with Lineage 1 isolates. However, PL2 was also not correlated with the colonization index (CI) (Table 5.3), the variable that should have the strongest mechanistic relationship with foliage retention. Thus, our results are not consistent with a direct relationship between Lineage 2 and SNC severity. Furthermore, the results of our linear model suggested that, on average, after accounting for distance from the coast (an environmental gradient that is strongly associated with variation in disease and the relative abundance *N. gaeumannii* Lineage 2), PL2 was not significantly correlated with AFR (Figure 5.3). Given our current understanding of the mechanisms of disease in this pathosystem, where the foliage loss associated with SNC results from cumulative occlusion of the stomata by the pseudothecia of *N. gaeumannii* (Manter et al., 2000; Stone et al., 2008a), the most likely mechanism by which Lineage 2 could cause more severe defoliation would be by producing more pseudothecia relative to Lineage 1. However, our analyses, which did not find any relationship between CI and PL2 (Table

5.3), do not support such a mechanism. The main environmental variable associated with the spatial distribution of Lineage 2 (winter temperature) is also strongly correlated with the variable that most strongly influences needle colonization (spring/early summer dew point temperature) (Table 5.3). This suggests that the environment that is most conducive to needle colonization is also favorable for *N. gaeumannii* Lineage 2, as suggested by Winton and Stone (2004).

Distance from the coast and elevation are two geographic variables that had significant associations with both PL2 and disease severity in our data. These geographic variables do not directly affect biological processes that influence *N. gaeumannii* abundance or SNC severity. Their effects on the biological system are a reflection of interacting climatic and environmental factors along a gradient from the low-elevation forests along the western slopes of the Coast Range to the higher elevation forests further east in the Coast Range. Indeed, distance from the coast and elevation were strongly correlated with one another, and were significantly correlated with the combination of environmental variables included in this study. We have used distance from the coast as a proxy for continentality, a complex combination of environmental conditions that vary along this geographic gradient.

The multivariate NMS ordination of sites in relation to genetic distance revealed strong spatial genetic differentiation between inland and coastal sample sites. This approach allowed for a visualization of statistical relationships between genetic variation and pertinent environmental, geographic, and disease variables. The spatial distribution of genetic variation was highly correlated with mean winter temperature, mean summer

temperature, and mean average dew point temperatures in the year prior to sampling (Figure 5.5, Table 5.4). The distribution of *N. gaeumannii* Lineage 2 was most strongly correlated with mean winter temperature (Figure 5.5, Table 5.4). Foliage retention varied most strongly with mean summer temperature, elevation, and longitude, and was negatively correlated with mean average May-July dew point temperature (Figure 5.5, Table 5.4). Sites with lower AFR values and higher CI values generally occurred at lower elevations nearest the coast where summers were cooler and spring/early summer dew point temperatures were warmer (Figure 5.5). *Nothophaeocryptopus* populations occurring in these sites appeared to be genetically differentiated from the higher elevation inland sites where the winters were colder, summers were hotter, and AFR was greater (Figure 5.5, Table 5.1). These results also suggest that climate may influence the genetic structure of *N. gaeumannii* populations via natural selection and adaptation. Although the SSR markers used here are presumed to be selectively neutral, and thus are not directly influenced by the environment, they provided a tool with which to detect genetic differentiation between populations that may be associated with adaptation to local climate.

Because the occlusion of stomata causes the foliage loss associated with SNC, we expected the correlation between AFR and CI to be stronger, as it has been in previous studies (Manter et al., 2003; Watt et al., 2010). In our dataset there was considerable variation in AFR for a given value of CI, suggesting that there is broad host variation in tolerance (i.e. some host genotypes can tolerate higher levels of infection before needle abscission occurs). This phenomenon has been investigated for SNC in coastal Douglas-

fir (Temel et al., 2004). In that study, the authors concluded that there was some genetic variation in host tolerance due to historical SNC pressure in the environment where the host genotype evolved (Temel et al., 2004). Generally, Douglas-fir provenances from regions where rainfall and humidity are low are less tolerant of SNC because natural selection has not favored tolerant individuals where disease pressure is historically low (Hood, 1982; Mcdermott and Robinson, 1989; Temel et al., 2004). The variation observed in our study may also be a factor of some direct interaction between environment and disease. It seems reasonable to assume that some unfavorable environmental conditions may lead to greater foliage loss at lower levels of infection, and that favorable conditions may allow hosts to maintain a healthy level of foliage with higher levels of infection.

A synthesis of the results from this study provides a framework for understanding the factors influencing SNC severity and the genetic structure of *N. gaeumannii* populations. In general, the sites with the most severe SNC and the highest relative abundances of Lineage 2 were at low elevations (< 300 m) within ~ 20 km of the coast along the western slopes of the Oregon and Washington Coast Ranges where winter temperatures were the warmest (~6–10 ˚C), summers were coolest (~14–16 ˚C), and the dew point temperatures (the temperature at which the air was saturated with water vapor) were warmest (~9–11 ˚C). These observations are in agreement with previous studies that demonstrated that warmer winter temperatures and abundant moisture in the spring/early summer favor *N. gaeumannii* abundance and thus SNC severity (Lee et al., 2017, 2016, 2013; Manter et al., 2005; Stone et al., 2008b, 2007; Watt et al., 2010). Our observations

are also in agreement with studies that suggested that high temperatures inhibit the growth of *N. gaeumannii* (Rosso and Hansen, 2003), resulting in lower SNC severity (Lee et al., 2017; Manter et al., 2005; Stone et al., 2008b, 2007; Watt et al., 2011, 2010; Zhao et al., 2012). Climate change will likely exacerbate SNC severity, leading to an intensification of symptoms in areas already affected by SNC, but also an expansion of the area affected by SNC (Coop and Stone, 2010; Lee et al., 2017; Stone et al., 2008b; Watt et al., 2011, 2010). In the future, modeling of geographic variation in SNC severity should consider the relationships between climate and the proportion of Lineage 2, which may be a good predictor of SNC severity even if there is not a causal association between those two variables.

Not only does climate influence SNC severity through direct effects on growth rate and reproduction of *N. gaeumannii*, but it is also correlated with spatial genetic differentiation in the *N. gaeumannii* population and the divergence of two non-interbreeding fungal lineages. It appears that the two *N. gaeumannii* lineages are adapted to slightly different environmental conditions, and thus exhibit different habitat distributions that are determined, directly or indirectly, by climate. The local environment has the potential to be a driver of further genetic change in *N. gaeumannii* populations. The *N. gaeumannii* isolates collected from sites with the most severe disease appeared to be genetically differentiated from collected at sites with less severe disease (Figure 5.4), suggesting that some adaptation to local climate or natural selection for advantageous genotypes has occurred in the geographic regions where SNC is most severe. Whether *N. gaeumannii* isolates in the coastal SNC epidemic zone are more aggressive or have

increased fitness (and thus cause more severe SNC) is still unclear and should be the focus of future studies.

In the present study, sample sizes (i.e. the numbers of sites, isolates, trees, needles, etc.) were much larger than those in Winton et al. (2006), and disease severity was measured systematically for each tree, as opposed to a coarse-scale visual estimation of foliage discoloration and canopy density. This sampling strategy likely provided a better estimate of the relationship between relative abundance of Lineage 2 and SNC severity. However, the accuracy of our estimates of the relative proportion of Lineage 2 from each site was dependent upon sample size. In our study, there were cases where the number of trees sampled at a given site was quite small, and there were also cases where the number of isolates sampled from a site were few as well (e.g. eight isolates from two trees from CB5-2). Thus, the estimated proportion of Lineage 2 (and the estimated relationships between the relative proportion of Lineage 2 and the other variables) may have been biased due to sampling bias. The isolates collected from CB5-2 were not included in the NMDS analysis because we determined that this site was an outlier that had a disproportionate influence on the ordination. The sample of eight isolates from this site had MLGs that were very dissimilar from those collected from the other sites in that block. The fact that the isolates collected from CB5-2 were all Lineage 1, but the site existed in a region where Lineage 2 is relatively abundant, also influenced the fitting of the geographic variables in the NMDS, especially latitude. This suggests that the isolates at CB5-2 were more similar to sites further north, even though this site is near the southern coast of Oregon. Had we collected more isolates from this site, we may have

detected MLGs that were more similar to those from other sites in that block. Another reason for this could be that infected Douglas-fir seedlings sourced from a nursery further north, or further inland where Lineage 2 is much less abundant, were planted at this site. Given that we do not know the history of this site, or where the seedlings were sourced this explanation would be difficult to verify. It is also possible that the environment at this site disfavors Lineage 2, as mean summer temperature was much higher (~ 17.2 ˚C) than would be expected given its proximity to the coast. In this regard, this site more closely resembled an inland site where Lineage 2 might be much less abundant.

The scope of this study was limited due to the use of highly variable neutral markers, which are useful for identifying populations and estimating genetic differentiation, but cannot be used for analyses of natural selection and adaptation. Thus, a thorough demonstration of the role of environment in structuring populations of *N. gaeumannii* was not possible with the available molecular tools. Recent advances in population genomics have enabled the identification of the molecular mechanisms involved in adaptation to local environmental conditions (Branco et al., 2017; Ellison et al., 2011). For instance, a recent study of genomic variation between populations of *Neurospora crassa* identified several cryptic lineages that appeared to be associated with adaptation to local climate, and found that genes encoding an RNA helicase enzyme, an important part of the cold stress response in microbes, were present in divergent regions of the genome (Ellison et al., 2011). Further analyses of growth rates in mutant strains of *N. crassa* suggested that climate had selected for individuals with helicase enzymes that conferred increased cold tolerance (Ellison et al., 2011). Studies of population

differentiation and local adaptation to climate have also been applied to the ectomychorrizal fungus *Suillus brevipes* (Branco et al., 2017). Those authors found that regions of the genome that were highly divergent among populations from different environments contained genes involved in membrane transport, which is thought to be associated with environmental stress responses (Branco et al., 2017). The application of these tools to *N. gaeumannii* should be the next step towards elucidating the environmental factors contributing to spatial genetic variability in its populations and identifying the mechanistic influences of these environmental factors on its biology.

5.6 Acknowledgements

Thanks to Michelle Agne, Gabriela Ritóková, and Dave Shaw for coordinating the sampling of the SNCC plot network and providing foliage samples and disease severity data. Thanks to Amy Ramsey and Dan Omdal for providing access to the WA DNR sampling plots and the associated SNC severity data. Special thanks to B. McCune for valuable assistance in the implementation and interpretation of the NMDS analyses, and L. Ganio and A. Muldoon for assisting in the development of the linear model. This research was made possible by financial contributions from the Swiss Needle Cast Cooperative, Portland Garden Club, Puget Sound Mycological Society, Cascade Mycological Society, Oregon Mycological Society, Washington Department of Natural Resources, U.S.D.A. Forest Service, the Oregon State University Graduate School, and the Oregon Lottery. The authors are very grateful for their generous support.

5.7 Literature Cited

Bennett, P., Stone, J., 2016. Assessments of population structure, diversity, and phylogeography of the Swiss needle cast fungus (*Phaeocryptopus gaeumannii*) in the U.S. Pacific Northwest. *Forests* 7, 14. doi: 10.3390/f7010014

Branco, S., Bi, K., Liao, H.-L., Gladieux, P., Badouin, H., Ellison, C.E., Nguyen, N.H., Vilgalys, R., Peay, K.G., Taylor, J.W., Bruns, T.D., 2017. Continental-level population differentiation and environmental adaptation in the mushroom *Suillus brevipes*. *Molecular Ecology* 26, 2063–2076. doi: 10.1111/mec.13892

Capitano, B.R., 1999. The infection and colonization of Douglas-fir needles by the Swiss needle cast pathogen, *Phaeocryptopus gaeumannii* (Rhode) Petrak (MS Thesis). Oregon State University, Corvallis, Oregon.

Coop, L.B., and Stone, J.K., 2010. Climate models for predicting distribution and severity of Swiss needle cast. pp. 66–80 in *Swiss Needle Cast Cooperative Annual Report 2010*. Mulvey, R., and Shaw, D. (eds.). College of Forestry, Oregon State University, Corvallis, OR. http://sncc.forestry.oregonstate.edu/annual-reports

Ellison, C.E., Hall, C., Kowbel, D., Welch, J., Brem, R.B., Glass, N.L., Taylor, J.W., 2011. Population genomics and local adaptation in wild isolates of a model microbial eukaryote. *Proceedings of the National Academy of Sciences* 108, 2831–2836. doi: 10.1073/pnas.1014971108.

Gerritsen, H., 2014. mapplots: data visualization on maps. R package version 1.5. https://CRAN.R-project.org/package=mapplots

Hansen, E.M., Stone, J.K., Capitano, B.R., Rosso, P., Sutton, W., Winton, L., Kanaskie, A., McWilliams, M.G., 2000. Incidence and impact of Swiss needle cast in forest plantations of Douglas-fir in coastal Oregon. *Plant Disease* 84, 773–778.

Harrell, F.E.J., 2017. Hmisc: Harrell miscellaneous. R package version 4.0-3. https://CRAN.R-project.org/package=Hmisc

Hood, I.A., 1982. *Phaeocryptopus gaeumannii* on *Pseudotsuga menziesii* in Southern British Columbia. *New Zealand Journal of Forestry Science* 12, 415–24.

Jombart, T., 2008. adegenet: a R package for the multivariate analysis of genetic markers. Bioinformatics 24, 1403–1405. doi: 10.1093/bioinformatics/btn129.

Kamvar, Z.N., Brooks, J.C., Grunwald, N.J., 2015. Novel R tools for analysis of genome-wide population genetic data with emphasis on clonality. *Frontiers in Genetics* 6. doi: 10.3389/fgene.2015.00208

Kamvar, Z.N., Tabima, J.F., Grünwald, N.J., 2014. *Poppr*: an R package for genetic analysis of populations with clonal, partially clonal, and/or sexual reproduction. *PeerJ* 2, e281. doi: 10.7717/peerj.281

Lee, E.H., Beedlow, P.A., Waschmann, R.S., Burdick, C.A., Shaw, D.C., 2013. Tree-ring analysis of the fungal disease Swiss needle cast in western Oregon coastal forests. *Canadian Journal of Forest Research* 43, 677–690. doi: 10.1139/cjfr-2013-0062

Lee, E.H., Beedlow, P.A., Waschmann, R.S., Tingey, D.T., Cline, S., Bollman, M., Wickham, C., Carlile, C., 2017. Regional patterns of increasing Swiss needle cast impacts on Douglas-fir growth with warming temperatures. *Ecology and Evolution* 00, 1–30. doi: 10.1002/ece3.3573.

Lee, E.H., Beedlow, P.A., Waschmann, R.S., Tingey, D.T., Wickham, C., Cline, S., Bollman, M., Carlile, C., 2016. Douglas-fir displays a range of growth responses to temperature, water, and Swiss needle cast in western Oregon, USA. *Agricultural and Forest Meteorology* 221, 176–188. doi: 10.1016/j.agrformet.2016.02.009.

Manter, D.K., Bond, B.J., Kavanagh, K.L., Rosso, P.H., Filip, G.M., 2000. Pseudothecia of Swiss needle cast fungus, *Phaeocryptopus gaeumannii*, physically block stomata of Douglas fir, reducing CO_2 assimilation. *The New Phytologist* 148, 481–491.

Manter, D.K., Reeser, P.W., Stone, J.K., 2005. A climate-based model for predicting geographic variation in Swiss needle cast severity in the Oregon Coast Range. *Phytopathology* 95, 1256–1265. doi: 10.1094/PHYTO-95-1256.

Manter, D.K., Winton, L.M., Filip, G.M., Stone, J.K., 2003. Assessment of Swiss needle cast disease: temporal and spatial investigations of fungal colonization and symptom severity. *Journal of Phytopathology* 151, 344–351.

McCune, B., Grace, J.B., Urban, D.L., 2002. Analysis of ecological communities. MjM Software Design, Gleneden Beach, OR. doi: 10.1016/S0022-0981(03)00091-1.

Mcdermott, J.M., Robinson, R.A., 1989. Provenance variation for disease resistance in *Pseudotsuga menziesii* to the Swiss needle-cast pathogen, *Phaeocryptopus gaeumannii*. *Canadian Journal of Forest Research* 19, 244–246.

Mote, P.W., Salathé, E.P., 2010. Future climate in the Pacific Northwest. *Climatic Change* 102, 29–50. doi: 10.1007/s10584-010-9848-z.

Peakall, R., Smouse, P.E., 2012. GenAlEx 6.5: genetic analysis in Excel. Population genetic software for teaching and research--an update. *Bioinformatics* 28, 2537–2539. doi: 10.1093/bioinformatics/bts460.

Peakall, R., Smouse, P.E., 2006. GenAlEx 6: genetic analysis in Excel. Population genetic software for teaching and research. *Molecular Ecology Notes* 6, 288–295. doi: 10.1111/j.1471-8286.2005.01155.x.

R Core Team, 2017. R: A language and environment for statistical computing. R Foundation for Statistical Computing, Vienna, Austria. https://www.R-project.org/

Ramsey, A., Omdal, D., Dozic, A., Kohler, G., and Boderck, M., 2015. Swiss needle cast aerial and ground survey coastal Washington. pp. 12-18 in *Swiss Needle Cast Cooperative Annual Report 2015*. Ritóková, G., and Shaw, D. (eds.). College of Forestry, Oregon State University, Corvallis, OR. http://sncc.forestry.oregonstate.edu/annual-reports

Ritóková, G., Shaw, D., Filip, G., Kanaskie, A., Browning, J., Norlander, D., 2016. Swiss needle cast in western Oregon Douglas-fir plantations: 20-year monitoring results. *Forests* 7, 155. doi: 10.3390/f7080155.

Rogers, J.S., 1972. Measures of genetic similarity and genetic distances, in: Studies in Genetics. University of Texas Publishers, pp. 145–153.

Rosso, P.H., Hansen, E.M., 2003. Predicting Swiss needle cast disease distribution and severity in young Douglas-fir plantations in coastal Oregon. *Phytopathology* 93, 790–798.

Stabler, B., 2013. shapefiles: read and write ESRI shapefiles. R package version 0.7. https://CRAN.R-project.org/package=shapefiles

Stone, J.K., Capitano, B.R., Kerrigan, J.L., 2008a. The histopathology of *Phaeocryptopus gaeumannii* on Douglas-fir needles. *Mycologia* 100, 431–444.

Stone, J.K., Coop, L.B., Manter, D.K., 2008b. Predicting effects of climate change on Swiss needle cast disease severity in Pacific Northwest forests. *Canadian Journal of Plant Pathology* 30, 169–176.

Stone, J.K., Hood, I.A., Watt, M.S., Kerrigan, J.L., 2007. Distribution of Swiss needle cast in New Zealand in relation to winter temperature. *Australasian Plant Pathology* 36, 445. doi: 10.1071/AP07049.

Temel, F., Johnson, G.R., Stone, J.K., 2004. The relationship between Swiss needle cast symptom severity and level of *Phaeocryptopus gaeumannii* colonization in coastal Douglas-fir (*Pseudotsuga menziesii var. menziesii*). *Forest Pathology* 34, 383–394.

Watt, M.S., Stone, J.K., Hood, I.A., Manning, L.K., 2011. Using a climatic niche model to predict the direct and indirect impacts of climate change on the distribution of Douglas-fir in New Zealand. *Global Change Biology* 17, 3608–3619. doi: 10.1111/j.1365-2486.2011.02486.x.

Watt, M.S., Stone, J.K., Hood, I.A., Palmer, D.J., 2010. Predicting the severity of Swiss needle cast on Douglas-fir under current and future climate in New Zealand. *Forest Ecology and Management* 260, 2232–2240. doi: 10.1016/j.foreco.2010.09.034.

Wickham, H., 2016. ggplot2: elegant graphics for data analysis. Springer-Verlag, New York. http://ggplot2.org

Winton, L.M., 2001. Phylogenetics, population genetics, molecular epidemiology, and pathogenicity of the Douglas-fir Swiss needle cast pathogen *Phaeocryptopus gaeumannii*. PhD dissertation. Oregon State University, Corvallis, OR, USA.

Winton, L.M., and Stone, J.K. 2004. Microsatellite population structure of *Phaeocryptopus gaeumannii* and pathogenicity of *P. gaeumannii* genotypes/lineages. pp. 42-48 in *Swiss Needle Cast Cooperative Annual Report 2004*, Mainwaring, D. (ed.). College of Forestry, Oregon State University, Corvallis, OR. http://sncc.forestry.oregonstate.edu/annual-reports

Winton, L.M., Hansen, E.M., Stone, J.K., 2006. Population structure suggests reproductively isolated lineages of *Phaeocryptopus gaeumannii*. *Mycologia* 98, 781–791.

Winton, L.M., Stone, J.K., Hansen, E.M., 2007. Polymorphic microsatellite markers for the Douglas-fir pathogen *Phaeocryptopus gaeumannii*, causal agent of Swiss needle cast disease. *Molecular Ecology Notes* 7, 1125–1128. doi: 10.1111/j.1471-8286.2007.01802.x.

Zhao, J., Maguire, D.A., Mainwaring, D.B., Kanaskie, A., 2012. Climatic influences on needle cohort survival mediated by Swiss needle cast in coastal Douglas-fir. *Trees* 26, 1361–1371.

Zhao, J., Mainwaring, D.B., Maguire, D.A., Kanaskie, A., 2011. Regional and annual trends in Douglas-fir foliage retention: Correlations with climatic variables.

Forest Ecology and Management 262, 1872–1886. doi: 10.1016/j.foreco.2011.08.008.

5.8 Figures and Tables

Table 5.1: Site variables, sample sizes, and disease severity estimates for the 35 sites from which Douglas-fir foliage was collected for isolation of *Nothophaeocryptopus gaeumannii*.

Table 5.1

Site	Year	Distance from the coast (km)	Elevation (m)	N_{trees}	$N_{isolates}$	L1[a]	L2[b]	CI[c]	AFR (%)[d]
Oregon									
Tillamook									
T0-1	2014	5.3	134	9	53	26	27	23.1	42.3
T0-2	2014	4.2	169	5	16	3	13	19.6	52.3
T0-3	2014	8.3	127	5	26	13	13	24.9	30.5
T5-3	2014	16.7	158	5	28	22	6	42.8	32.8
T5-5	2014	17.9	293	5	24	19	5	36.3	46.3
T15-1	2014	28.1	459	4	49	27	22	16.1	67.1
T15-2	2014	36.2	576	5	31	17	14	6.7	88.5
T25-2	2014	49.5	591	5	101	101	0	3.7	88.8
T25-3	2014	49.2	521	5	63	62	1	6.4	88.5
Newport									
N0-1	2015	4.7	146	4	28	0	28	22.9	37.3
N5-2	2015	14.2	457	3	23	0	23	8.8	64.0
N15-3	2015	32.3	411	3	13	6	7	8.3	83.2
N25-5	2015	50.8	251	2	10	10	0	9.6	89.3
Florence									
F0-2	2015	2.7	31	5	11	0	11	19.2	43.3
F5-1	2015	11.2	160	3	13	0	13	12.7	37.8
F15-1	2014	40.6	595	5	32	28	4	15.3	77.8
F15-3	2014	38.0	223	2	15	4	11	17.4	85
F25-2	2014	50.0	498	5	38	25	13	18.5	78.8
Coos Bay									
CB0-1	2015	8	51	2	11	0	11	29.3	56.5
CB5-2	2015	25	114	2	8	8	0	34.4	57.0
CB15-2	2015	42	283	5	12	7	5	17.4	71.3
CB25-2	2015	57	549	1	23	16	7	4.1	76.5
Gold Beach									
G0-1	2015	1.8	159	3	19	0	19	18.3	56.5
G0-2	2016	2.2	98	2	10	0	10	21.7	40.5

Table 5.1 (Continued)

Washington									
N Olympic Peninsula									
WDNR70	2015	5.9	16	5	37	20	17	21.8	78.9
WDNR71	2015	12.6	105	5	39	21	18	27.2	71.1
WDNR49	2015	20.4	163	5	41	30	11	27.0	76.7
WDNR68	2015	34.6	116	5	31	29	2	23.5	70.1
WDNR66	2015	43.7	47	5	53	52	1	32.8	60.0
S Olympic Peninsula									
WDNRQ	2015	4.3	37	5	31	2	29	NA	NA
WDNR64	2015	11.8	67	5	38	2	36	22.4	51.7
WDNR63	2015	21.9	265	5	40	17	23	8.4	75.2
WDNR32	2015	30.6	482	5	46	46	0	14.2	86.5
SW Washington									
DNRL25-2	2014	58	228	5	25	19	6	18.1	80.3
DNRS25-1	2014	48	355	5	23	14	9	19.4	78.8
Total:				150	1061	646	415		

[a] L1 = number of *Nothophaeocryptopus gaeumannii* Lineage 1 isolates recovered from the site, [b] L2 = number of *N. gaeumannii* Lineage 2 isolates recovered from the site, [c] CI = colonization index (average percentage of stomata occluded by pseudothecia), [d] AFR (%) = average foliage retention (average percentage of needles remaining across four needle age classes).

Table 5.2: Summary of variations in geographic, disease, and environmental variables across the 35 sites in Oregon and Washington from which Douglas-fir foliage was sampled for isolation of *Nothophaeocryptopus gaeumannii*.

Variable	Mean	SD	Min	Max
Geography				
Lat[a]	45.5	1.8	42.1	48.2
Long[b]	-123.9	0.4	-124.6	-123.3
Elev[c]	261.7	185.3	16.0	595.0
Dist[d]	26.0	18.3	1.8	57.6
Disease				
CI[e]	19.2	9.4	3.7	42.8
AFR[f]	65.3	18.4	30.5	89.3
PL2[g]	0.5	0.4	0.0	1.0
Environment				
MADT[h]	9.2	0.8	7.3	10.5
TmSummer[i]	15.9	0.9	14.2	17.8
TmWinter[j]	6.4	1.9	4.1	10.3

[a] Lat = latitude (decimal degrees), [b] Long = longitude (decimal degrees), [c] Elev = elevation (meters), [d] Dist = distance from the coast (km), [e] CI = colonization index (average percentage of stomata occluded by pseudothecia), [f] AFR (%) = average foliage retention (average percentage of needles remaining across four needle age classes), [g] PL2 = relative proportion of *NothoPhaeocryptopus gaeumannii* Lineage 2 recovered from a site (number of Lineage 2 isolates/ total isolates), [h] MADT = mean average dew point temperature (˚C) (May-July year prior to sampling), [i] TmSummer = mean summer temperature (˚C) (May-September year prior to sampling), [j] TmWinter = mean winter temperature (˚C) (November-March prior to sampling)

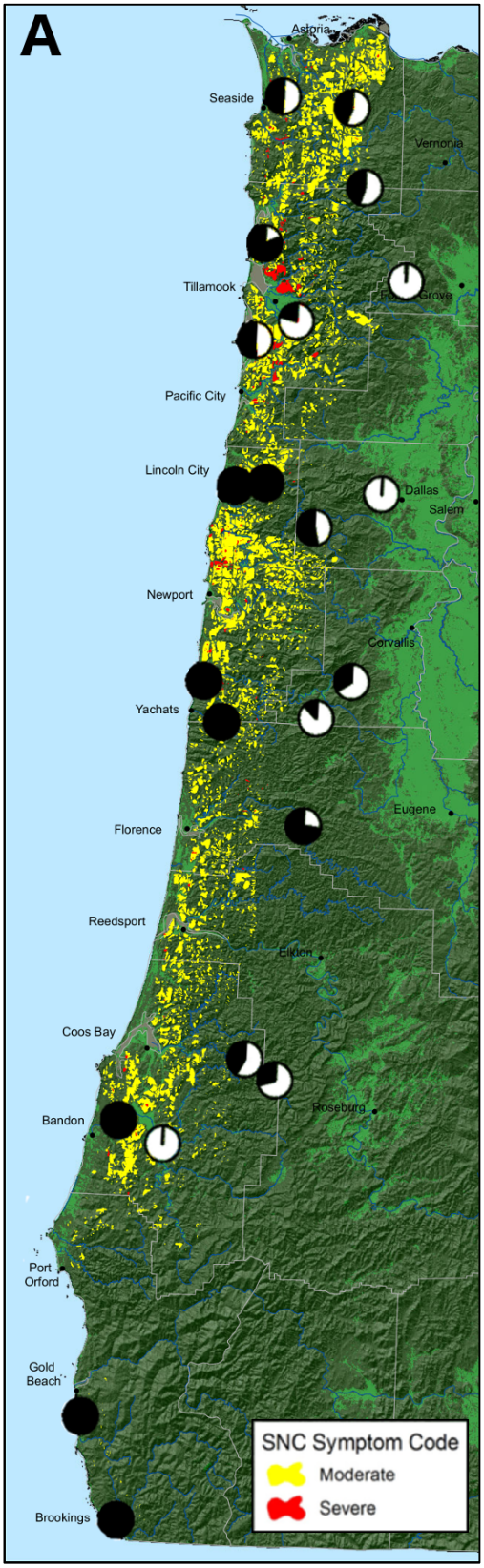
A
Astoria
Seaside
Vernonia
Tillamook
Grove
Pacific City
Lincoln City
Dallas
Salem
Newport
Corvallis
Yachats
Eugene
Florence
Reedsport
Elkton
Coos Bay
Roseburg
Bandon
Port Orford
Gold Beach
Brookings
SNC Symptom Code
Moderate
Severe

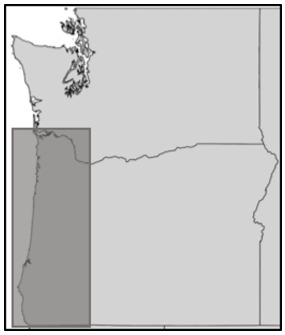

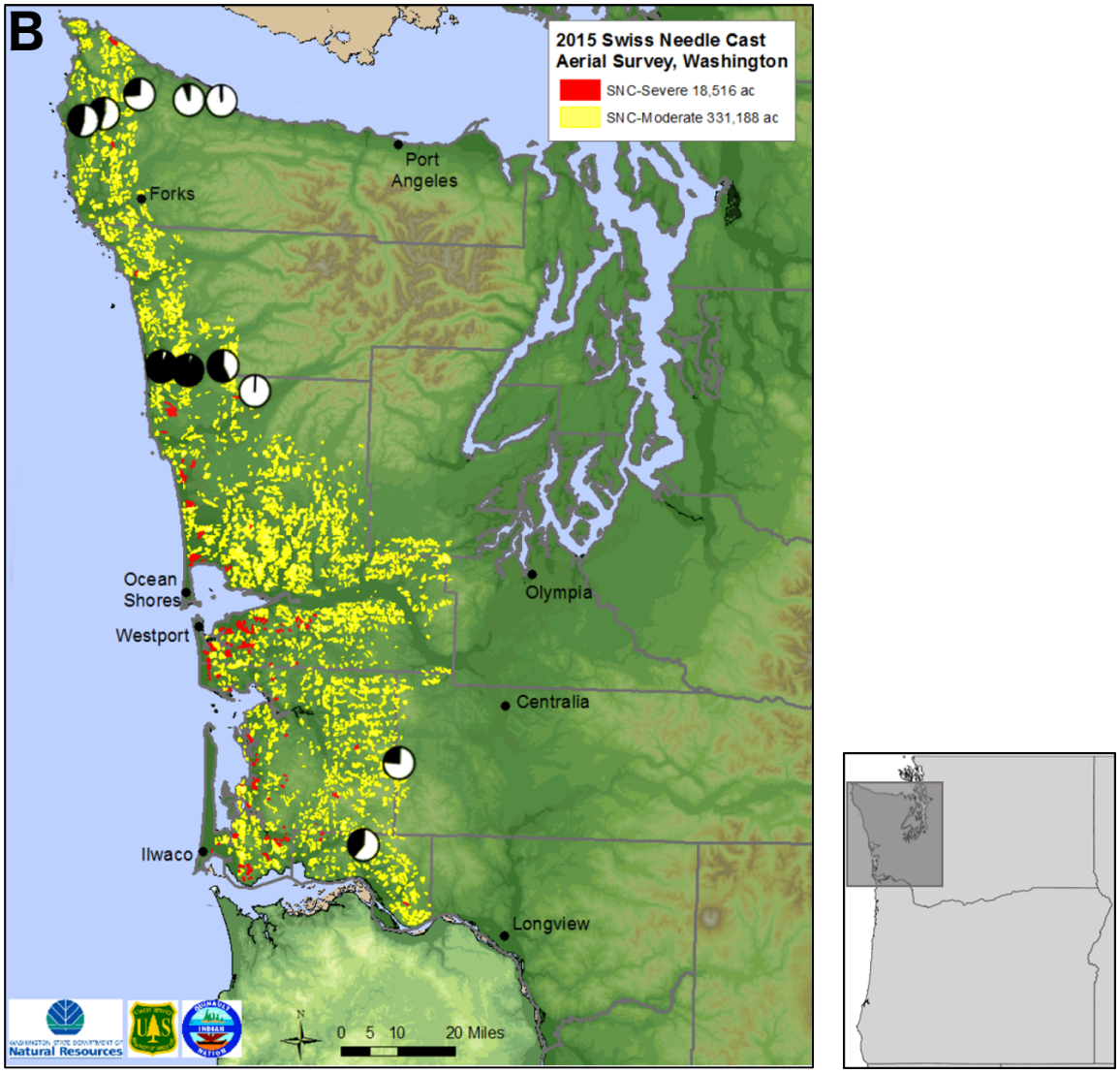

Figure 5.1: Swiss needle cast aerial survey maps (Ramsey et al., 2015; Ritóková et al., 2016) with pie charts showing the geographic distributions of *Nothophaeocryptopus gaeumannii* Lineage 1 (white) and Lineage 2 (black) in **A)** 24 sites in western Oregon (for two of the pie charts, data from adjacent sites were pooled to avoid overlap), and **B)** 11 sites in western Washington.

Table 5.3: Pearson's correlation coefficients (*r*) for the relationships between each of the environmental and geographic variables used for this study. Numbers in parentheses represent computed P-values for the correlation coefficient.

	CI[a]	AFR[b]	PL2[c]	MADT[d]	TmSummer[e]	TmWinter[f]	Elev[g]	Dist[h]
CI	–							
AFR	-0.59 (*0.000*)	–						
PL2	-0.03 (*0.857*)	-0.51 (*0.002*)	–					
MADT	0.65 (*0.000*)	-0.58 (*0.000*)	0.26 (*0.144*)	–				
TmSummer	-0.33 (*0.053*)	0.38 (*0.025*)	-0.21 (*0.236*)	-0.2 (*0.257*)	–			
TmWinter	0.2 (*0.262*)	-0.48 (*0.004*)	0.51 (*0.002*)	0.6 (*0.000*)	0.07 (*0.707*)	–		
Elev	-0.66 (*0.000*)	0.6 (*0.000*)	-0.38 (*0.027*)	-0.8 (*0.000*)	0.39 (*0.023*)	-0.48 (*0.004*)	–	
Dist	-0.41 (*0.016*)	0.73 (*0.000*)	-0.69 (*0.000*)	-0.55 (*0.001*)	0.49 (*0.004*)	-0.47 (*0.005*)	0.63 (*0.000*)	–

[a] colonization index (average proportion of stomata occluded by pseudothecia), [b] Average foliage retention (%), [c] relative proportion of Lineage 2 isolates from sample site (Lineage 2 isolates/total isolates), [d] Mean average dewpoint temperature (˚C), [e] mean summer temperature (˚C), [f] mean winter temperature (˚C), [g] Elevation (meters), [h] distance from the coast (km).

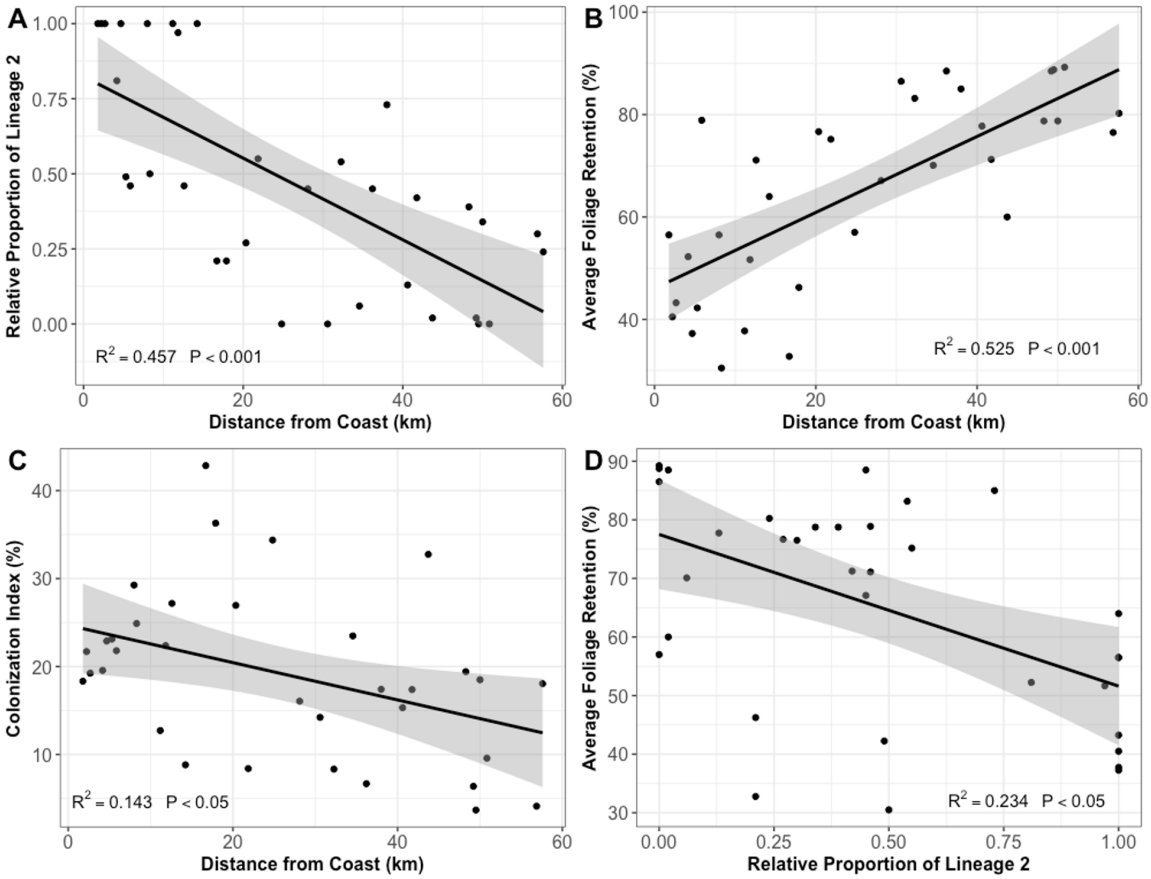

Figure 5.2: The relationships between distance from the coast (km) and **A)** the relative proportion of isolates corresponding to *Nothophaeocryptopus gaeumannii* Lineage 2, **B)** average foliage retention (AFR) (%), and **C)** the colonization index (i.e. the average proportion of stomata occluded by *N. gaeumannii* pseudothecia). **D)** The relationship between the relative proportion of Lineage 2 and average foliage retention when the distance from the coast (a major confounding variable) is not taken into account. Shaded regions represent 95% confidence intervals for the fitted lines. Relative proportion of Lineage 2 = the number of isolates of *N. gaeumannii* Lineage 2 recovered from the site/ total isolates from the site.

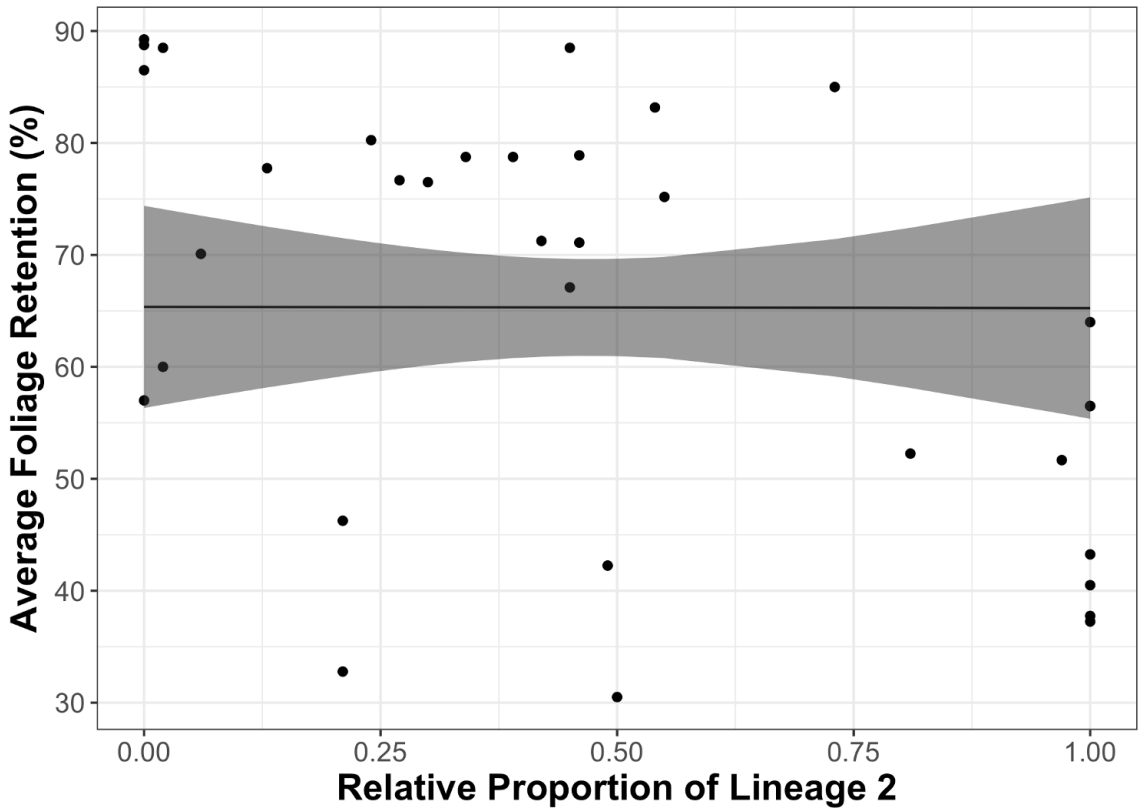

Figure 5.3: The relationship between average foliage retention (AFR) (%) and the relative proportion of *Nothophaeocryptopus gaeumannii* Lineage 2, after accounting for distance from the coast. Each point corresponds to one of the 34 sites for which disease severity data were available. The line corresponds to predicted values from the model when the distance from the coast is fixed at its mean (26 km), with the shaded region representing the 95% confidence intervals for the predicted values.

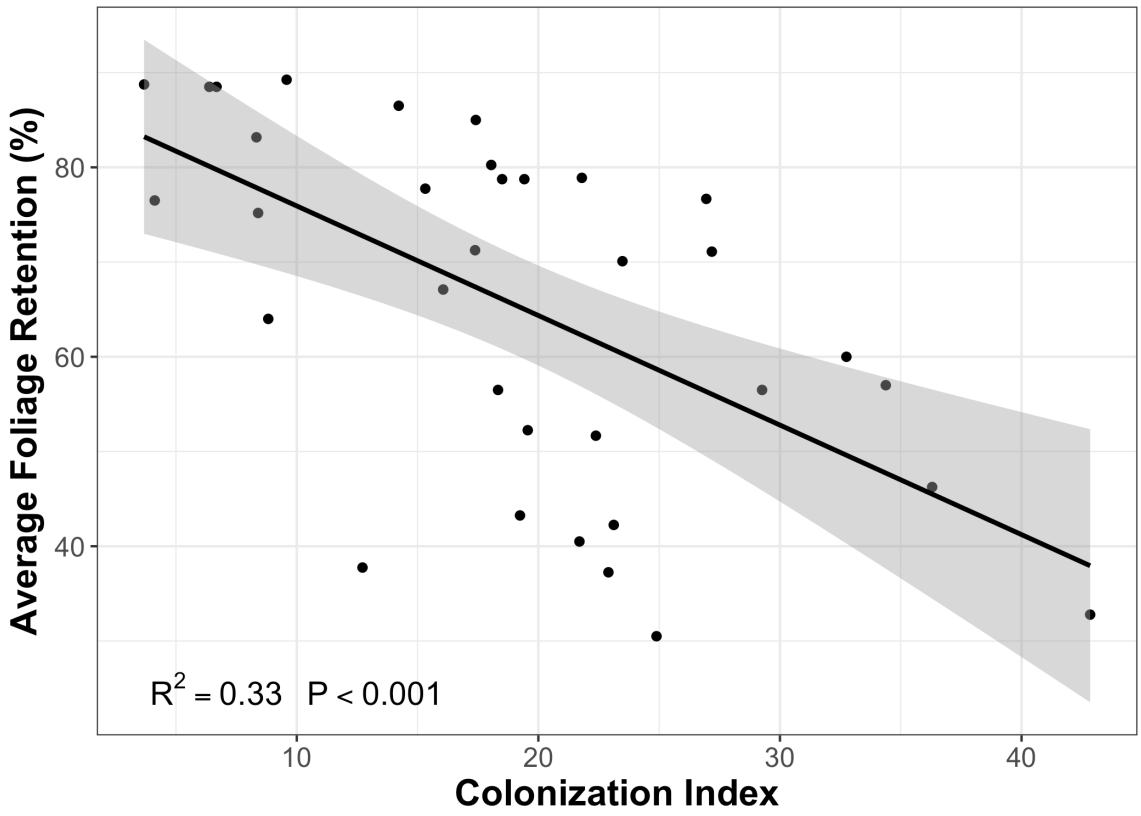

Figure 5.4: The relationship between average foliage retention (AFR) (%), estimated for ten Douglas-fir trees from each of the 34 sites, and the colonization index (CI), an estimate of the average percentage of stomata occluded by pseudothecia of *Nothophaeocryptopus gaeumannii*.

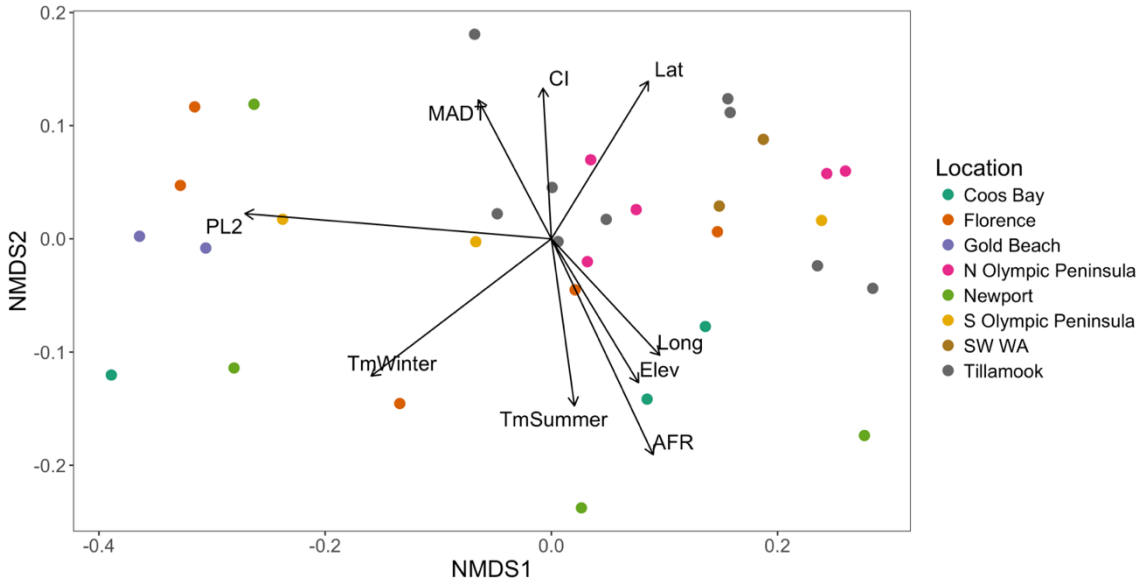

Figure 5.5: Non-metric multidimensional scaling (NMDS) ordination based on the genetic distances between 33 sample sites calculated from multilocus SSR genotypes of *Nothophaeocryptopus gaeumannii* isolates. Joint-plot vectors show correlations between environmental variables and the ordination. Vector labels correspond to the variables listed in Table 5.4. Final stress = 0.095. Locations in legend correspond to the sampling blocks. One Coos Bay site was removed from the ordination because it was an outlier, and one S Olympic Peninsula site was not included because disease severity estimates were not available.

Table 5.4: Environmental, geographic, and disease variables used in the joint-plot for the NMDS analysis based on the genetic distance *Nothophaeocryptopus gaeumannii*.

Variable	Description	R^2 [a]	P [b]
Lat	Latitude (decimal degrees)	0.342	0.004
Long	Longitude (decimal degrees)	0.253	0.017
TmWinter	mean winter temperature (˚C) (November-March prior to sampling)	0.513	0.001
TmSummer	mean summer temperature (˚C) (May-September year prior to sampling)	0.284	0.012
MADT	Mean average dewpoint temperature (˚C) (May-July year prior to sampling)	0.247	0.015
PL2	Relative proportion of Lineage 2 isolates in sample site (Number of Lineage 2 Isolates/Total Number of Isolates)	0.947	0.001
AFR	Average foliage retention (% foliage remaining across 4 needle age classes from branches in the mid canopy)	0.569	0.001
CI	Colonization index (average percentage of stomata occluded by pseudothecia)	0.228	0.016
Elev	Elevation (meters)	0.283	0.009

[a] R^2 reflects the correlation between environmental variables and ordination scores.
[b] P-value calculated from 999 permutations of the data.

5.9 Supplementary Figures

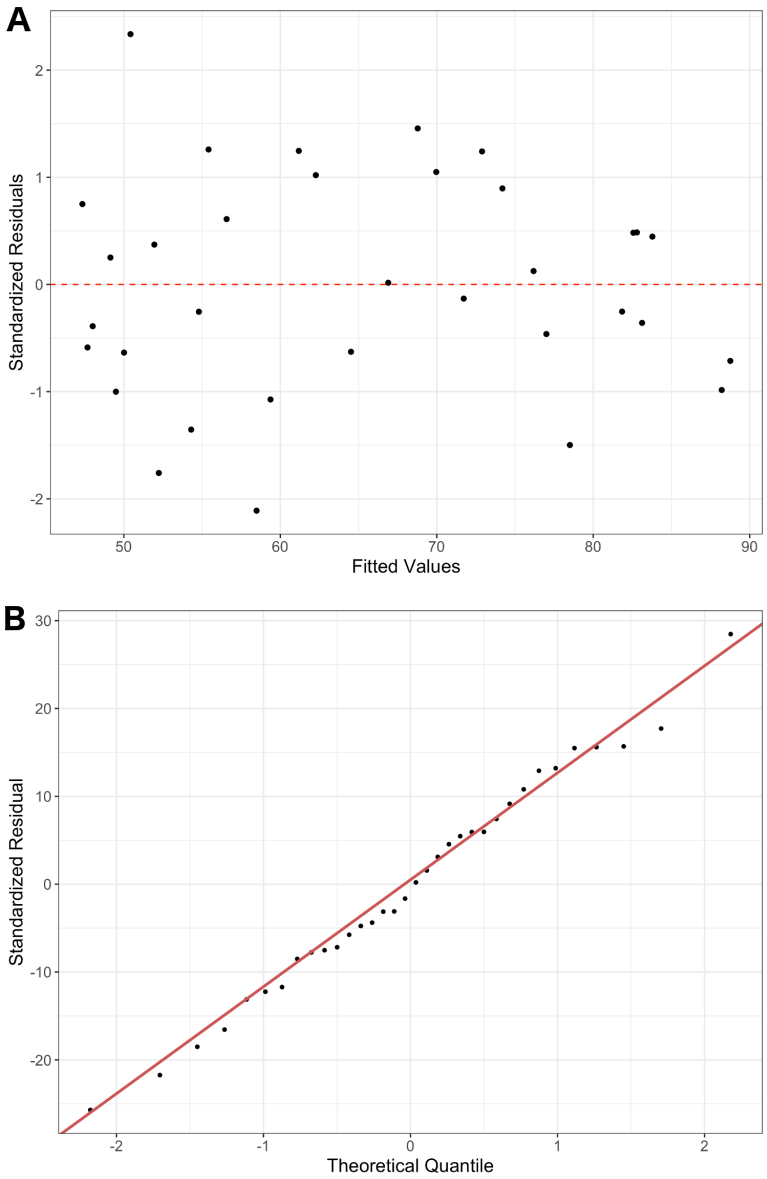

Figure S5.1: Diagnostic plots for the linear model of average foliage retention as a function of the relative proportion of *Nothophaeocryptopus gaeumannii* Lineage 2 and distance from the coast (km). **A)** Standardized residuals plotted against the fitted values from the model. The equal distribution of values around the zero line indicates that the assumption of constant variance has not been violated. **B)** Standardized residuals plotted against the theoretical quantiles. Here, the relationship does not deviate considerably from a straight line, suggesting that the assumption of normally-distributed residuals has not been violated.

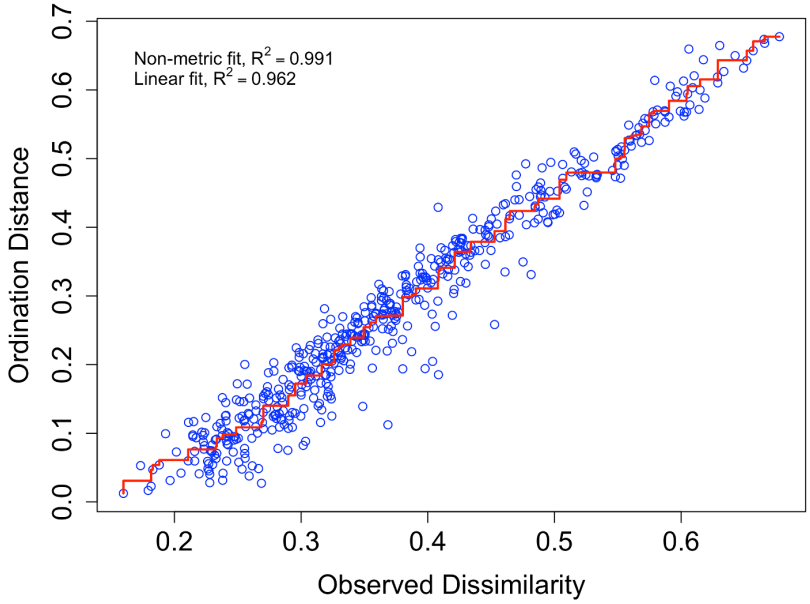

Figure S5.2: Stress plot from the non-metric multidimensional scaling ordination (NMDS) based on the genetic distances between sites from which *Nothophaeocryptopus gaeumannii* isolates were collected. This plot shows the relationship between ordination distances and the observed dissimilarity (i.e. pairwise genetic distances between sites). R^2 values provide a measure of goodness-of-fit. Non-metric fit is based on stress (*S*), and is defined as $R^2 = 1\text{-}S*S$ (Oksanen et al., 2017). The linear fit is the squared correlation between fitted values and ordination distances (Oksanen et al., 2017).

Chapter 6: Conclusions

This dissertation represents a significant contribution towards an understanding of the factors influencing the spatial genetic structures of native and introduced fungal populations. Our findings may serve as a foundation for future studies of the evolutionary biology of *N. gaeumannii*, interactions between environment, population structure and SNC severity. Here, we investigated the influences of reproductive mode, population bottlenecks following founder events, dispersal, and the environment, on the genetic structure of *N. gaeumannii* populations.

In Chapter 2, we described the genetic structure of populations of *N. gaeumannii* within the native range of Douglas-fir in western Oregon and Washington. Given that asexual reproduction via conidia is not known to occur in this fungus, the presence of repeated multilocus genotypes suggests that it is capable of reproducing via homothallism. We observed the heterogeneous spatial distributions of two non-interbreeding lineages in Oregon and Washington, provided the first evidence that *N. gaeumannii* Lineage 2 is present in Washington, and determined that these lineages are admixed within individual Douglas-fir needles in plantations in the western Coast Ranges in Oregon and Washington. These analyses also provided support for the hypothesis that the two lineages are reproductively isolated. Despite the fact that the two lineages are sympatric within Douglas-fir canopies and within individual needles, they do not appear to interbreed, suggesting that they are genetically incompatible.

We also provided evidence that the observed spatial genetic structure may be influenced by dispersal abilities of this fungus. Individual trees were host to as many as 20 distinct genotypes, and genotypes were shared between trees within sites, suggesting

that gene flow occurs between them via ascospore dispersal. However, the local *N. gaeumannii* populations at coastal sites and inland sites appeared to be genetically isolated in many cases. This could be the result of dispersal limitations, but may also reflect differing environmental preferences among the lineages or may have resulted from the human-mediated transfer of infected Douglas-fir seedlings that were used to establish timber plantations. There were identical genotypes that occurred between Oregon and Washington at sites up to 300 km apart. Assuming that these arose due to shared ancestry and were not the result of homoplasy, this suggests that gene flow occurs between these sites. The data analyzed here did not allow us to infer whether this gene flow occured via natural dispersal or human-mediated migration.

Similar analyses were performed with isolates collected from an introduced population of *N. gaeumannii* in New Zealand, where the fungus first was documented in 1959. Here, we presented the first evidence that Lineage 2 is present outside of the western Coast Range in Oregon, and found that unique Lineage 2 genotypes were present in the South Island that were not detected in the North Island where the initial introduction occurred. It is possible that the observed distribution of these genotypes resulted from subsequent independent introductions of *N. gaeumannii* from coastal forests in western North America. In addition to the presence of the two non-interbreeding lineages in New Zealand, we observed an abundance of repeated genotypes that must have resulted from self-fertilization. These factors had a significant influence on linkage disequilibrium in the population. Even after the removal of repeated genotypes and the separation of the two lineages, linkage among loci was still significantly higher

than expected under linkage equilibrium. One overrepresented genotype that was shared among nearly 300 individuals at 17 sites was recovered from sites that were over 1,000 km apart. Although we could not directly test spore dispersal capabilities, the spatial distribution of genotypes observed in New Zealand is unlikely to be reflective of long distance dispersal. Rather, it suggests either that anthropogenic activities have resulted in the movement of infected plant material or that a "stepping-stone" model of dispersal has occurred between the discontinuous and often spatially distant Douglas-fir plantations in the North and South Islands.

We then combined data for genotypes from 1,061 isolates from western Oregon and Washington, 2,085 isolates collected in New Zealand, and over 680 additional isolates from Idaho and New Mexico, the eastern United States, Europe, Australia, and Chile to assess the population structure and diversity in *N. gaeumannii* globally. Genotypic clustering methods were used to analyze the similarities among genotypes from these disparate populations, and approximate Bayesian computation with *DIYABC* allowed us to test competing hypothesis about the origins and sources of introduction of these global *N. gaeumannii* populations. These analyses revealed that North America is the center of diversity of *N. gaeumannii*, providing further support for this region as the evolutionary origin of the pathogen. Isolates from Europe, New Zealand, and Chile were much more similar to those from North America than those from Australia, and the *DIYABC* analysis suggested that North America was the source of the introductions to Europe, New Zealand, and Chile. Although Australia and New Zealand are closer to each another than either is to Europe or North America, and the two countries have strong

commercial and cultural ties, the ABC analyses suggested that their populations had separate origins. The cluster analyses also suggested that despite their relative proximity and commercial ties, gene flow has not occurred between them. The *DIYABC* scenario with the highest statistical support suggested that each of the introduced populations have undergone a genetic bottleneck, i.e. the loss of allelic richness and genetic diversity associated with founding events. This suggests that a small number of migrants was introduced to each location in one (or a few) discrete events, and genetic drift led to the loss or fixation of alleles at random in subsequent generations. New Zealand stood out as being much more diverse than the other introduced populations, even after accounting for unequal sample sizes. This suggests that there may have been multiple introductions there, or that the individuals introduced in the initial founding event were relatively diverse. Given the spatial separation between these populations and those in northwestern North America (where *N. gauemannii* and Douglas-fir are native) and Europe (where the first introduction occurred), the best explanation for the observed distribution of *N. gaeumannii* is that infected Douglas-fir seedlings were inadvertently introduced for establishing timber plantations, or for the ornamental nursery trade.

We also examined relationships between *N. gaeumannii* Lineage 2, SNC severity, and environment to test the hypotheses that Lineage 2 is more aggressive and that environmental factors influence the spatial distributions of both lineages. It initially appeared that the relative abundance of Lineage 2 was higher in Douglas-fir stands where SNC symptoms are more severe. This was true for both the landscape-level distribution of visible SNC symptoms (as assessed via aerial disease survey), and foliage retention

measured in the Douglas-fir stands from which our isolates were collected. The spatial distribution of Lineage 2 was most strongly correlated with mean winter temperature, a variable that also influences SNC severity. Needle colonization was higher, and foliage retention lower, where mean winter temperature and spring/early summer dew point temperatures were warmest. Where summers were hot and dry, colonization was much lower and foliage retention was much higher. These variables, as well as the spatial distribution of *N. gaeumannii* Lineage 2, were strongly correlated with distance from the coast, a variable that is associated with continentality. After accounting for this environmental gradient across which our samples were collected, there was no evidence to suggest an association between the relative abundance of Lineage 2 and SNC severity. These results do not support the hypothesis that Lineage 2 is more aggressive, but instead showed that the correspondence between Lineage 2 and disease severity is a consequence of environment. The same environmental factors that are most conducive to SNC also appear to be favorable for *N. gaeumannii* Lineage 2. Our multivariate statistical analyses suggested that isolates collected from the stands with the most severe SNC symptoms were highly differentiated genetically from those collected from stands with the least severe symptoms. The relative abundance of Lineage 2 did not differ between these sites, providing additional evidence that Lineage 2 is not more aggressive. It is not clear whether the genetic differentiation observed between these sites is due to environment, reflecting local adaptation to climate, or whether there is some selection for aggressive isolates occurring where SNC is most severe. The possibility that this genetic differentiation is due to genetic drift, or is the result of anthropogenic activities could not

be ruled out. The fact that the genetic structure of *N. gaeumannii* populations as well as SNC severity are so closely linked with the existing environmental variation in the low-elevation coastal Douglas-fir forests in western Oregon and Washington suggests that climate change may have a major impact on both the disease and the pathogen. Climate change is expected to lead to an expansion of the region that is most conducive to SNC (Stone et al., 2008b; Lee et al., 2017). The results of this study suggest that these environmental changes will also influence the genetic structure of *N. gaeumannii* populations in the coming decades.

All of these separate lines of evidence point to a clear set of conclusions regarding the evolutionary forces influencing the genetic structure of *N. gaeumannii* populations. First is the presence of two highly differentiated non-interbreeding lineages, which are the primary component of the substructure within the *N. gaeumannii* population. Their existence seems to be maintained by the fact that they are reproductively incompatible, as there are no obvious physical barriers to gene flow between them. Reproductive mode also has a profound influence on the structure of its populations. There is ample evidence to suggest that this fungus is homothallic. The most convincing of which is the presence of repeated multilocus genotypes in nearly all of the populations that we sampled. Given that this fungus does not mate in culture (Stone et al., 2008a), it would be difficult to definitively demonstrate the reproductive mode in a laboratory setting. However, an examination of the mating type loci via nucleotide sequencing may provide further evidence as to the mating system and may also provide insights into the potential genetic incompatibility between the two lineages.

Our results also provided evidence that the spatial genetic structure observed in *N. gaeumannii* populations is influenced by the environment. The spatial distributions of the lineages are correlated with temperature, and thus it appears that they adapted to slightly different environmental conditions. Lineage 1 is far more abundant than Lineage 2 where mean winter temperatures are colder, and where summers are warmer and drier. Lineage 2 is more abundant than Lineage 1 where winters are warmer. This suggests that Lineage 1 has adapted to cooler climates, while Lineage 2 has adapted to warmer climates.

Given the high level of differentiation observed between the two lineages, and evidence that suggests that they are genetically incompatible, it seems reasonable to conclude that they should be described as separate species. If full genome sequences were available for both lineages, one would expect to be able to identify regions of the genome in which the two lineages are divergent. This sequence divergence could then be combined with available genome sequences from closely related fungi to construct a phylogenetic tree that depicts evolutionary relationships among the groups based on genome-wide variation. This could provide valuable insights into the phylogenetic relationships between the two lineages, and may also allow researchers to identify regions of the genome that are under selection that may be responsible for their divergence.

Although the evolutionary origins of these two lineages have not been investigated, we might assume that they occupied separate geographic ranges at some point in their evolutionary histories. This would explain their genetic divergence, as fungi are not known to speciate without some form of allopatry (Giraud et al., 2008; Giraud

and Gourbiere, 2012; Restrepo et al., 2014). The fact that there appear to be coastal and inland "forms" of *N. gaeumannii* seems to coincide with the fact that there are coastal and interior varieties of their Douglas-fir host (i.e. *P. menziesii* var. *menziesii* and *P. menziesii* var. *glauca*). Although the Douglas-fir trees from which Lineage 1 and Lineage 2 isolates were collected in Oregon and Washington were all of the coastal form (*P. menziesii* var. *menziesii*), the Lineage 1 isolates from Idaho and New Mexico were collected from foliage of the interior variety, *P. menziesii* var. *glauca*. One possible scenario is that Lineage 1 evolved on the interior Douglas-fir form, and Lineage 2 on the coastal Douglas-fir form. These infraspecific varieties of Douglas-fir diverged during the Pliocene, and were geographically isolated for a long periods of time due to glaciation (Gugger et al., 2010; Lavender and Hermann, 2014). During this time, they were confined to their respective glacial refugia along the west coast, and in the Rocky Mountains (Gugger et al., 2010; Lavender and Hermann, 2014). This hypothesis would provide an explanation for the geographic isolation that would have been required to achieve strong genetic divergence and complete reproductive isolation between the *N. gaeumannii* lineages. After the glaciers receded, both Douglas-fir forms experienced major climatic shifts and subsequently migrated gradually to occupy their current distributions in which their populations are admixed, and they often hybridize, in the eastern Coast Range in southern British Columbia (Lavender and Hermann, 2014). This scenario would have resulted in a relatively recent reunion of the two *N. gaeumannii* lineages in northwestern North America, and could explain many of our observations concerning their environmental preferences, their spatial distributions, and their genetic

structures. To test this hypothesis, one could compare phylogenies of both host and fungus and apply coalescence analyses to approximate the time since divergence of the two *N. gaeumannii* lineages. If the timing of this evolutionary divergence were to coincide with known glaciation events or the estimated time of divergence of the host varieties, then that would suggest a potential mechanism leading to their speciation.

6.1 Literature Cited

Giraud, T., Gourbiere, S., 2012. The tempo and modes of evolution of reproductive isolation in fungi. *Heredity* 109, 204. doi: 10.1038/hdy.2012.30.

Giraud, T., Refrégier, G., Le Gac, M., de Vienne, D.M., Hood, M.E., 2008. Speciation in fungi. *Fungal Genetics and Biology* 45, 791–802. doi: 10.1016/j.fgb.2008.02.001

Gugger, P.F., Sugita, S., Cavender-Bares, J., 2010. Phylogeography of Douglas-fir based on mitochondrial and chloroplast DNA sequences: testing hypotheses from the fossil record. *Molecular Ecology* 19, 1877–1897. doi: 10.1111/j.1365-294X.2010.04622.x.

Lee, E.H., Beedlow, P.A., Waschmann, R.S., Tingey, D.T., Cline, S., Bollman, M., Wickham, C., Carlile, C., 2017. Regional patterns of increasing Swiss needle cast impacts on Douglas-fir growth with warming temperatures. *Ecology and Evolution* 00, 1–30. doi: 10.1002/ece3.3573.

Stone, J.K., Capitano, B.R., Kerrigan, J.L., 2008a. The histopathology of Phaeocryptopus gaeumannii on Douglas-fir needles. *Mycologia* 100, 431–444.

Stone, J.K., Coop, L.B., Manter, D.K., 2008b. Predicting effects of climate change on Swiss needle cast disease severity in Pacific Northwest forests. *Canadian Journal of Plant Pathology* 30, 169–176.